

**EFFECT OF ULTRASONICATION ON COLLOIDAL,
THERMOPHYSICAL AND RHEOLOGICAL PROPERTIES
OF ALUMINA–WATER NANOFLUID**

MOHAMMED MAHBUBUL ISLAM

**FACULTY OF ENGINEERING
UNIVERSITY OF MALAYA
KUALA LUMPUR**

2015

EFFECT OF ULTRASONICATION ON COLLOIDAL,
THERMOPHYSICAL AND RHEOLOGICAL PROPERTIES
OF ALUMINA–WATER NANOFLUID

MOHAMMED MAHBUBUL ISLAM

THESIS SUBMITTED IN FULFILLMENT OF THE
REQUIREMENTS FOR THE DEGREE OF
DOCTOR OF PHILOSOPHY

FACULTY OF ENGINEERING
UNIVERSITY OF MALAYA
KUALA LUMPUR

2015

UNIVERSITY OF MALAYA

ORIGINAL LITERARY WORK DECLARATION

Name of the candidate: **Mohammed Mahbubul Islam**

Registration/Matric No: **KHA 120076**

Name of the Degree: **Doctor of Philosophy**

Title of Thesis (This Work): **Effect of Ultrasonication on Colloidal, Thermophysical and Rheological Properties of Alumina–Water Nanofluid**

Field of Study: **Energy (Mechanics and Metal Work)**

I do solemnly and sincerely declare that:

- (1) I am the sole author/writer of this Work;
- (2) This Work is original;
- (3) Any use of any work in which copyright exists was done by way of fair dealing and for permitted purposes and any excerpt or extract from, or reference to or reproduction of any copyright work has been disclosed expressly and sufficiently and the title of the Work and its authorship have been acknowledged in this Work;
- (4) I do not have any actual knowledge nor do I ought reasonably to know that the making of this work constitutes an infringement of any copyright work;
- (5) I hereby assign all and every rights in the copyright to this work to the University of Malaya (“UM”), who henceforth shall be owner of the copyright in this work and that any reproduction or use in any form or by any means whatsoever is prohibited without the written consent of UM having been first had and obtained;
- (6) I am fully aware that if in the course of making these works I have infringe any copyright whether intentionally or otherwise, I may be subject to legal action or any other action as may be determined by UM.

Candidate’s Signature

Date

Subscribe and solemnly declare before,

Witness Signature

Date

Name :

Designation :

ABSTRACT

Nanofluids are promising fluids for heat transfer applications. Low stability and high viscosity are two important drawbacks for practical applications of nanofluids. The aggregation and sedimentation of nanoparticles are related to the colloidal dispersion characteristics, which directly affect the stability and thermophysical properties. An ultrasonic homogenizer can break the aggregation of particles and disperse them into a fluid to improve the stability of the suspension. Therefore, sound energy is needed to improve thermal energy. However, the research question is whether the improvement achieved in thermal application is feasible for the amount of used ultrasound energy. The aim of this research was to study the effect of the ultrasonic treatment on colloidal dispersion characteristics, thermophysical and rheological properties, and thermal performance analysis for a nanofluid. Specifically, a 0.5 vol.% of Al_2O_3 -water nanofluid was prepared using a horn or probe (tip) ultrasonic dismembrator and 0 to 5 h of durations were applied. The microstructure, particle size distribution, and zeta potential were analyzed as the colloidal dispersion characteristics at 25% and 50% amplitude of the sonicator power. The thermophysical (thermal conductivity, viscosity, and density) and rheological properties of the nanofluids subjected to ultrasonic treatment for different durations were measured at different temperatures from 10 to 50 °C. Thermal performance characteristics as: thermal resistance, heat transfer coefficient, pumping power, and figures of merit were also analyzed for a mini channel heat sink at different flow rates. It was found that higher sonicator amplitude took fewer periods to disperse the particles. An optimum dispersion of particles with high stability was observed at ~5 and ~3 h of ultrasonication duration with 25% and 50% power amplitudes, respectively. Thermal conductivity and density ratio were found to be increased, but viscosity ratio was decreased with increasing sonication time and temperature. At lower temperature, nanofluid showed Newtonian behavior at lower

shear rate, but it showed non-Newtonian at higher shear rates. Nevertheless, at higher temperature, nanofluids were found to be almost non-Newtonian with shear thickening behavior. Moreover, a slight decrease in yield stress with increasing sonication time was also observed and it was found to be lower at a higher temperature. Higher heat transfer coefficient was observed for 4 h of ultrasonication duration, which was more effective at high-flow rates. However, pumping power was increased with the increase of sonication time and with low flow rates. Figure of merit analysis showed that a 4 h of ultrasonication could give optimum thermal performance. Nevertheless, the longer duration of ultrasonication is not fruitful in terms of productivity, considering the usage of sound energy and the gain in thermal engineering.

ABSTRAK

Nanofluids adalah cecair yang amat sesuai untuk aplikasi pemindahan haba. Kestabilan yang rendah dan kelikatan yang tinggi adalah dua kekurangan utama untuk aplikasi praktikal *nanofluids*. Pengumpulan dan pemendapan *nanopartikel* adalah berkait dengan ciri-ciri serakan koloid, memberi kesan yang secara langsung kepada kestabilan dan sifat termofizikal. Homogenizer ultrasonik boleh memecahkan pengumpulan partikel dan menghamburkan mereka ke dalam cecair untuk meningkatkan kestabilan penyebaran. Oleh itu, tenaga bunyi diperlukan untuk meningkatkan tenaga haba. Walau bagaimanapun, persoalan kajian ialah sama ada peningkatan kejuruteraan haba sesuai untuk jumlah tenaga *ultrasound* digunakan. Tujuan kajian ini adalah untuk mengkaji kesan rawatan ultrasonik pada ciri-ciri serakan koloid, sifat termofizikal dan reologi, dan analisis prestasi termal untuk sesuatu *nanofluid*. Secara khusus, *nanofluid* 0.5 vol.% daripada Al_2O_3 -air *dismembrator* ultrasonik jenis tanduk (hujung) dengan tempoh yang berbeza dari 0 hingga 5 j. Struktur mikro, taburan saiz zarah, dan potensi zeta telah dikaji sebagai ciri-ciri serakan koloid pada amplitud 25% dan 50% daripada kuasa sonicator. Sifat termofizikal (kekonduksian terma, kelikatan dan ketumpatan) dan reologi *nanofluid* yang disediakan oleh jangka masa ultrasonikasi yang berlainan diukur untuk suhu yang berbeza dari 10 hingga 50 °C. Ciri-ciri prestasi haba sebagai: rintangan termal, pekali pemindahan haba, kuasa pam, dan angka merit juga dianalisis untuk saluran mini tenggelam haba pada kadar aliran yang berbeza. Didapati bahawa amplitud sonikator yang tinggi mengambil masa yang sedikit untuk menyuraikan partikel. Serakan partikel yang optimum dengan kestabilan yang tinggi diperhati dari ~5j dan ~3j masing-masing untuk tempoh ultrasonikasi dengan amplitud kuasa 25% dan 50%. Kekonduksian terma dan kepadatan telah meningkat, tetapi kelikatan telah menurun dengan peningkatan masa sonication dan suhu. Pada suhu yang lebih rendah, *nanofluid* menunjukkan tingkah laku *Newtonian* pada kadar ricih yang lebih rendah, tetapi ia

menunjukkan *non-Newtonian* pada kadar ricih yang lebih tinggi. Walau bagaimanapun, nanofluids dijumpai hampir *non-Newtonian* dengan tingkah laku ricih penebalan. Selain itu, tegasan alah telah didapati menurun dengan peningkatan masa sonikasi juga diperhatikan dan didapati bahawa lebih rendah pada suhu yang tinggi. Pekali pemindahan haba yang lebih tinggi diperhatikan untuk tempoh ultrasonikasi selama 4 j, yang lebih berkesan pada kadar aliran tinggi. Walau bagaimanapun, kuasa pam meningkat dengan peningkatan masa sonikasi dan kadar aliran. Rajah analisis merit menunjukkan bahawa 4 j daripada ultrasonikasi boleh memberikan prestasi terma yang optimum. Namun, tempoh ultrasonik yang lama tidak berkesan dari segi produktiviti, memandangkan penggunaan tenaga bunyi dan keuntungan dalam kejuruteraan termal.

ACKNOWLEDGEMENTS

In the Name of Allah, The Beneficent, The Merciful, I would like to express my utmost gratitude and thanks to the almighty Allah (s.w.t) for the help and guidance that He has given me through all these years. My deepest appreciation is to my family for their blessings and supports.

I would like to express my sincere gratefulness and gratitude to my supervisors, **Professor Dr. Saidur Rahman** and **Dr. Amalina Binti Muhammad Afifi**. I am grateful to them for their brilliant supervision, guidance, encouragement and supports in carrying out this research work. I am deeply indebted to them. I acknowledge the effort of my internal examiner **Dr. Poo Balan Ganesan** for his constructive and valuable comments to improve the quality of the thesis at the final stage.

Finally, thanks to Ministry of Education Malaysia and University of Malaya for financial support, privileges, and opportunities to conduct this study. This project was carried out under the UM MoE High Impact Research Grant (HIRG) Scheme (Project no. UM.C/HIR/MoHE/ENG/40). I gratefully acknowledge to the staff and students of Mechanical Engineering Department of University of Malaya in helping me and for suggestion and advices in completing this research work.

TABLE OF CONTENTS

| | |
|--|--------------|
| ORIGINAL LITERARY WORK DECLARATION | ii |
| ABSTRACT | iii |
| ABSTRAK | v |
| ACKNOWLEDGEMENTS | vii |
| TABLE OF CONTENTS | viii |
| LIST OF FIGURES | xi |
| LIST OF TABLES | xvi |
| LIST OF SYMBOLS AND ABBREVIATIONS | xviii |
| CHAPTER 1: INTRODUCTION | 1 |
| 1.1 Background..... | 1 |
| 1.2 Colloidal systems and nanofluid..... | 2 |
| 1.2.1 Colloid | 2 |
| 1.2.1.1 Particle structure (size and shape)..... | 4 |
| 1.2.1.2 Particle aggregate | 4 |
| 1.2.1.3 Polydispersity..... | 5 |
| 1.2.1.4 Zeta potential..... | 6 |
| 1.2.2 Nanofluid | 7 |
| 1.3 Ultrasonication and nanofluid preparation..... | 9 |
| 1.4 Thermophysical properties | 12 |
| 1.4.1 Thermal conductivity | 13 |
| 1.4.2 Viscosity | 14 |
| 1.4.3 Density..... | 14 |
| 1.4.4 Specific heat..... | 14 |
| 1.5 Rheology | 15 |
| 1.6 Thermal performance parameters | 16 |
| 1.7 Importance and scope of the research..... | 19 |
| 1.8 Objectives of the research | 23 |

| | |
|---|-----------|
| 1.9 Outline of the thesis | 23 |
| CHAPTER 2: LITERATURE REVIEW | 25 |
| 2.1 Introduction | 25 |
| 2.2 An overview on nanofluid preparation and ultrasonication process..... | 25 |
| 2.3 Studies conducted on effect of ultrasonication on colloid | 28 |
| 2.4 An overview on influence of ultrasonication on thermophysical properties..... | 34 |
| 2.4.1 Thermal conductivity | 34 |
| 2.4.2 Viscosity | 37 |
| 2.4.3 Density..... | 38 |
| 2.5 An overview on influence of ultrasonication on rheology | 39 |
| 2.6 Studies conducted on effect of ultrasonication on thermal performance..... | 40 |
| 2.7 Summary of the available studies | 41 |
| 2.8 Research gap and action..... | 43 |
| CHAPTER 3: METHODOLOGY | 45 |
| 3.1 Introduction | 45 |
| 3.1.1 Materials | 45 |
| 3.1.2 Equipment..... | 47 |
| 3.2 Ultrasonication..... | 49 |
| 3.2.1 Bulk heat measurement | 49 |
| 3.2.2 Nanofluid preparation..... | 49 |
| 3.3 Colloidal dispersion inspection | 53 |
| 3.4 Thermophysical properties measurement..... | 54 |
| 3.4.1 Thermal conductivity measurement | 55 |
| 3.4.2 Viscosity measurement..... | 57 |
| 3.4.3 Density measurement | 59 |
| 3.5 Rheology analysis | 61 |
| 3.6 Thermal performance analysis..... | 62 |

| | |
|--|------------|
| 3.6.1 Heat sink data validation | 67 |
| CHAPTER 4: RESULTS AND DISCUSSIONS | 70 |
| 4.1 Introduction | 70 |
| 4.2 Effect of ultrasonication in bulk heating | 70 |
| 4.3 Colloidal dispersion characteristics | 71 |
| 4.3.1 Microstructures | 71 |
| 4.3.2 Aggregate size..... | 90 |
| 4.3.3 Polydispersity index | 97 |
| 4.3.4 Zeta potential | 99 |
| 4.4 Thermophysical properties | 104 |
| 4.4.1 Thermal conductivity | 104 |
| 4.4.2 Viscosity | 114 |
| 4.4.3 Density..... | 120 |
| 4.5 Rheology | 124 |
| 4.6 Thermal performance characteristics | 138 |
| CHAPTER 5: CONCLUSIONS AND RECOMMENDATIONS..... | 150 |
| 5.1 Introduction | 150 |
| 5.2 Conclusions | 150 |
| 5.3 Limitations of the study | 154 |
| 5.4 Recommendations..... | 154 |
| REFERENCES | 156 |
| LIST OF PUBLICATIONS AND PAPERS PRESENTED..... | 167 |
| APPENDIX A: ELEMENTAL COMPOSITION OF NANOPARTICLES BY FESEM-EDAX ANALYSIS | 169 |
| APPENDIX B: PARTICLES SIZE MEASUREMENT AFTER ULTRASONICATION | 171 |
| APPENDIX C: MEASURED VALUES OF EFFECTIVE THERMOPHYSICAL PROPERTIES | 177 |
| APPENDIX D: FITTING PARAMETERS FOR RHEOLOGICAL MODELS..... | 180 |
| APPENDIX E: UNCERTAINTIES IN MEASUREMENTS | 182 |

LIST OF FIGURES

| | |
|---|----|
| Figure 1.1: Some real life examples of nanometer to micrometer scale substances (Özering et al., 2010)..... | 3 |
| Figure 1.2: An example of cluster or aggregate size of particles. | 5 |
| Figure 1.3: Pictorial description of polydispersity index. | 6 |
| Figure 1.4: Relationship between absolute zeta potential values with stability of suspension. | 7 |
| Figure 1.5: Thermal conductivities of heat transfer fluids (at 300 K) and solid materials (metals and metal oxides)..... | 9 |
| Figure 1.6: Schematic example of (a) direct sonication and (b) indirect sonication. | 11 |
| Figure 1.7: Example of stable and unstable colloidal suspension (a) well dispersed and stable nanofluid, and (b) aggregation, sedimentation, and unstable nanofluid..... | 12 |
| Figure 1.8: Types of flow behaviors of fluids or suspensions..... | 16 |
| Figure 1.9: Schematic illustration of a rectangular mini channel heat sink. | 19 |
| Figure 3.1: TEM images showing the microstructure of 1h ultrasonicated Al ₂ O ₃ –water nanofluids of (a) 0.01, (b) 0.1, (c) 0.5, and (d) 1 vol.% concentrations. | 47 |
| Figure 3.2: Representation of nanofluid preparation process..... | 52 |
| Figure 3.3: Accuracy of the KD2 Pro thermal properties analyzer (Decagon, USA) compared by the sample (glycerine) supplied by the manufacturer. | 55 |
| Figure 3.4: Schematic illustration of thermal conductivity measurement. | 56 |
| Figure 3.5 Accuracy of the rheometer after calibration with standard viscosity fluid..... | 58 |
| Figure 3.6 Schematic illustration of viscosity measurement..... | 59 |
| Figure 3.7: Accuracy of the DA 130N portable density meter (KYOTO, Japan) compared by water at 25 °C. | 60 |
| Figure 3.8: Schematic illustration of density measurement. | 61 |
| Figure 3.9: Schematic illustration of the mini channel thermal performance measurement setup. | 63 |
| Figure 3.10: Cross section of the copper mini channel heat sink. | 64 |

| | |
|---|----|
| Figure 3.11: Comparison of heat sink inlet temperature by water. | 68 |
| Figure 3.12: Comparison of heat sink base temperature by water. | 69 |
| Figure 3.13: Comparison of heat sink outlet temperature by water. | 69 |
| Figure 4.1: Effect of ultrasonication in bulk heating of liquid. | 71 |
| Figure 4.2: FESEM images of Al ₂ O ₃ nanoparticles at (a) in 10- and (b) 1- μm scales. | 72 |
| Figure 4.3: Microstructure of Al ₂ O ₃ –water nanofluid prepared by without ultrasonication (0 h). Figure 4.3 (a), (b), (c), and (d) stand for 6300×, 12500×, 20000×, and 31500× magnifications. | 74 |
| Figure 4.4: Microstructure of Al ₂ O ₃ –water nanofluid at 1 h ultrasonication duration. | 75 |
| Figure 4.5: Microstructure of Al ₂ O ₃ –water nanofluid at 2 h ultrasonication duration. | 77 |
| Figure 4.6: Microstructure of Al ₂ O ₃ –water nanofluid at 3 h ultrasonication duration. | 79 |
| Figure 4.7: Microstructure of Al ₂ O ₃ –water nanofluid at 4 h ultrasonication duration. | 81 |
| Figure 4.8: Microstructure of Al ₂ O ₃ –water nanofluid at 5 h ultrasonication duration. | 82 |
| Figure 4.9: Histogram of individual particle diameter after 0 h (without ultrasonication). | 84 |
| Figure 4.10: Histogram of individual particle diameter after 1 h of ultrasonication duration. | 85 |
| Figure 4.11: Histogram of individual particle diameter after 2 h of ultrasonication duration. | 86 |
| Figure 4.12: Histogram of individual particle diameter after 3 h of ultrasonication duration. | 87 |
| Figure 4.13: Histogram of individual particle diameter after 4 h of ultrasonication duration. | 88 |
| Figure 4.14: Histogram of individual particle diameter after 5 h of ultrasonication duration. | 89 |
| Figure 4.15: Average final particle sizes of Al ₂ O ₃ nanoparticles after different durations of ultrasonication. | 90 |
| Figure 4.16: Particle size distribution (based on intensity) of Al ₂ O ₃ nanoparticles at different durations of ultrasonication with different power amplitudes. | 92 |

| | |
|---|-----|
| Figure 4.17: Average cluster sizes of Al ₂ O ₃ nanoparticles after varying ultrasonication durations, at 25% and 50% amplitudes..... | 94 |
| Figure 4.18: Distribution of cluster sizes of Al ₂ O ₃ nanoparticles after different ultrasonication durations with 50% amplitudes..... | 95 |
| Figure 4.19: Average cluster sizes of Al ₂ O ₃ nanoparticles after different durations of ultrasonication. | 97 |
| Figure 4.20: Polydispersity index after varying ultrasonication durations. | 99 |
| Figure 4.21: Absolute zeta potential of Al ₂ O ₃ –water nanofluid after different durations of ultrasonication at 25% and 50% amplitude..... | 100 |
| Figure 4.22: Absolute zeta potential of Al ₂ O ₃ –water nanofluid after different durations of ultrasonication. | 102 |
| Figure 4.23: pH value of Al ₂ O ₃ –water nanofluid after different durations of ultrasonication at 50% amplitude..... | 104 |
| Figure 4.24: Enhancement percentage of thermal conductivity of 0.5 vol.% of Al ₂ O ₃ –water nanofluids after different durations of ultrasonication. | 106 |
| Figure 4.25: Mechanism of influence of ultrasonication duration on thermal conductivity..... | 108 |
| Figure 4.26: Different colloidal states during thermal conductivity measurement for the nanofluid prepared by lower ultrasonication duration. | 109 |
| Figure 4.27: Precision of thermal conductivity measurements. | 110 |
| Figure 4.28: Variations of thermal conductivity enhancement with temperatures for 0.5 vol.% of particles concentration..... | 112 |
| Figure 4.29: Enhancement percentage of thermal conductivity at 25 °C temperature after different durations of sample preparation. | 113 |
| Figure 4.30: Enhancement percentage of viscosity of 0.5 vol.% of Al ₂ O ₃ –water nanofluids after different durations of ultrasonication..... | 116 |
| Figure 4.31: Mechanism of influence of ultrasonication duration on viscosity. | 117 |
| Figure 4.32: Variations of viscosity enhancement with temperatures. | 119 |
| Figure 4.33: Enhancement percentage of viscosity at 25 °C temperature after different durations of sample preparation..... | 120 |
| Figure 4.34: Enhancement percentage of density of 0.5 vol.% of Al ₂ O ₃ –water nanofluids after different duration of ultrasonication. | 121 |
| Figure 4.35: Mechanism of influence of ultrasonication duration on density. | 122 |

| | |
|--|-----|
| Figure 4.36: Variations of density enhancement with temperatures. | 123 |
| Figure 4.37: Enhancement percentage of density at 25 °C temperature after different durations of sample preparation. | 124 |
| Figure 4.38: Relation of shear stress of Al ₂ O ₃ –water nanofluid with shear rates. | 125 |
| Figure 4.39: Shear stresses at different shear rates for the Al ₂ O ₃ –water nanofluid prepared by (a) 0, (b) 1, (c) 2, (d) 3, (e) 4, and (f) 5 h of ultrasonication. | 127 |
| Figure 4.40: Viscosity of Al ₂ O ₃ –water nanofluid at different shear rates. | 129 |
| Figure 4.41: Viscosity at different shear rates for the Al ₂ O ₃ –water nanofluid prepared by (a) 0, (b) 1, (c) 2, (d) 3, (e) 4, and (f) 5 h of ultrasonication. | 132 |
| Figure 4.42: Relations of microstructure of colloids with rheology. | 134 |
| Figure 4.43: Effect of ultrasonication duration on yield stress point of Al ₂ O ₃ –water nanofluid. | 135 |
| Figure 4.44: Effect of ultrasonication duration on flow behavior index for the Al ₂ O ₃ –water nanofluid. | 137 |
| Figure 4.45: Effect of ultrasonication duration on flow consistency index for the Al ₂ O ₃ –water nanofluid. | 138 |
| Figure 4.46: Effect of ultrasonication duration on thermal resistance of the mini channel heat sink. | 140 |
| Figure 4.47: Effect of ultrasonication duration on log mean temperature difference of the mini channel heat sink. | 142 |
| Figure 4.48: Effect of ultrasonication duration on the heat transfer coefficient of the mini channel heat sink. | 145 |
| Figure 4.49: Effect of ultrasonication duration of Al ₂ O ₃ –water nanofluids on pumping power of the mini channel heat sink. | 147 |
| Figure 4.50: Figures of merit of the mini channel heat sink after different durations of ultrasonication. | 149 |
| Figure 5.1: Example of ultrasound tip erosion. | 155 |
| Figure A1: EDAX analysis of Al ₂ O ₃ nanoparticles at point 1. | 169 |
| Figure A2: FESEM image of Al ₂ O ₃ nanoparticles during EDAX analysis with the marking of point 1. | 169 |
| Figure A3: EDAX analysis of Al ₂ O ₃ nanoparticles at point 2. | 170 |
| Figure A4: FESEM image of Al ₂ O ₃ nanoparticles during EDAX analysis with the marking of point 2. | 170 |

| | |
|---|-----|
| Figure B1: TEM microstructure of Al ₂ O ₃ –water nanofluid prepared by without ultrasonication (0 h) on a 50 nm scale (31500× magnifications) with particle size measurements. | 171 |
| Figure B2: TEM microstructure of Al ₂ O ₃ –water nanofluid prepared by 1 h of ultrasonication on a 50 nm scale (31500× magnifications) with particle size measurements. | 172 |
| Figure B3: TEM microstructure of Al ₂ O ₃ –water nanofluid prepared by 2 h of ultrasonication on a 50 nm scale (31500× magnifications) with particle size measurements. | 173 |
| Figure B4: TEM microstructure of Al ₂ O ₃ –water nanofluid prepared by 3 h of ultrasonication on a 50 nm scale (31500× magnifications) with particle size measurements. | 174 |
| Figure B5: TEM microstructure of Al ₂ O ₃ –water nanofluid prepared by 4 h of ultrasonication on a 50 nm scale (31500× magnifications) with particle size measurements. | 175 |
| Figure B6: TEM microstructure of Al ₂ O ₃ –water nanofluid prepared by 5 h of ultrasonication on a 50 nm scale (31500× magnifications) with particle size measurements. | 176 |
| Figure C1: Thermal conductivity of 0.5 vol.% of Al ₂ O ₃ –water nanofluids after different duration of ultrasonication. | 177 |
| Figure C2: Effective thermal conductivity of 0.5 vol.% of Al ₂ O ₃ –water nanofluids at 25 °C after different periods from sample preparation. | 177 |
| Figure C3: Effective viscosity of 0.5 vol.% of Al ₂ O ₃ –water nanofluids after different duration of ultrasonication. | 178 |
| Figure C4: Effective viscosity of 0.5 vol.% of Al ₂ O ₃ –water nanofluids at 25 °C after different periods from sample preparation. | 178 |
| Figure C5: Effective density of 0.5 vol.% of Al ₂ O ₃ –water nanofluids after different duration of ultrasonication. | 179 |
| Figure C6: Effective density of 0.5 vol.% of Al ₂ O ₃ –water nanofluids at 25 °C after different periods from sample preparation. | 179 |

LIST OF TABLES

| | |
|--|-----|
| Table 1.1: Some typical colloidal systems (Everett, 1988)..... | 3 |
| Table 1.2: Effect of different variables on thermophysical properties of nanofluids. | 13 |
| Table 2.1: Summary of different types of the synthesis process that have been using by the researchers during nanofluid preparation. | 27 |
| Table 2.2: Summary of the available literatures on effect of ultrasonication. | 42 |
| Table 3.1: Properties of Al ₂ O ₃ nanoparticles used in the study. | 46 |
| Table 3.2: List of equipment used in the research. | 48 |
| Table 3.3: Sonication energy for different durations. | 51 |
| Table 3.4: Details specification of the copper mini channel heat sink. | 64 |
| Table A1: Elemental composition of Al ₂ O ₃ nanoparticles by EDAX analysis at point 1. | 169 |
| Table A2: Elemental composition of Al ₂ O ₃ nanoparticles by EDAX analysis at point 2. | 170 |
| Table D1: Fitting parameters for rheological models. | 180 |
| Table E1: Uncertainties in aggregate size measurement for 50% power amplitude. | 182 |
| Table E2: Uncertainties in polydispersity index measurement for 50% power amplitude..... | 182 |
| Table E3: Uncertainties in zeta potential measurement for 50% power amplitude. | 183 |
| Table E4: Uncertainties in thermal conductivity measurement. | 183 |
| Table E5: Uncertainties in thermal conductivity measurement after certain periods | 183 |
| Table E6: Uncertainties in viscosity measurement..... | 184 |
| Table E7: Uncertainties in viscosity measurement after certain periods at 25 °C..... | 184 |
| Table E8: Uncertainties in density measurement. | 184 |
| Table E9: Uncertainties in density measurement after certain periods at 25 °C..... | 184 |
| Table E10: Uncertainties in rheology measurement at 10 °C..... | 185 |

| | |
|--|-----|
| Table E11: Uncertainties in rheology measurement at 20 °C..... | 186 |
| Table E12: Uncertainties in rheology measurement at 30 °C..... | 187 |
| Table E13: Uncertainties in rheology measurement at 40 °C..... | 188 |
| Table E14: Uncertainties in rheology measurement at 50 °C..... | 189 |
| Table E15: Uncertainties in the measured parameters of the heat sink. | 190 |

LIST OF SYMBOLS AND ABBREVIATIONS

Abbreviations

| | |
|-----------|--|
| A | Area (m^2) |
| AFM | Atomic force microscopy |
| ANOVA | Analysis of variance |
| cm | Centimeter |
| CNT | Carbon nanotube |
| C_p | Specific heat ($\text{J/kg}\cdot\text{K}$) |
| CPU | Central Processing Unit |
| d | Diameter of nanoparticles (nm) |
| \bar{d} | Average diameter of nanoparticles (nm) |
| D_h | Hydraulic diameter of the fluid flow (m) |
| DIW | Deionized water |
| DLS | Dynamic light scattering |
| d_p | Nanoparticle diameter (nm) |
| DW | Distilled water |
| EDAX | Energy dispersive X-ray analysis |
| EG | Ethylene glycol |
| EO | Engine oil |
| FESEM | Field emission scanning electron microscope |
| FOM | Figure of merit |
| g | Grams |
| GA | Gum Arabic |
| h | Hour (s) |
| h | Heat transfer coefficient ($\text{W}/\text{m}^2\cdot\text{K}$) |

| | |
|------------|--|
| H | Height (mm) |
| HRTEM | High resolution transmission electron microscope |
| HTC | Heat transfer coefficient ($\text{W}/\text{m}^2 \cdot \text{K}$) |
| k | Thermal conductivity ($\text{W}/\text{m} \cdot \text{K}$) |
| K | Consistency index/coefficient (Pa.s) |
| L | Length (mm) |
| m | Mass (kg) |
| \dot{m} | Mass flow rate (kg/s) |
| min | Minute (s) |
| ml | Milliliter |
| MWCNT's | Multi-walled carbon nanotubes |
| n | Flow behavior index (dimensionless) |
| N | Number of channel |
| P | Power (W) |
| ΔP | Pressure drop (Pa) |
| PCS | Photon correlation spectroscopy |
| PG | Propylene glycol |
| P_p | Pumping power (W) |
| PU | Polyurethane |
| PVD | Physical Vapor Deposition |
| Q | Heat flow (W) |
| Q | Total heat dissipation from heater (W) |
| r | Particle radius (nm) |
| SDS | Sodium dodecyl sulfate |
| sec | Second (s) |
| SEM | Scanning electron microscope |

| | |
|-----------|--|
| t | Interfacial layer thickness (m) |
| T | Temperature (K) |
| TEM | Transmission electron microscope |
| THW | Transient hot wire |
| TNT | Titanate nanotube |
| ULA | Ultra low adapter |
| UV | Ultraviolet |
| UV-Vis | Ultraviolet visible spectrophotometer |
| \dot{V} | Volumetric flow rate (m ³ /s) |
| vol.% | Volume concentration of particles |
| W | Water |
| W | Watt |
| W | Width (mm) |
| wt.% | Weight concentration of particles |

Greek letters

| | |
|----------|----------------------------------|
| Δ | Change rate with the system |
| ϕ | Particle volume fraction |
| γ | Shear rate (s ⁻¹) |
| η | Efficiency |
| μ | Dynamic viscosity (mPa.s) |
| ρ | Density (kg/m ³) |
| τ | Shear stress (N/m ²) |
| τ_o | Yield stress (N/m ²) |
| ζ | Zeta |

Dimensionless number

Re Reynolds number

Subscripts

av Average

b Base

bf Base fluid

ch Channel

eff Effective

LMTD Log mean temperature difference

f Fluid

hs Heat sink

l Liquid

n Nanoparticle

nf Nanofluid

p Particle

tc Thermocouple

th Thermal

Superscript

n Flow behavior index (dimensionless)

CHAPTER 1: INTRODUCTION

1.1 Background

In this modern era, customers are looking for high-performance equipment but in compact size with less weight. The performance of heat transfer equipment depends on the following equation:

$$Q = hA\Delta T \quad (1.1)$$

Where, Q is the heat flow, h is the heat transfer coefficient (HTC), A is heat transfer area, and ΔT is the temperature gradient.

Therefore, heat transfer improvement can be made by increasing (i) heat transfer area, (ii) temperature, and (iii) HTC (Saidur et al., 2011). The case (i) is usually tried to be avoided because increasing the heat transfer area will increase the bulkiness (size and weight) of the equipment. Case (ii) needs more input power to increase the temperature as a result operating cost will be increased. Therefore, technologies have already reached to their limit for the cases (i) and (ii). Tremendous researches are going on for the case (iii) by changing different parameters. Now researchers are trying to increase the HTC of liquids by mixing solid particles into these liquids. These types of heterogeneous mixtures are called colloidal systems, which are made up of dispersed phase and dispersion medium. As the addition of solid particles in liquid, increase the viscosity of the suspension as a result pumping power and pressure drop increase, also clogging and blockage of the flow passage could be happened. Therefore, nano-sized (10^{-9} m) solid particles (called nanoparticles and mostly in powder form) are proposed to mix with heat transfer fluids to increase their HTC.

1.2 Colloidal systems and nanofluid

1.2.1 Colloid

The study of physics and chemistry introduces three states of matter: solid, liquid, and gas as well as the transformations (melting, sublimation, and evaporation) among them (Everett, 1988). Besides the pure substances, there are solutions, which are homogenous/heterogeneous dispersion of two or more similar or different species mixed together in a molecular scale. System of this kind is called “colloids”, where one component is finely dispersed in another (Everett, 1988). Table 1.1 shows example of some typical colloidal systems. Previously, Thomas Graham distinguished substances into two types as crystalloids and colloids based on diffusion characteristics. If a substance can directly diffuse a parchment membrane is termed as crystalloids, e.g. acids, bases, sugars, and salts. On the other hand, if a substance very slowly diffuses through parchment paper is termed as colloids, e.g., glue. However, later these distinguished was proved as inappropriate, as with the change of environmental conditions these states could be changed. Hiemenz and Rajagopalan (1997) define colloid as “any particle, which has some linear dimension between 10^{-9} m (1 nm) and 10^{-6} m (1 μ m) is considered a colloid.” Nevertheless, these limits are not rigid, for some special cases (emulsion and some typical slurry) particles of larger size are present. Figure 1.1 shows some real-life examples of nanometer to micrometer scale substances.

Table 1.1: Some typical colloidal systems (Everett, 1988).

| Example | Class | Disperse phase | Dispersion medium |
|--|--------------------------------|-----------------|-------------------|
| Fog, mist, tobacco smoke, aerosol sprays | Liquid aerosol | Liquid | Gas |
| Industrial smokes | Solid aerosol | Solid | Gas |
| Milk, butter, mayonnaise | Emulsions | Liquid | Liquid |
| Inorganic colloids | Sols or colloidal suspensions | Solid | Liquid |
| Clay slurries, toothpaste, muds | Paste | Solid | Liquid |
| Opal, pearl, stained glass, pigmented plastics | Solid suspension or dispersion | Solid | Solid |
| Froths, foams | Foam | Gas | Liquid |
| Meerschaum | Solid foam | Gas | Solid |
| Jellies, glue | Gels | Macro-molecules | Solvent |

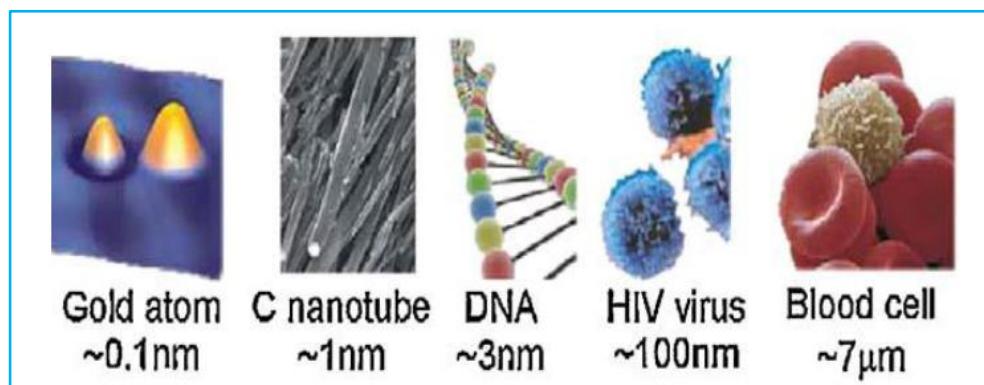


Figure 1.1: Some real life examples of nanometer to micrometer scale substances

(Özering et al., 2010).

Colloid science is an interdisciplinary subject; its field of interest overlaps chemistry, physics, biology, material science, and several other disciplines (Hiemenz & Rajagopalan, 1997). It is the particle dimension - not the chemical composition (organic or inorganic) or physical state (e.g., one or two phases) that are the attention. The last century has been seen as renaissance for colloid (Everett, 1988). Therefore, the

important properties of colloids have been identified. Some common physical properties of colloids that are studied to evaluate the dispersion characteristics are:

1.2.1.1 Particle structure (size and shape)

One of the most important features of colloidal particle is their physical dimension, the defining characteristic of colloids. Particle movement depends on its' size and shape. Many other properties (e.g., specific surface area, aggregation behavior, and microstructure) are strongly influenced by dimension. Thermophysical properties, e.g., thermal conductivity, viscosity, and specific heat capacity also depend on particle size and shapes (Baheta & Woldeyohannes, 2013; Timofeeva et al., 2009; Timofeeva et al., 2010). The easiest particle structure is considered as uniform-size particles with spherical geometry. However, colloidal particles come in all sizes and shapes.

1.2.1.2 Particle aggregate

The primary particles of a dispersed system tend to associate into larger structures known as aggregates. The inter-particle forces are responsible for this aggregation. In most cases, the dispersed phase is present as aggregates, not as primary particles. In such cases, it is the size, shape, and concentration of the aggregates that determine the properties of the dispersion itself. Particle size distribution (PSD) is analyzed to check the aggregate size. Figure 1.2 shows the effective particle diameter also called cluster or aggregate size of particles, which could be several times (\times) larger than a single-particle diameter.

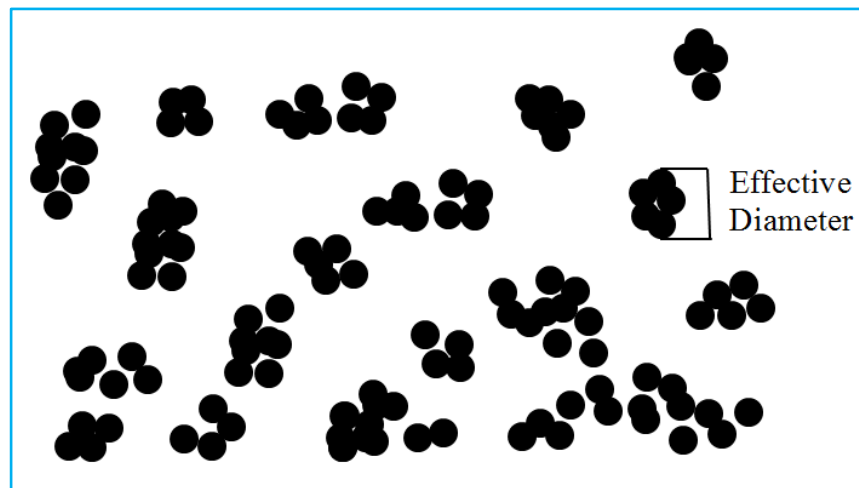


Figure 1.2: An example of cluster or aggregate size of particles.

It is noteworthy that two types of aggregates are possible in nanofluids. One type of aggregate occurs when nanoparticles are agglomerated in dry powder form. These aggregates are unlikely to be broken apart when nanoparticles are suspended into fluid with high shear or ultrasound. Another type of aggregate happens when loose single crystalline nanoparticles are suspended, each particle acquires a diffuse layer of fluid intermediating particle-particle interactions in nanofluid. Due to weak repulsion, those nanoparticles can form aggregate-like ensembles moving together (Timofeeva et al., 2009). Furthermore, few aggregated nanoparticles (small cluster) could form a further large cluster.

1.2.1.3 Polydispersity

When there are different ranges of particle sizes present in any disperse systems are called polydispersity. The term “polydisperse” could easily be understood from its converse term “monodisperse”. If all the particles of any disperse systems are of (approximately) the same size are called monodisperse (Everett, 1988). Polydispersity indexes are in the range from 0 to 1; where very close or equal to 1, indicating to extremely broad size distribution means a polydisperse system, but if it is closer to zero

means only one size of particle is present, which denotes a monodisperse system. Figure 1.3 shows a schematic illustration of polydispersity index.

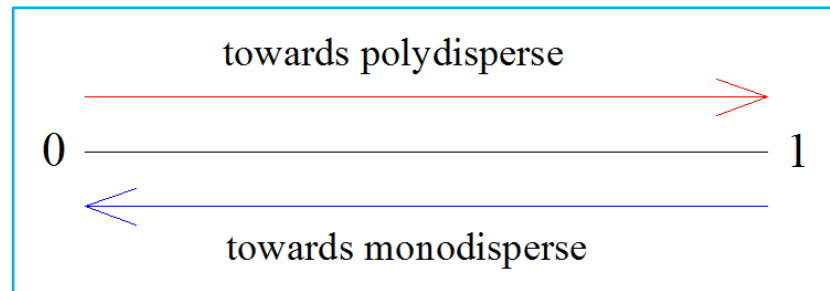


Figure 1.3: Pictorial description of polydispersity index.

1.2.1.4 Zeta potential

This is an electrokinetic phenomenon of colloidal systems. Some other colloidal dispersion characteristics are related to the zeta potential (or electrical charge) of the particles. The inter particle energy can be obtained from zeta potential distribution. This inter particle force is related to the stability of a suspension, which are linked with coagulation and flow behavior. It is pronounced that the absolute zeta potential value over 60 mV show excellent stability, above 30 mV are physically stable, below 20 mV has limited stability and lower than 5 mV are evident to agglomeration (Müller, 1996). Figure 1.4 shows the relationship between absolute zeta potential values with stability of suspension. The sedimentation behaviors of colloidal suspensions and flotation behaviors of mineral ores are also related to the zeta potential (Hunter, 1981).

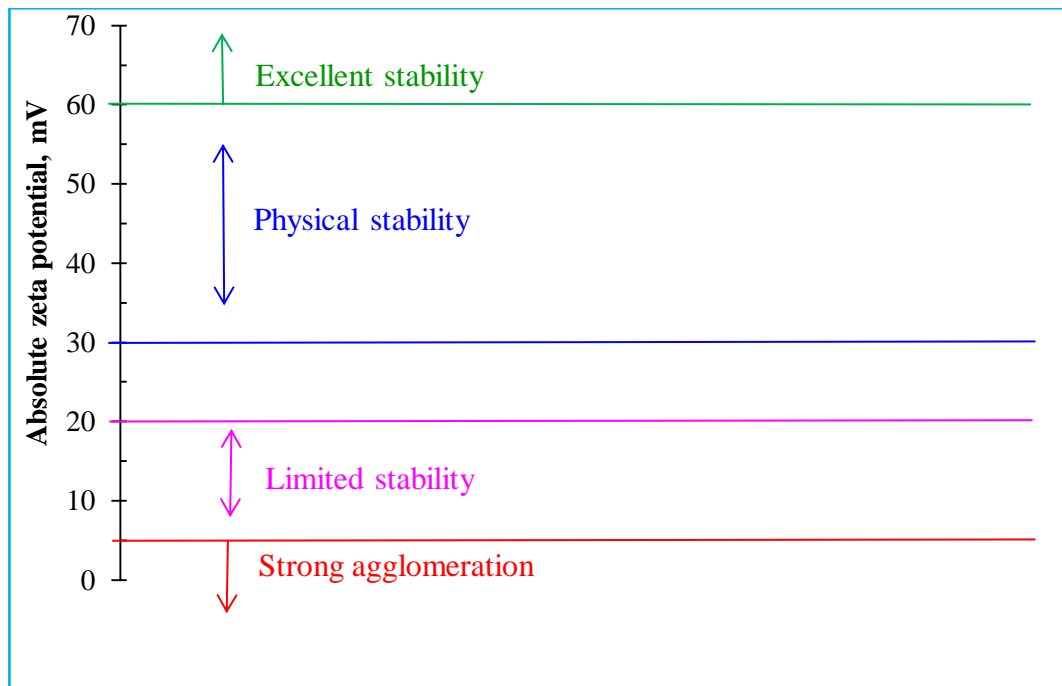


Figure 1.4: Relationship between absolute zeta potential values with stability of suspension.

1.2.2 Nanofluid

Nanofluids are the colloidal suspensions of nanoparticles (with average particle size within 1–100 nm at least in one dimension) dispersed in base fluids to enhance their thermal performance. This is a special kind of heat transfer fluid, which has higher thermal conductivity than that of the traditional host fluids (e.g. ethylene glycol (EG), water, engine oil, and so on). Nanoparticles that used to prepare nanofluids can be metals (e.g. Cu, Ni, Al, etc.), oxides (e.g. Al_2O_3 , TiO_2 , CuO , SiO_2 , Fe_2O_3 , Fe_3O_4 , BaTiO_3 , etc.) and other compounds (e.g. CNT, Graphene, SiC, CaCO_3 , TNT, etc.) (Mahbubul et al., 2013). For very small size and large specific surface areas of the nanoparticles, nanofluid possess better heat transfer properties like: high thermal conductivity, less clogging in flow passages, long-term stability, and homogeneity (Chandrasekar et al., 2010).

Stephen Choi from National Argonne Laboratory (USA) is the pioneer who for the first time demonstrated that the use of nanoparticles enhances the heat transfer performances of liquids in 1995 (Choi & Eastman, 1995). Since then a lot of research has been going on tremendously about thermal conductivity, viscosity, density, specific heat, different modes of heat transfer, pressure drop, pumping power, different properties of nanofluids (e.g. fundamental, thermal, physical, optical, magnetic, etc.), etc. Most widely used heat transfer fluids such as water, oil, EG, and refrigerants have poor heat transfer properties; however, their huge applications in the field of power generation, chemical processes, heating and cooling processes, transportation, electronics, automotive, and other micro-sized applications make the re-processing of these heat transfer fluids to have better heat transfer properties reasonably necessary (Mahbubul et al., 2012). Figure 1.5 shows that, at the ambient temperatures, thermal conductivity of metallic solids is an order-of-magnitude greater than that of fluids (e.g. thermal conductivity of copper is about 700 and 3000 times greater than the thermal conductivity of water and engine oil, respectively) (Islam, 2012). Therefore, thermal conductivity of the solid metallic or non-metallic particles suspended fluids are significantly higher than the thermal conductivity of the traditional heat transfer fluids (Murshed et al., 2008a). Recently, many researchers found that dispersing nano-sized particles into the liquids result in higher HTC of this newly developed fluid called nanofluids compared to the traditional liquids.

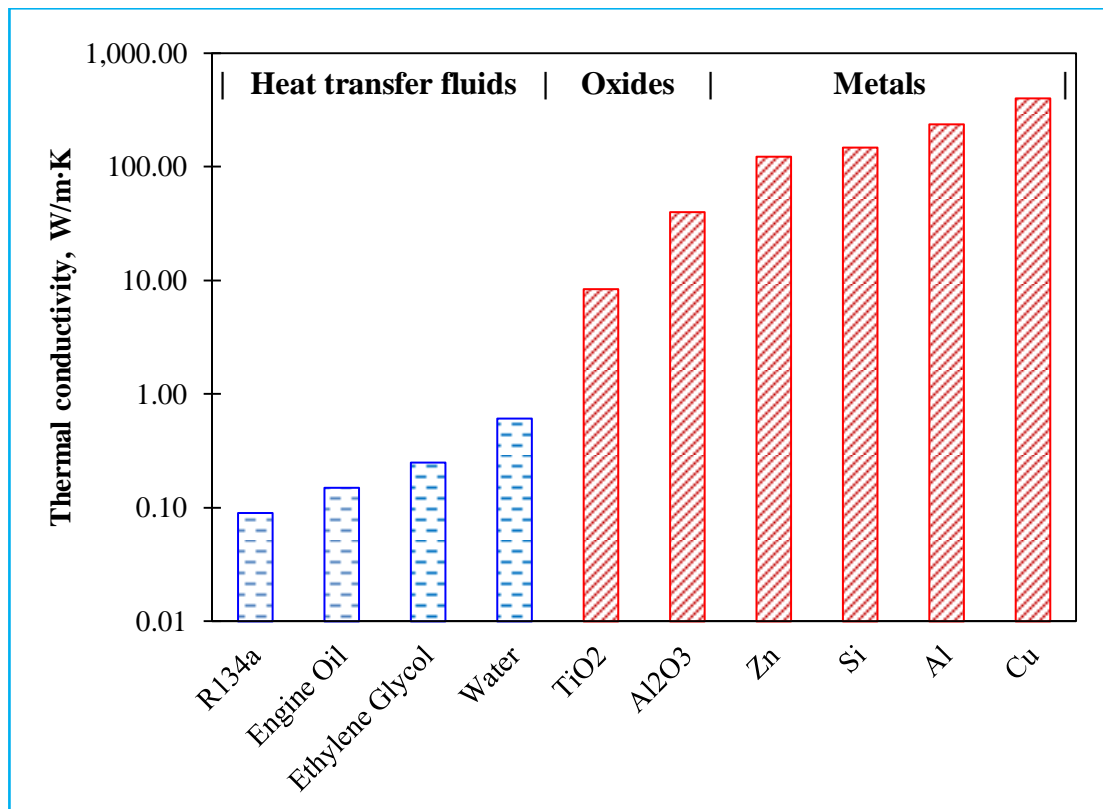


Figure 1.5: Thermal conductivities of heat transfer fluids (at 300 K) and solid materials (metals and metal oxides).

1.3 Ultrasonication and nanofluid preparation

The stability of nanofluids is a critical factor that must be taken into account because it affects the performance of any system. In this regard, nanofluids are desired to have thermodynamic, kinetic, chemical, and dispersion stabilities (Zhu et al., 2007). For practical application of nanofluid, it is necessary that the nanoparticles will be uniformly dispersed in fluids to make a stable suspension (Lee et al., 2008). Nanoparticles tend to agglomerate easily over time because of their high surface energies. The aggregation of nanoparticles is a reason for sedimentation meaning that nanoparticles are at the bottom, which are not taking part in the performance and decreases the thermal conductivity of nanofluids (Li et al., 2009). In addition, the sizes of nanoparticle agglomerates also affect the viscosity of nanofluids that will increase pressure drop and pumping power; blocking the flow passages; and, consequently, lead

to lower heat transfer performance (Ruan & Jacobi, 2012). According to Everett (1988), “It is a fundamental principle of thermodynamics that, if a system is kept at a constant temperature, it will tend to change spontaneously in a direction which will lower its free energy. This is exemplified by the simple mechanical case of a weight that falls under the influence of gravity” (Everett, 1988).

Ruan and Jacobi (2012) report that ultrasonication is a common way to break up agglomeration and promote dispersion of nanoparticles into base fluids to obtain more stable nanofluid. The ultrasonication techniques affect the surface and structure of nanoparticles and prevent the agglomeration of particles to achieve stable nanofluids (Ghadimi et al., 2011). Addition of surfactant is another method that is used to increase the stability of nanofluids. Surfactants, also known as surface-active agents, are chemical compounds that reduce the surface tension of a liquid and increase the immersion of particles. Use of a surfactant is necessary for insoluble particles such as carbon nanotubes (CNTs) that do not disperse in most solvents (Rashmi et al., 2011). However, some surfactants, such as gum arabic (GA), increase the viscosity of nanofluids, causing an increase in pressure drop and pumping power, especially in industrial applications (Garg et al., 2009). Thus, ultrasonication methods are popular among researchers.

The ultrasonication process could be direct sonication as the immersion of ultrasonic probe or horn into the mixture, or indirect sonication where the sample inside a container that submerged into a bath having liquid (mostly water) over which ultrasonic waves are transmitted (Taurozzi et al., 2012). Figure 1.6 shows the illustrated examples of direct and indirect sonication. Indirect sonication is not suitable for the dispersion of dry powders, even not effective for high viscous fluid based nanofluid. Therefore,

ultrasonic probe or “horn” is more effective for nanofluid preparation (Chung et al., 2009; Taurozzi et al., 2012). Nevertheless, there is no standard procedure for the ultrasonication process to prepare nanofluid. Therefore, researchers are struggling to prepare stable and well-dispersed nanofluids. Figure 1.7 shows the example of stable and unstable nanofluids. Moreover, inconsistent outcomes have been reported in the literature even for the same type of nanofluid because of the lack of the standard preparation process. Therefore, to get the maximum benefit from nanofluid, it is necessary to study the optimum sonication time required to prepare stable nanofluids.

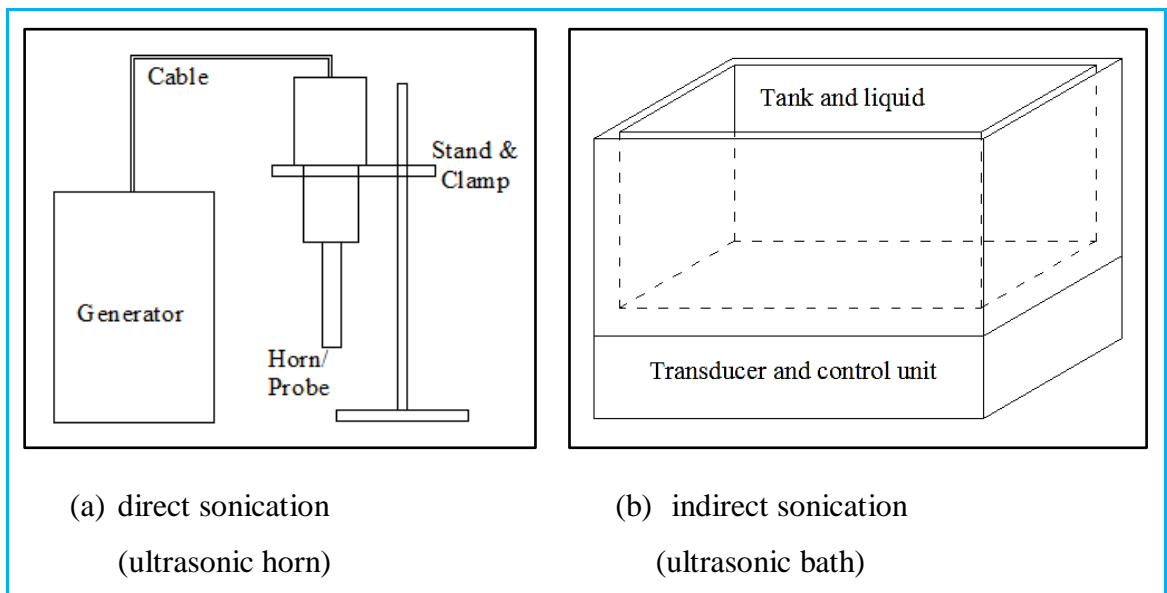


Figure 1.6: Schematic example of (a) direct sonication and (b) indirect sonication.

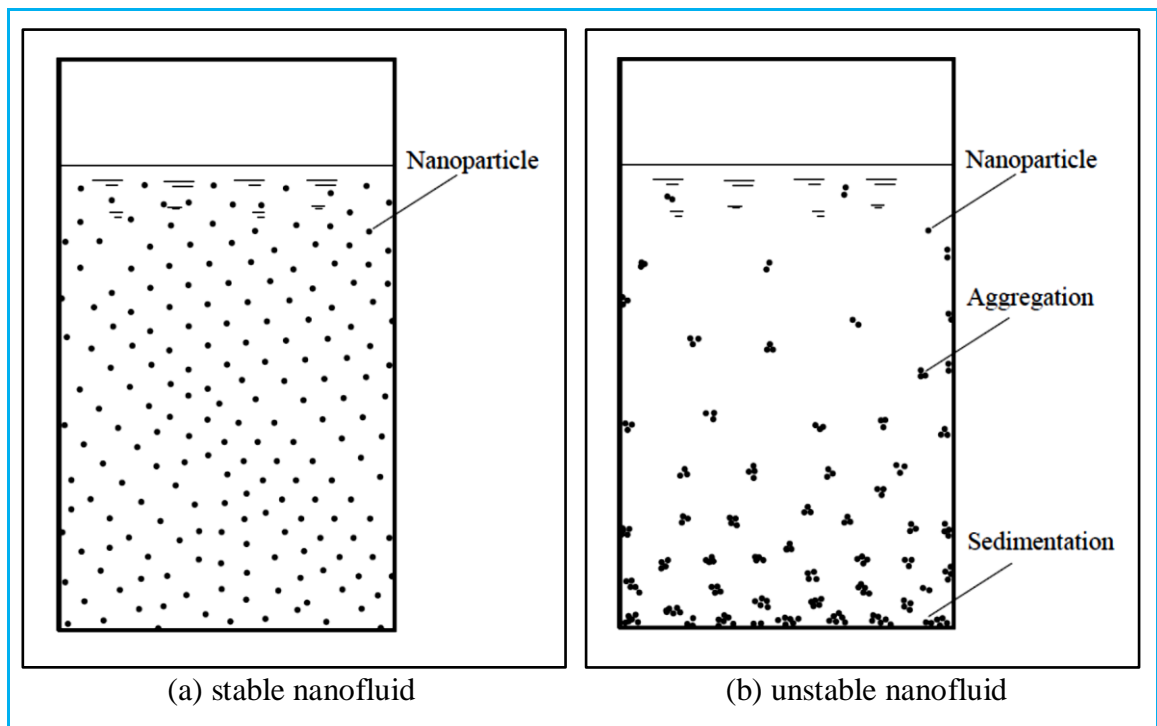


Figure 1.7: Example of stable and unstable colloidal suspension (a) well dispersed and stable nanofluid, and (b) aggregation, sedimentation, and unstable nanofluid.

1.4 Thermophysical properties

Thermophysical properties are the physical properties of a substance, which are variable with temperature. Thermal conductivity and diffusivity, viscosity, density, and specific heat capacity are some common thermophysical properties. These properties depend not only temperature but also affected by the type and amount of solid concentration, particle size and shape, base fluid type, surfactant, and many other parameters. The effects of nanoparticle concentration, temperature, and particle size on thermophysical properties of nanofluids are shown in Table 1.2.

Table 1.2: Effect of different variables on thermophysical properties of nanofluids.

| Properties | Solid concentration | Temperature | Particle size | Effect | Reference |
|----------------------|---|---|--|---|------------------------|
| Thermal conductivity |  |  |  |  | Murshed et al. (2008b) |
| Viscosity |  |  |  |  | Mahbubul et al. (2012) |
| Density |  |  |  |  | Elias et al. (2014) |
| Specific heat |  |  |  |  | Shahrul et al. (2014) |

[Note:  denotes increasing trend;  denotes decreasing trend;  denotes contradictory results;  denotes not available]

1.4.1 Thermal conductivity

Thermal conductivity is an inherent property of a substance, and it is related to heat conduction. The amount of heat conducted/transferred within in a unit temperature gradient through a unit thickness perpendicular to a unit surface area is called thermal conductivity. It is denoted by the symbol k or λ and the unit is W/m·K. Thermal conductivity of suspensions mainly depends on the particle volume concentrations, particle size and shape, thermal conductivity of particles and fluids, and fluid temperature (Chandrasekar et al., 2012; Ghadimi et al., 2011). It increases accordingly with the augmentation of nanoparticle concentration and temperature. Still, there are contradictions about the effect of particle size, shape and cluster size on thermal conductivity of nanofluids (Murshed et al., 2008b).

1.4.2 Viscosity

Viscosity defines the internal resistance of a fluid to flow. It is related to the motion of the neighboring molecules of a fluid. If the internal collision of particles is higher meaning higher friction and higher viscosity; on the other hand, lower viscosity is the result of little internal collision. Viscosity is denoted by μ or η and unit is $\text{kgm}^{-1}\text{s}^{-1}$ which is equal to Pascal-second (Pa·s) and it is mostly used. It increases with the intensification of nanoparticle concentrations, but it falls with the rise of fluid temperature (Mahbubul et al., 2012). As like thermal conductivity, the effects of particle size and shape on viscosity of nanofluids are still inconsistent (Mahbubul et al., 2012).

1.4.3 Density

Density is the mass per unit volume and qualitatively it means “heaviness”. It is denoted by ρ and unit is kg/m^3 . Density is strongly dependent on the nanoparticle material used, whereas the other parameters such as nanoparticles size, shape, zeta potential and additives do not affect the density of nanofluids significantly (Timofeeva et al., 2011). Solids have a greater density compared to liquids; therefore, the density of nanofluids is increased with the enhancement of nanoparticle concentration. Same as viscosity, density also decreases as the rise of liquid temperatures (Elias et al., 2014).

1.4.4 Specific heat

Specific heat is the amount of heat needed to increase a unit temperature of a body. It is denoted by C_p and the unit is $\text{J/kg}\cdot\text{K}$. Generally specific heat capacity of nanofluids decreases with the addition of nanoparticles. However, there are also some negative results, which indicate that specific heat of nanofluids increases after adding nanoparticles (Shahrul et al., 2014). It depends on nanoparticle size, shape, material, and temperature. There are contradictory results available about the effect of particle size and temperature on specific heat of nanofluids. Nevertheless, some researchers agreed

upon the fact that specific heat increases by the increase of particle diameter. Mostly, specific heat capacities of fluids are measured by using different types of differential scanning calorimeter (DSC). Based on the measurement principle of DSC, it analyzes a very little amount of liquid, which can be as much as in milligram (mg) scale. It is very difficult to differentiate the effect of an ultrasonication period during nanofluid preparation by considering only a fraction of mg of fluid. Therefore, in this study the effect of ultrasonication on specific heat capacity of nanofluid was not considered for analysis.

1.5 Rheology

Rheology is one of the important properties that describe the flow and/or deformation of matter under the influence of extremely imposed mechanical forces. It could be defined as properties of matter determining its behavior, i.e., its reaction to deformation and flow. Different types of flow behaviors are demonstrated in Figure 1.8. In general, if the viscosity of a fluid or suspension remains constant with different applied shear rates, then the fluid is considered as Newtonian. However, if viscosity changed with the applied shear rates, then the fluid is non-Newtonian. Moreover, if viscosity increased with shear rates, then it is called dilatant or shear thickening; conversely, if viscosity decreased with shear rates, then it is called pseudo plastic or shear thinning behavior.

Various parameters like material type, base fluid type, percentage of concentration, size and shape of particles, surfactants, temperature, shear stress, shear rate (applied force), and time effect on rheology. Specifically, in the case of nanofluid researchers are studied the rheological properties of nanofluid as viscosity as a function of volume concentration, temperature and shear rate (to check the flow characteristics, whether Newtonian or non-Newtonian). Leong et al. (1993) reported that aggregate size of particle proportionally effect on shear stress and viscosity of a sample. Therefore, the

effects of cluster size on rheological properties are needed to be studied and the cluster size relates to the preparation process. The knowledge of rheology is necessary in fluid mechanics, polymer science, mining, food and chocolate processing and many other applications. Although, it is a colloidal property, however, due to the importance of this property (in fluid mechanics and mechanical engineering), rheology deserves extra attention. That is why in this study it will be discussed as a separate sub-section from colloidal properties.

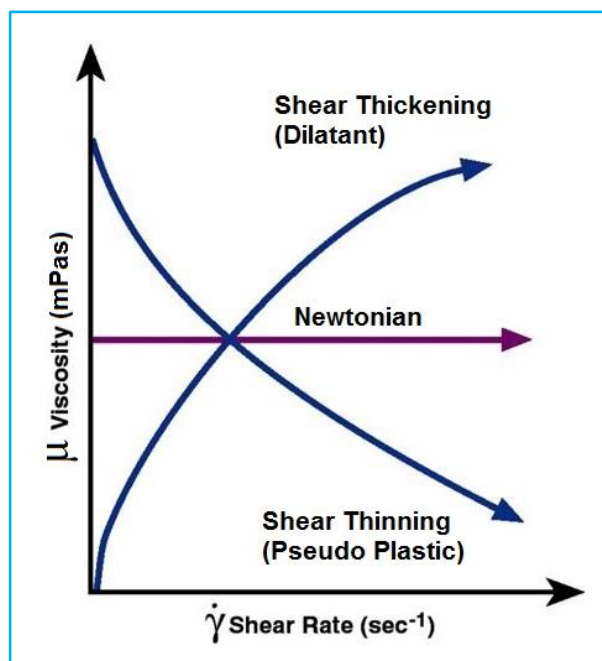


Figure 1.8: Types of flow behaviors of fluids or suspensions.

1.6 Thermal performance parameters

The colloidal characteristics are the internal states of a fluid, which will indicate the consistency of other parameters or performance of a system. Thermophysical and rheological properties are used to estimate the performance of a thermal system; however, these properties are not the performance characteristics of a system. The performance parameters of thermal systems are temperature and HTC (Zhang et al., 2010). Mostly log mean temperature difference (LMTD) is considered as a performance

parameter. Thermal resistance is another important parameter of thermal performance (Hirschi, 2008). If a thermal system is related to fluid flow, then pressure drop and pumping power also considered as performance parameters. Figure of merit (FOM) analysis is considered an important criterion where the increase of HTC compared to base fluid is divided by the ratio of pumping power of nanofluid by that of base fluid (Yu et al., 2012b).

Thermal performance can be calculated from thermophysical properties. However, during calculation, it considers only the value, which is determined by standard machines. Nevertheless, the effect of colloid and microstructure in some cases ignored during thermophysical properties measurement. For example, mostly viscometers are: cone and plate/parallel disks/coaxial cylinders (Couette) type (Mewis & Wagner, 2012). Likewise, thermal conductivity is measured by a needle or plate like sensor. However, a real thermal system may be in different shapes like: rectangular heat sink, plate heat exchanger; where the physical effect of nanofluid will be different. Therefore, this study wants to check the real effect of nanofluid in a system. Specifically, nanofluid is promising for thermal applications based on literature. However, yet, no practical/industrial application started. Dispersion of nanoparticle in refrigerant is promising for energy saving (Bi et al., 2011; Bi et al., 2008). Nevertheless, due to the small tube of refrigeration system, nanoparticle may block the passage due to this reason no commercial application is observed.

To verify the influence of ultrasonication durations of nanofluids on the performance of a thermal system, very small channel system is necessary. Simply considering a straight tube or shell and tube or helical tube heat exchangers (where the lowest diameter considered about 8 mm) could not be able to differentiate the significance of sonication

periods of nanofluids as the tube diameter is large enough to agglomeration size of particles. Because, most cluster sizes of nanofluids are within micro meter ranges (Ghadimi et al., 2011).

Different types of the mini channel heat sink have been proposed for cooling of electronics devices with the aid of nanofluid as operating fluid. Copper or aluminum is used for the fabrication of mini channel because of their high thermal conductivity. Figure 1.9 shows a typical mini channel heat sink that is designed for electronics' cooling. Mostly, the channel diameters of mini channels are about millimeter range. Therefore, the effect of cluster size of nanoparticle could have significant effect on a mini channel thermal performance. In addition, mini channels heat sinks are promising in thermal management of electronic devices; specifically, to cool the processor of personal computer. Khaleduzzaman et al. (2014) analyzed the cooling effect of using nanofluid in micro channel heat sink to cool CPU. This was so attract the scientific community that American Chemical Society has produced a press release on that and different news media highlighted this research (American Chemical Society, 2014). Therefore, based on the importance of such heat sink, this study will consider such a mini channel heat sink to analyze the effect of ultrasonication on thermal performance.

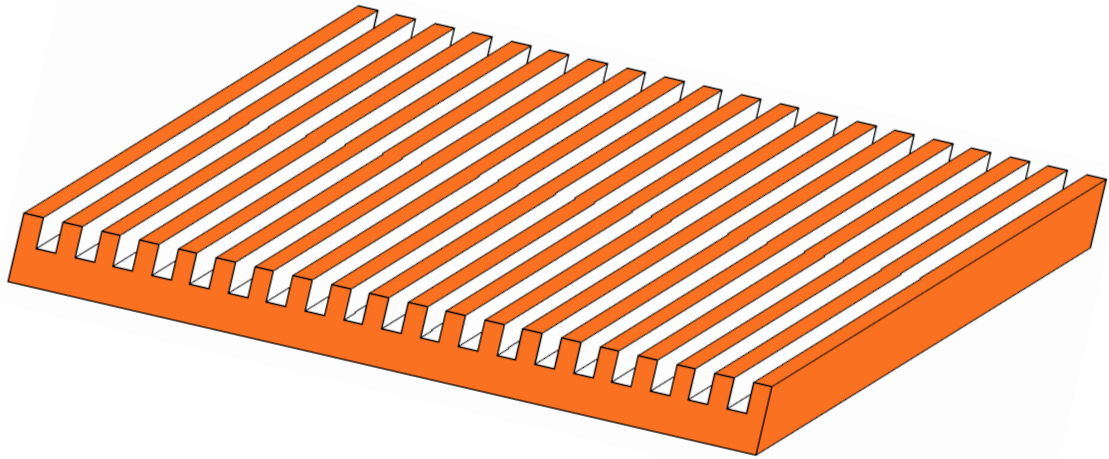


Figure 1.9: Schematic illustration of a rectangular mini channel heat sink.

1.7 Importance and scope of the research

Energy is being considered as the peak of the “Top Ten” worldwide problems of mankind for the next fifty (50) years (Smalley, 2005). Heat transfer enhancement is emphasized for energy-saving purposes that could lead to the better quality of human life and meet the aim of sustainable development. Nanotechnology plays a vital role in heat transfer enhancement. Nanofluids are promising fluids for heat transfer applications and have the potentiality to enhance heat transfer performance by decreasing the amount of energy needed to operate the thermal systems that related heat transfer fluids. Hopefully, the application of nanofluid will save energy as well as will reduce the emission, global warming potential, and greenhouse-gas effect. The performance of nanofluids depends on the stability, which is related to proper dispersion of nanoparticles. Due to the surface energy of nanoparticles, they do not want to disperse in fluids rather want to agglomerate. Ultrasonication process can break the agglomeration and disperse the nanoparticles in suspensions. However, for proper dispersion of nanoparticles it is necessary to know the required amount of sonication time that can overcome the surface energy of particles. As nanofluids are colloidal

suspensions so, the dispersion behavior of nanofluids could be analyzed from its colloidal properties. Therefore, it is necessary to study the effect of ultrasonication duration on colloidal properties of nanofluids. If nanofluids are not stable, clogging, aggregation and sedimentation would happen that decline the performance of suspensions via decreasing thermal conductivity and increasing viscosity.

Therefore, the following scientific questions need to be considered:

- i. How to form a colloidal dispersion?
- ii. What are the factors that could determine whether a colloid is stable or not?
- iii. How to control a colloid in the dispersed state, and stable?
- iv. How can unwanted colloids be destructed?
- v. What are the special properties needed to be analyzed for a colloidal system?
- vi. How to handle the colloidal systems?

The above questions are the main concerns of many industries, including chemical manufacturing, food industry, energy industries, and many others. Preparation of stable colloids is necessary in the industrial applications of paints, inks, pharmaceutical and cosmetic products, biological activities, drilling muds, agricultural chemicals, firefighting foams. Earlier of this chapter introduced the formation of colloidal dispersion. Aggregated particles are rapidly sediment due to the gravitational effect. The knowledge to destruct the unwanted colloid is required for water purification, fining of wines and beer, sewage disposal, breaking of oil emulsions and foams, dewatering of sludge, dispersal of aerosol and fog, disposal of radioactive waste (Everett, 1988). The microstructure analyses are necessary to study the colloidal dispersion characteristics as particle size, shape, aggregation, and polydispersity. Stability of nanofluids is an

important phenomenon that needs to be characterized. Zeta potential study gives the idea about stability of a suspension.

Thermophysical properties are calculated to determine the performance parameter, e.g. HTC, pressure drop, energy efficiency of a thermal system. Among the thermophysical properties, thermal conductivity is being considered as the most important property of any fluid for heat transfer application. Thermal conductivity is directly related to HTC that related to the performance of any system. Viscosity is a significant parameter for all heat transfer applications related to fluids (Nguyen et al., 2007). Viscosity becomes an important transport phenomenon for the design of the chemical process. The performances of heat exchangers are measured by HTC, which is also influenced by viscosity as well as distillation calculation and other heat transfer performances are influenced by viscosity (Smith et al., 2003). Stability of suspension is related to the density of particles. Density is needed to calculate the required weight and space (volume) required for a system to operate with nanofluids. It is also necessary for consumer products during packaging and in order to bottles. The most important influence of viscosity and density is to design piping system as pressure drop and pumping power are depended on these properties of a fluid.

In oil recovery and refinery industries, drilling muds, food and additive processing industries, their rheological properties are very important for handling. Rheological behavior will give idea about flow characteristics which, is significant to design required pumping power and pressure drop. Mostly, nanofluid will be used under flow conditions (Kwak & Kim, 2005). Different fluids have various flow characteristics and even for the same base fluid various types of results (both Newtonian and non-Newtonian) have been reported in the literature (Chen et al., 2009b). Extensive use of

numerical models (e.g. thermal conductivity, viscosity, density) related to Newtonian fluids are using for non-Newtonian nanofluids have been observing in literatures (Banerjee, 2013). For example, Einstein's equation is improper to assume the viscosity of nanofluids in most cases, as it is suitable for Newtonian fluids with spherical particles. Even this model has been using to estimate the viscosity of tubular shape particles (CNT, TNT) suspended nanofluids, which is not appropriate. It has been observed that even for a little concentration of nanoparticles, typical Newtonian fluids often become non-Newtonian (Banerjee, 2013). Even rheological knowledge is required to understand the interactions of fluid-particles and particles-particles in fluid. Furthermore, it gives the idea about the microstructure under both static and dynamic conditions (Kwak & Kim, 2005). Wang and Guo (2006) suggest to prepare colloidal suspensions in different methods as the aggregate size of particle proportionally affect the shear stress and viscosity of a sample (Leong et al., 1993). Due to the significance of rheology in fluid mechanics, extensive investigations of rheological properties of nanofluids are necessary.

Due to the tremendous advances in technology, the electronics products are designing in compact size, less weight but with a higher processing speed. Therefore, high-heat fluxes are generated, and traditional air cooling is not enough (Tullius et al., 2011). Even by changing the design of heat sink or increasing the speed of air velocity could not manage the high-heat generation. Liquid cooling of the electronics device is inevitable and nanofluid could be a promising fluid for thermal management of electronics cooling (Khaleduzzaman et al., 2014). HTC is being considered the most important performance parameter. It is normally expressed the rate of heat passing from one material/medium to another. According to Hirschi (2008), thermal resistance is an important parameter to characterize the thermal performance of an interface material

and thermal conductivity is a part to calculate the thermal resistance. Pressure drop and pumping power are considered during pump and pipe flow design. The rise of pumping power for nanofluid is considered a negative impact of nanofluid. Therefore, to get an optimum benefit from nanofluid for a specific application, FOM is analyzed (Yu et al., 2010) by considering the penalty of pumping power.

1.8 Objectives of the research

Based on the importance discussed above, the objectives of the research have been designed as follows:

- ❖ To investigate the effect of sonicator amplitude and ultrasonication duration on colloidal dispersion characteristics of 0.5 vol.% Al_2O_3 –water nanofluid;
- ❖ To investigate the effect of ultrasonication duration on thermophysical properties of the nanofluid;
- ❖ To investigate the effect of ultrasonication duration on rheological properties of the nanofluid;
- ❖ To investigate the effect of ultrasonication duration on thermal performance of the nanofluid with a copper mini channel heat sink.

1.9 Outline of the thesis

This thesis contains five (05) chapters. The contents of the chapters have been outlined as follows:

Chapter 1: This chapter is started with some background information, then introduced colloidal systems and nanofluids, ultrasonication and nanofluid preparation, thermophysical and rheological properties, and thermal performance parameters as well as described the importance and objectives of the thesis.

Chapter 2: This chapter is the summary of past literature about ultrasonication and nanofluid preparation methods, the effect of the ultrasonication process of nanofluids on

colloidal, thermophysical and rheological properties, and thermal performance parameters. This chapter is ended up with the summary of known items, research questions about unknown things, and the action needed to fulfill the research gap.

Chapter 3: It describes the experimental setup, materials, procedures and equipment that have been used during nanofluid preparation, determination of colloidal properties (e.g. microstructures, particle size, cluster size, polydispersity, and zeta potential), thermophysical (thermal conductivity, viscosity, and density), and rheological (shear rates, shear stress, viscosity, yield stress, flow index) properties of nanofluids. It also discussed about the experimental setup and procedure used to investigate the effect of ultrasonication on thermal performance in a mini channel heat sink.

Chapter 4: This chapter analyzes the outcomes of the effect of the ultrasonication process on colloidal, thermophysical, and rheological properties; and influence of ultrasonication on thermal performance of a mini channel heat sink. It also includes the discussions of “why” and “how” analyses of the outcomes.

Chapter 5: This is the last chapter and wraps up the thesis with some concluding remarks, recommendations for future work, and some precautions for ultrasonication.

CHAPTER 2: LITERATURE REVIEW

2.1 Introduction

This chapter contains extensive background information on past studies and current knowledge related to this research topic. It included the overview of other related studies, their approach development and significance in this study in order to set up the objectives of the research. Pertinent literatures in the form of journal articles, thesis, reports, conference papers, Internet sources, and books collected from different sources are used for this study. It may be mentioned that about 80–90% of the literatures were collected from most related and prestigious peer reviewed international referred journals such as: Applied Physics Letters, International Journal of Heat and Mass Transfer, International Journal of Thermal Science, Journal of Colloid and Interface Science, Materials Science and Engineering A, Powder Technology, Ultrasonics Sonochemistry. Moreover, some relevant information has been collected through personal communication with the key researchers around the world in this research area. The subsequent section started with the brief discussion about available literatures on ultrasonication and nanofluid preparation and followed by studies conducted on the effect of ultrasonication of nanofluids on colloidal, thermophysical and rheological properties, and thermal performance parameters.

2.2 An overview on nanofluid preparation and ultrasonication process

Preparation of nanofluids is not just simply the mixture of solid particles into base fluids. Generally, two techniques have been using to prepare nanofluids: a) single step method and b) two-step method. When both the preparation of nanoparticles as well as the mixture of nanofluid is done in a joint process is called a single step method. Some commonly used techniques for single step method of nanofluid preparation include: physical vapor deposition (PVD) technique (Eastman et al., 2001) or liquid chemical

method (Zhu et al., 2004). This single step method has both merits and demerits. One of the most important advantages is the enhanced stability and minimized agglomeration. Only the low-pressure fluids could be synthesized by this process, which is the vital drawback of this method. In a two-step method (Paul et al., 2011; Yu et al., 2011), first the nanoparticles are primarily arranged and then mixed with the fluid using high shear (Pak & Cho, 1998; Wen & Ding, 2005) or ultrasound (Goharshadi et al., 2009). Nowadays, nanoparticles are available from commercial sources. This method has attracted scientists and commercial users. The disadvantage of this method is that the particles quickly agglomerate prior to disperse into the medium and partial dispersion of nanoparticles has also been observed.

Table 2.1 shows typical synthesis processes of two step method used by the researchers to prepare nanofluids. The ultrasonication time used by the researchers is also mentioned in the Table 2.1. From the Table 2.1, it is clear that, different researchers used different ultrasonication duration. Even though, ultrasonication methods are popular among researchers, nevertheless, there is no standard procedure for the ultrasonication process to prepare nanofluid (specifically, types of ultrasonic processor and duration of sonication). Taurozzi et al. (2012) report that ultrasonic bath is not suitable for the dispersion of dry powders. However, it could be seen in Table 2.1 that most researchers using ultrasonic bath for nanofluid preparation. Also, there are no standard guidelines about the percentage of amplitude and pulse on-off duration. Even most researchers are ignored ultrasonication duration, sonicator types, amplitudes, and the sequence of pulses as they do not mention this information on their papers (Elias et al., 2014; Murshed et al., 2008a; Murshed et al., 2008c; Sohel et al., 2014; Turgut et al., 2009). However, some other methods, e.g., ball mill, shaker, mechanical stirring have also been used to prepare nanofluids.

Table 2.1: Summary of different types of the synthesis process that have been using by the researchers during nanofluid preparation.

| Base fluid | Nanoparticle (dia. in nm) | Volume (%) | Synthesis process | Sonication duration | Reference |
|--------------|--|---------------|-------------------|---------------------|--------------------------|
| Water | Al ₂ O ₃ (37) | 0.01–0.16 | Ball mills | 24 h | (Tseng & Wu, 2002) |
| Terpineol | Ni (300) | 3–10 | Ball mills | 24 h | (Tseng & Chen, 2003) |
| Water | TiO ₂ (7–20) | 5–12 | Ball mills | 24 h | (Tseng & Lin, 2003) |
| Ethanol | SiO ₂ (35,94 & 190) | 1.4–7 | Stirring | 2 h | (Chevalier et al., 2007) |
| R141b | Al ₂ O ₃ (13) | 1–5 | Shaker | 24 h | (Islam, 2012) |
| DW, EG, EO | Al ₂ O ₃ (28) | 1–6 | Ultrasonic bath | 30 min | (Wang et al., 1999) |
| EG–W(60:40) | CuO (29) | 0–6.12 | Ultrasonic bath | 30 min | (Namburu et al., 2007a) |
| DW | TiO ₂ (20) | 0.024–1.18 | Ultrasonic bath | 30 min | (He et al., 2007) |
| R113 | CNT's | 0.2–1.0 | Ultrasonic bath | 30 min | (Jiang et al., 2009a) |
| R113 | Cu, Ni, Al, CuO, Al ₂ O ₃ | 0.1–1.2 | Ultrasonic bath | 30 min | (Jiang et al., 2009b) |
| DW | CaCO ₃ (20–50) | 0.12–4.11 | Ultrasonic bath | 1–45 min | (Zhu et al., 2010) |
| EG–W (60:40) | CuO (30), Al ₂ O ₃ (45), SiO ₂ (50) | 0–6.12 | Ultrasonic bath | 2 h | (Kulkarni et al., 2009) |
| Water, EG | Al ₂ O ₃ (50) | 0.5–6 | Ultrasonic bath | 2 h | (Anoop et al., 2009) |
| EG | TiO ₂ (25) | 0–8 wt. % | Ultrasonic bath | 20 h | (Chen et al., 2007a) |
| EG | TiO ₂ (25) | 0.1–1.86 | Ultrasonic bath | 20 h | (Chen et al., 2007b) |
| EG | TiO ₂ (~10), L=100 nm | 0–8 wt. % | Ultrasonic bath | 20 h | (Chen et al., 2009a) |
| DW | CNT | 0.1–0.5 wt. % | Ultrasonic bath | 24 h | (Ding et al., 2006) |

Table 2.1, continued

| Base fluid | Nanoparticle (dia. in nm) | Volume fraction (%) | Synthesis process | Duration of sonication | Reference |
|--------------------|--------------------------------------|---------------------|-------------------|------------------------|-------------------------|
| EG | CuO (12) | 0.002 | Ultrasonic bath | 1– 30 h | (Kwak & Kim, 2005) |
| Water | MWCNTs (20–30), L=10–30 μ m | 0.24–1.43 | Ultrasonic probe | 10 min | (Phuoc et al., 2011) |
| Water | MWCNTs (10–20) | 1 wt. % | Ultrasonic probe | 20, 40, 60, 80 min | (Garg et al., 2009) |
| Car engine coolant | Al ₂ O ₃ (<50) | 0.1–1.5 | Ultrasonic probe | 3 h | (Kole & Dey, 2010) |
| DIW | TiO ₂ (21) | 0.2–3 | Ultrasonic probe | No information | (Turgut et al., 2009) |
| EO, EG | Al (80) | 1–3 | Ultrasonic probe | No information | (Murshed et al., 2008a) |
| EG–W (60:40) | SiO ₂ (20,50 & 100) | 0–10 | No information | No information | (Namburu et al., 2007b) |

2.3 Studies conducted on effect of ultrasonication on colloid

Few studies reported some comparative analysis about the effect of ultrasonication duration of nanofluids on colloidal characteristics. Based on the dispersion criteria (microstructures, cluster size, zeta potential, and others), some researchers point out that highest ultrasonication duration is better. Yang et al. (2006) studied the effect of ultrasonication on agglomeration size for nanotube-in-oil dispersions. They characterize by TEM and found that cluster size decreased with increasing sonication time/energy. Amrollahi et al. (2008) applied ultrasonication for 20 h to homogenize CNT in EG. They analyzed the results with TEM and as settling time by naked eye. The precipitation measured by human eye is not a precise method even though the author claimed that the precision was ± 10 min. The author reported that at lower ultrasonication, nanofluids with higher particle concentrations were rapidly sediment because of strong closed packed clusters existed on the suspension, which were not

broken by limited sonication period. However, with the increase of ultrasonication duration, these clusters became loose and further prolonged ultrasonication; they become very small cluster and then become individual particles, therefore, sedimentation rate decrease. The authors also observed the above stated phenomena with TEM microstructure even though they analyze TEM only after three durations as 15 min, 5 h, and 20 h of ultrasonication and for only 2.5 vol.% concentration of particles. Ruan and Jacobi (2012) applied 5, 40, 140, 520, and 1355 min of ultrasonication duration to homogenize multi-walled carbon nanotube (MWCNT) in EG. The nanofluids were prepared by using both continuous and pulses mode of ultrasonication. Microstructure, agglomerate size, and nanotube length and aspect ratio were determined by TEM to study the effect of ultrasonication. They observed that average cluster size, nanotube length, and aspect ratio of nanotube decreased with increasing sonication time or energy.

Also, Yu et al. (2012a) conducted a set of experiments to find out the effect of the ultrasonication parameters with the sonicator maximum power of 120 W and frequency of 20 kHz. They conducted the research for single-walled carbon nanotubes (SWCNT) with de-ionized water (DIW) and ultrasonicated for 10 to 120 min with 10 min interval. They also set five different power (20, 40, 60, 80, 100 and 120 W) of the homogenizer and characterize with UV-visible spectrophotometer and atomic force microscopy (AFM). They found that, nanotube length was decreased with the increase of sonication durations. They recommend that, sonication power is more influential parameter compared to sonication time and larger sonicator tip diameter performed better. However, they collect 1.5 ml (3 vol.% of initial solution) of sample every after 10 min of ultrasonication that has two types of effect. One is the sonication process is interrupted and the other which is more important is that the specific power per

volume/gram is geometrically increased as volume decreasing and power increasing. However, during the calculation and comparison only linear relation considered as time and power increasing, the volume decreasing could not consider. Again, after collecting the sample the solutions were centrifuged for 2 h and finally, the supernatant (upper 60% of the volume) was used for analysis. Therefore, the actual effect of colloid could not be achieved after centrifuge as most particle precipitate by this method, which were not considered for analysis.

Another study concerned with the dispersion stability of alumina–water nanofluids, which were one-year-old, was performed by Elcioglu and Okutucu-Ozyurt (2014). PSD of the nanofluids was analyzed in a weekly manner to monitor any changes. On the other hand, the nanoparticles formed aggregates over 1 year. The authors ultrasonicated the nanofluids via an ultrasonic bath, up to 5 h. A reduction in the aggregate size was observed, to some extent, in almost every week compared to before ultrasonication values; but the after-ultrasonication particle size approached to the one-week before value within a short period of time. The study was indicative of the requirement of performing such measurements in a frequent and periodic manner. Sadeghi et al. (2014) studied the effect of ultrasonication duration up to 180 min for alumina–water nanofluid with an ultrasonic vibrator (200 W and 24 kHz). They analyzed zeta potential, cluster size and polydispersity index (PDI). They observed that zeta potential was increased with the increase of ultrasonication. They also found that PDI and cluster size decreased with increasing ultrasonication duration and reported that during the first 30 min PDI and cluster size rapidly decreased and after that slowly decreased.

However, some other researchers report that there are specific ideal ultrasonication durations existed based on different conditions of nanofluids e.g., particle concentration

and type, and amount of base fluid (Kabir et al., 2007). Kwak and Kim (2005) studied the optimum ultrasonication duration for CuO–EG nanofluid. They ultrasonicated the mixture for between 1 and 30 h and characterized the nanofluid by dynamic light scattering (DLS) and zeta potential measurements. They found that 9 h of sonication was optimum and that, after longer sonication, the particles coalesced again. Furthermore, they found the highest zeta potential value for 9 h of ultrasonication. Nevertheless, they could not describe any specific reason behind this phenomenon. Lam et al. (2005) studied the effect of ultrasonication durations in nanoclay/epoxy composites. The samples were first mixed by hand stirring and then ultrasonicated for 5, 10, 15, 30, and 60 min of durations and characterized with scanning electron microscopy (SEM). They report that cluster sizes were decreased with the increase of ultrasonication durations. The authors report that due to the lack of enough energy, the nanoclay platelets will not be able to escape from the clusters. Again, they urged that, the effect of too much energy will create larger cluster as the collision of each single platelet will increase and they will tangle up and react. Chen et al. (2007b) ultrasonicated TiO₂–EG suspension up to 40 h for the same objective as to find out the optimum sonication duration. Their characterization with light scattering for agglomeration size shows that, 20 h of homogenization is best that was 140 nm size. After which further size reduction was could not be achieved. However, the authors claimed that, based on the principle of that Zetasizer, the given result was quite larger than the actual.

Also, Yu et al. (2007) studied the dispersion behavior of MWCNTs under varying sonication times. They prepared nanofluid with 0.1 wt.% MWCNT in distilled water with 0.15 wt.% of sodium dodecyl sulfate (SDS) as the surfactant. A continuous power of 20 W was used for sonication with various durations of 0, 5, 15, 30, 40, 50, and 120

min. They characterized the colloid with UV-visible spectrophotometer and TEM and reported that maximum achievable dispersion of MWCNTs was reached after certain sonication energy (sonication time). Kabir et al. (2007) analyzed the influence of ultrasonication on nanofibers/polyurethane foam composite and report that there is an optimum ultrasonication duration for a specific nanoparticle concentration; lower sonication period is required for higher amplitudes and vice versa; and higher ultrasonication duration is essential for higher concentration also for a higher amount of base fluids. Lee et al. (2008) ultrasonicated Al_2O_3 nanoparticles in water for durations of 0, 5, 20, and 30 h. TEM and zeta potential measurements were used to characterize the nanofluid. It was found that a sonication duration of ~5 h gave the best results. Garg et al. (2009) investigated the effect of sonication time of nanofluid on dispersion behaviors. They prepared four samples of 1 wt.% MWCNT in DIW with GA as additives and subjected the samples to ultrasonication for 20, 40, 60, and 80 min. They analyze TEM and found that the optimum ultrasonication time for homogenization was 40 min, using a 130 W and 20 kHz ultrasonicator.

Zhu et al. (2010) determine the influence of ultrasonication time on average cluster size. They analyzed the solutions of CaCO_3 -water, which were ultrasonicated for 1–45 min and found that the cluster size rapidly decreased within 20 min of ultrasonication after that slightly increased with ultrasonication duration. As their primary substance was in paste form, therefore, most of the aggregates were soft, and broken up rapidly as within 20 min. Nguyen et al. (2011) studied the effect of ultrasonication duration, power, and pulsed mode on de-agglomeration of alumina nanoparticles in water where the maximum input power of the machine was 400 W with a frequency of 20 kHz. They used 10%, 30%, and 60% of vibration amplitude with different pulsed mode and optimal break-up of agglomeration were found for 30% amplitude. In the case of 60%

amplitude, cluster size again increased after 300 sec of ultrasonication; therefore; the author's point out that higher power of ultrasonication could re-agglomerate the particles. Nevertheless, for 10% and 30% amplitudes, the aggregate sizes were continuously decreased with the increase of sonication time. They used different modes of pulsed as continuous and pulsed with long and short durations; however, no difference and similar outcomes were observed.

Rashmi et al. (2011) analyzed the effect of ultrasonication duration on stability of 0.01 and 0.1 wt.% CNT–water–GA nanofluid with the aid of UV-visible spectrophotometer. They homogenized the mixtures for the period of 1, 4, 8, 16, and 20 h using an ultrasonic bath and reported 4 h to be the optimum duration for both concentrations. The authors focused that the structure of CNT was damaged as bending, buckling, and dislocations, which were the reasons for lower stability after prolonged ultrasonication. Chakraborty et al. (2012) analyzed the influence of ultrasonication durations on TiO₂ nanofluid. They added 0.1, 0.2, and 0.4 wt.% of silver (Ag) nanoparticles and ultrasonicated for 10, 20, and 30 min of durations. They observed the settling time and report that for lower concentration of particles; ultrasonication did not have a significant role. Kole and Dey (2012) ultrasonicated ZnO nanoparticles in EG up to 100 h and characterized the PSD and microstructure. They reported that the lowest cluster size was obtained for 60 h of sonication and after that cluster size again increased. LotfizadehDehkordi et al. (2013) studied (with an ultrasonic disruptor) the effective ultrasonication period for TiO₂–water nanofluids through the analysis with Box- Behnken design to investigate the influence of ultrasonication power (20–80%), ultrasonication time (2–20 min), the volume concentration (0.1–1.0 vol.%); and the significances of the models were tested by the analysis of variance (ANOVA). The experiments were performed using a UV-visible spectrophotometer for after-one-week

and after-one-month intervals. Their results showed that, longer duration of sonication and high power decreased the stability of nanofluid.

Furthermore, two different trends have also been observed by the same study. Chung et al. (2009) dispersed two types (A and B) of ZnO nanopowder in water and ultrasonicated the dispersions for 60 min. They characterized the effect of various sonication times using TEM and photon correlation spectroscopy (PCS). The PCS results showed that ultrasonication reduced the mean cluster size to 100 nm within 60 min for powder A and within 20 min for powder B, whereas further ultrasonication up to 60 min could not reduce the cluster size. Nevertheless, the TEM results showed that aggregates still existed in the suspension.

From the above studies, no noticeable conclusion could be drawn. Some of the researchers recommend that the higher sonication time is better. However, others found the minimum agglomeration was after certain duration of ultrasonication. Nevertheless, there is no specific or common duration of ultrasonication suggested by the researchers that could be followed for better solution. Based on the above literatures, it could be recommended that the studies about the effect of ultrasonication are still immature.

2.4 An overview on influence of ultrasonication on thermophysical properties

There are some but very few such as studies available in literature about the effect of sonication time on thermophysical properties of nanofluid.

2.4.1 Thermal conductivity

In the case of thermal conductivity, there are three types of outcomes have been reported for the effect of ultrasonication. Some researchers found that, thermal conductivity of nanofluid enhanced with increasing ultrasonication duration. Among

them, Amrollahi et al. (2008) analyzed the thermal conductivity of MWCNT–EG nanofluid for ultrasonication time up to 24 h. Their study reports that longer sonication time gives the higher thermal conductivity ratio, which is more noteworthy for higher concentrations and thermal conductivity ratio rapidly increased for the first three h of ultrasonication durations. Ruan and Jacobi (2012) investigated the effects of sonication on the thermal conductivity of MWCNT–EG–GA nanofluid. First, they measured thermal conductivity for different sonication modes (continuous and pulse mode) and found no significant impact on results. They again studied the effect of prolonged ultrasonication duration (up to 22 h) on thermal conductivity and indicated that the maximum enhancement of thermal conductivity was obtained using longer sonication times and it continuously increased with sonication time. Moreover, for the first 160 min of ultrasonication, it increased rapidly. The authors compared their results with Amrollahi et al. (2008), which was also MWCNT–EG and found 5% higher thermal conductivity ratio and they claim that this high value may be due to the use of surfactant. However, Amrollahi et al. (2008) used 0.5% volume fraction and Ruan and Jacobi (2012) considered 0.5% weight fraction. This could be a possible reason for the variation of their outcomes. Hays et al. (2006) studied the effect of sonication time on thermal conductivity of 2 vol.% Al_2O_3 –deionized water nanofluid. They found that thermal conductivity enhancement ratio was increased with the increase of sonication time until 60 min and initially, the enhancement ratio was rapidly increased with sonication time until 30 min and then slowly increased with ultrasonication durations. The author claim that as with the start of ultrasonication and continuous ultrasonication, nanoparticle size is decreased, therefore, thermal conductivity increased for smaller particle sizes.

Conversely, Yang et al. (2006) reported different trend as the thermal conductivity ratio of the CNT–oil dispersions were decreased with the rise of the sonication time or the dispersion energy. They discuss that fluids with larger agglomeration have higher thermal conductivity but by applying higher ultrasonication decreased the agglomeration size, also break the CNT so thermal conductivity decreased (Yang et al., 2006).

Furthermore, some authors report that there is specific optimum sonication time available after which thermal conductivity value decrease. Hong et al. (2005) and Hong et al. (2006) studied the effect of ultrasonication duration on thermal conductivity enhancement ratio. They disperse 0.55 vol.% of Fe nano powder in ethylene glycol and ultrasonicated for the durations of 0, 10, 30, 50, and 70 min. They observed that thermal conductivity ratio increased almost with a linearly trend for the nanofluid prepared by until 50 min of durations. However, thermal conductivity ratio found to be decreased for the sample prepared by 70 min of ultrasonication in comparison to that one of 50 min. Garg et al. (2009) investigated the effects of sonication time on the thermal conductivity of nanofluids. The authors prepared four samples of 1 wt.% MWCNTs in GA and water and subjected the samples to ultrasonication for 20–80 min. They found that the thermal conductivity increased with the ultrasonication duration, but the optimum enhancement of the thermal conductivity ratio was obtained for 40 min of sonication. The author discussed that the aspect ratio and three-dimensional networks of the samples are the reason of such outcomes. Kole and Dey (2012) also analyzed the effect of ultrasonication duration up to 100 h for thermal conductivity of ZnO–EG nanofluid. The authors found a rapid increment of thermal conductivity up to 30 h and optimum thermal conductivity found for 60 h, up to which thermal conductivity increased and

further sonication it decreased. The author reported that the decreasing trend for >60 h, is for the increase of aggregate size and their separation from the base liquid.

In contradiction to the above, a decreasing and then increasing trend has been reported. Sadeghi et al. (2014) investigated the influence of ultrasonic mixing time on thermal conductivity of 2 and 3 vol.% Al₂O₃-water nanofluids. The authors ultrasonicated the nanofluid up to 150 min and measured the thermal conductivities at different temperatures. They reported that with the start of ultrasonication thermal conductivity of nanofluid decreased up to 30 min but further ultrasonication it was slowly increased. They observed the same trend for both concentrations and at different temperatures. They discuss that the reason behind these phenomena is the Brownian motion, which enhanced for the decrease of cluster size.

It could be noted that, cluster size of nanoparticles (in nanofluid) is directly related to ultrasonication power. Zhu et al. (2006) observed that thermal conductivity is influenced by nanoparticle clustering. Murshed et al. (2008b) urged that there is are sufficient studies available about the consequence of clustering of particles on thermal conductivity of nanofluids even though it is an important factor.

2.4.2 Viscosity

There are two types of outcomes have been reported in literature for the effect of ultrasonication on viscosity of nanofluids. Some authors report that viscosity decreased with the increase of sonication time. Among them, Yang et al. (2006) found that the viscosity of nanofluids kept decreasing with increasing dispersion energy for nanotube-in-oil dispersions and that the sonication time was proportional to the dispersion energy. The authors reported that a prolonged ultrasonication time affected the size and aspect ratio of particles, reducing the viscosity of the suspension.

Contradiction to the above result has also been reported in literature. Wang and Guo (2006) studied the effect of milling time of nanofluid preparation on viscosity for $\text{Al}_2\text{O}_3/\text{ZrO}_2$ suspensions containing polyelectrolyte. They used two different compositions of binary systems and found that viscosity of both mixtures increased with increasing ultrasonication duration.

However, some researchers argued that, viscosity of nanofluids first increase with the increase of sonication duration and after reaching a highest level, it decreased towards the base fluids. Garg et al. (2009) investigated the effects of sonication time on the viscosity of nanofluids. The authors prepared four samples of 1 wt.% MWCNTs in GA and water and subjected the samples to ultrasonication for 20–80 min. They found that the viscosity initially increased until 40 min and then decreased with further increasing of sonication time. Ruan and Jacobi (2012) investigated the effects of sonication on viscosity of 0.5 wt.% CNTs in GA and EG. They homogenized the suspension up to 1355 min and measured the viscosity of the samples at different shear rates. They indicated that the minimum increase in viscosity was obtained using longer sonication times. They found that the maximum viscosity rise of the nanofluid was obtained after a sonication time of 40 min, finally decreasing to the viscosity of the pure base fluid level at a sonication time of 1355 min. The similar trends have observed at different shear rates.

2.4.3 Density

Literatures about the density of nanofluids are still scarce. Specifically, the author could not find any literature about the influence of ultrasonication on density of nanofluids. Nevertheless, there are some literatures that reported the effect of particle volume fraction, and temperature on the density of nanofluids. Pak and Cho (1998) for the first

time, measured the density of $\gamma\text{Al}_2\text{O}_3$ and TiO_2 with distilled water and found that densities of nanofluids were increased with increasing particle concentration. It is found that, mostly, density of nanofluid increases with the increment of nanoparticle volume concentration (Timofeeva et al., 2011). Moreover, Mariano et al. (2013) reported that the density of nanofluid increases with increasing applied pressures. On the other hand, the density of nanofluids decreased with increasing temperature (Mariano et al., 2013).

2.5 An overview on influence of ultrasonication on rheology

Very few comparative studies on the effect of ultrasonication duration on rheological properties of nanofluids are available in the literature. Yang et al. (2006) studied the influence of ultrasonication on rheology of the CNT–oil dispersions. They observed clear shear thinning behavior for very low and very high concentration of dispersant. However, in the case of 3 wt.% dispersant, almost Newtonian trend was observed. Again, for higher applied shear stress almost similar and Newtonian flow curve have been observed. The authors indicated that lengthy ultrasonication decreased the agglomeration size, also break the CNT and the result is the decreased of viscosity (Yang et al., 2006). Wang and Guo (2006) reported that aggregate size of particle proportionally effect on shear stress and viscosity of a sample. Therefore, the effects of cluster size on rheological properties are needed to be studied and the cluster size relates to the preparation process. Kabir et al. (2007) investigated the influence of ultrasound sonication on compressive yield strength of carbon nanofibers doped polymer. They reported that optimum sonication time depends on sonicator power, nanoparticle concentration and amount of base fluid.

Also, Garg et al. (2009) investigated the effects of sonication time on the rheological behavior of MWCNT with DIW and GA. They found a non-Newtonian trend with shear

thinning or pseudoplastic style as decrease of viscosity with increase of shear rate especially at 15 °C. Almost similar flow behavior has been observed for the nanofluid prepared by different periods of ultrasonication. The unique flow characteristics may be due to the lower applied shear rate range for the study that was up to 75 s^{-1} of shear rate. They suggest more related studies to understand these criteria. Ruan and Jacobi (2012) also studied the rheological properties of MWCNT but with EG as the base fluid and a shear thinning behavior was observed. However, they found different flow curves for the nanofluids prepared by different durations of ultrasonication. For example, viscosity of nanofluid prepared by 40, 140 and 520 min showed high viscosity and they rapidly decreased by the increase of shear rates. However, nanofluid prepared by 1355 min showed slower viscosity variation with shear rates, even at higher shear rates viscosity values were found to be near to base fluid. Conversely, nanofluid prepared without sonication (0 min) showed various flow characteristics as initially viscosity decreased with increasing shear rate and then increased, and finally unchanged with shear rates. These limited literatures are not enough to understand the flow characteristics of nanofluids with the variation of the ultrasonication period during their preparation.

2.6 Studies conducted on effect of ultrasonication on thermal performance

Literature about effect of ultrasonication on thermal performance parameters is rare. The only study was found for the effect of ultrasonication durations (20, 40, 60, and 80 min) on convective HTC by Garg et al. (2009). They used a straight copper tube having the length of 914.40 mm and 1.55 mm inner diameter. A constant heat flux 0.6 W/cm^2 and three flow rates (40, 60, and 80 mL/min) were maintained, where the flow conditions were laminar and the Reynolds number for water at these conditions were about 600, 900, and 1200, respectively. The authors found that convective HTC increases with the increase of axial distance. For all the three flow rates, they found highest convective HTC for the nanofluid prepared by 40 min of ultrasonication. They

found highest increment about 32% for the sample prepared by 40 min of ultrasonication for the Reynolds number 600 ± 100 . They indicated that the increments of convective HTC were higher compared to the increase of thermal conductivity. It is notable that, they found highest increment of thermal conductivity about 20% for the sample prepared by 40 min of ultrasonication.

2.7 Summary of the available studies

The available literatures about the effect of ultrasonication have been shortened in Table 2.2. From the Table 2.2 it is obvious that, very few studies have done about the effect of ultrasonic energy. Nevertheless, among the available studies, most are related only characterization and checked only the agglomeration size with ultrasonication duration. However, to get a good conclusion, different evaluation techniques simultaneously need to be carried out (Ghadimi et al., 2011). TEM, DLS, zeta potential all need to be carried out to verify a result. Furthermore, thermophysical properties measurements depend on the colloidal dispersion state of nanofluid. Also, rheology is an important phenomenon that also depends on a sonication period. Unlikely, no complete research has been found that conducted colloidal, thermophysical, and rheological properties of nanofluids by considering the effect of ultrasonication duration. Therefore, in this study, effect of ultrasonication on colloidal dispersion, thermophysical, and rheological properties will be determined as well as thermal performance characteristics will be analyzed.

Table 2.2: Summary of the available literatures on effect of ultrasonication.

| Investigator | Nanofluid | Sonication time | Investigation | Findings |
|-------------------------|---------------------------------------|-----------------|---|---------------------|
| Kwak and Kim (2005) | CuO-EG | 0-30 h | Cluster size, Zeta potential | 9 h is best |
| Yang et al. (2006) | CNT-oil | 5-30 min | TEM, Thermal conductivity, Viscosity | Highest is best |
| Chen et al. (2007b) | TiO ₂ -EG | 0-40 h | Cluster size | 20 h is optimum |
| Yu et al. (2007) | MWCNT-DW | 0-120 min | UV-vis, TEM | Highest is best |
| Lee et al. (2008) | Al ₂ O ₃ -water | 0-30 h | TEM, Zeta Potential | ~ 5 h is best |
| Amrollahi et al. (2008) | CNT-EG | 15-1200 min | TEM, Thermal conductivity | Highest is best |
| Chung et al. (2009) | ZnO-water | 0-60 min | Cluster size | Highest is best |
| Garg et al. (2009) | MWCNT-DIW | 20-80 min | TEM, Thermal conductivity, Viscosity, HTC | No optimum result |
| Zhu et al. (2010) | CaCO ₃ -DW | 1-45 min | Cluster size | 20-30 min is better |
| Nguyen et al. (2011) | Al ₂ O ₃ -water | 0-600 sec | Cluster size | Highest is best |
| Rashmi et al. (2011) | MWCNT-DW | 1-24 h | UV-vis | 4 h is optimum |
| Kole and Dey (2012) | ZnO-EG | 4-100 h | DLS, TEM, Thermal conductivity | 60 h is optimum |
| Yu et al. (2012a) | SWCNT-DIW | 10-120 min | UV-vis, AFM | Highest is best |
| Ruan and Jacobi (2012) | MWCNT-EG | 5-1355 min | TEM, Thermal conductivity, Viscosity | Highest is best |
| Ghadimi et al. (2013) | TiO ₂ -DW | 0-15 min | UV-vis, TEM | Highest is best |
| Sadhegi et al. (2014) | Al ₂ O ₃ -water | 0-180 min | PSD, Zeta potential, UV-vis, Thermal conductivity | Highest is best |

2.8 Research gap and action

From the above limited literature, no concrete conclusions can be drawn. Also most of the above studies did not consider as much as dispersion criteria (microstructures, cluster size, polydispersity, particle size, zeta potential, and others), to conclude their results. Even most of the outcomes concluded based on by considering only one or two of the above criteria. The following questions could not be answered from the limited available literature as how much sonication energy needs to prepare nanofluids and how long should be homogenized for better suspension of colloids. Therefore, more studies need to determine the standard ultrasonication duration to prepare stable nanofluid.

Furthermore, most studies are concerned with CNT nanofluids because of their high thermal conductivity despite some drawbacks such as being insoluble in most liquids and having high costs and a difficult manufacturing process. The effect of ultrasonication is significant in CNT nanofluids because of the high aspect ratio (length-to-diameter ratio) of CNTs. The length usually tends to break down because of the force created during the sonication period. Furthermore, CNTs are in the tubular shape that has different type of motion in the particle movement, which are directly affected on rheological properties and very difficult to link the particles' movement with flow behavior. Again, the surfactants or dispersants used to dissolve CNT has complex flow behaviors (Garg et al., 2009; Sanchez et al., 2002).

The Al_2O_3 is a potential nanoparticle as it disperses easily in most fluids. It is inexpensive, as its manufacturing is easy and it is produced on a large industrial scale. Because alumina has a spherical shape in most cases, it has a minimum aspect ratio (about 1). Therefore, the effect of the reduction of the aspect ratio could be ignored for Al_2O_3 nanofluids. Again, spherical particles have only one type of motion. Therefore,

the real effect of ultrasonication could be easily analyzed for Al_2O_3 nanofluids with numerical explanation of particle motions. Moreover, to the best of the author's knowledge, no study available on the effects of ultrasonication duration on the colloidal, thermophysical and rheological properties, and thermal performance parameters of Al_2O_3 -based nanofluids is available. Thus, in this study, the effects of ultrasonication duration on the colloidal dispersion, thermophysical, and rheological properties, and thermal performance with a mini channel heat sink for 0.5 vol.% Al_2O_3 -water nanofluid have been studied. Based on the above literature, the highest optimum ultrasonication duration was found to be 5 h for Al_2O_3 -water nanofluid by Lee et al. (2008). Nguyen et al. (2011) studied the effect of ultrasonication approximately up to 600 sec only and Sadeghi et al. (2014) analyzed up to 180 min for Al_2O_3 -water nanofluid. Therefore, based on those, this study was designed to analyze up to 5 h of ultrasonication.

CHAPTER 3: METHODOLOGY

3.1 Introduction

The aim of this chapter is to describe the materials, equipment, experimental settings and to introduce the various parameters that have been used to conduct the research. Moreover, the related equations used in this research are presented. The subsequent sections start from the description of the materials and their properties and estimation of the suitable concentration of Al_2O_3 nanoparticles for this study and brief information about the equipment that were used. The sections are followed by the experimental procedure to prepare nanofluids; the methodology to analyze the colloidal dispersion (microstructure, PSD, polydispersity, and zeta potential); the measurement procedure of thermophysical properties (thermal conductivity, viscosity, and density); experimental setup for rheology measurement and mathematical models for rheology analysis; finally, the experimental setup and methodology to analyze the influence of ultrasonication on thermal performance of a mini channel heat sink.

3.1.1 Materials

This section is started with the discussion of the nanoparticle and base fluid used to study the effect of the ultrasonication process. Al_2O_3 nanoparticles (manufactured by Sigma-Aldrich, USA, and directly purchased from Sigma-Aldrich, Malaysia) with the manufacturer defined an average particle diameter of 13 nm with spherical shape and a purity of 99.5% were used in this study. Distilled water was used as the base fluid for these experiments. Table 3.1 shows the properties of Al_2O_3 nanoparticles.

Table 3.1: Properties of Al₂O₃ nanoparticles used in the study.

| Property (unit) | Value |
|--------------------------------|--------------|
| Molecular mass (g/mol) | 101.96 |
| Average particle diameter (nm) | 13 |
| Density (kg/m ³) | 4000 |
| Thermal conductivity (W/m·K) | 40 |

First, four volume concentrations (0.01, 0.1, 0.5, and 1 vol.%) of Al₂O₃–water nanofluids have been prepared using 50% ultrasonication amplitude with 2 seconds ON and 2 seconds OFF pulses for 1 h of ultrasonication. Then the microstructures of these four samples were analyzed by a TEM (Model LIBRA 120, Zeiss, Germany). The TEM results are provided in Figure 3.1.

Based on the TEM analyses, the dispersion characteristics of the samples with varying nanoparticle concentrations can be observed in Figure 3.1. It is revealed from the TEM micrographs that, the particles were in a rather involved and overlapping condition for 1 vol.% nanofluid compared to the 0.01, 0.1 and 0.5 vol.% samples. Such an observation of the sample microstructure can give preliminary conclusions on the nanoparticle-clustering tendency, which is inevitable in the long term. In order not to render the possible improvements in thermophysical properties coming with the increased nanoparticle concentration, 0.5 vol.% nanofluid is selected for further investigation as it appeared to be the preferable one among the concentrations studied, in terms of the nanoparticle dispersion. The sample of 1 vol.% was found to be the most concentrated nanofluid. However, 0.01 vol.% was observed to have the most diluted concentration. Hence, 0.5 vol.% of Al₂O₃–H₂O nanofluids have been further investigated for the effective ultrasonication parameters.

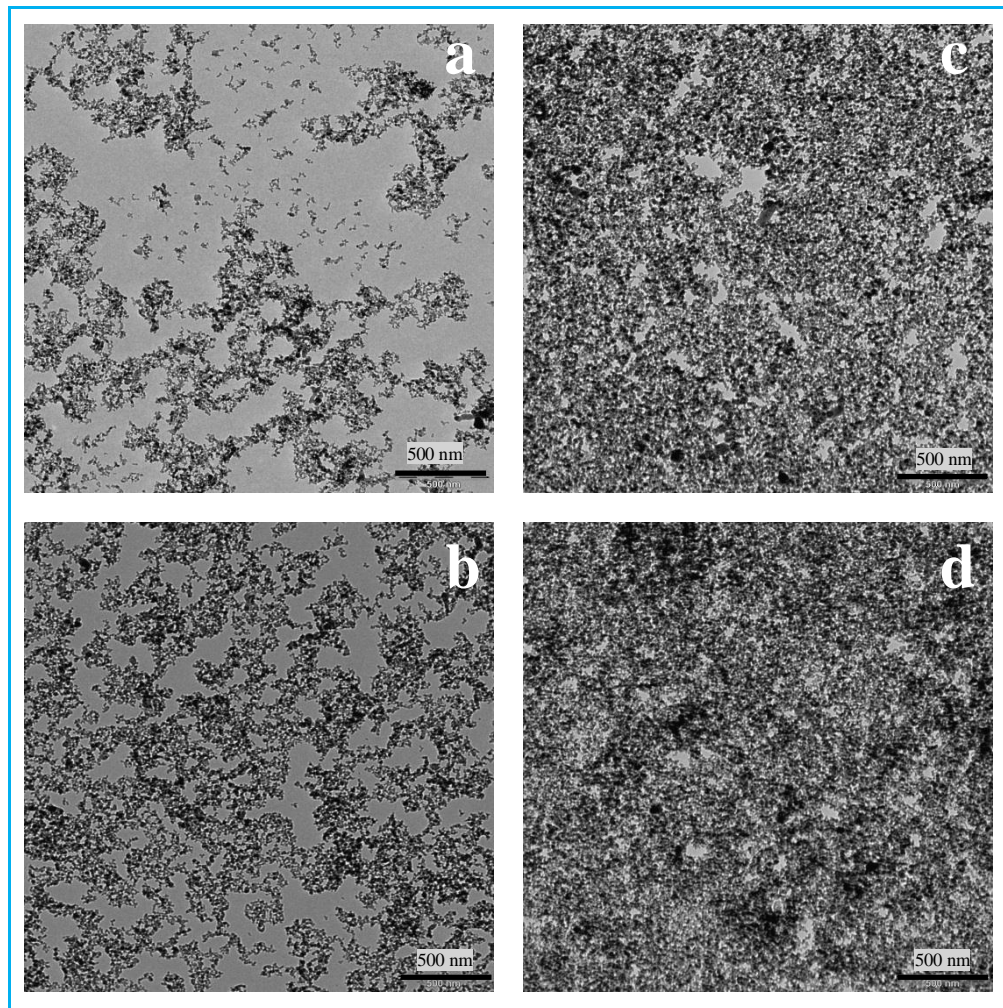


Figure 3.1: TEM images showing the microstructure of 1h ultrasonicated Al₂O₃-water nanofluids of (a) 0.01, (b) 0.1, (c) 0.5, and (d) 1 vol.% concentrations.

3.1.2 Equipment

Table 3.2 shows the summary of the equipment list used in this study with their information, purpose, and accuracy. The details of the purpose of the equipment with other controlled parameters will be discussed in the next sub-sections.

Table 3.2: List of equipment used in the research.

| Equipment | Manufacturer | Model | Purpose | Accuracy |
|--|---------------------|---------------|---|---------------------------|
| Precision analytical balance | AND | GR-200 | To weigh nanoparticles | ± 0.1 mg |
| Ultrasonic homogenizer | Fisher Scientific | 505 | To prepare nanofluids | |
| Refrigerated circulator bath | CPT Inc. | C-DRC 8 | To maintain constant temperature during nanofluid preparation | ± 0.02 °C |
| Field emission scanning electron microscope (FESEM) | Zeiss | AURIGA | To analyze the particle size, shape, and composition | |
| High resolution transmission electron microscope (HRTEM) | JEOL | JFM-2100F | To analyze the particle size, shape, and distribution | |
| Transmission electron microscope (TEM) | Zeiss | TEM LIBRA 120 | To analyze the particle size, shape, and distribution | |
| Zetasizer | Malvern | 3000HS | PSD, polydispersity, zeta potential | |
| Pen type pH meter | HXS | PH-009 (I) | pH measurement | ± 0.1 pH |
| Thermal properties analyzer | DECAGON | KD2-Pro | To measure thermal conductivity | ± 0.01 W/m·K |
| Programmable rheometer | Brookfield | LVDV-III | To measure rheology | $\pm 1\%$ |
| Portable density meter | Kyoto | DA-130 | To measure density | ± 1 kg/m ³ |
| Advanced digital refrigerated circulator bath | PolyScience | AD07R-40-12E | To maintain constant temperature during measurements | ± 0.01 °C |
| Digital photo camera | Samsung | ES65 | To capture photo | |

3.2 Ultrasonication

3.2.1 Bulk heat measurement

Before being started on the nanofluids preparation, the heat generations into the liquid have been analyzed. To study the effect of bulk heating of the liquid, the horn (tip) ultrasonic dismembrator machine (Model 505, Fisher Scientific, USA) was operated continuously 5 min in four different volume of distilled water as 25, 50, 100, and 200 ml with 50% amplitude (as for the ½-inch standard tip, this is highest recommended % of amplitude), and continuous pulse mode. The capacity of the machine is designed as 20 kHz operating frequency and 500 W maximum input power. It could be noted that, 25, 50, 100, and 200 ml water were filled in 50, 50, 100, and 250 ml standard beaker, respectively. For all the cases, a new sample was operating after the sonicator probe became at normal (room temperature). At least 2.5 cm of the sonicator tip was immersed (from the top surface of water level) into the water and at least 1 cm clearance between the beaker inner surface (bottom) and tip end surface was maintained. A temperature probe (having capacity of -100 to 300 °C with accuracy of ± 1.0 °C) was immersed into the water and data recorded in computer.

3.2.2 Nanofluid preparation

A two-step method was employed to prepare these nanofluids, where nanoparticles were primarily arranged and then mixed with the fluid using ultrasound (Goharshadi et al., 2009). The experimental procedure for the preparation of nanofluids includes the following steps: weighing the desired amount of nanoparticle, m_n and put them into a vessel; in the next step adding the required amount of fluid, m_l into that vessel. A precision analytical balance (GR-200, AND, Japan) was used to measure the weight of nanoparticles. This equipment has an accuracy of ± 0.0001 g. The precision of nanoparticle weight and water volume were maintained as ± 0.001 g and ± 0.5 ml,

respectively. First, 0.5 vol.% Al_2O_3 nanoparticles were suspended in distilled water to prepare the nanofluid. After the nanoparticles had been suspended in the base fluid, the mixtures were stirred by a very narrow (3 mm diameter) glass tube for 1 min to enable the nanoparticles to subside into the base fluid completely.

Then, the nanofluids were sonicated for the durations of 30, 60, 90, 120, and 150 min using the homogenizer separately with 25% and 50% amplitudes for 0.5 vol.% of the nanofluids. Pulses with a sequence of 2 sec ON and 2 sec OFF were used during the sonication process. Such an approach is generally recommended, since operating in pulsed mode slowed down the rate of temperature enhancement of the ultrasonicated material; hence reducing undesirable results and permitting well temperature control compared to continuous mode operation (Taurozzi et al., 2012). A refrigerated circulator bath (Model C-DRC 8, CPT Inc., South Korea) was connected to a recursion beaker, and the nanofluids were prepared inside the beaker at 15 °C temperature to avoid vaporization. The nanofluid preparation process is depicted in (a) schematic and (b) pictorial in Figure 3.2.

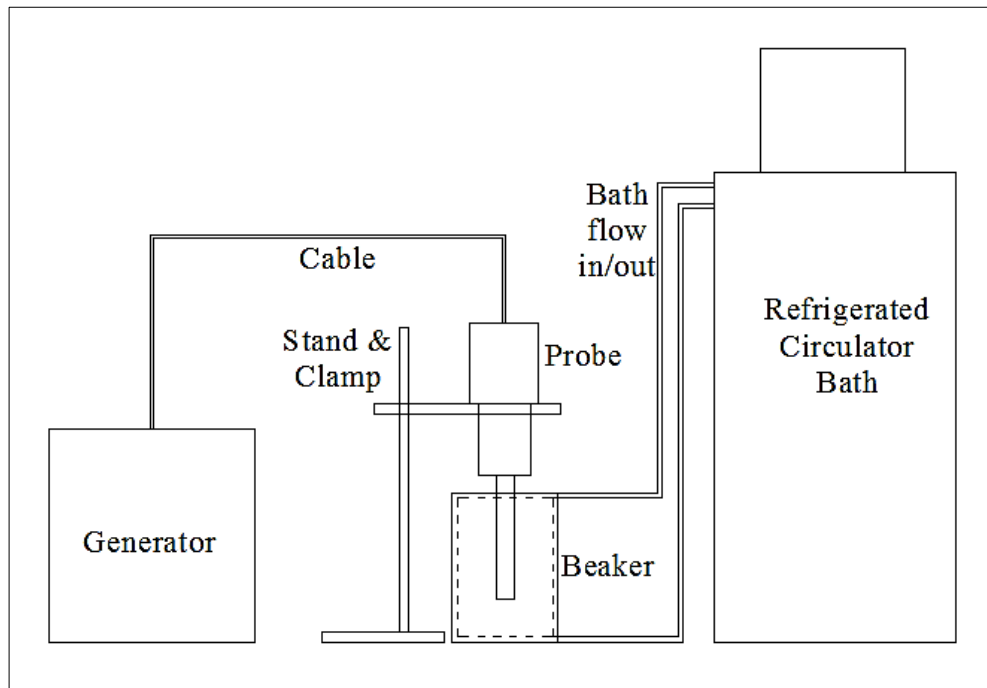
It is noteworthy that, for the setting of the above mentioned durations; the total elapsed durations of sonication were the double periods (as for the setting of 2 sec ON and 2 sec OFF pulses, homogenizer machine counted only the ON/running periods). Therefore, for the effective ultrasonication periods of 30, 60, 90, 120, and 150 min, total ultrasonication durations were taken 1, 2, 3, 4, and 5 h, respectively. As the homogenizer unit was run/operate until 1, 2, 3, 4, and 5 h of periods, therefore, the author would like to address the sonication durations as 1, 2, 3, 4, and 5 h in this and in other chapters of the thesis. Another sample was considered for analysis was termed as “0 h” (zero hour) that means without ultrasonication just mixed by stirring the narrow

glass tube. Some other desired ultrasonication durations in between 0–5 h were used with 50% sonicator amplitudes. The energy values of the machine used are tabulated in Table 3.3.

Table 3.3: Sonication energy for different durations.

| Duration, h | Sonication energy, J |
|--------------------|-----------------------------|
| 30 | 8,460 |
| 60 | 16,920 |
| 90 | 25,380 |
| 120 | 33,840 |
| 150 | 42,300 |

For colloid characterization, 50 ml nanofluids of each sample were prepared in a 50 ml standard beaker. In the case of thermophysical properties, rheological behavior, and thermal performance analysis 100, 25, and 200 ml nanofluids were prepared, respectively inside 100, 25, and 250 ml standard beaker at a time (in a single running/operation of the homogenizer). For the measurement of nanofluid properties after 10, 20, and 30 days of the preparation of the samples, nanofluids were separated on the first day of preparation and they were stored inside air conditioned room to avoid vaporization. At least 2 cm homogenizer horn was submerged in liquid and 1 cm clearance was maintained in between the tip end and the beaker inside bottom surface.



(a) Schematic



(b) Pictorial

Figure 3.2: Representation of nanofluid preparation process.

The equation was used to determine the volume concentration of nanofluids is:

$$\varphi = \frac{m_n / \rho_n}{m_n / \rho_n + m_l / \rho_l} \quad (3.1)$$

Where, φ is the particle volume fraction (vol.%); m_n and m_l are the mass of nanoparticle and base fluid, respectively; and ρ_n and ρ_l are the density of nanoparticle and base fluid, respectively.

3.3 Colloidal dispersion inspection

The microstructure and composition of the nanoparticles were characterized by FESEM (Model AURIGA, Zeiss, Germany). As-received nanoparticles were characterized by FESEM at 1 kV accelerating voltage without any treatment. Magnification scales on $1000\times$ and $10000\times$ were used to capture the image within 10- and 1- μm plots, respectively. The elemental compositions of the nanoparticles have also been checked by SEM-EDAX analysis, which confirm the composition of Al_2O_3 nanoparticles. The EDAX results have been reported in Appendix A (Table A1 and A2, Figure A1 and A3).

HRTEM with 200 kV accelerating voltage (Model JEM-2100F, JEOL, Japan) and TEM with 120 kV accelerating voltage (Model LIBRA 120, Zeiss, Germany) were used to capture the microstructures of the nanofluid for the purpose of analyzing the colloidal dispersion. Samples for TEM were prepared immediately after the preparation of the nanofluid or at least within 30 min after the nanofluid preparation. TEM samples were prepared in a transparent and thin film of “Formvar” with an evaporated layer of carbon on 300 mesh copper grid. A droplet of nanofluids was placed on the surface of the

copper grid and waited about 3 min to absorb the nanofluid. Then edge of high-quality filter paper was used to extract the remaining nanofluid from the grid. After that, nanofluid over the grid was dried by normal airflow inside an air-conditioned room for about 1 min. Finally, the TEM samples were stored inside Petri dish over filter paper and putted inside a desiccator at room temperature (about 25 °C). Magnification scales of 6300 \times , 12500 \times , 20000 \times , and 31500 \times were used to capture the image within 500-, 200-, 100-, and 50-nm plots, respectively. At least twenty images for each TEM sample (at five different locations with the above four magnification scales) were recorded for analysis. The average particle diameter for all ultrasonication durations was also measured as an arbitrary distance by TEM. At least two images on the 50-nm scale were analyzed for each sample, and 40-120 nanoparticles' diameter was measured to check the effect of ultrasonication on particle size of nanofluids after each sonication period.

A Zetasizer 3000HS instrument (Malvern Instruments, U.K.) was used to check the average aggregate size as PSD, polydispersity, and zeta potential after sonication of each sample. The Zetasizer analysis was conducted at 25 °C temperature, 24 h after nanofluid preparation and without diluting the concentration. The zeta potential was analyzed without changing the pH of the suspension. The zeta potential analysis was repeated after 30 days of nanofluid preparation to study the significance of ultrasonication duration of nanofluid after long time. A pen types pH meter (Model PH-009 (I), HXS, China) was used to measure the pH of the samples.

3.4 Thermophysical properties measurement

Thermophysical properties were measured at different temperatures for the nanofluids prepared with various ultrasonication durations. The experimental procedures are discussed here.

3.4.1 Thermal conductivity measurement

For thermal conductivity measurement, a KD2 Pro thermal properties analyzer (Decagon, USA) was used. The KS-1 sensor (length 60 mm and diameter 1.3 mm) of the device is used for the measurement of thermal conductivity of liquids within the range of 0.02 to 2.00 W/m·K. The accuracy/sensor performance of the KD2 Pro device was measured with glycerol (recommended and supplied by manufacturer) and plotted in Figure 3.3. It is found from the Figure 3.3 that the accuracy of the device was within $\pm 1.5\%$. The thermal conductivities of 0.5 vol.% $\text{Al}_2\text{O}_3/\text{H}_2\text{O}$ nanofluid were studied (on the same day of nanofluid preparation) for 10 to 50 °C temperatures with the aid of an advanced digital refrigerated water bath that has temperature stability of ± 0.01 °C (Model AD07R-40-12E, Polyscience, USA). Again, thermal conductivity values were measured after 10, 20, and 30 days after the preparation of the samples.

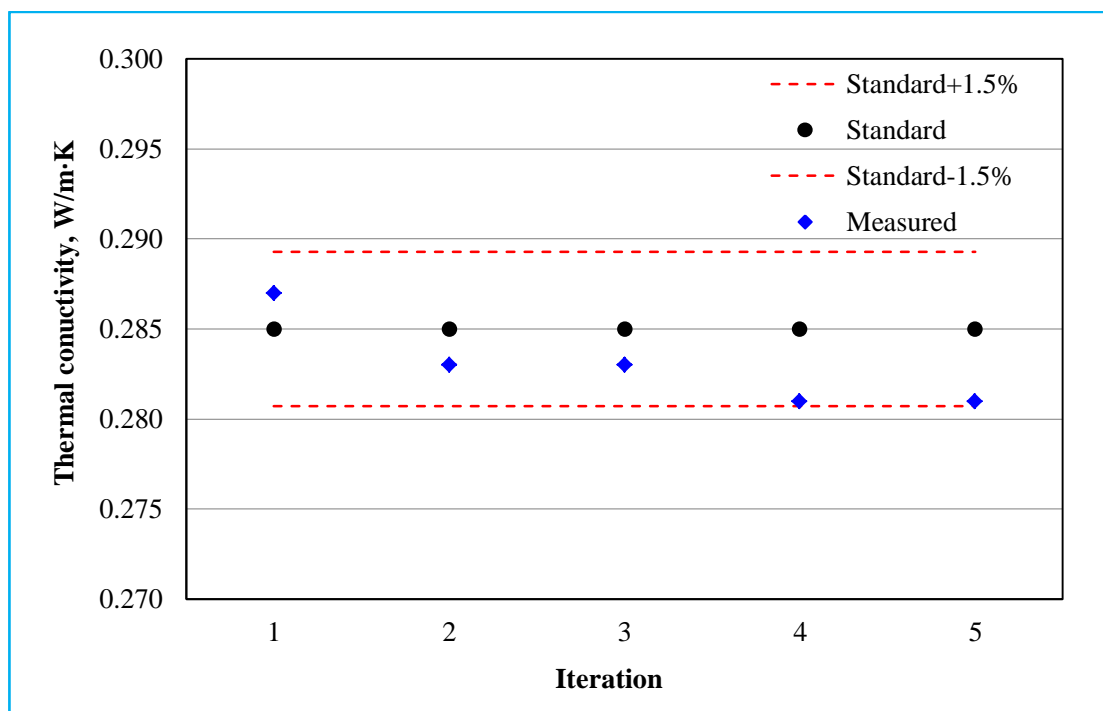


Figure 3.3: Accuracy of the KD2 Pro thermal properties analyzer (Decagon, USA) compared by the sample (glycerine) supplied by the manufacturer.

About 45 ml of sample was poured into a closed bottle, and KD2 Pro sensor was fully submerged into the sample. The sample with sensor was submerged into the thermal bath. The illustration of the thermal conductivity measurement setup is shown in Figure 3.4. The precisions of temperature measurements were considered up to ± 0.5 °C. The experiment for each parameter (each temperature of each sample) was repeated at least 15 times to get values that are more precise, and the average value was considered for analysis. Approximately, 10% of data was omitted considering them outliers. The uncertainties in measurement of thermal conductivity were calculated, and average uncertainty was found to be $\pm 4.49\%$. The details of uncertainties in measurement of thermal conductivity have reported in Table E1 and E2 (Appendix E).

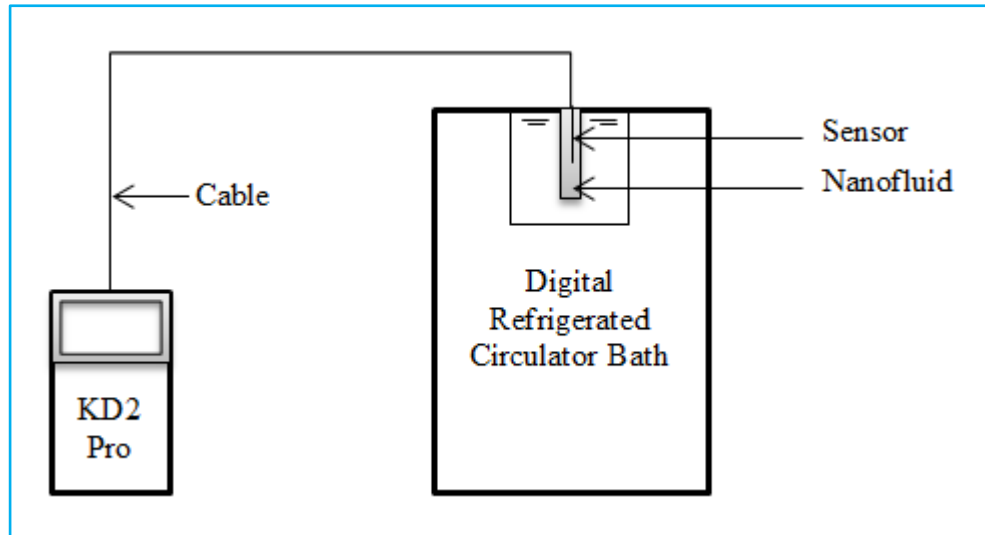


Figure 3.4: Schematic illustration of thermal conductivity measurement.

Sitprasert et al. (2009) model that consider the effect of volume concentration, particle diameter and temperature was used to predict thermal conductivity of the nanofluids to compare with the experimental values.

$$k_{eff} = \frac{(k_p - k_{lr})\phi k_{lr} [2\beta_1^3 - \beta^3 + 1] + (k_p + 2k_{lr})\beta_1^3 [\phi\beta^3 (k_{lr} - k_f) + k_f]}{\beta_1^3 (k_p + 2k_{lr}) - (k_p - k_{lr})\phi [\beta_1^3 + \beta^3 - 1]} \quad (3.2)$$

Where, k_l , k_p , k_f are the thermal conductivity of interfacial layer, solid particles and base fluid, respectively. $\beta = 1 + \frac{t}{r_p}$, $\beta_1 = 1 + \frac{t}{2r_p}$; The thickness of interfacial layer, t depends on temperature where $t = 0.01(T - 273)r_p^{0.35}$, and the thermal conductivity of the interfacial layer can be found from $k_l = C \frac{t}{r_p} k_r$; where $C = 30$, a constant for Al_2O_3 nanoparticles, T is the temperature in Kelvin and r_p is the radius of nanoparticles.

3.4.2 Viscosity measurement

In this study, a programmable rheometer (model LVDV-III ultra, Brookfield, USA) was used to measure the viscosity of the nanofluids. Mecomb Malaysia Sdn Bhd (an authorized dealer of Brookfield Engineering) calibrated the rheometer with standard viscosity fluids and accuracy of the machine was found to be $\pm 1\%$. The accuracy of the equipment after calibration has plotted in Figure 3.5. For viscosity measurement, the machine was connected to a personal computer via USB cable, and Rheocalc 32 software was used for data collection and storage. The spindle was connected to the viscometer and submerged into the nanofluid. The viscosity was developed against the spindle as a result of deflection of the calibrated spring. Ultra low adapter (ULA) was coupled with the main unit to measure viscosity with a lower amount of sample (about 16 ml is necessary). The viscosity of each sample was measured (on the same day of nanofluid preparation) at a constant shear rate of 73.38 s^{-1} while the ULA spindle was rotating at 60 rpm. Again, viscosity values were measured after 10, 20, and 30 days after the preparation of the samples. For the temperature variation, the advanced digital refrigerated circulator bath that has temperature stability of $\pm 0.01 \text{ }^\circ\text{C}$ (model AD07R-40-12E, PolyScience, USA) was connected to the water jacket of the ULA that was attached to the rheometer. The temperature of each sample was varied from 10 to $50 \text{ }^\circ\text{C}$

at 10 °C intervals to investigate the effect of temperature on the viscosity of the nanofluid. The precision of temperature measurements was within the range of ± 0.2 °C. A schematic of the viscosity measurement system is shown in Figure 3.6. Each experiment was repeated at least three times to obtain values that were more precise. The mean value of the three data points was considered for the analysis. The uncertainties in measurement of viscosity were calculated and the average uncertainty was found to be $\pm 0.57\%$. The details of uncertainties in measurement viscosity have reported in Table E3 AND E4 (Appendix E).

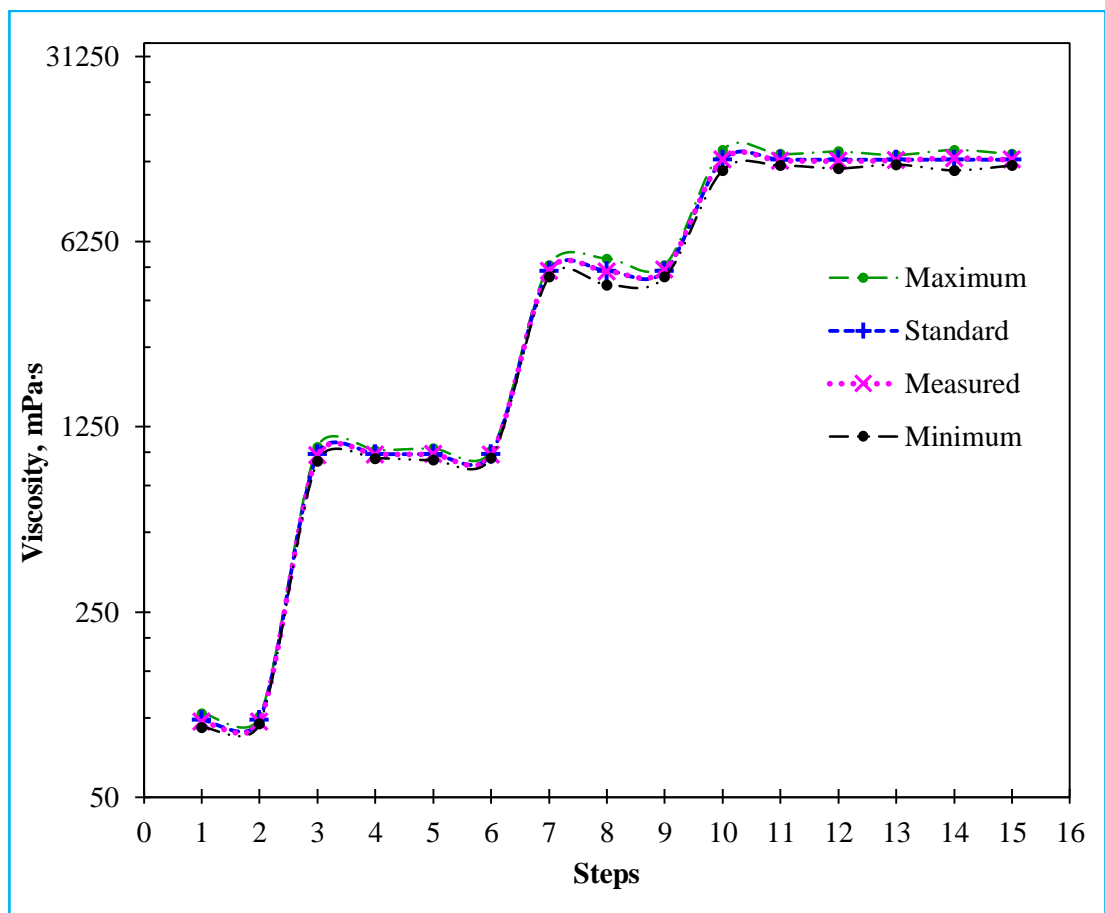


Figure 3.5 Accuracy of the rheometer after calibration with standard viscosity fluid.

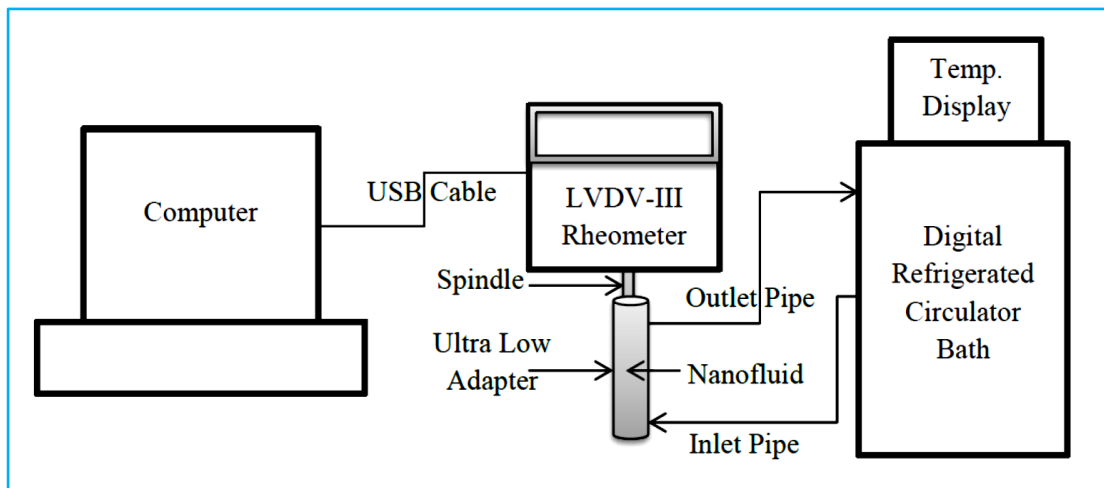


Figure 3.6 Schematic illustration of viscosity measurement.

3.4.3 Density measurement

The density of the nanofluids was measured by KEM-DA130N portable density meter (KYOTO, Japan). It could measure the density within a range of 0 to 2000 kg/m³ with a accuracy of ± 1 kg/m³ and the resolution of 0.0001 g/cm³ (1 kg/m³). This machine can measure density within a temperature range of 0 to 40 °C. Therefore, density of each sample was measured (on the same day of nanofluid preparation) for the temperature of 10 to 40 °C with 10 °C intervals. Again, density values were measured after 10, 20, and 30 days after the preparation of the samples. For the temperature variation, about 30 ml of nanofluid was poured in a small bottle (capacity of 40 ml) that was placed inside the advanced programmable refrigerated water bath (Model AD07R-40-12E, Polyscience, USA). The accuracy of the machine was measured for water and plotted in Figure 3.7. The comparison of the measured data with standard data base at 25 °C shows the maximum deviation to be only about 0.1%. The schematic of the density measurement system is shown in Figure 3.8. The experiment was repeated about 10 times for each sample and each temperature to get values that are more precise and the average value was taken for analysis. The uncertainties in measurement of density were calculated and average uncertainty was found to be $\pm 0.01\%$. The details of uncertainties in measurement of density have reported in Table E5 and E6 (Appendix E). Again, Pak

and Cho (1998) model was used to assume density of nanofluids to compare with the experimental outcomes at different temperatures.

$$\rho_{nf} = (1 - \varphi)\rho_f + \varphi\rho_p \quad (3.3)$$

Where, ρ_{nf} , ρ_p , ρ_f are the density of nanofluid, solid particles, and base fluid, respectively.

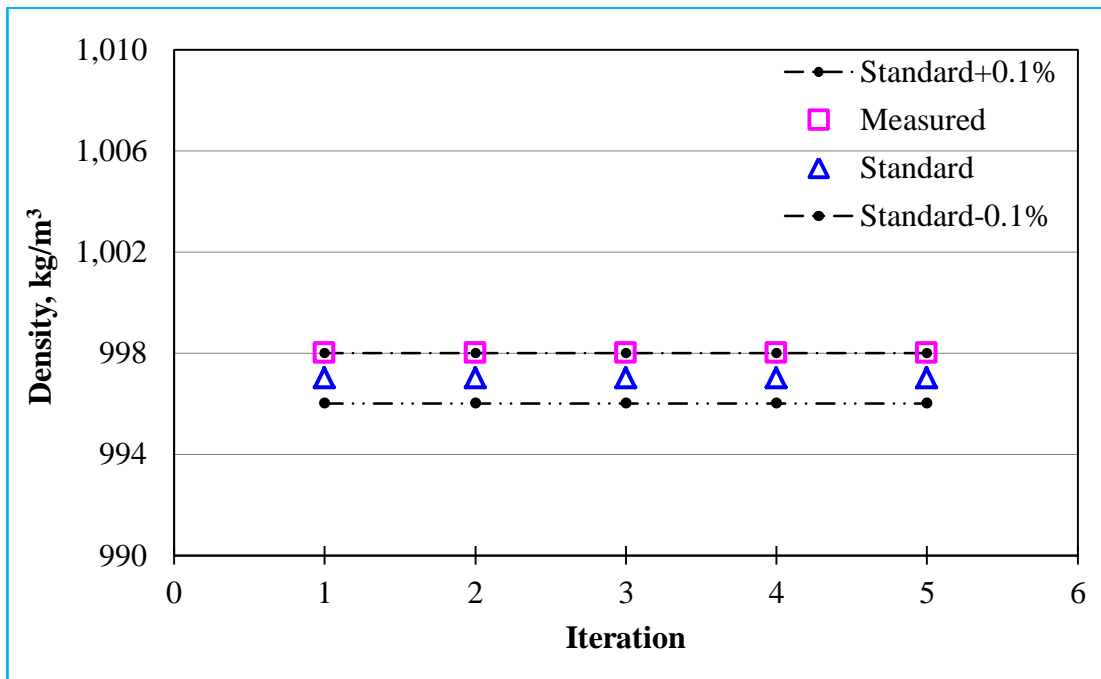


Figure 3.7: Accuracy of the DA 130N portable density meter (KYOTO, Japan) compared by water at 25 °C.

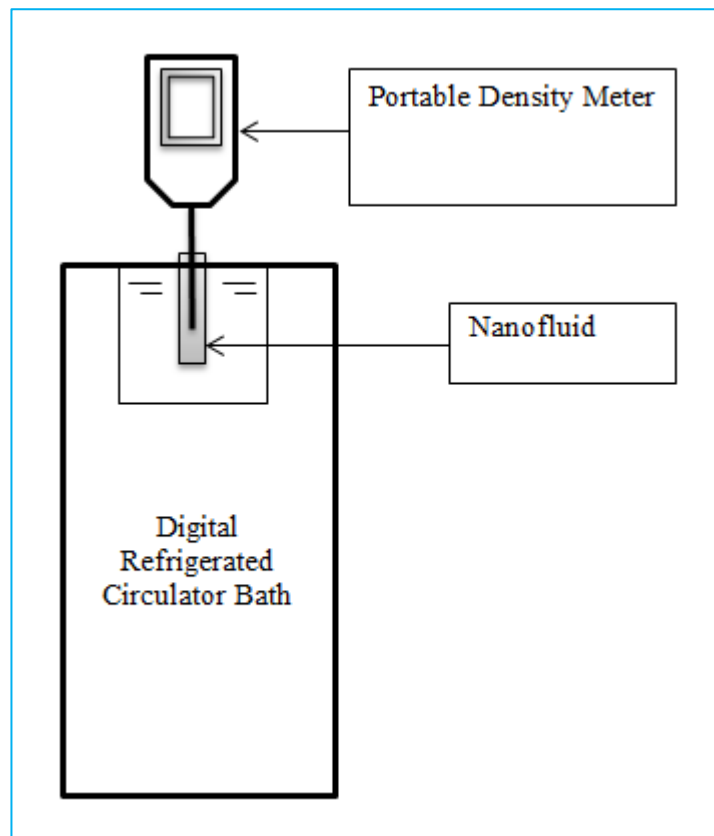


Figure 3.8: Schematic illustration of density measurement.

3.5 Rheology analysis

The rheological properties measurements were accomplished with the same equipment and procedure discussed in section 3.4.2 (viscosity measurement) that was portrayed in Figure 3.6. However, for rheology analysis, the shear stresses and viscosities of all samples were measured at shear rates from 12.23 to 305.75 s^{-1} while the ULA spindle rotating was 10 to 250 rpm. The experiments were conducted at least four times to get values that are more precise and the average value was considered throughout the analysis. The uncertainties in measurement of rheology were calculated and average uncertainties were found to be $\pm 1.52\%$ and $\pm 1.70\%$ for viscosity and shear stress, respectively at different shear rates. The details of uncertainties in rheology measurement have reported in Table E7–E11 (Appendix E).

Herschel-Bulkey mathematical model (Herschel & Bulkley, 1926) was used to analyze the yield stress point of the nanofluids prepared by different durations of ultrasonication. The equation is expressed as:

$$\tau = \tau_0 + K\gamma^n \quad (3.4)$$

Where, τ is the shear stress (Pa), τ_0 is the yield stress, γ is the shear rate (s^{-1}), K is the consistency coefficient (Pa.s), and n is the flow behavior index (dimensionless).

The most frequently applied Power law model has been used to analyze the flow characteristic that is expressed as:

$$\tau = K\gamma^n \quad (3.5)$$

3.6 Thermal performance analysis

A copper mini channel heat sink that is an existing set up (available in Energy Lab 2, Faculty of Engineering, University of Malaya) was used to study the effect of ultrasonication of nanofluids on some thermal performance parameters. The closed-loop experimental setup of the mini channel heat sink has shown in Figure 3.9. The setup is mainly comprised of a mini channel, storage tank, pump, flow meter, pressure transducer, heaters, radiator cooler, thermocouples, and data logger. The mini channel was a customized unit having copper material. Copper material was used because of its high thermal conductivity. The mini channel was cuboid shaped with the overall dimensions of 50 mm x 50 mm x 10 mm (L x W x H) and fabricated by using a wire electrical discharge machine. The cross section of the rectangular mini channel heat sink is shown in Figure 3.10. (An illustration of the rectangular heat sink has shown in

Figure 1.9 that described a clear idea about shape). All the channel and fin had same space of 0.5 mm and channel height was 0.8 mm. Table 3.4 shows the details specifications of the copper mini channel heat sink that used in this study.

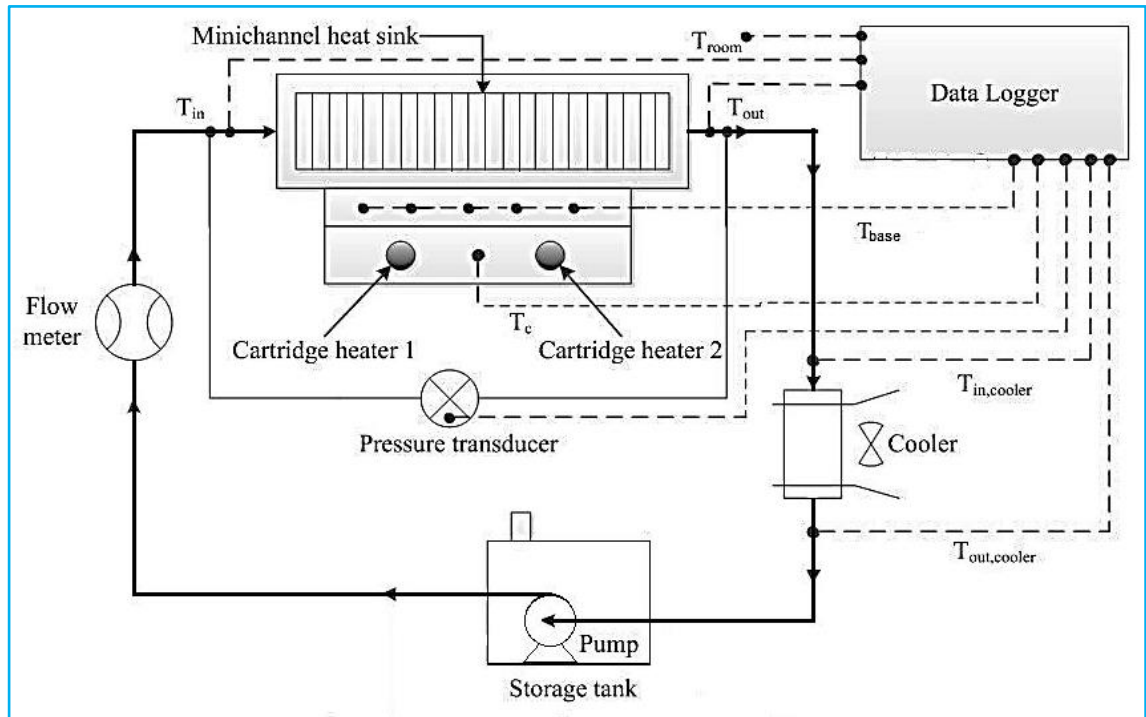


Figure 3.9: Schematic illustration of the mini channel thermal performance measurement setup.

Two cartridge heaters with capacity of each unit 200 W was used to heat the mini channel from its bottom/base. Glass wool and Teflon were used as insulation for the heat sink to minimize any possible heat loss in environment. Five units of RTD type thermocouples were used to monitor the base temperature, and the average of the five points was recorded in the data logger. About 1500 ml nanofluid was used to operate the setup and forced by a pump to flow through the system. Polyurethane (PU) tubes having the outer diameter of 16 mm and inner diameter of 11 mm were used to connect and the closed system. A volumetric flow meter was used to control the flow of the nanofluid. The inlet and outlet temperatures of mini channel were recorded in a data-acquisition

system by using RTD type thermocouples. A differential pressure transducer was used and linked with the data logger to record the pressure drop of nanofluid (for in and out of the mini channel). A radiator cooler was used to cool down the nanofluid before it reached to the storage tank as inside the mini channel, nanofluid as a coolant absorbed heat. The in and out temperatures of the radiator cooler (temperature of nanofluid before and after passing the radiator cooler) and room temperatures were also recorded in data logger using RTD type thermocouples.

Table 3.4: Details specification of the copper mini channel heat sink.

| Parameter (unit) | Value |
|-------------------------------|-------|
| Heat sink total length (mm) | 50 |
| Heat sink total width (mm) | 50 |
| Heat sink total height (mm) | 10 |
| Top cover height (mm) | 7.2 |
| Bottom part total height (mm) | 2.8 |
| Base height (mm) | 2 |
| Channel height (mm) | 0.8 |
| Channel length (mm) | 50 |
| Channel width (mm) | 0.5 |
| Fin width (mm) | 0.5 |
| Number of channels | 50 |

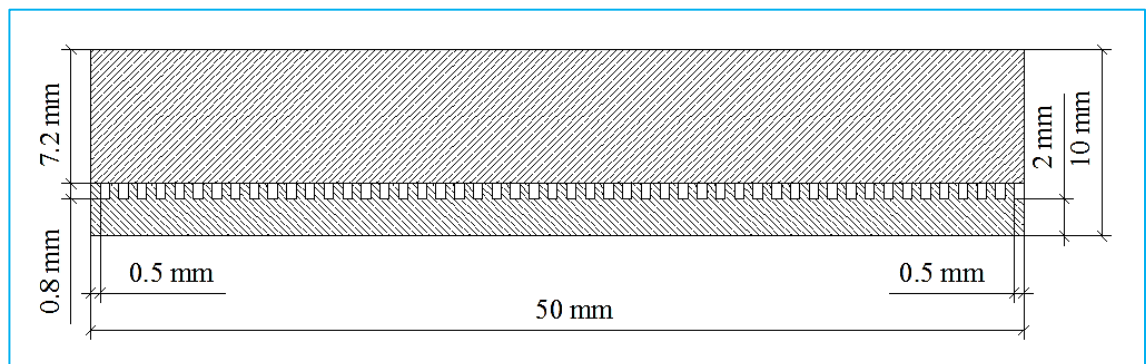


Figure 3.10: Cross section of the copper mini channel heat sink.

First, the setup was operated with water (base fluid) only. Later five samples prepared by 1, 2, 3, 4, and 5 h of ultrasonication durations were run through the system. For this purpose, 200 ml of 0.5 vol.% nanofluid was prepared at a time with 50% amplitudes and 2 sec ON and 2 sec OFF pulse mode, and the required amount of nanofluids were accumulated. After using any new sample, the setup was cleaned by water and compressed air to fully remove any remaining of the previous sample. Five different flow rates (0.500, 0.625, 0.750, 0.875, and 1.000) were used during this study and approximately 1 h duration was continued for each flow condition. To control high precision, data was recorded at every after 20 sec intervals during the 1 h operation for each condition and the average data were used for the analysis. The uncertainties in the measured parameters of the heat sink were calculated and found to be 0.73%, 1.03%, 1.14%, and 0.47% for base, inlet and outlet temperatures, and pressure drop, respectively. The details of the uncertainties of measurement related to the heat sink have reported in Table E12 (Appendix E). The following equations were used to calculate the performance parameters.

Thermal resistance of the heat transfer was calculated based on the following equation (Xie et al., 2009):

$$R_{th} = \frac{A_b(T_b - T_{in})}{Q} \quad (3.6)$$

The effective base temperature of the heat sink was calculated by considering the effect of the base height (Naphon & Nakharintr, 2013). The equation is expressed as:

$$T_b = T_{b,(av,tc)} - \left(\frac{QH_b}{k_{hs}A_b} \right) \quad (3.7)$$

The area of the heat sink base was calculated based on the following equation:

$$A_b = L_{ch} N(W_{ch} + W_{fin}) \quad (3.8)$$

The log mean temperature difference (ΔT_{LMTD}) was calculated using the effective base temperature (Ho & Chen, 2013), which is expressed as:

$$\Delta T_{LMTD} = \frac{(T_b - T_{in}) - (T_b - T_{out})}{\ln\left(\frac{(T_b - T_{in})}{(T_b - T_{out})}\right)} \quad (3.9)$$

The HTC was calculated using the following equation (Naphon & Nakharintr, 2013):

$$h = \frac{Q}{A_{eff} (\Delta T_{LMTD})} \quad (3.10)$$

Where, the effective surface area of the mini channel (Ijam et al., 2012) was calculated as:

$$A_{eff} = L_{ch} N(W_{ch} + 2\eta H_{ch}) \quad (3.11)$$

Where, η is the efficiency factor of the channel or used material and for copper material, η could be considered as 1 (Sohel et al., 2014).

Pumping power of the system was calculated using the following equation:

$$P_p = \dot{V} \Delta P \quad (3.12)$$

Here, \dot{V} is the volumetric flow rate, which was determined from the following equation:

$$\dot{V} = \frac{\dot{m}}{\rho_{nf}} \quad (3.13)$$

Therefore, the equation of pumping power becomes as below:

$$P_p = \frac{\dot{m}}{\rho_{nf}} \Delta P \quad (3.14)$$

Yu et al. (2012b) proposed the FOM as the ratio of HTC divided by the pumping power ratio, which was used to calculate the FOM for the nanofluids prepared by various durations of ultrasonication at different flow rates. The equation is expressed as:

$$FOM = \frac{(h_{nf} / h_{bf})}{(P_{nf} / P_{bf})} \quad (3.15)$$

3.6.1 Heat sink data validation

There are mainly three temperature measurements of the heat sink are: inlet temperature, base temperature, and outlet temperature. Before being analysis with nanofluid, these measurement points were checked with distilled water and compared

with the study of Rana (2014) and Shah (2015), who used the same experimental setup. Figure 3.11 shows the measured value of inlet temperature for water at different flow rates of the liquid. The maximum deviation of this study was found to be within 1.6 °C and trend is similar to the study of Rana (2014).

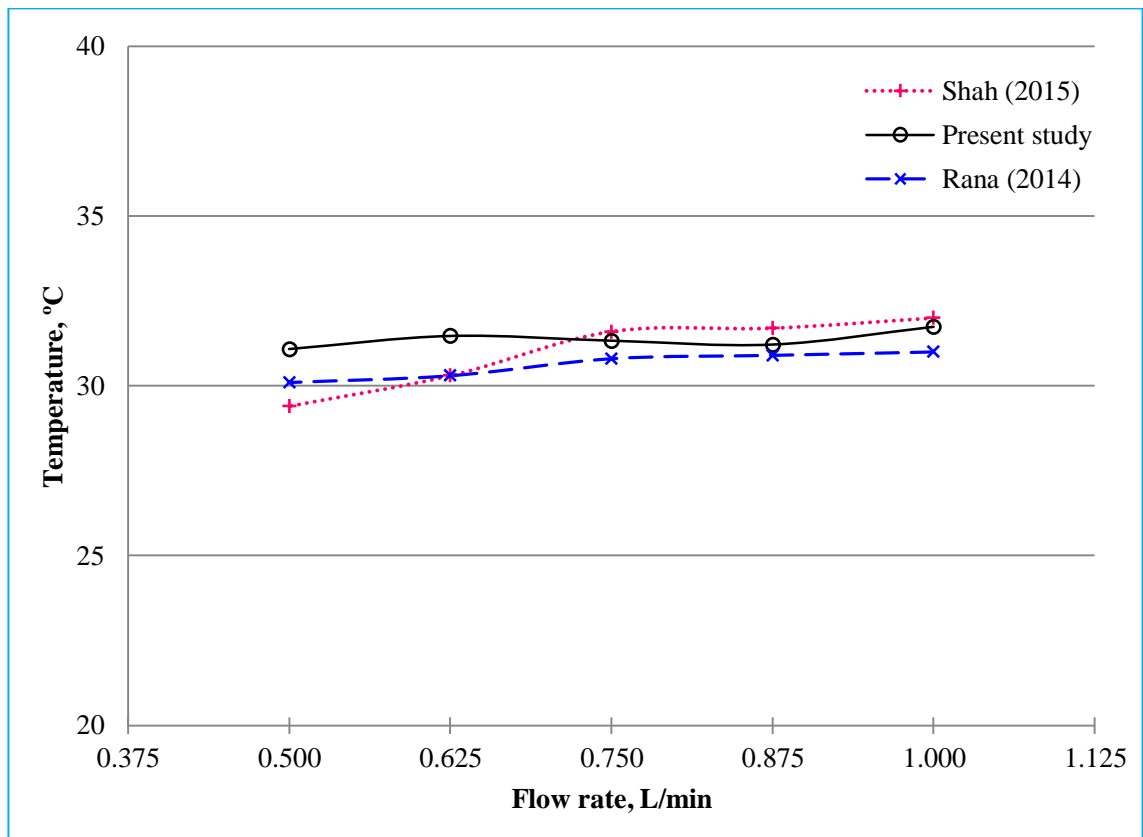


Figure 3.11: Comparison of heat sink inlet temperature by water.

Figure 3.12 shows the recorded data of base temperature for water at different flow rates of the liquid. The maximum deviation of this study was found to be within 1.6 °C and at higher flow rates the values of this study were almost similar with the value reported by Rana (2014) and Shah (2015). Figure 3.13 shows the measured data of outlet temperature for water of this study at different flow rates of the liquid. From Figure 3.13, the maximum deviation of this study was found to be within 0.8 °C with the study of Rana (2014) and Shah (2015).

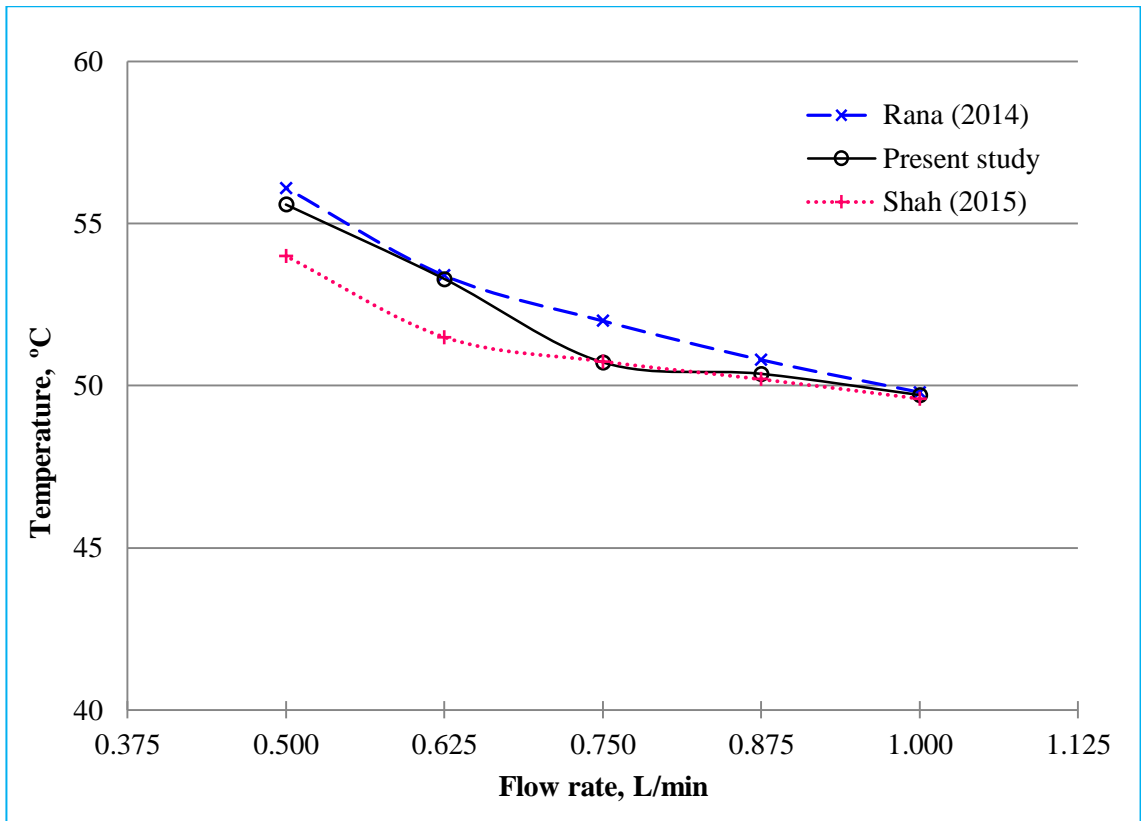


Figure 3.12: Comparison of heat sink base temperature by water.

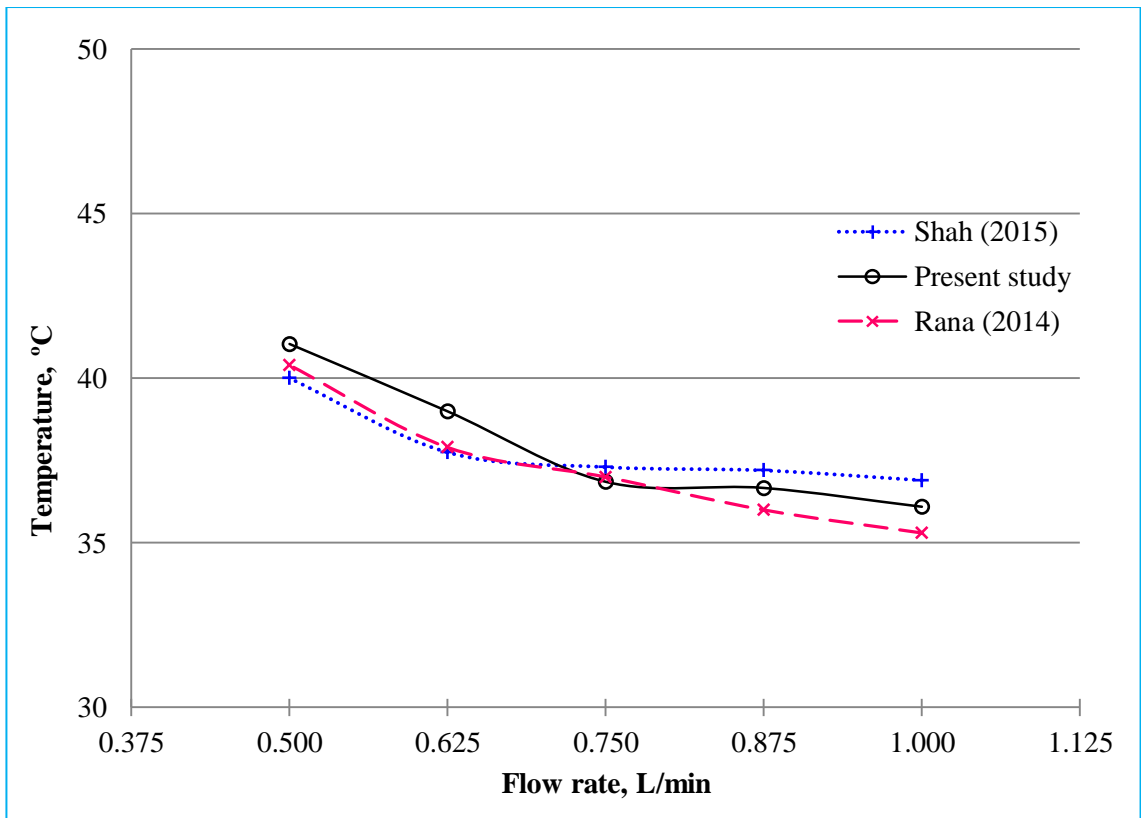


Figure 3.13: Comparison of heat sink outlet temperature by water.

CHAPTER 4: RESULTS AND DISCUSSIONS

4.1 Introduction

The aim of this chapter is to describe the obtained results and to discuss the outcomes with scientific explanations. The subsequent sections start with the effect of ultrasonication in bulk heating of liquids. Then it followed by the effect of ultrasonication durations on colloidal dispersion characteristics where microstructures, PSD, zeta potential and sedimentation rate. The sections also are followed by the effect of ultrasonication and temperature on thermophysical (e.g. thermal conductivity, viscosity, and density) and rheological properties (shear rate, shear stress, viscosity, yield stress, flow index) of nanofluids. Finally, the thermal performance analysis with a mini channel heat sink is discussed.

4.2 Effect of ultrasonication in bulk heating

The effect of ultrasonication in bulk heating of liquid has shown in Figure 4.1. the Y-axis value of the graph is the temperature difference, which were calculated by subtracting the measured temperature from initial liquid temperature (room temperature). It is seen from the Figure 4.1 that the influence of ultrasonication was more effective for lower liquid volume. Temperature was increased with the increase of sonication time and the increment rates were found to be higher for a lower amount of water. After the first min of ultrasonication, the increment rate was observed 18.3, 10.8, 5.6, and 3.8 °C for the liquid volume of 25, 50, 100, and 200 ml, respectively. Therefore, it is necessary to use thermal bath or ice bath to control the temperature rise during the ultrasonication process. Otherwise, nanofluid will be evaporated and total volume and concentration will be changed. Chung et al. (2009) observed that agitation by ultrasonic horn increase temperature by 10 °C/min initially. Furthermore, they report

that this increment rate was 1 °C/min in ultrasonic bath. They used 20 ml of DIW to study the effect of ultrasonication on the temperature rise.

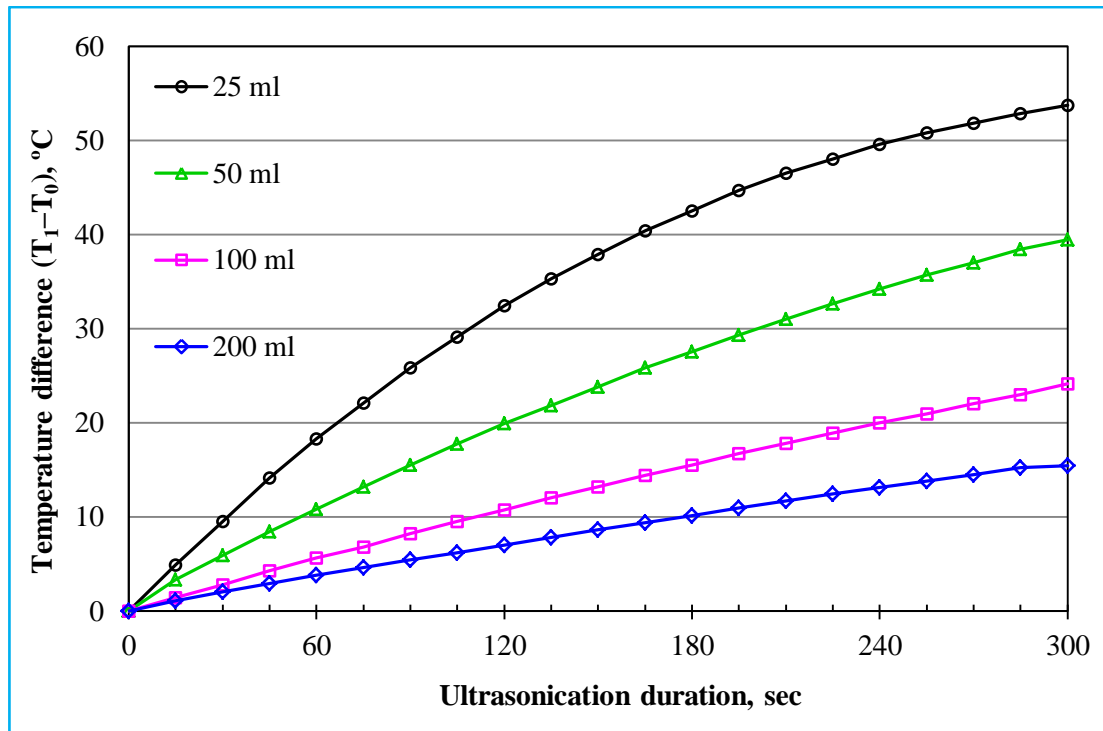


Figure 4.1: Effect of ultrasonication in bulk heating of liquid.

4.3 Colloidal dispersion characteristics

4.3.1 Microstructures

To study the effect of sonication time on the colloidal dispersion of Al_2O_3 –water nanofluid, the microstructure of Al_2O_3 nanoparticles was observed first, before they were mixed with water. The microstructures of Al_2O_3 nanoparticles taken by FESEM without any treatment (as received) are shown in Figure 4.2. In Figure 4.2 (a) in the 10- μm range, high agglomeration of the nanoparticles is observed. Figure 4.2 (b) shows the particles in the smaller range of 1 μm , in which the nanoparticles are found in loose clustered form and spherical shape. Therefore, it could be predicted that the nanoparticles will be easily dispersed in liquid with the vibration of ultrasonication.

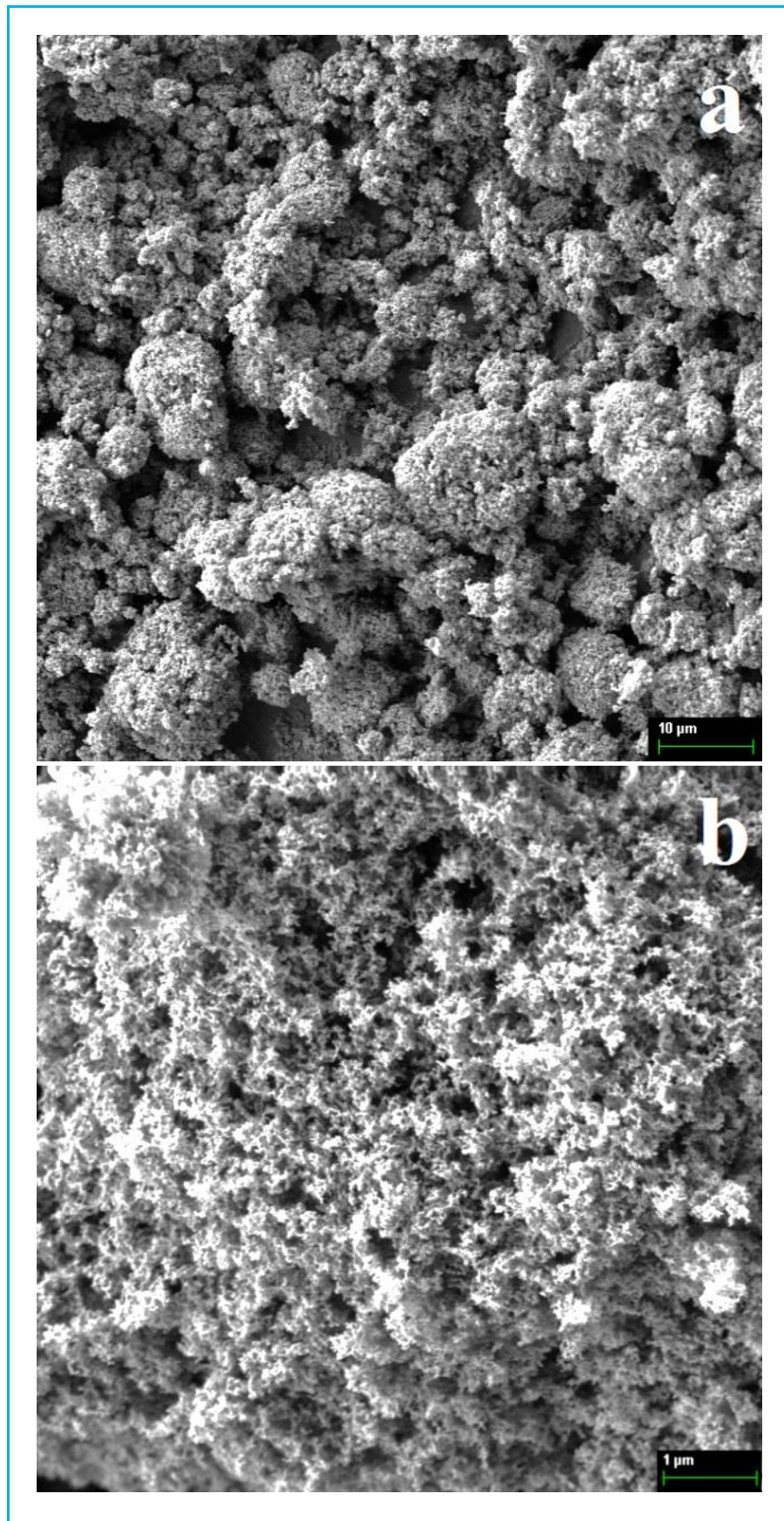


Figure 4.2: FESEM images of Al₂O₃ nanoparticles at (a) in 10- and (b) 1-μm scales.

After the Al_2O_3 nanoparticles had been suspended in water, the microstructure was again analyzed by TEM. The TEM images after suspended into water by stirring and without sonication is shown in Figure 4.3. To obtain a better understanding of the microstructure, the images were portrayed at four different magnifications (500-, 200-, 100-, and 50-nm scales). From Figure 4.3, it is clear that the nanoparticles were not properly dispersed and there was strong clustering among the nanoparticles. These aggregate occurs when the nanoparticles were agglomerated in dry powder form and even after mixing with water they are still existed. Therefore, ultrasound energy is necessary to breakdown such as aggregates. Some locations that are empty in the micrograph imply the presence of no particles, whereas some places are darker and show high aggregation of nanoparticles. The agglomerations are clear in Figure 4.3 (a) and 4.3 (d).

The TEM images of Al_2O_3 -water nanofluid after 1 h ultrasonication with 2 different amplitudes (25% and 50%) is shown in Figure 4.4. Figure 4.4 show that 1 h ultrasonication is not enough for well dispersion of nanoparticles. The left-side figures (Figure 4.4 (a)–(d)) are the micrograph of 25% amplitude, which show that there are a lot of aggregates of particles still existed. The right-side figures (Figure 4.4 (e)–(h)) are the micrograph of 50% amplitude and these microstructures show a better colloidal dispersion compared to that of 25% amplitude. Nevertheless, there are some clusters of particles were existed, which are visible in Figure 4.4 (g) and (h). Figure 4.4 state that better dispersion of nanoparticles is found for higher power (amplitude) of sonicator even for the same duration. Lam et al. (2005) reported that lack of enough energy, nanoparticles would not be able to escape from the clusters, as a result large aggregation will be observed. The higher aggregation was seen in the case of nanofluids prepared by 1 h of ultrasonication with 25% amplitude is being the result of the above statement.

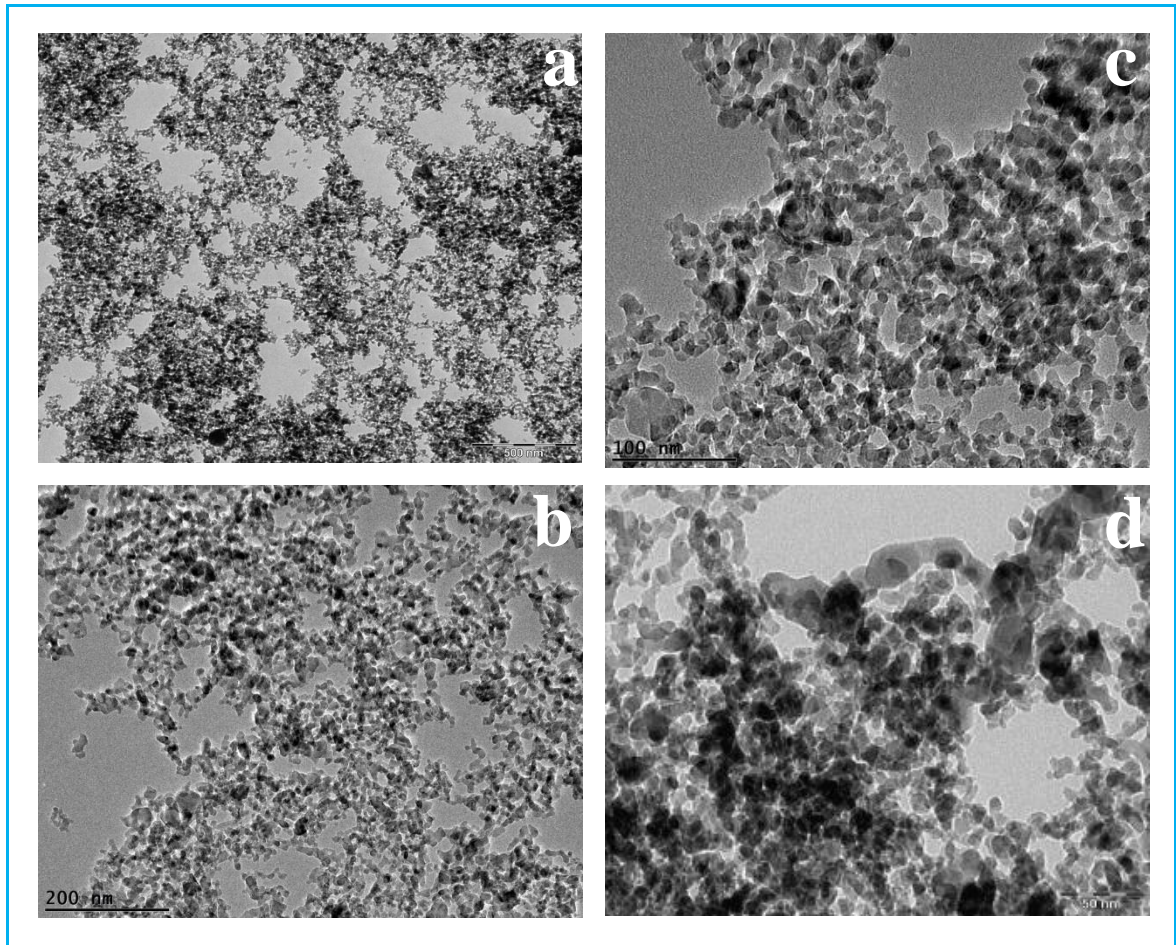


Figure 4.3: Microstructure of Al₂O₃–water nanofluid prepared by without ultrasonication (0 h). Figure 4.3 (a), (b), (c), and (d) stand for 6300×, 12500×, 20000×, and 31500× magnifications.

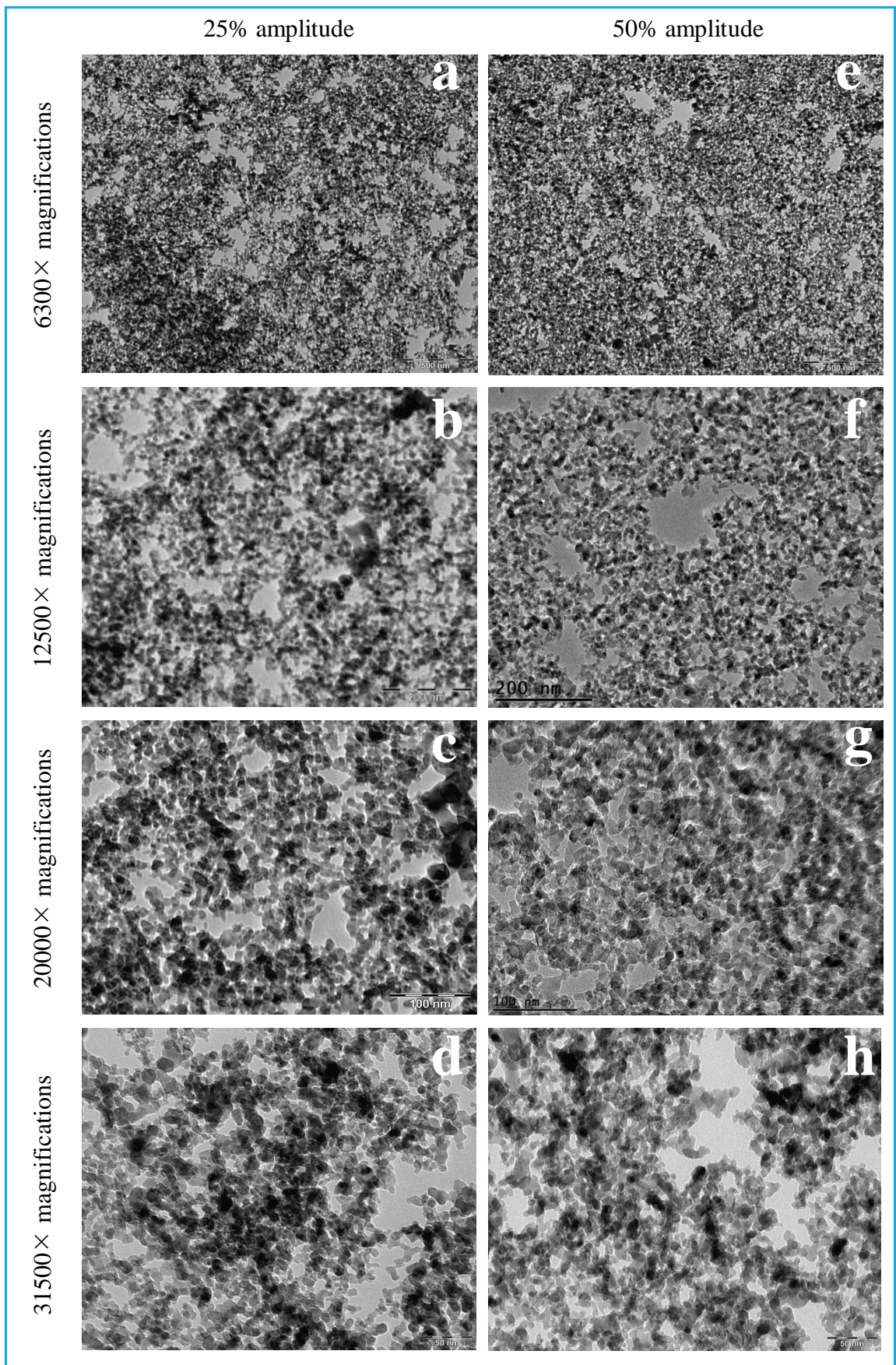


Figure 4.4: Microstructure of Al_2O_3 -water nanofluid at 1 h ultrasonication duration.

Figure 4.5 shows the microstructure of Al_2O_3 nanoparticle in water after 2 h of ultrasonication with 25% and 50% amplitude. Figure 4.5 (a)–(d) (the left-side figures) are the micrograph of 25% amplitude at $6300\times$, $12500\times$, $20000\times$, and $31500\times$ magnifications, respectively in 500-, 200-, 100-, and 50-nm scales, respectively. Similarly, the right-side figures (Figure 4.5 (e)–(h)) are stood for micrograph of 50% amplitude. It is clear from Figure 4.5 that the nanoparticles were well dispersed and almost similar type dispersion has been observed for the nanofluids prepared by 2 h of ultrasonication with 25% and 50% amplitude. Nevertheless, there are few small overlaps have been observed, which are the nano-clusters among the particles. Such nano-clusters could not be fully broken down, even after prolonged ultrasonication. It is impossible to get the initial size of particles after dispersed into fluid (Elcioglu & Okutucu-Ozyurt, 2014). PSD analysis gives the idea about the size of the nano-clusters. Ghadimi et al. (2011) report that the cluster of nanofluids will be at least three times higher than the average particle diameter.

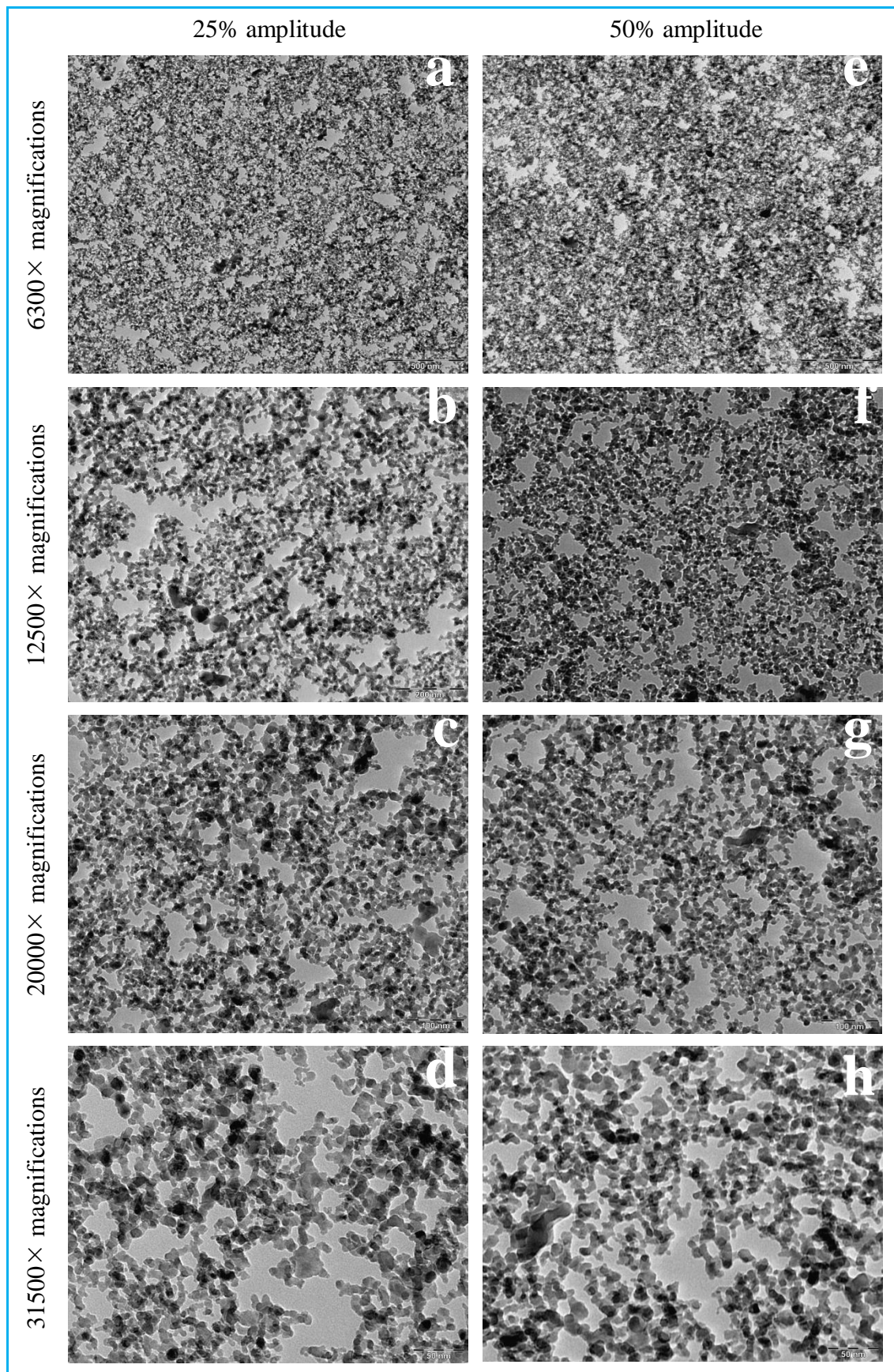


Figure 4.5: Microstructure of Al_2O_3 -water nanofluid at 2 h ultrasonication duration.

The microstructures of Al₂O₃–water nanofluid prepared by 3 h of ultrasonication with 2 different amplitudes (25% and 50%) are shown in Figure 4.6. The left-side figures (Figure 4.6 (a)–(d)) are the micrograph of 25% amplitude and the right-side figures (Figure 4.6 (e)–(h)) are the micrograph of 50% amplitude. More spreading of nanoparticles is seen from Figure 4.6. There are only few empty areas are visible in the micrograph. Even though, there is no large agglomeration was observed but there are small nano-clusters of particles are existed. Either the agglomeration of nanoparticles did not have enough energy to completely breakdown the clusters or the nanoparticles have received over energy and started to re-agglomerate. Nevertheless, it is impossible to completely breakdown the clusters of particles (Ghadimi et al., 2011). It is reported in literature (Kwak & Kim, 2005; Lam et al., 2005; Nguyen et al., 2011) that higher power of ultrasonication could re-agglomerate the particles as the collision of each particle will increase and they will tangle up. A comparative higher dispersion of particles is observed for the nanofluids prepared by 50% amplitude in comparison to 25% one. This indicates that using 25% amplitudes of sonicator power, even after 3 h of ultrasonication, nanoparticles do not get enough energy to completely be dispersed into water.

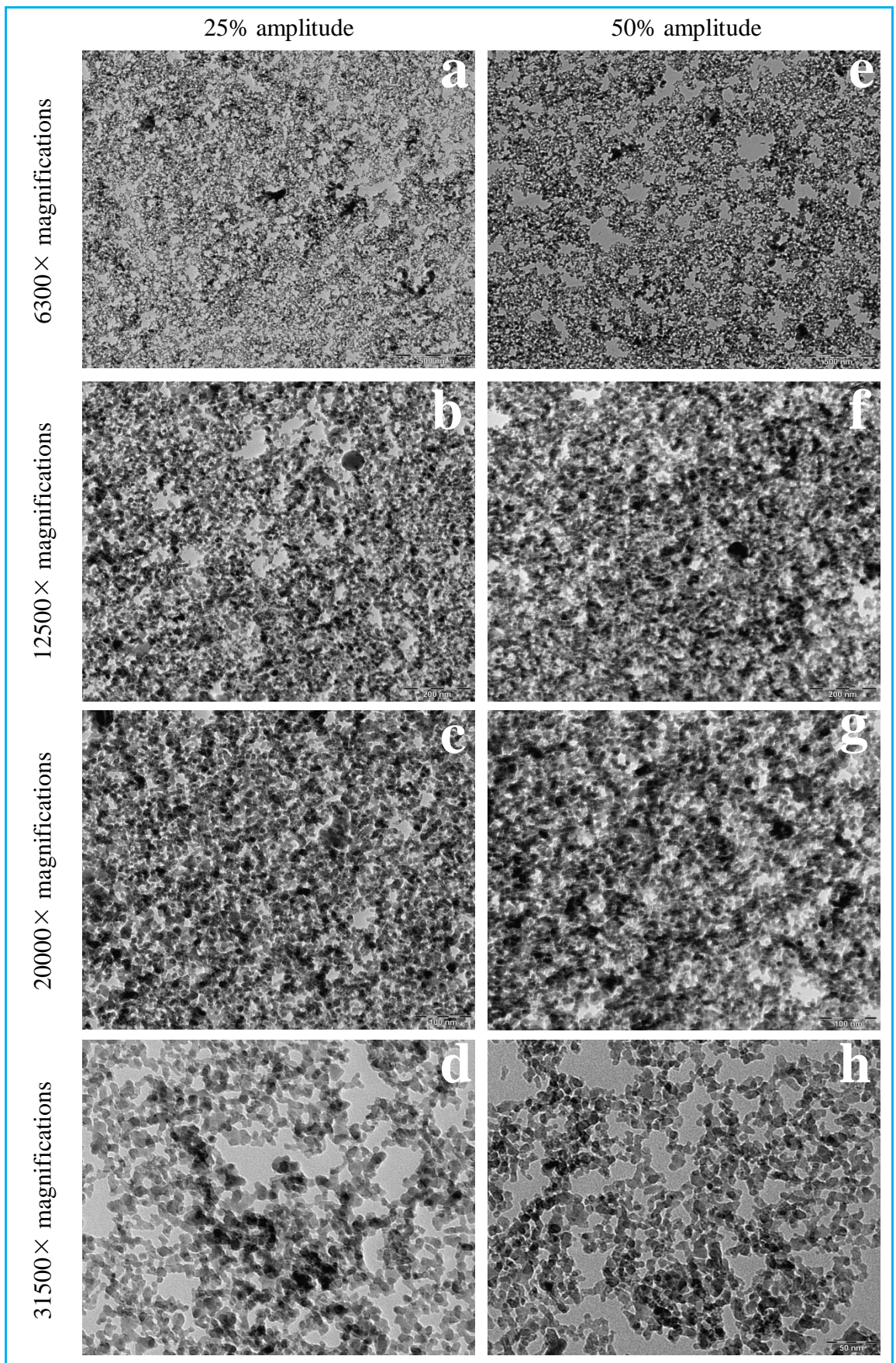


Figure 4.6: Microstructure of Al_2O_3 -water nanofluid at 3 h ultrasonication duration.

The micrographs taken by TEM for the nanofluids prepared by 4 h of ultrasonication with 25% and 50% amplitudes have shown in Figure 4.7. Figure 4.7 (a)–(d) (the left-side figures) are the micrograph of 25% amplitude at 6300 \times , 12500 \times , 20000 \times , and 31500 \times magnifications, respectively in 500-, 200-, 100-, and 50-nm scales, respectively. Similarly, the right-side figures (Figure 4.7 (e)–(h)) are standing for micrograph of 50% amplitude. More spreading of nanoparticles is seen in the figure. There are no significant empty areas are visible in the micrographs taken for the nanofluid prepared by 50% amplitude. However, still there are some but few empty areas could be seen for the nanofluids of 25% amplitude. Moreover, there are some clusters of particles were existed. Therefore, it could be expected that further higher ultrasonication with 25% amplitude could disperse more particles.

Figure 4.8 shows the microstructures of Al₂O₃–water nanofluid after 5 h of ultrasonication. The left-side figures (Figure 4.8 (a)–(d)) are the micrograph of 25% amplitude and the right-side figures (Figure 4.8 (e)–(h)) are the micrograph of 50% amplitude. More spreading of nanoparticles is seen in the figure for 5 h of ultrasonication and almost similar trend was observed for the applied power of 25 and 50% sonicator amplitude. However, there are minor overlaps of nanoparticles but no empty areas can be seen in Figure 4.8 (e)–(h) for 50% amplitude. A higher particle dispersion but with few empty areas and minor overlapping of particles have observed in Figure 4.8 (a)–(d) for 25% amplitude. Therefore, nanofluids prepared by 25% amplitudes did not have enough ultrasound energy yet. The images of Figure 4.8 are darker black color, which are more significant in Figure 4.8 (e)–(h) for 50% amplitude. This could be due to the erosion of a sonicator tip. Mandzy et al. (2005) reported that erosion of an ultrasonic tip could be contaminated with the fluid as a result of longer ultrasonication duration.

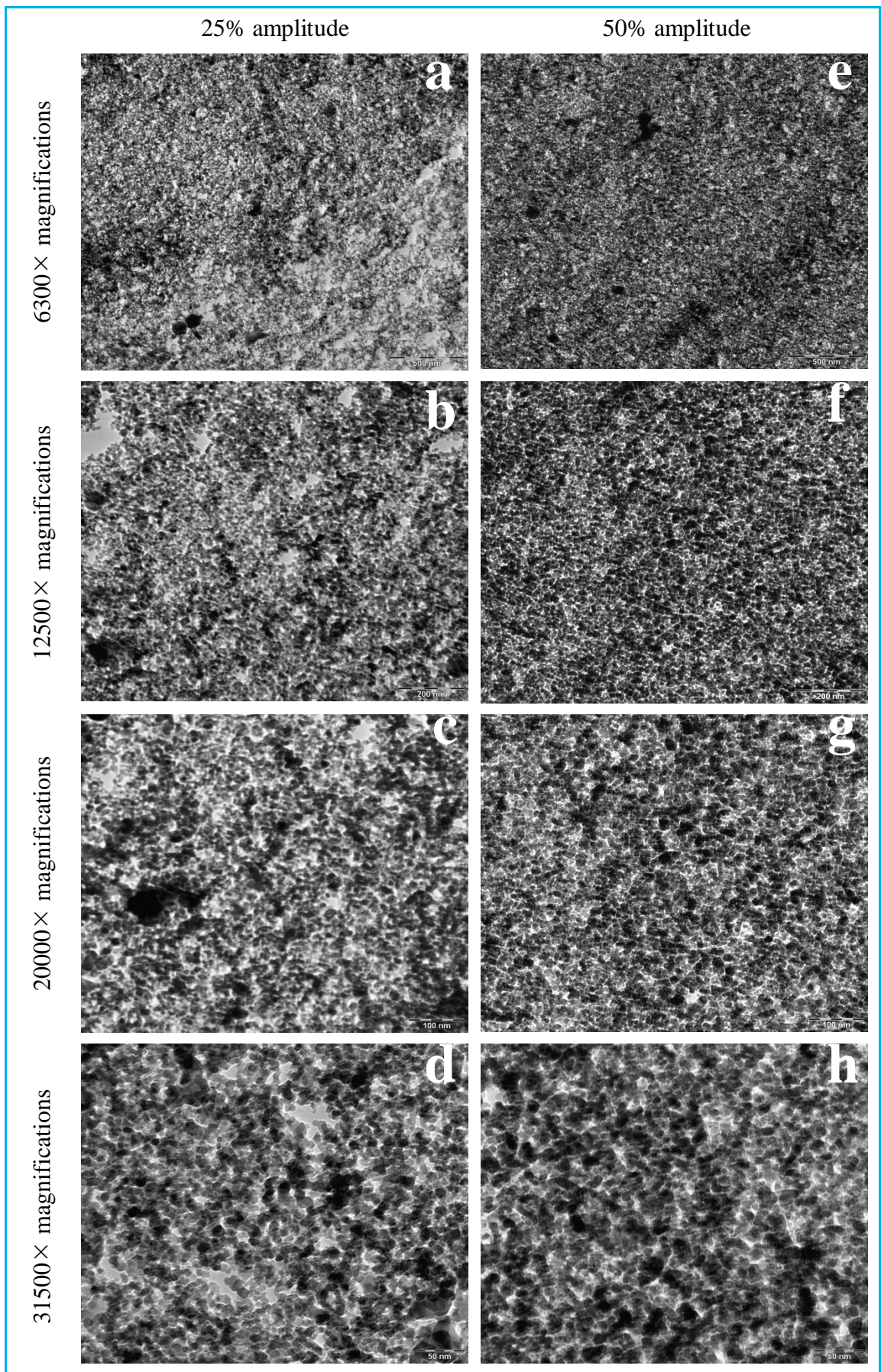


Figure 4.7: Microstructure of Al_2O_3 -water nanofluid at 4 h ultrasonication duration.

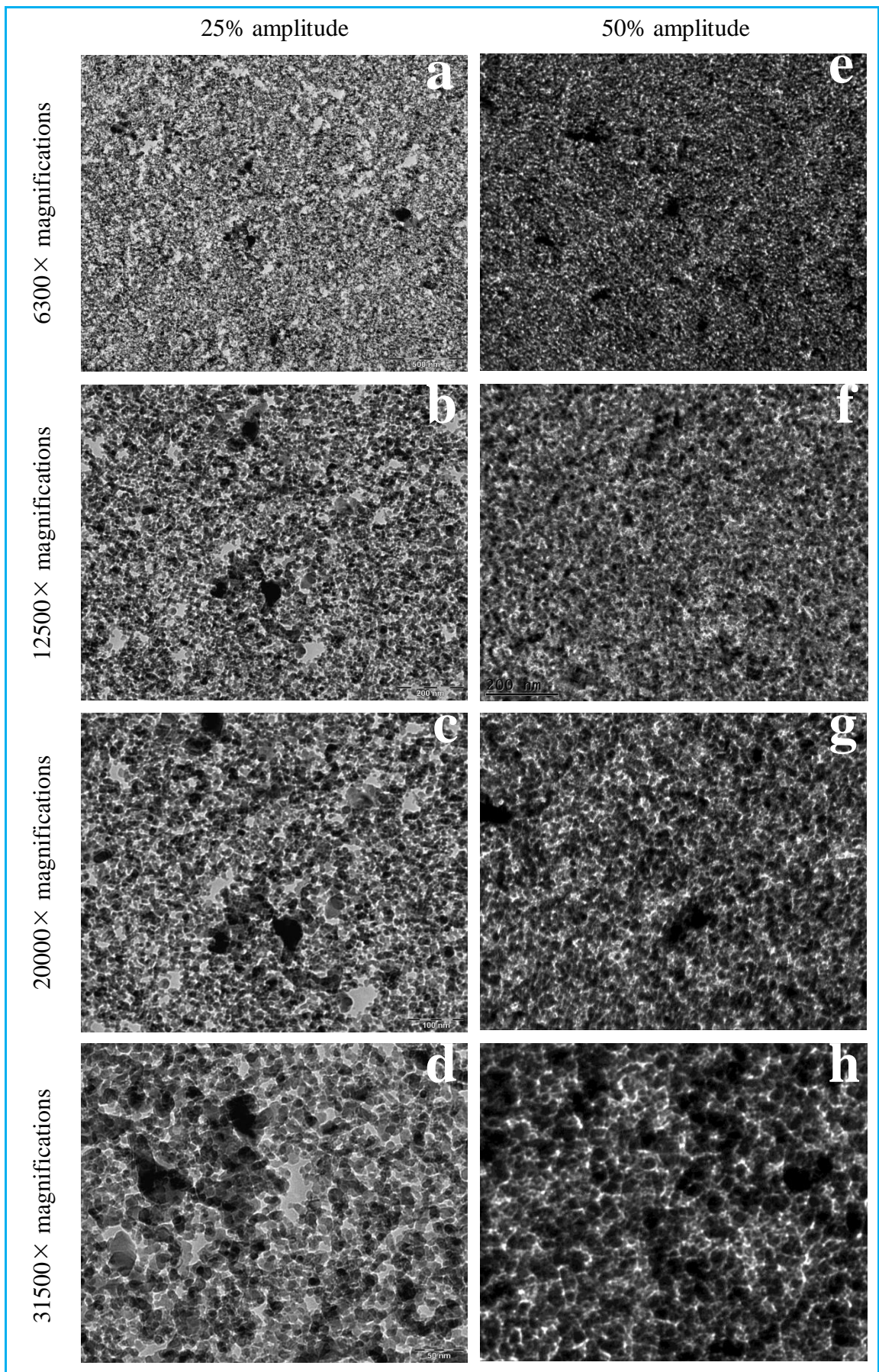


Figure 4.8: Microstructure of Al_2O_3 -water nanofluid at 5 h ultrasonication duration.

Therefore, a strong morphological change in the colloid occurs with the variation of the ultrasonication duration, as nanoparticles are dispersed until 2 h of sonication after which they start to coalesce. Kwak and Kim (2005) found a similar type of morphology, as further sonication after the optimum sonication time caused the nanoparticles to coalesce again.

The final particle sizes (average) of Al_2O_3 -water nanofluid after each ultrasonication was also measured from TEM images, and plotted as histograms of particle diameter. Figure 4.9 represents the histogram of particle sizes after 0 h of ultrasonication. Although the primary particle size (average) was 13 nm however, a wide range of particle sizes from 6 to 20 nm is observed in Figure 4.9 for the nanofluid prepared by 0 h of ultrasonication. Most of the nanoparticles were in the range of 10–14 nm, which are more than 50% of total population. A very few nanoparticle found to be over 20 nm size, which are not included in the histogram. The TEM microstructure of Al_2O_3 -water nanofluid after 0 h of ultrasonication on a 50-nm scale with particle size measurements is shown in Figure B1 (Appendix B).

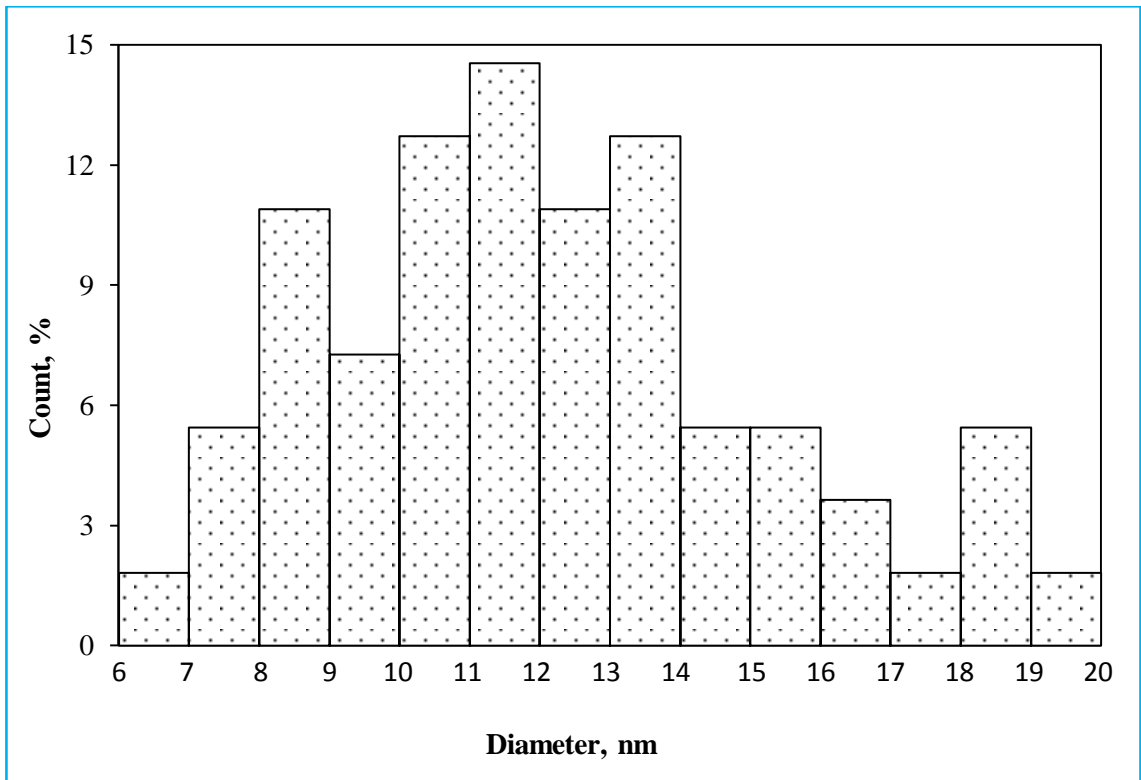


Figure 4.9: Histogram of individual particle diameter after 0 h (without ultrasonication).

The histogram of particle sizes after 1 h of ultrasonication show that particle sizes were within the range of 5 to 14 nm as reported in Figure 4.10. Here the particle size range is smaller than that of Figure 4.9 for 0 h of ultrasonication. Therefore, with the start of ultrasonication, nanoparticles are starting to break down and eroding also observed (Özcan-Taşkin et al., 2009). The particle-particle collision is also a reason of erosion. After 1 h of ultrasonication, most of the nanoparticles were found to be in the range of 9–11 nm. Almost 45% of total population was within this range. The TEM micrograph of the nanofluid after 1 h of ultrasonication on a 50 nm scale with particle size measurements is shown in Figure B2 (Appendix B).

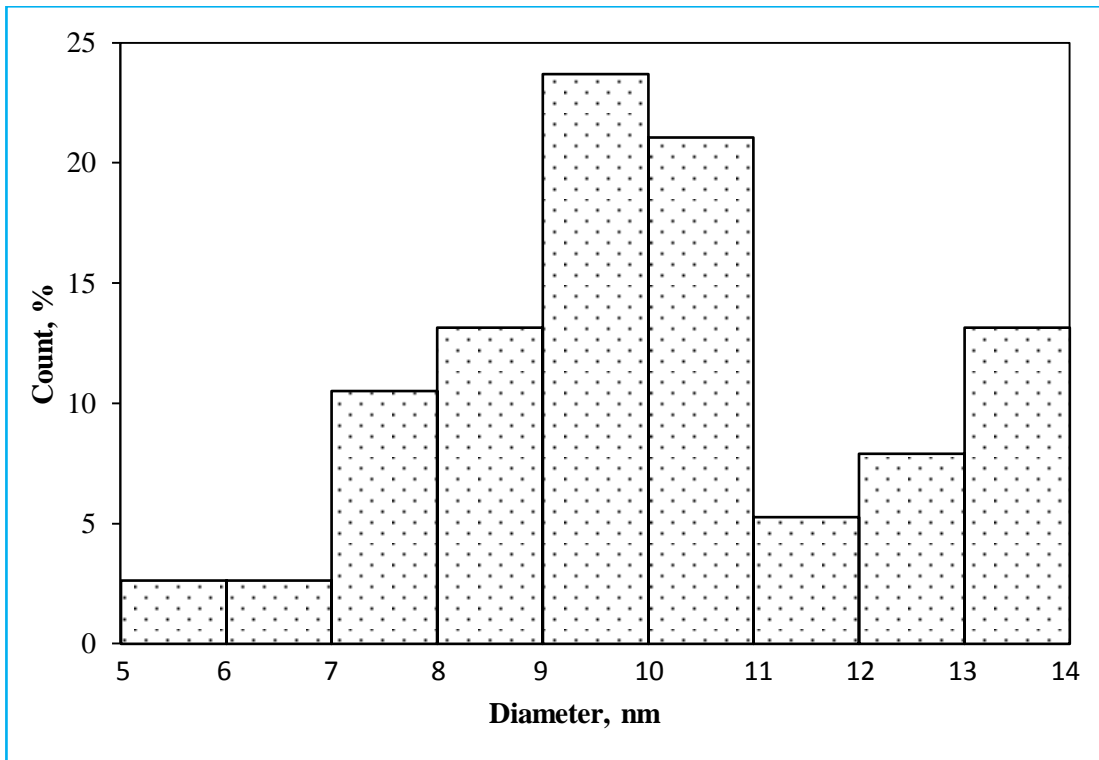


Figure 4.10: Histogram of individual particle diameter after 1 h of ultrasonication duration.

Figure 4.11 shows the histogram of particle sizes after 2 h of ultrasonication. It can be seen from Figure 4.11 that most of the nanoparticles were within the range of 8–11 nm, among them 10–11 nm range particles were large volume, which are approximately 31% among total volume. The highest nanoparticle diameter was observed about 12 nm, which is less than the primary average diameter (13 nm). Therefore, most of the particles were either broken or eroded by 2 h of ultrasonication. The TEM microstructure of Al_2O_3 –water nanofluid after 2 h of ultrasonication on a 50 nm scale with particle size measurements is shown in Figure B3 (Appendix B).

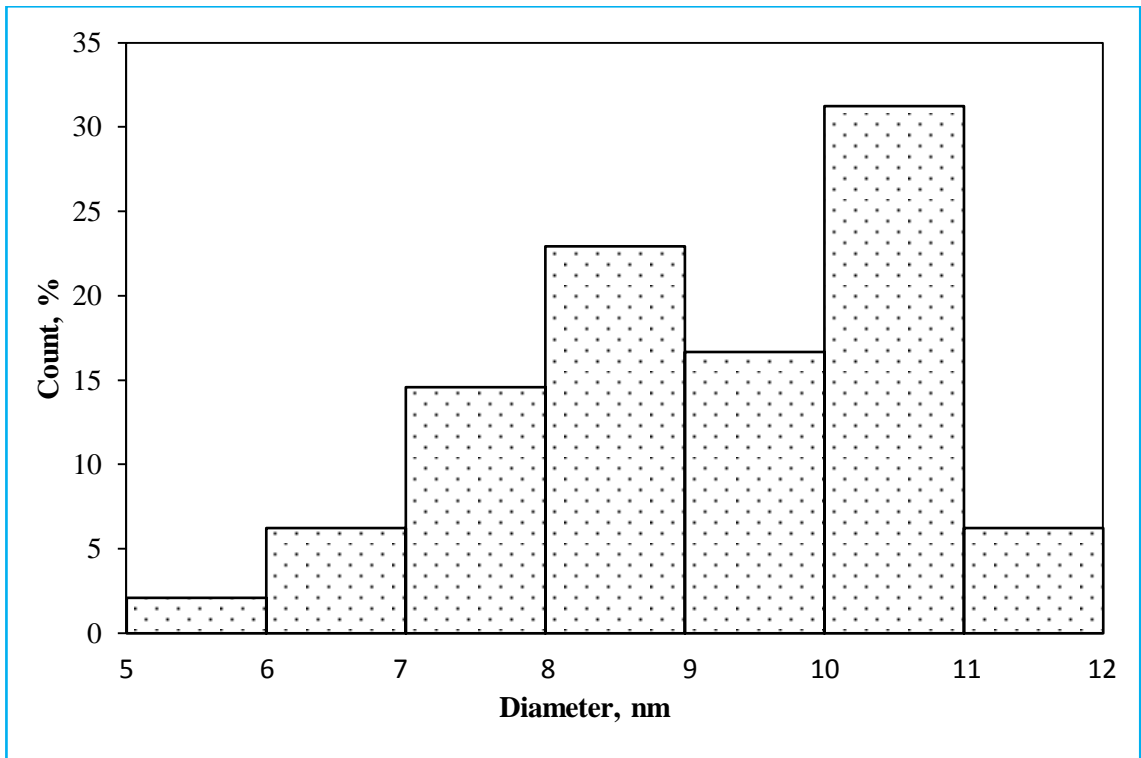


Figure 4.11: Histogram of individual particle diameter after 2 h of ultrasonication duration.

The histogram of particle sizes after 3 h of ultrasonication is shown in Figure 4.12. It can be seen from Figure 4.12 that after 3 h of ultrasonication, the particle sizes were again decreased. Most of the particles were within the range of 7 to 10 nm, which are the 70% to total population. Moreover, a 30% of total particles were within 8–9 nm diameter sizes. The TEM micrograph of the nanofluid after 3 h of ultrasonication on a 50 nm scale with particle size measurements is shown in Figure B4 (Appendix B).

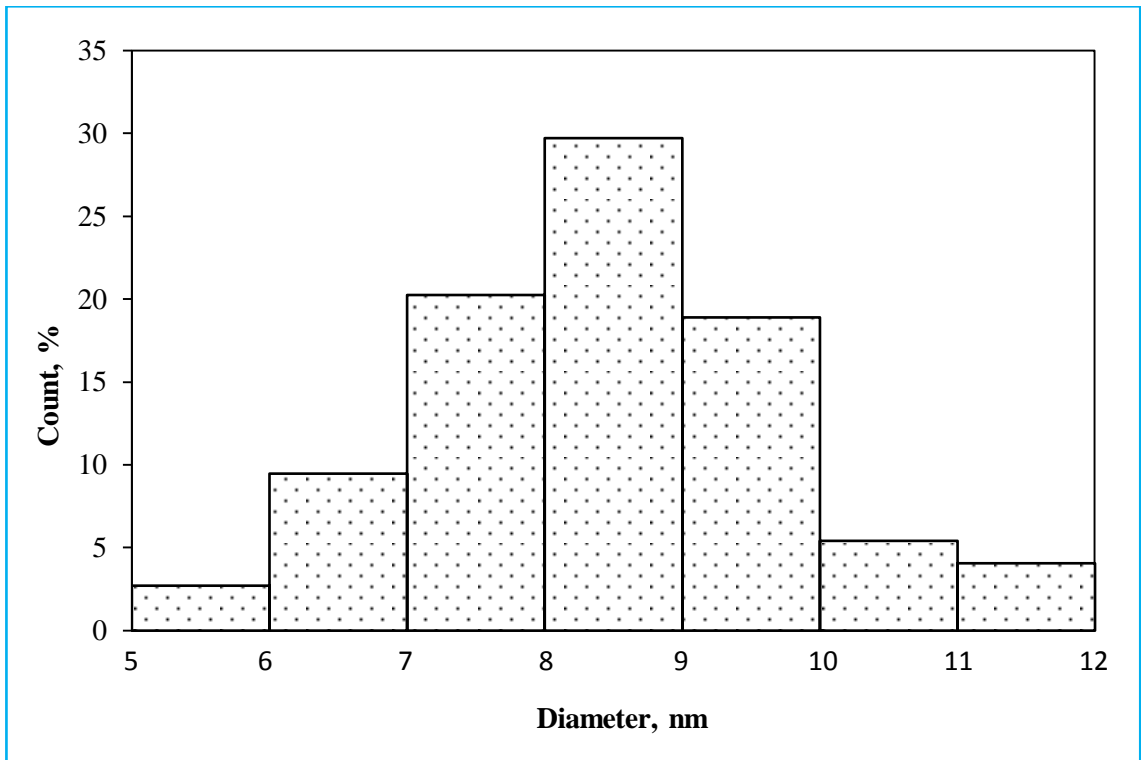


Figure 4.12: Histogram of individual particle diameter after 3 h of ultrasonication duration.

Figure 4.13 represents the histogram of particle sizes after 4 h of ultrasonication. Almost similar range of particle sizes reported in Figure 4.12 for 3 h of ultrasonication has been observed. However, here more than 75% of nanoparticles are within 7–10 nm range and about 32% of nanoparticles were in 8–9 nm range. Therefore, until 3 h of ultrasonication, nanoparticles diameters were rapidly decreased after that, no significant decrease of size with further sonication. The TEM microstructure of Al_2O_3 –water nanofluid after 4 h of ultrasonication on a 50 nm scale with particle size measurements is shown in Figure B5 (Appendix B).

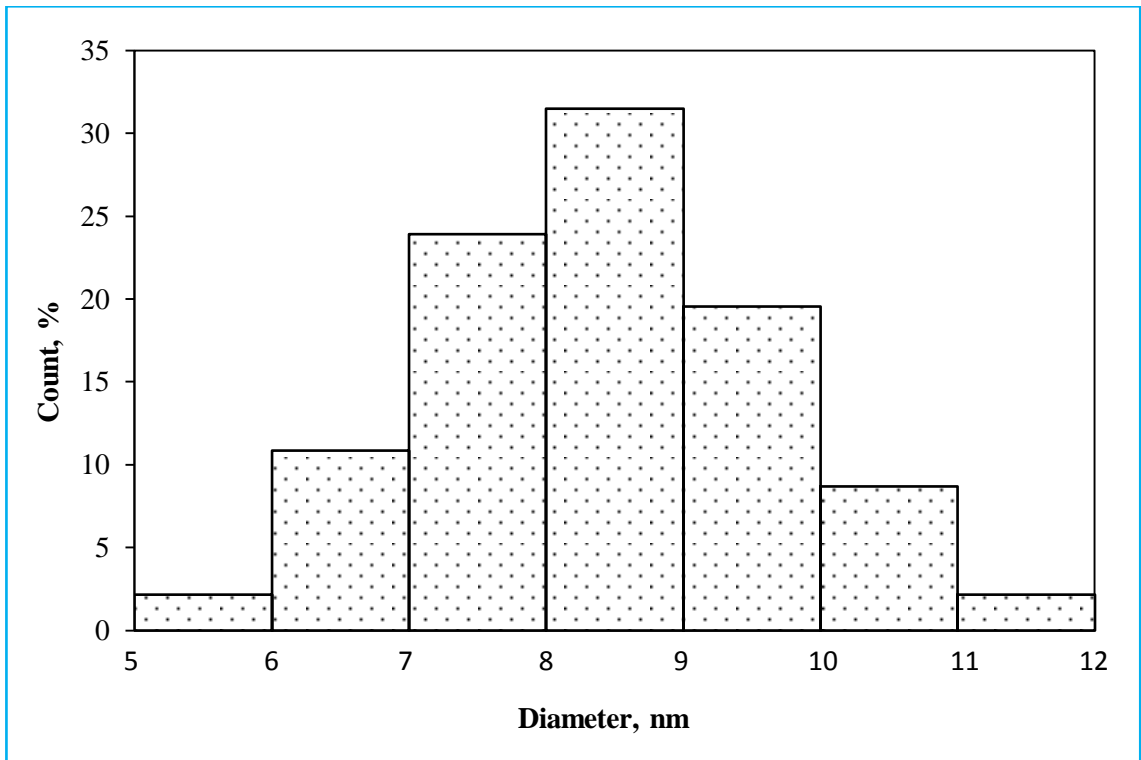


Figure 4.13: Histogram of individual particle diameter after 4 h of ultrasonication duration.

The histogram of particle sizes after 5 h of ultrasonication is reported in Figure 4.14. After 5 h of ultrasonication, most of the particle diameters were within the range of 7–10 nm and about 75% of total population was within this range. Furthermore, highest level of distribution (about 31% of particles) was in 8–9 nm range, which is almost similar that reported in Figure 4.12 and 4.13 for 3 and 4 h of ultrasonication, respectively. Therefore, even after 5 h of ultrasonication, the particles' diameter did not reduce from that of 3 h of ultrasonication. Nevertheless, the distribution of particles with a diameter less than 7 nm was observed to higher and particles having the diameter over 10 nm was found to be lower after 5 h of ultrasonication in comparison to that of 3 and 4 h of sonication. The TEM micrograph of the nanofluid after 5 h of ultrasonication on a 50 nm scale with particle size measurements is shown in Figure B6 (Appendix B).

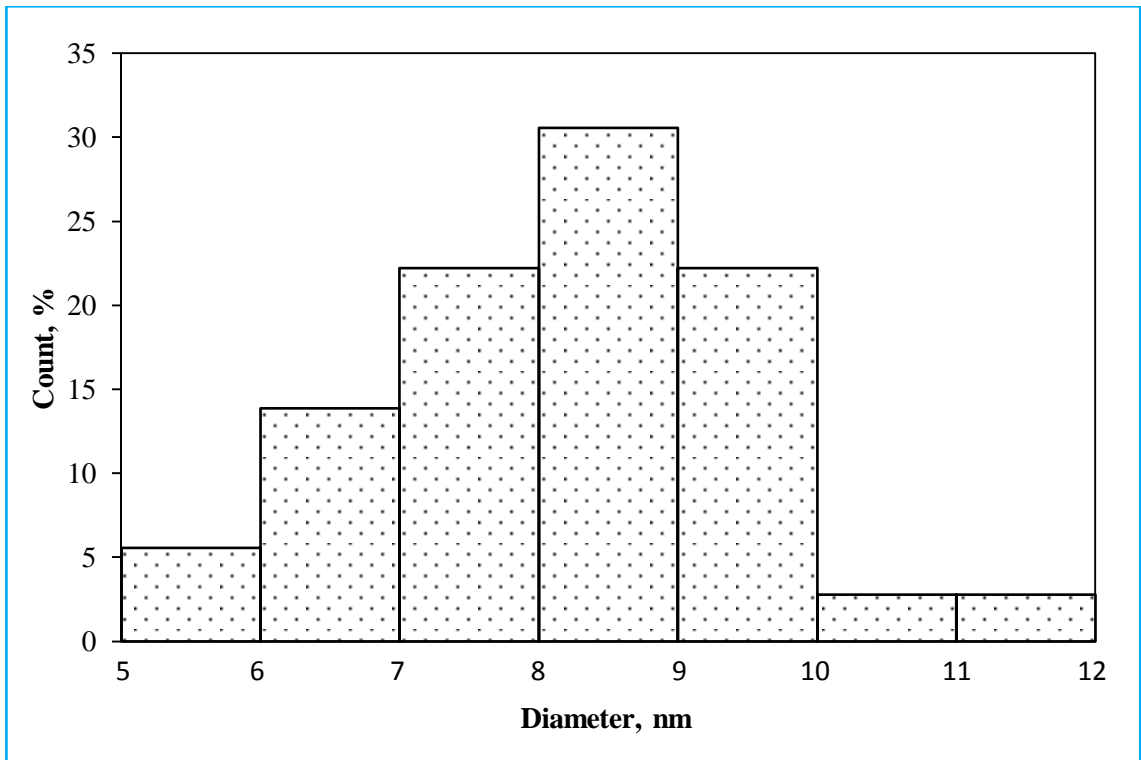


Figure 4.14: Histogram of individual particle diameter after 5 h of ultrasonication duration.

The final particle sizes (average) of Al₂O₃-nanofluid after each sonication is plotted in Figure 4.15. It can be seen in Figure 4.15 that the average nanoparticle size decreased with the increasing ultrasonication duration. An almost linear decreasing trend of particle size was observed up to 3 h of ultrasonication and the average final particle size was found to be 8.32 nm ± 0.05 nm after 3 h of ultrasonication. Therefore, this study supports the statement of Yang et al. (2006), who reported that prolonged ultrasonication time affects the size and aspect ratio of particles, which is more significant for nanotubes because of their larger particle length. However, with further ultrasonication, the average particle size was found to be same. Lee et al. (2008) reported that after 5 h of ultrasonication, most particles were smaller than the initial size of 30 nm ± 5 nm. However, the particle size is looked like 10 nm for their reported TEM image in the 50 nm scale (Lee et al., 2008).

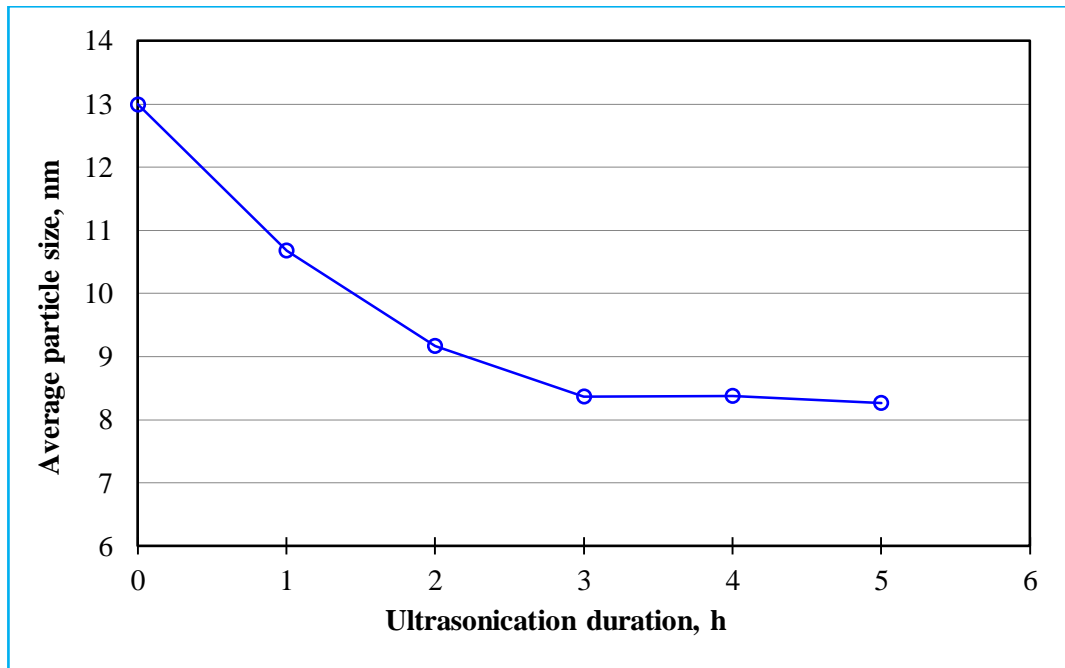


Figure 4.15: Average final particle sizes of Al₂O₃ nanoparticles after different durations of ultrasonication.

4.3.2 Aggregate size

There is uncertainty in the microstructure of nanofluids taken by TEM because this technique analyses a very small amount of sample. Even full sample could be observed at a time. Therefore, a Zetasizer instrument was used to analyze the aggregation of particles using the photon correlation spectroscopy (PCS) method. The effect of the ultrasonication process on PSD was measured for 1, 2, 3, 4, and 5 h of ultrasonication with 25% and 50% amplitude and reported in Figure 4.16. Figure 4.16 (a), (b), (c), (d), and (e) stand for 1, 2, 3, 4, and 5 h of ultrasonication with 25% amplitude and Figure 4.16 (f), (g), (h), (i), and (j) stand for 1, 2, 3, 4, and 5 h of ultrasonication with 50% amplitude. Considering the initial particle size (13 nm), the aggregated state of the nanoparticles can be observed through the PSD results presented in Figure 4.16. The aggregation is also evident in the FESEM image shown in Figure 4.2. According to the distributions in Figure 4.16, the largest particle aggregate detected by the Zetasizer device is approximately 200–250 nm. However, the frequency of such a large aggregate

is very low compared to that of smaller aggregate within the base liquid. Based on the analyses performed for each case in Figure 4.16, the range for the particle aggregate size has been obtained between 42–300 nm, approximately, depending on the ultrasonication duration and amplitude.

In addition to the aggregate size, their distribution characteristics are of great importance, as well. It is realized from Figure 4.16 that the PSDs of the samples ultrasonicated at 25% amplitude are mostly narrower than those for 50% amplitude, for the same ultrasonication duration. This result becomes more pronounced for longer ultrasonications. For a given ultrasonication duration, the only variable in the comparison for the character of PSDs is the ultrasonication amplitude. Hence, it can be concluded from Figure 4.16 that higher amplitude results in a more effective ultrasonication yielding smaller particles. However, for the PSD-sensitive and narrow PSD requiring applications, smaller amplitudes may be preferred, considering the advantages and drawbacks of having a slightly larger but narrower PSD.

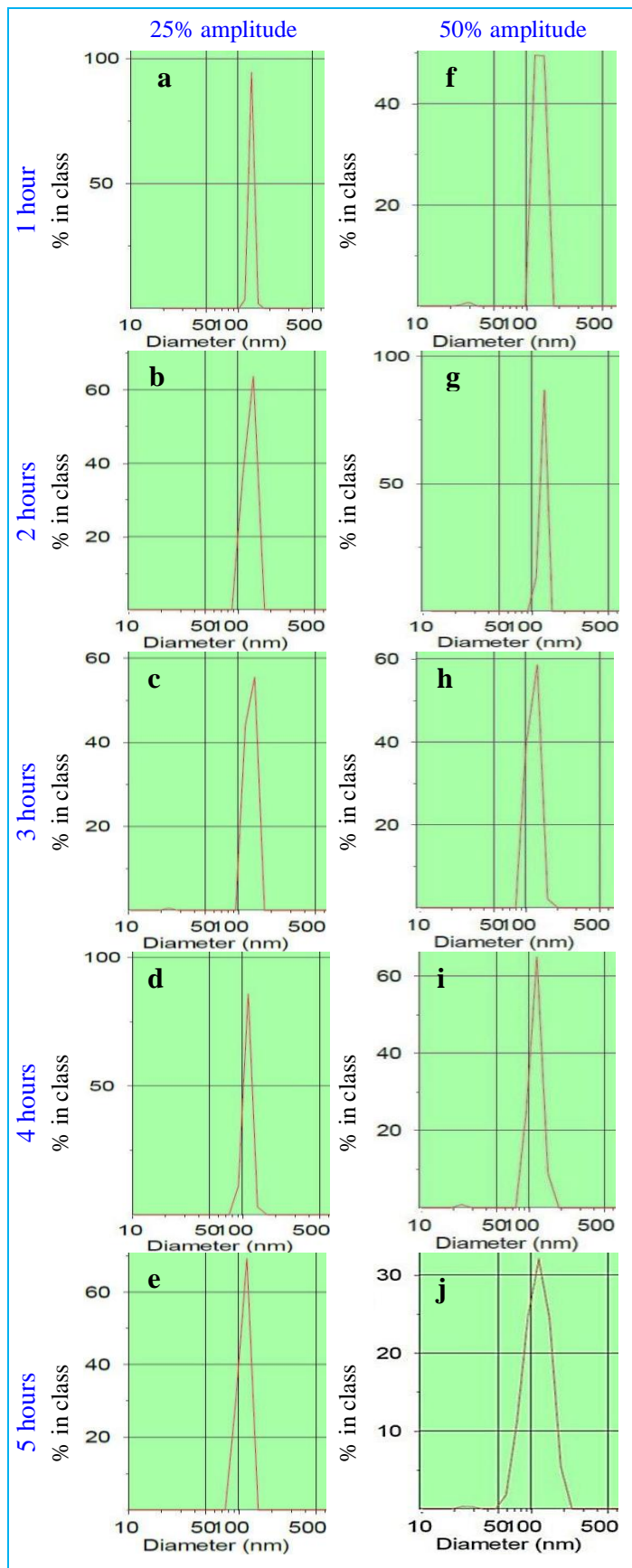


Figure 4.16: Particle size distribution (based on intensity) of Al_2O_3 nanoparticles at different durations of ultrasonication with different power amplitudes.

The average aggregate size variation with ultrasonication duration at different amplitudes is provided in Figure 4.17. As illustrated in Figure 4.17, the average cluster size decreased with increasing ultrasonication duration. As the ultrasonication duration increases, the total amount of ultrasonication energy that the sample is subjected to increases, according to the relation $E = P \times t$, where E , P , and t stand for the total amount of energy delivered to the suspension, the applied power, and the total amount of time (Taurozzi et al., 2012). Having quantitatively realized the nanoparticle aggregation through PSD analyses, reduction in the average particle size can be observed for increasing ultrasonication durations from 1 to 5 h. In addition, the higher the amplitude, the lower the aggregate size was observed. However, after 5 h of ultrasonication, the cluster size was almost same for the nanofluids prepared by 25% and 50% amplitudes. This phenomenon could be because the lowest attainable cluster size was reached after 5 h and further ultrasonication may not decrease the cluster size. Such as criteria have been reported in literature (Chen et al., 2007b; Chung et al., 2009).

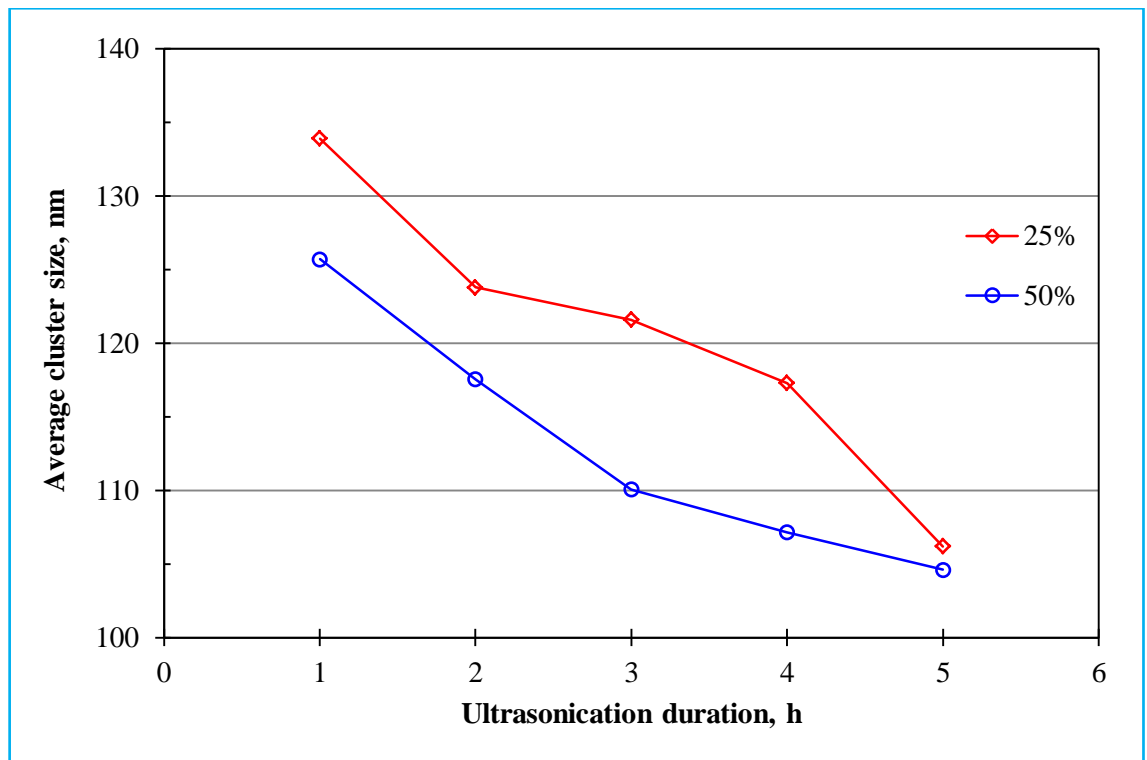


Figure 4.17: Average cluster sizes of Al_2O_3 nanoparticles after varying ultrasonication durations, at 25% and 50% amplitudes.

The cluster size distributions of Al_2O_3 nanoparticles after different durations of ultrasonication with 50% amplitudes are shown in Figure 4.18. The distribution curves are plotted in a single figure to understand the effect of ultrasonication duration on aggregate sizes. Only the 50% amplitude is considered here to concentrate only on the effect of the sonication period. From the Figure 4.18, it is observed that the highest aggregates were about 300 nm but within the range of distribution from 92–300 nm for 0 h of ultrasonication. The TEM images of Figure 4.3 were also evidence of large aggregation of particles for 0 h of ultrasonication. The narrowest distribution was observed for 2 h of ultrasonication, which was approximately 70–168 nm. Even best dispersion and very few clusters were observed for in the TEM micrograph of Figure 4.5 for 2 h of ultrasonication. The most broad distribution range was observed for 0 h and followed by 5 h of ultrasonication, which were approximately 92–300 nm and 42–210 nm, respectively. Because of the longest duration (5 h), a wide range of aggregation

is created. Most agglomerations were broken down, but some small clusters could have coalesced again with prolonged ultrasonication (Kwak & Kim, 2005).

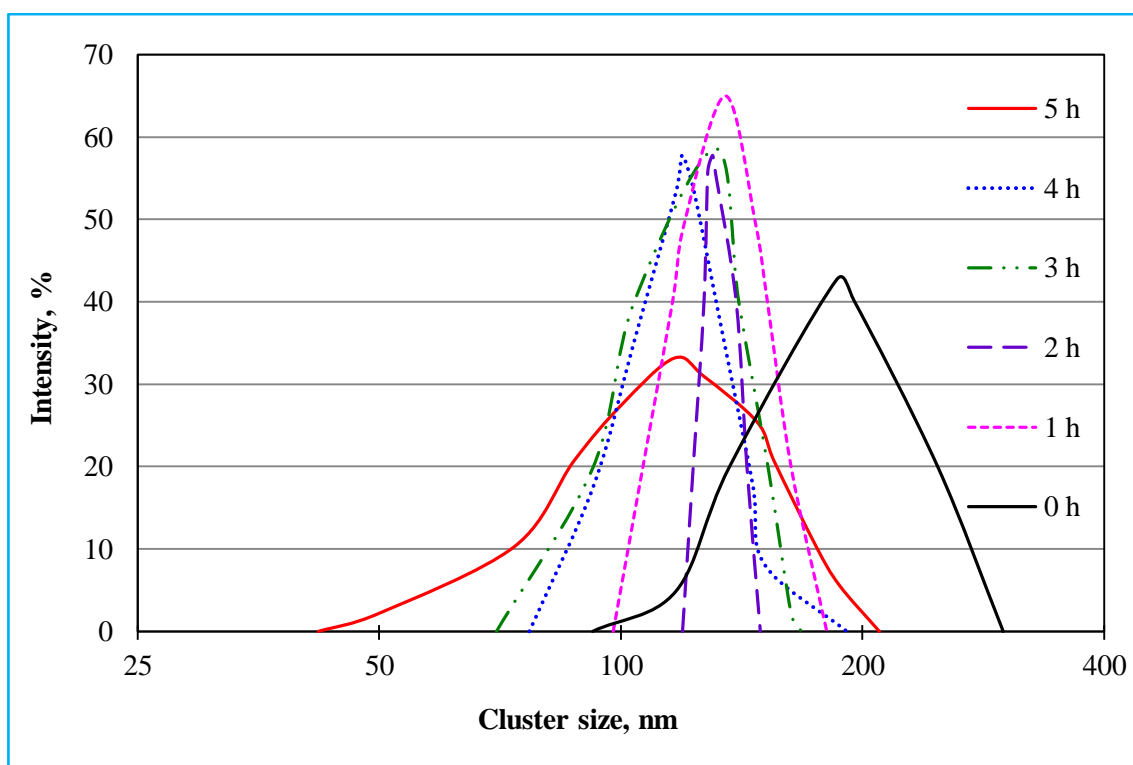


Figure 4.18: Distribution of cluster sizes of Al_2O_3 nanoparticles after different ultrasonication durations with 50% amplitudes.

The effect of ultrasonication duration on the average cluster size is reported in Figure 4.19. Some more PSD results were brought here for some of the intermediate durations of ultrasonication of this study (e.g., 0.5, 1.5, 2.5, 3.5, and 4.5 h). It can be seen in Figure 4.19 that the aggregation size decreased with increasing sonication time. The average cluster size rapidly decreased with the start of sonication. The aggregation of nanoparticles started breakdown with the ultrasonication vibration. Initially, the decreasing rate of aggregation size was found to be higher. After a certain duration, the rate of decrease was lower. As the ultrasonication duration increases, the total amount of ultrasonication energy that the sample is subjected to increases the total amount of energy and delivered to the suspension. In this study, the average cluster size decreased

from 212 nm (for 0 h, i.e., without ultrasonication) to 139 nm with 0.5 h of ultrasonication. However, with further ultrasonication, the average aggregate size was slowly decreased after 0.5 h of ultrasonication. For example, it was found to be 126 nm for 1 h of ultrasonication yet it was 105 nm for 5 h of sonication. Therefore, during the first 1 h of ultrasonication, average cluster size decreased 86 nm (212–126 nm) but after 1 h of ultrasonication by using 4 h of further ultrasonication (from 1 to 5 h) the aggregate size reduced only 21 nm (126–105 nm). Sadeghi et al. (2014) also found the similar trend of decreasing rate of cluster size with ultrasonication and reported that during first 0.5 h cluster size rapidly decreased and after that almost constant. The result of this study is compared with the outcomes of Sadeghi et al. (2014), and portrayed in Figure 4.19. It is observed that the average cluster sizes were obtained by Sadeghi et al. (2014) was higher than the result of this study. It may be because their primary nanoparticle size was 25 nm diameter and the nanoparticles may have initially high level of agglomeration as seen in Figure 4.19. Their achievable minimum cluster size was about 158 nm for 3 h of ultrasonication for Al_2O_3 -water nanofluid. Nevertheless, Nguyen et al. (2011) found 150 nm of cluster size only after 180 s of ultrasonication and their primary size of nanoparticle was 13 nm. Chen et al. (2007b) found a lowest aggregate size of ~140 nm for TiO_2 nanoparticles after 20 h of ultrasonication, where the primary particle size was 25 nm. Therefore, aggregate size depends more on initial primary size than the sonication power (Özcan-Taşkin et al., 2009).

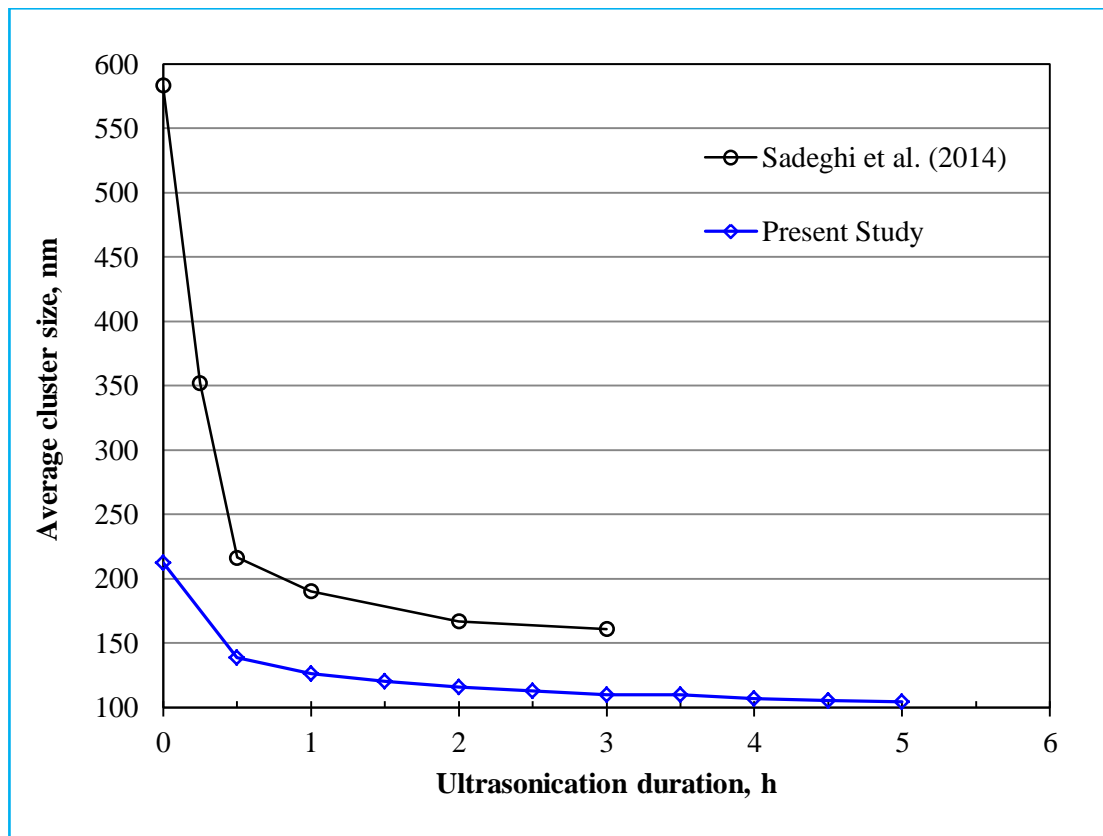


Figure 4.19: Average cluster sizes of Al₂O₃ nanoparticles after different durations of ultrasonication.

4.3.3 Polydispersity index

The relation of ultrasonication durations on the polydispersity index (PDI) has studied for 50% amplitude sonicator power, and reported in Figure 4.20. From the Figure 4.20, it can be seen that the highest PDI value was found to be 0.34 for the nanofluid prepared without ultrasonication (0 h). The PSD results of Figure 4.18 also support it as the range of cluster size for nanofluid prepared by 0 h of ultrasonication was 92–300 nm, which is the widest range among the results. The TEM images of Figure 4.2 also show that there were a large number of agglomerations were existed for the nanofluid prepared by 0 h of ultrasonication. The results of average particle size after ultrasonication reported in Figure 4.9 (a) also support it, as broad sizes (6–20 nm) of particles were existed for 0 h of sonication. PDI was decreased with the increase of ultrasonication duration until 2 h and the lowest PDI value was found to be 0.22 for 2 h of ultrasonication. The

distribution of agglomerate sizes reported in Figure 4.18 also supports the above result. The cluster sizes of nanoparticles for 2 h of sonication were within the range of 119 to 150 nm, which is the smallest range among the results. The TEM images of Figure 4.5 show that there were fewer clusters of particles after 2 h of ultrasonication. Further ultrasonication after 2 h show that PDI was increased with sonication periods. The results of Figure 4.18 show that the range of the cluster sizes of nanoparticles were further increased after 2 h of ultrasonication. It is known that ultrasonication can break down the cluster, however; further agglomeration could be the result of prolonged ultrasonication (Taurozzi et al., 2012). Moreover, longer ultrasonication could agglomerate the nanoparticles again. The similar trend has also been reported in literature (Kwak & Kim, 2005). The PDI results of this study were also compared with other published results of Sadeghi et al. (2014) and portrayed in Figure 4.20. They found that PDI of Al₂O₃ nanoparticles was decreased with the increase of the sonication period. They reported a rapid decrement of PDI with the start of ultrasonication until 15 min after which PDI decreased slowly and after 3 h of ultrasonication, the PDI became approximately 0.15.

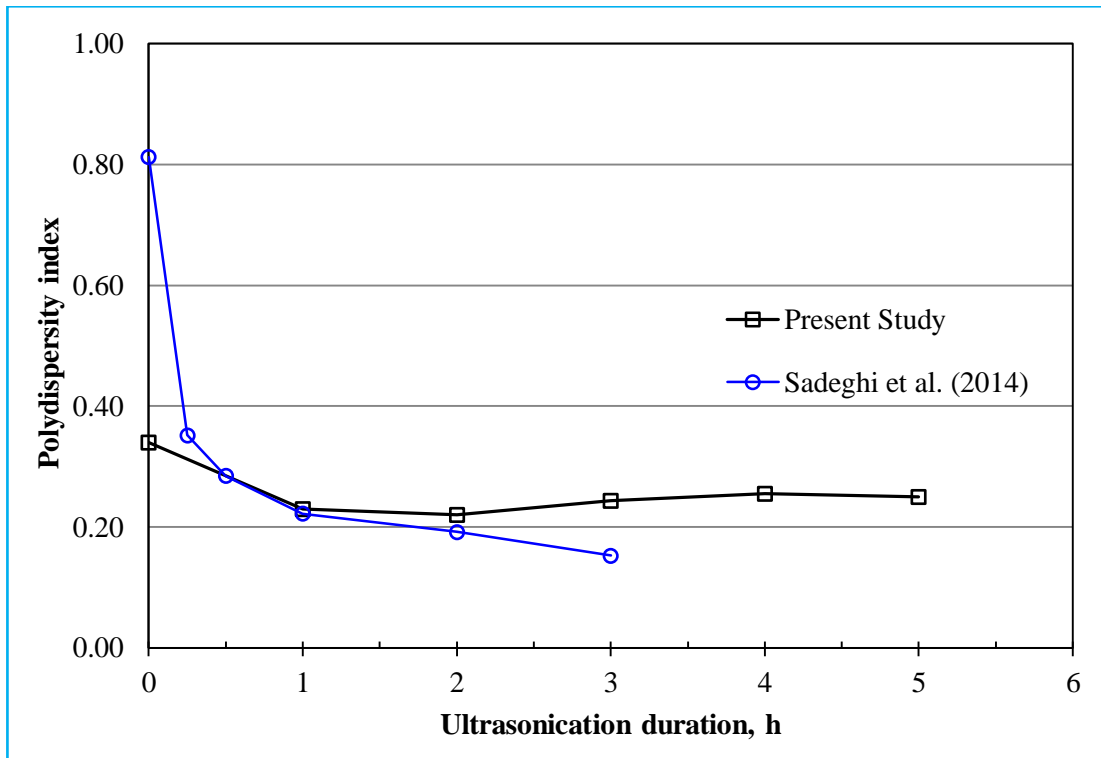


Figure 4.20: Polydispersity index after varying ultrasonication durations.

4.3.4 Zeta potential

Zeta potential was measured for each sample to quantify the stability of the nanofluid. The zeta potential of the 0.5 vol.% of Al_2O_3 -water nanofluid have been investigated for 1, 2, 3, 4, and 5 h of ultrasonication durations and with 25% and 50% sonicator amplitudes. The results are illustrated in Figure 4.21, together with the limits of excellent and physical stability (Müller, 1996). As it is apparent in Figure 4.21, the zeta potential of the sample is always lying on the maximum limit of the physical stability and is approaching the excellent stability. In this study, the highest zeta potential value 58.4 mV was observed for 3 h of ultrasonication with 50% amplitude of power and further sonication until 5 h could not increase the value. In the case of 25% amplitude, the zeta potential value was slowly increased until 5 h of sonication and the highest value was 57.5 mV at this ultrasonication period. Therefore, it could be predicted that with 50% amplitude, the nanoparticles received highest ultrasound energy at 3 h of duration. However, in the case of 25% amplitude, the ultrasound energy was effective

until 5 h period. Almost similar types of trends were also observed in TEM microstructures of Figure 4.4 where nanoparticles ultrasonicated with 25% amplitudes were not properly homogenized due to the lack of sufficient sonication power. Again, the result of average particle size after each ultrasonication reported in Figure 4.15 show that particle sizes were not changed after 3 h of ultrasonication (with 50% amplitudes). It can be predicted that for longer ultrasonication durations with 25% amplitudes, the zeta potential value can increase and may shift to the excellent stability range. Nevertheless, the electro-dynamic stability of the prepared samples can be considered as outstanding.

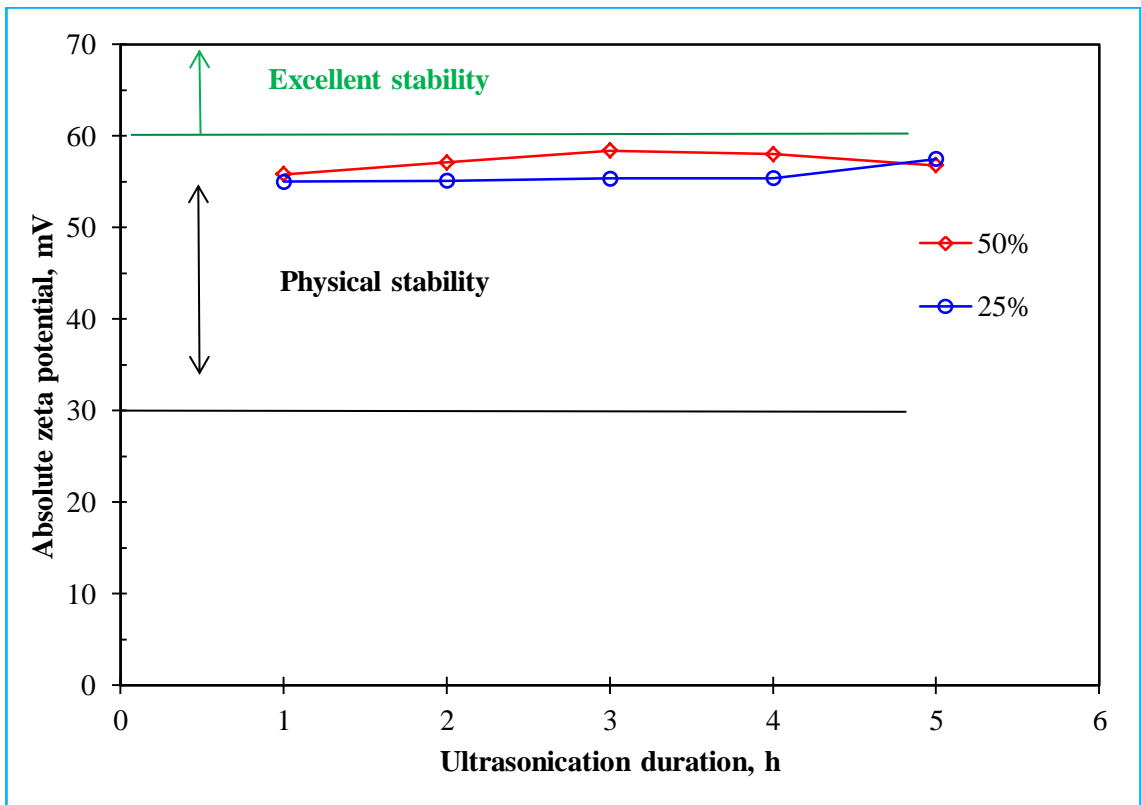


Figure 4.21: Absolute zeta potential of Al_2O_3 -water nanofluid after different durations of ultrasonication at 25% and 50% amplitude.

As highest zeta potential was found to be 58.4 mV for 3 h of ultrasonication with 50% amplitude of sonicator power, therefore, to investigate whether the peak value of zeta

potential some more intermediate duration before 3 h of ultrasonication was considered for analysis. The zeta potential values of 0, 0.5, 1, 1.5, 2, 2.5, 3, 4, and 5 h of ultrasonication is shown in Figure 4.22. Again, the absolute zeta potential value was found to be increased accordingly with ultrasonication duration up to 3 h as seen in Figure 4.22. With the starting of ultrasonication, zeta potential increases to a higher value and further ultrasonication it rises slowly. Highest zeta potential value was found to be 58.4 mV for 3 h of ultrasonication. Kwak and Kim (2005) found the highest absolute zeta potential value about 50 mV for 9 h of sonication whereas further ultrasonication until 30 h could not increase the value. Lee et al. (2008) found about 34.5 mV zeta potential for 5 h of sonication. They observed that further ultrasonication, zeta potential was decreased.

A comparison was drawn between the values of zeta potential after 1 day and after 30 days of preparation. It was observed that, after 30 days, the zeta potential values decreased and the difference between 1 day and 30 days were higher for lower sonication time. Thirty days after preparation, the absolute value was found to be 15 mV for the sample prepared without sonication (termed as 0 h). Even after 30 days of preparation, the absolute zeta potential value was found to be 56.8 mV for an ultrasonication duration of 5 h that is the same value observed after 1 day of preparation with this period of sonication. Therefore, longer sonication durations increased the stability of the nanofluid. It is pronounced that absolute zeta potential values over 60 mV indicate excellent stability, those above 30 mV indicate physical stability, those below 20 mV indicate limited stability, and those lower than 5 mV are evidence of agglomeration (Müller, 1996). Hence, the electro-dynamic stability of the prepared samples can be considered as outstanding. Furthermore, the experimental results of this study were also compared with other published results of Sadeghi et al. (2014) and

plotted in Figure 4.22. However, they studied until 3 h of sonication and measured the zeta potential immediately after the preparation of samples. They reported that the zeta potential values were continuously increased accordingly with sonication time. They observed the highest zeta potential value of 52 mV for 3 h of ultrasonication. Based on their results, it could be predicted that further ultrasonication after 3 h will increase the zeta potential value. However, they did not mention the used amplitude of sonicator power. Moreover, they diluted the concentration during the measurement of this electrostatic charge.

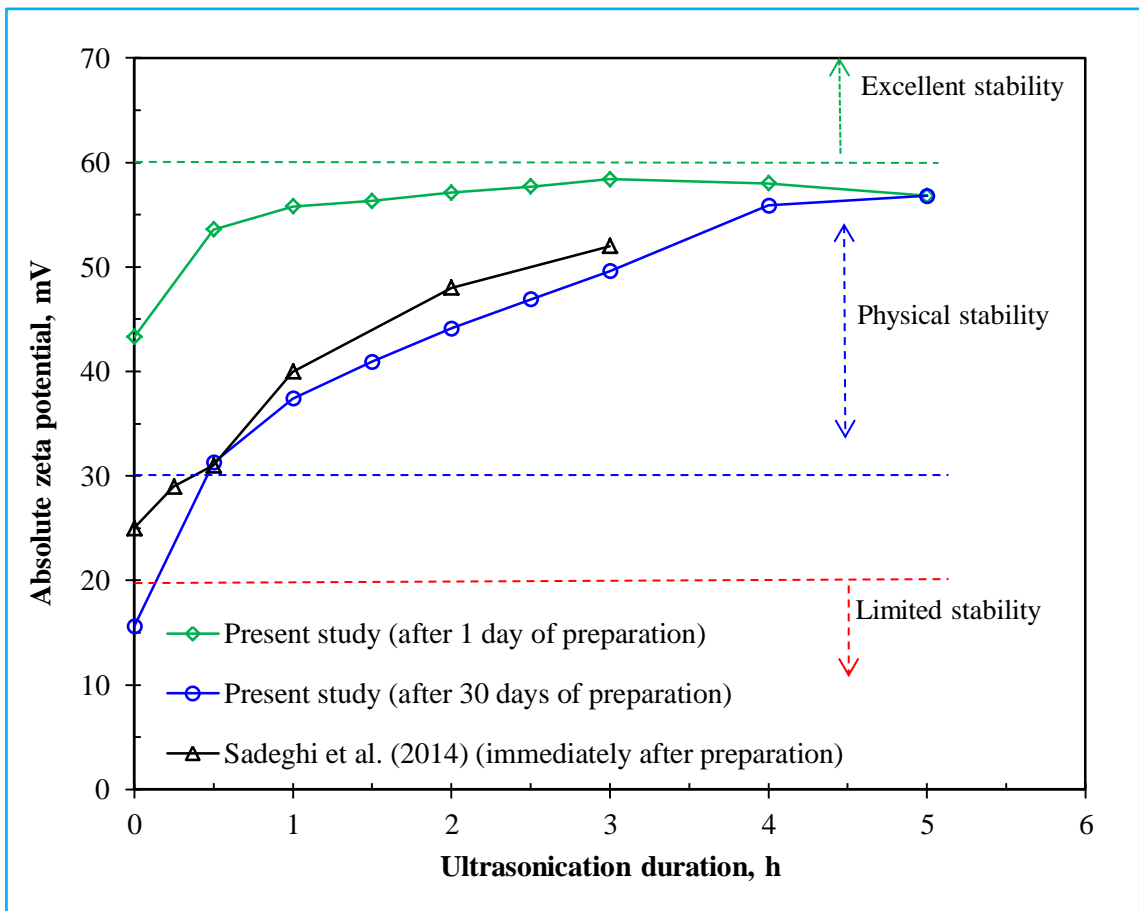


Figure 4.22: Absolute zeta potential of Al_2O_3 -water nanofluid after different durations of ultrasonication.

The pH of the specimens were measured at 25 °C and reported in Figure 4.23. The pH of the samples was found to be 5.1 ± 0.1 for the nanofluids prepared by different durations of ultrasonication. However, the pH of nanofluid prepared without ultrasonication was found to be 5.6 ± 0.2 . Lee et al. (2008) was found a pH of 6.04 and Chandrasekar et al. (2010) found to be around 5 for Al₂O₃-water nanofluid at 25 °C. This minor difference of the pH values of this study with the values reported in literatures (Chandrasekar et al., 2010; Lee et al., 2008) may be because of the variation of particle concentration and source of nanoparticle, which is related to the percentage of composition. Xie et al. (2008) measured the isoelectric point of Al₂O₃ nanoparticles and found to be 9.2. The author urged that if the pH of a suspension is far from this isoelectric point, then the nanoparticles are expected to be well dispersed as the repulsive forces of nanoparticles are increased. On the other hand, if pH value is near to 9.2, then the repulsive forces among nanoparticles are decreased and lead to coagulation and aggregation of nanoparticles. As there is an extreme distance between the obtained pH of this study with the isoelectric point, therefore, the nanofluid could be considered as stable. The zeta potential values of this study reported in Figure 4.21 and 4.22 provide more evidence in support of the above statement.

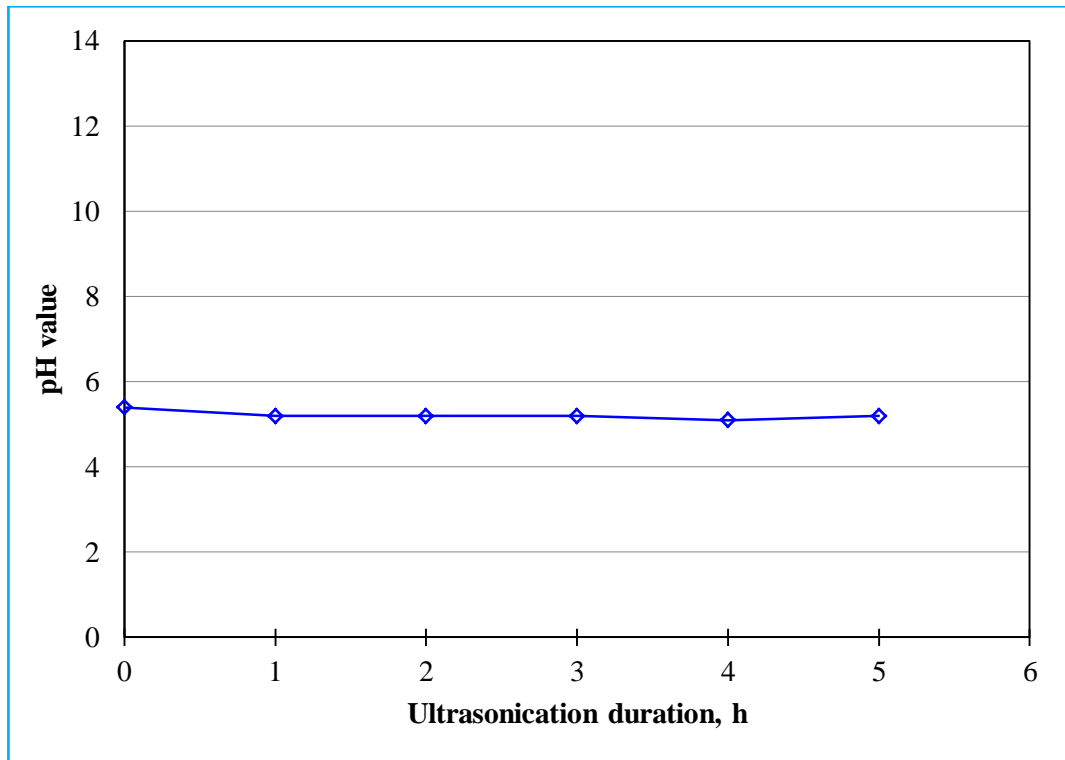


Figure 4.23: pH value of Al_2O_3 -water nanofluid after different durations of ultrasonication at 50% amplitude.

Based on the above analysis it is determined that higher amplitude is better for colloidal dispersion. Based on this study, 50% amplitude is the highest limit of the sonicator that will be kept for the following experiments. Another important parameter is the optimum ultrasonication duration need to be used for better dispersion of nanofluid. The TEM, PSD, and zeta potential prove that the optimum sonication duration was 3 h with 50% amplitude of sonicator power.

4.4 Thermophysical properties

4.4.1 Thermal conductivity

Figure 4.24 shows the effect of ultrasonication durations (as 0, 1, 2, 3, 4, and 5 h) on the thermal conductivity enhancement percentage of the Al_2O_3 - H_2O nanofluid for 0.5 volume concentration (%) of nanoparticles. It can be seen in Figure 4.24 that the

thermal conductivity enhancement percentage increased accordingly with the increase of ultrasonication duration. From the Figure 4.24, it is found that highest thermal conductivity values were obtained for the nanofluid that prepared by 5 h of ultrasonication. Thermal conductivities of nanofluid prepared by 4 h of ultrasonication were almost similar to those values for 5 h of ultrasonication. The lowest thermal conductivity values were observed for the nanofluid prepared by 1 h of ultrasonication. Even the thermal conductivities of nanofluid prepared by without ultrasonication were higher than those values for 1 h of ultrasonication. This phenomenon can be explained as without ultrasonication, the nanoparticles are not able to spread homogeneously in the base fluid and there was strong agglomeration and larger cluster size was existed. Moreover, this study was started with the measurement of thermal conductivity of 10 °C and at this low temperature; there was less motion of the nanoparticles. Furthermore, as the measurement was started just after the preparation of nanofluid, therefore, the nanoparticles do not have enough time to sediment and the strong clusters of nanoparticles could be aligned with the sensor of the thermal conductivity measurement device and higher values were observed (Zhu et al., 2006). After starting the ultrasonication, cluster sizes reduced and thermal conductivity drops (Sadeghi et al., 2014). Maximum deviation of thermal conductivity enhancement was observed about 1.90% only for the use of ultrasonication duration until 5 h. Therefore, the effect of ultrasonication duration does not have enough significations on thermal conductivity enhancement. One possible reason could be the measurement principle of transient hot wire (THW) method of KD2 pro analyzer. As heat dissipated in the wire increases the temperature of the nanofluid and measure the thermal conductivity of the sample (Paul et al., 2010). Therefore, the effect of preparation parameters are not significant in this method as small amount of sample is considered where the hot wire dissipated heat. The measured values of effective thermal conductivities at different temperatures for the

nanofluid prepared by different durations of ultrasonication have reported in Figure C1 (Appendix C).

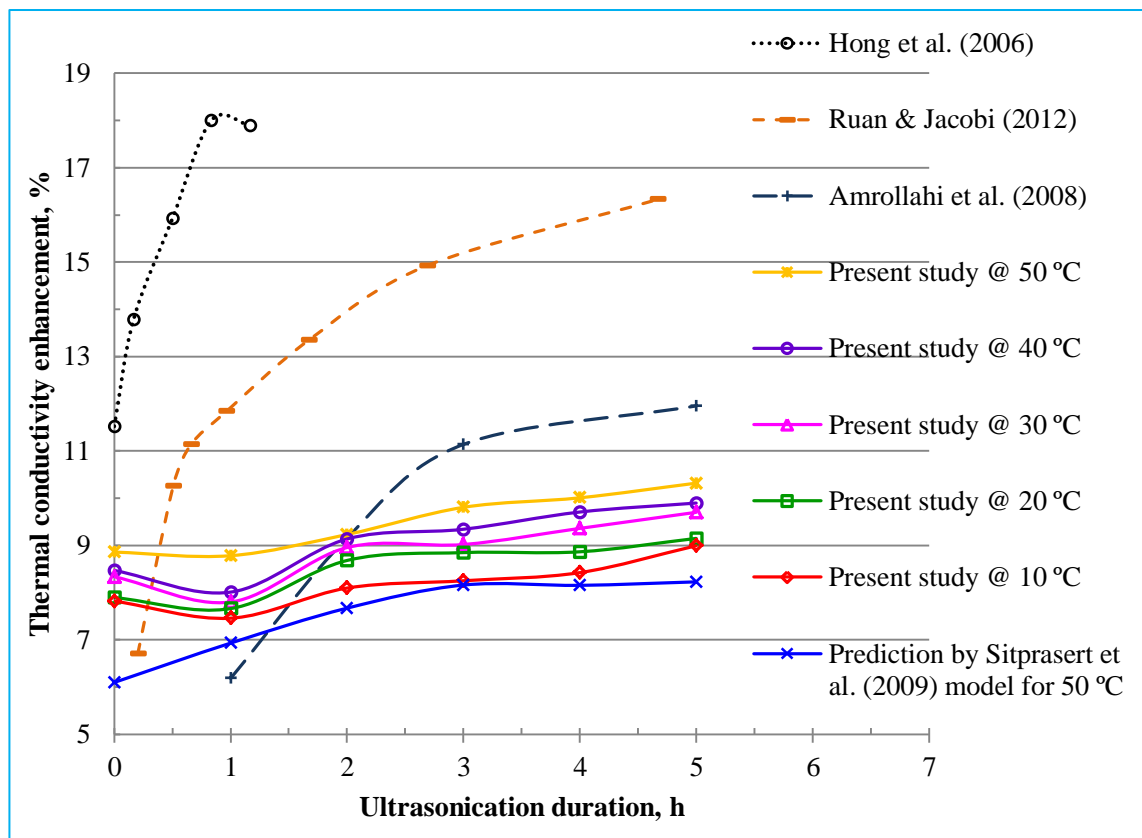


Figure 4.24: Enhancement percentage of thermal conductivity of 0.5 vol.% of Al_2O_3 -water nanofluids after different durations of ultrasonication.

The experimental results of this study were compared with the results reported in literature (Amrollahi et al., 2008; Hong et al., 2006; Ruan & Jacobi, 2012) and almost a similar trend of thermal conductivity enhancement with ultrasonication time was observed. However, thermal conductivity enhancement percentage of this study was found to be lower than the values reported by (Amrollahi et al., 2008; Hong et al., 2006; Ruan & Jacobi, 2012); even though, all the considered literatures were with 0.5 vol.% of nanoparticles. The possible reason is the variation of nanoparticles types. Hong et al. (2006) disperse 0.55 vol.% of Fe nano powder in ethylene glycol and ultrasonicated for the durations of 0, 10, 30, 50, and 70 min. They observed that thermal conductivity ratio

increased almost with a linearly trend for the nanofluid prepared by until 50 min of durations. However, thermal conductivity ratio found to be decreased for the sample prepared by 70 min of ultrasonication in comparison to that one of 50 min. As Fe has a thermal conductivity value several times higher than Al_2O_3 particle. Ruan and Jacobi (2012) and Amrollahi et al. (2008) used MWCNT that has the most highest thermal conductivity. Therefore, significantly their thermal conductivity enhancement percentage will be higher than this study. Based on these studies it could be concluded that if thermal conductivity value of a nanoparticle is too high then the effect of ultrasonication duration will be significant. Again, the outcome of this study was compared with the prediction made by Sitprasert et al. (2009) model as this correlation consider particle size and temperature effect. This prediction was based on the average particle size after each of the ultrasonication duration reported in Figure 4.15. An almost similar trend was observed for the measured and predicted thermal conductivity enhancement percentage. Average deviation of the enhancement for measured and predicted was about 2% only.

Again, the effect of ultrasonication duration on thermal conductivity ratio could be discussed according to the study of Zhu et al. (2006) about effect of particle clustering and alignment. Figure 4.25 shows the colloidal state of nanofluids. The effect of particle clustering and alignment will be significant for the nanofluids prepared with less ultrasonication durations. Figure 4.25 (a) shows the colloidal state of nanofluids prepared by without or shorter ultrasonication period, where there are strong aggregations of nanoparticles are observed. The PSD results portrayed in Figure 4.19 are evident to higher aggregation of nanoparticles at lower ultrasonication. Figure 4.25 (b) shows the colloidal dispersion of nanofluids prepared by higher ultrasonication durations and no strong aggregation is significant (refer to Figure 4.8, TEM micrograph

after 5 h of sonication), therefore, thermal conductivity values were found to be consistent.

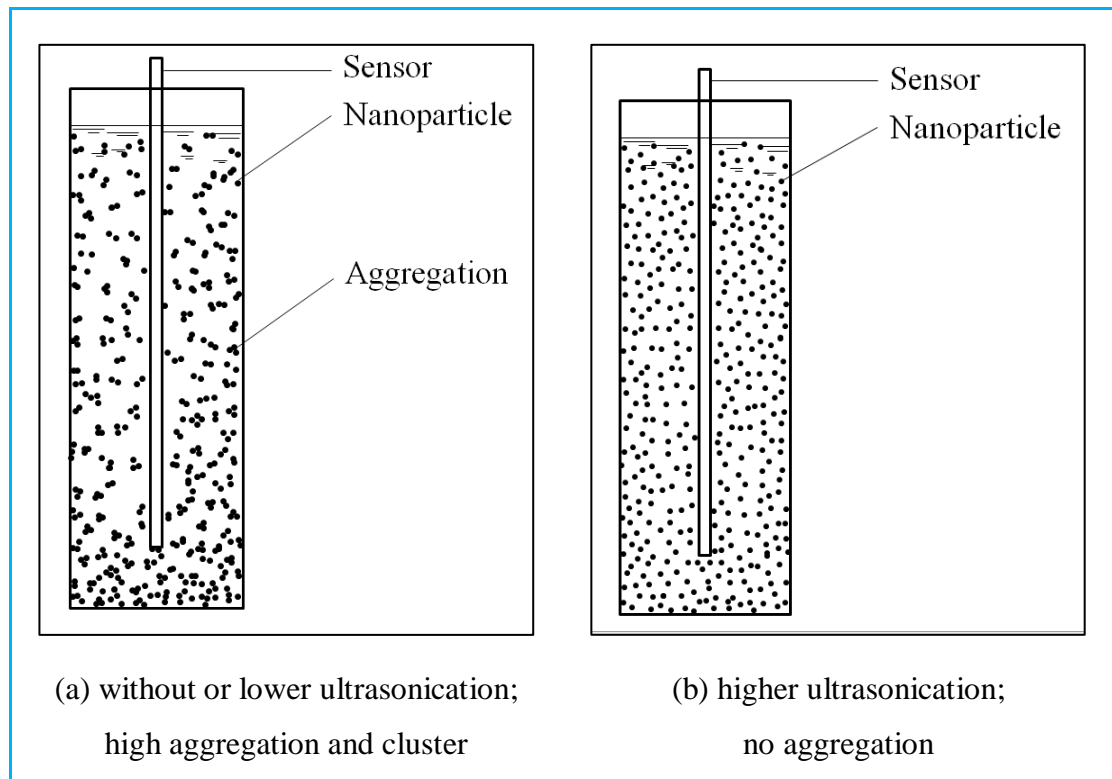
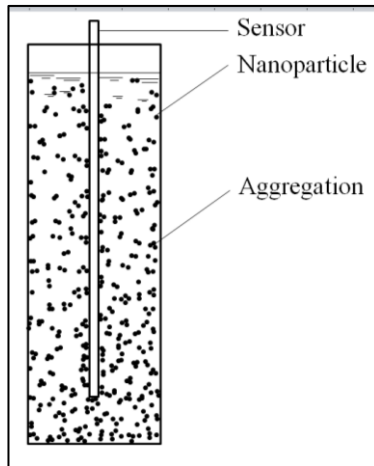
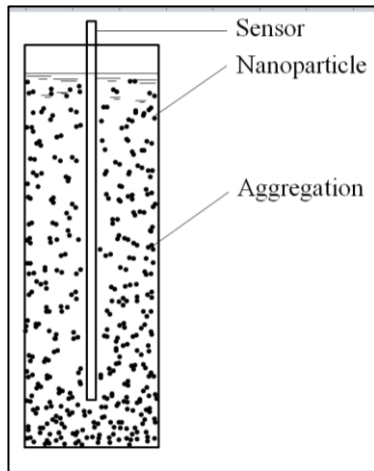


Figure 4.25: Mechanism of influence of ultrasonication duration on thermal conductivity.

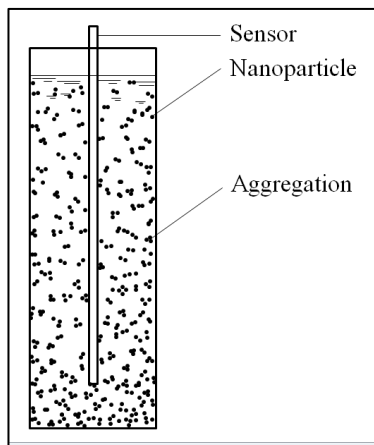
Again, the colloidal state for the nanofluids prepared by without ultrasonication or shorter periods (as portrayed in Figure 4.25 (a)) during thermal conductivity measurement could be among the three states as shown in Figure 4.26. Here in Figure 4.26 (a) shows that the clusters of nanoparticles could be very close and aligned with the thermal conductivity sensor, this will result higher thermal conductivity (Zhu et al., 2006). Again, the clusters could be apart from the sensor and lower thermal conductivity will be observed as shown in Figure 4.26 (b). Even there are chances that, the clusters will be neither as close nor so apart from the sensor as shown in Figure 4.26 (c).



(a) clusters are close to sensor;
outcome high thermal conductivity



(b) clusters are apart from sensor;
outcome low thermal conductivity



(c) clusters are neither so close nor apart
from sensor

Figure 4.26: Different colloidal states during thermal conductivity measurement for the nanofluid prepared by lower ultrasonication duration.

The phenomena stated in Figure 4.24 could be discussed again with the precision of measurements of thermal conductivity as portrayed in Figure 4.27. Figure 4.27 (a) and (b) show the precision of measurements of the thermal conductivity at 10–50 °C temperatures for the nanofluid prepared by 0 and 5 h of ultrasonication, respectively. In comparison to the Figure 4.27 (a) and (b), it is observed that the thermal conductivity values were more precise for the nanofluid prepared by higher ultrasonication. Both the Figure 4.27 (a) and (b) show that at lower temperatures, the thermal conductivity values were more precise because of fewer movements of particles. Nevertheless, at every temperature, the thermal conductivity values were almost same for the nanofluids prepared by 4 and 5 h of ultrasonication as reported in Figure 4.24. This could be discussed as with the ultrasonication of 4 and 5 h, stability of nanofluids reached to the pick level as well as thermal conductivity values showed consistent and higher.

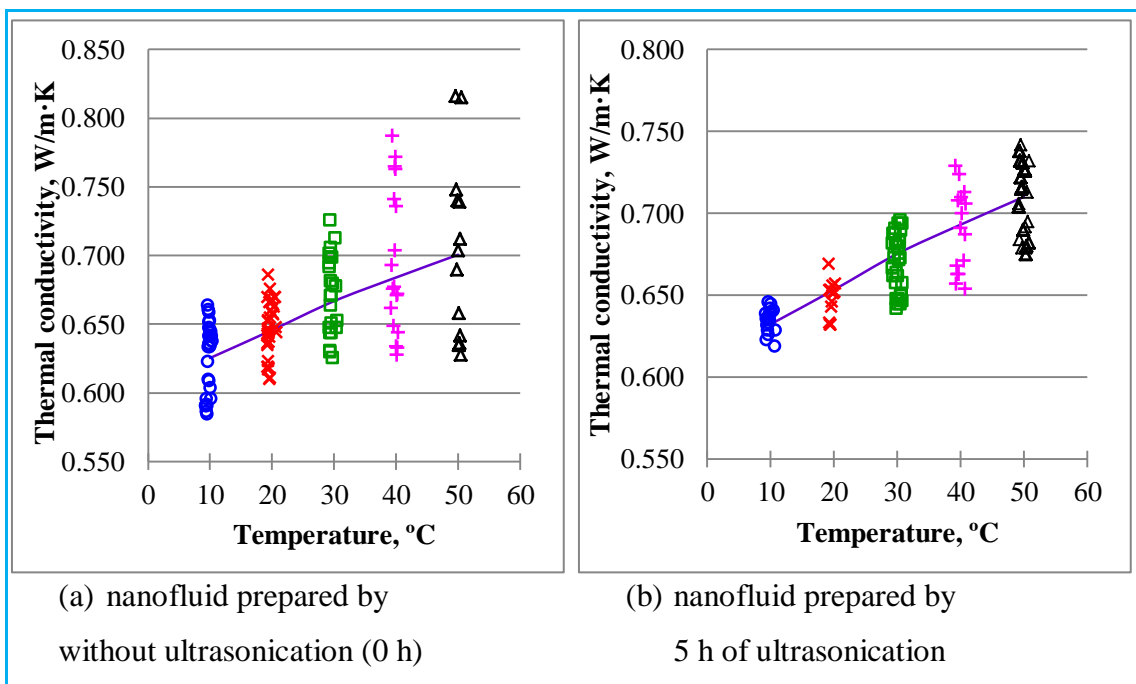


Figure 4.27: Precision of thermal conductivity measurements.

The effect of temperature on thermal conductivity enhancement percentage of nanofluids is portrayed in Figure 4.28. It can be seen in Figure 4.28 that thermal conductivity ratio increases with the increase of temperature. Higher nanofluid temperature increases the Brownian motion of nanoparticles and enhanced the thermal conductivity. However, at lower temperatures (10 and 20 °C), for the less movement of the particles, comparatively lower thermal conductivity enhancement was observed. An average increase of 1.33% of thermal conductivity enhancement was observed for the temperatures variations from 10 to 50 °C. The maximum variation was observed about 1.58% for the nanofluid prepared by 4 h of ultrasonication. Thermal conductivity increment ratio of this study was compared with some other studies reported in (Amrollahi et al., 2008; Kole & Dey, 2012; Patel et al., 2010). Among these studies, Amrollahi et al. (2008) observed the highest increment of about 7% from the temperature variation of 25 to 50 °C. This may be because of their high thermal conductivity particles (MWCNT). Kole and Dey (2012) found an irregular trend as thermal conductivity ratio decreased from 10 to 30 °C and again it increased for temperature variation of 30 to 50 °C. The result of Patel et al. (2010) for alumina–water was found to be very close with the present study. They found an increment of 3% for the temperature variation of 20 to 50 °C. Again, they observed a higher increment rate with temperature intensification for alumina–EG nanofluid.

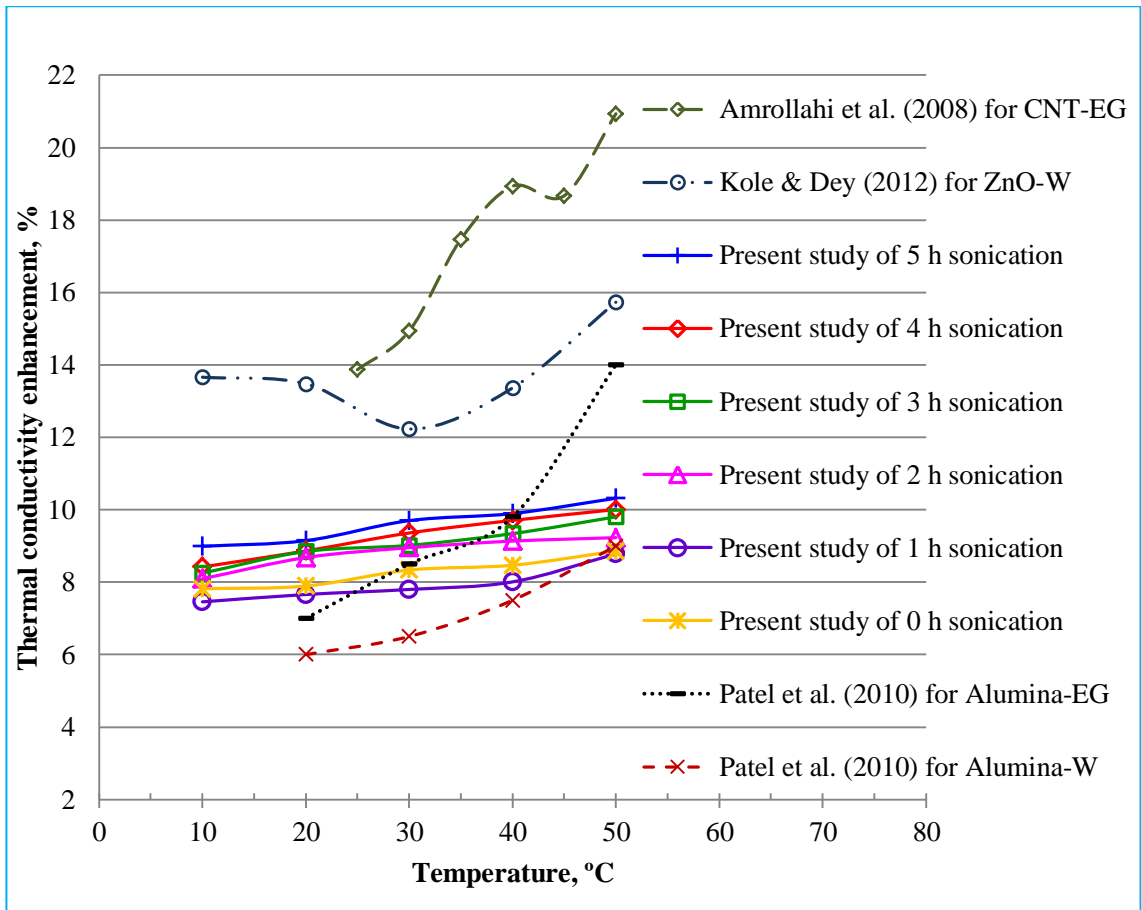


Figure 4.28: Variations of thermal conductivity enhancement with temperatures for 0.5 vol.% of particles concentration.

Again, thermal conductivity values were measured after 0, 10, 20, and 30 days after the preparation of the samples. These samples were measured only at 25 °C temperature so that the internal colloidal state may not change with temperature variation and the effect of sedimentation on thermal conductivity could be predicted. The enhancement percentage of thermal conductivities after 0, 10, 20, and 30 days of sample preparation are reported in Figure 4.29. It can be seen in Figure 4.29 that the thermal conductivity ratio was decreased with the periods sample kept. The reason is the sedimentation of particles over time. As the sedimented particles do not have participation in the flow therefore, the effective thermal conductivity values are decreased. It is found that after 30 days of sample preparation, thermal conductivity enhancement was decreased about 1.37% for the nanofluid prepared by 5 h of ultrasonication duration. However, this

decrement was found to be 1.76% for the nanofluid prepared by 0 h of ultrasonication. Therefore, the effect of ultrasonication duration was not effective over the thermal conductivity enhancement percentage. The measured values of effective thermal conductivities after 0, 10, 20, and 30 days of sample preparation have reported in Figure C2 (Appendix C). Ijam et al. (2015) studied the effective thermal conductivity value over time until seven days after preparation for graphene oxide–DIW/EG nanofluid. They observed almost constant values until seven days. The possible reasons are: the production method was different and the other important side is the viscosity of the base fluid was higher. Mostly, the higher the viscosity of the base fluid, the lower the sedimentation rate is observed.

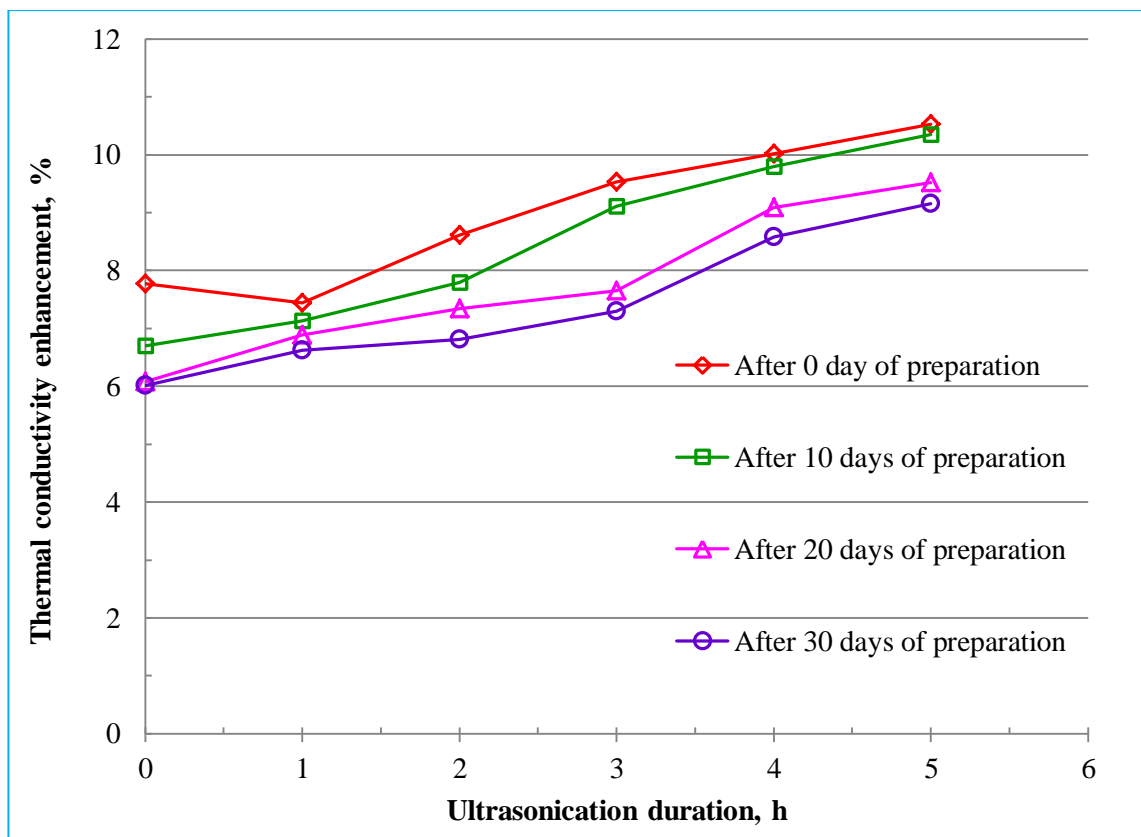


Figure 4.29: Enhancement percentage of thermal conductivity at 25 °C temperature after different durations of sample preparation.

4.4.2 Viscosity

The effects of ultrasonication durations at different temperatures on the viscosity enhancement of 0.5 vol.% of Al₂O₃–water nanofluid are shown in Figure 4.30. It is found that the viscosity of Al₂O₃–water nanofluid decreased with increasing sonication time, as shown in Figure 4.30. This trend is similar to the results obtained by Yang et al. (2006). Figure 4.30 shows that, during the 1st h of ultrasonication, viscosity decreased rapidly and further ultrasonication decreased slowly. This mechanism could be discussed with the aid of Figure 4.31. Figure 4.31 (a) shows the dispersion condition of nanoparticles for 0 h of ultrasonication (meaning without ultrasonication). Here nanoparticles are in highly clustered form and aggregated that was seen in Figure 4.3 as TEM and Figure 4.19 as PSD. These clusters are not taken part into the flow rather making resistance to flow and viscosity was increased. Figure 4.31 (b) shows a well dispersion of nanoparticles that have been started after 1 h of ultrasonication and so on. As there is less aggregation of particles, therefore, the nanoparticles take part in the flow and they create less resistance to the spindle and lower viscosity was observed. The TEM microstructure of Figure 4.4 to 4.8 also supports the above statement. As in the micrographs, it has been seen that with 1 h of ultrasonication and so on, agglomerations of nanoparticles are started to break down, however, without ultrasonication (0 h), there are strong clusters and agglomerations existed. In addition, for further ultrasonication until 5 h, the viscosity of the Al₂O₃–water nanofluid decreased slowly, approaching to the viscosity of the base fluid. The same trends were also found at different temperatures from 10 to 50 °C. At 10 °C, the viscosity of the Al₂O₃–water nanofluid without ultrasonication (0 h) was the highest compared to those of the other ultrasonicated nanofluids. This can be explained by the fact that, without ultrasonication, the nanoparticles were able to spread homogenously in the base fluid and, therefore, a strong agglomeration occurred. The viscosity enhancement was

decreased about 8–15% from 0 to 1 h of ultrasonication. However, from 1–5 h of ultrasonication, it was decreased only 5–6%. Therefore, first hour of ultrasonication is more effective for minimization of viscosity enhancement. The measured effective viscosity values at different temperatures for the nanofluid prepared by different durations of ultrasonication have reported in Figure C3 (Appendix C). The trend of this study for viscosity enhancement of ultrasonication duration was compared with the study of Garg et al. (2009). They observed a higher viscosity enhancement, which is probably for the higher concentration of particles that was 1 wt.%. Also, they used MWCNT that has higher particle size and aspect ratio as well as complex motion, which increase viscosity enhancement. They found a different trend as the viscosity initially increased until 40 min and then decreased with further increasing of sonication time. This possible reason for this phenomenon could be as they used MWCNT and 20 min of sonication was not enough so most of the particles may be were sedimented and lower viscosity was observed. It could be noted that the viscosity enhancement for 80 min of sonicated samples were found to higher than that of 20 min.

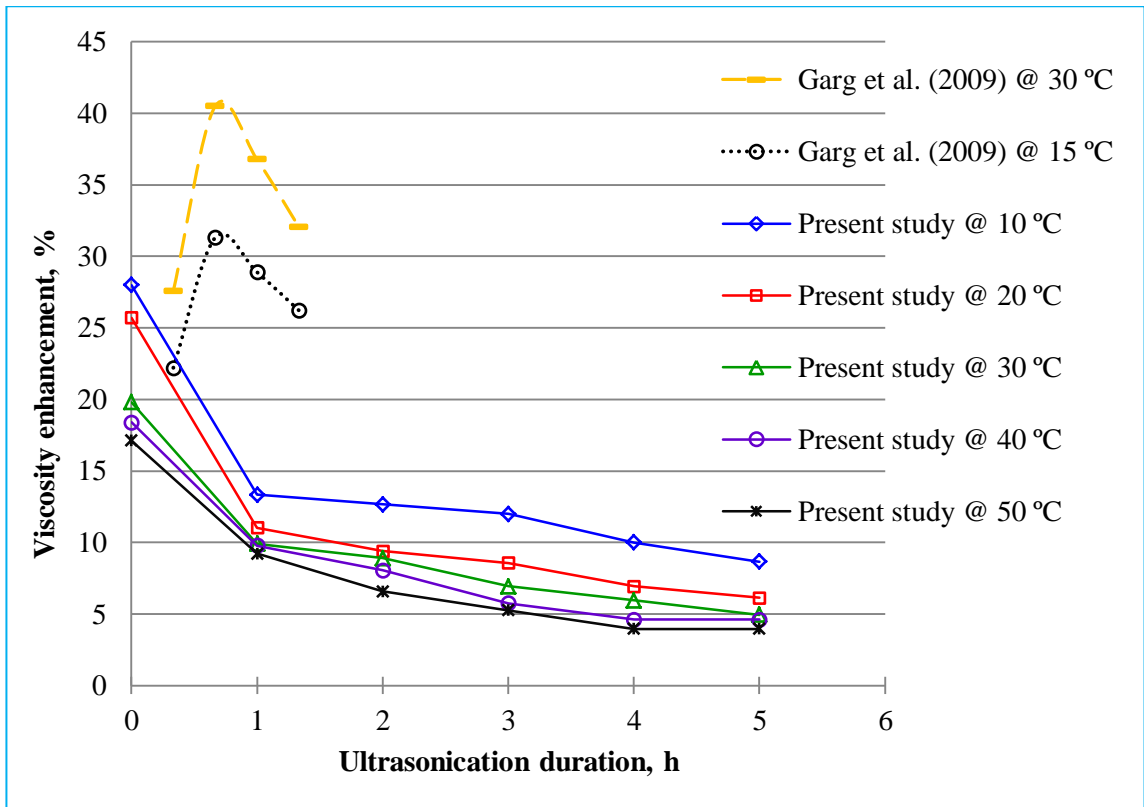


Figure 4.30: Enhancement percentage of viscosity of 0.5 vol.% of Al₂O₃–water nanofluids after different durations of ultrasonication.

It can be observed from Figure 4.30 that there are strong relationships between temperature and ultrasonication duration with the viscosity of the nanofluid. This phenomenon is also due to the effect of Brownian motion and van der Waals forces. It is also observed that, at the lower temperatures, it takes more ultrasonication duration to reach to the lowest viscosity level. However, at the higher temperatures, it takes less ultrasonication duration to reach to the lowest viscosity level. At the lower temperatures, the decrease of viscosity with the increase of ultrasonication duration was found to be higher compare to higher temperature. For example, at 10 °C viscosity enhancement was decreased about 20% for 0 to 5 h of ultrasonication, while viscosity enhancement decreased about 13%, at 50 °C for 0 to 5 h of ultrasonication. Therefore, longer sonication periods are not required to decrease the viscosity of the nanofluids, if the nanofluids are used at high-temperature applications.

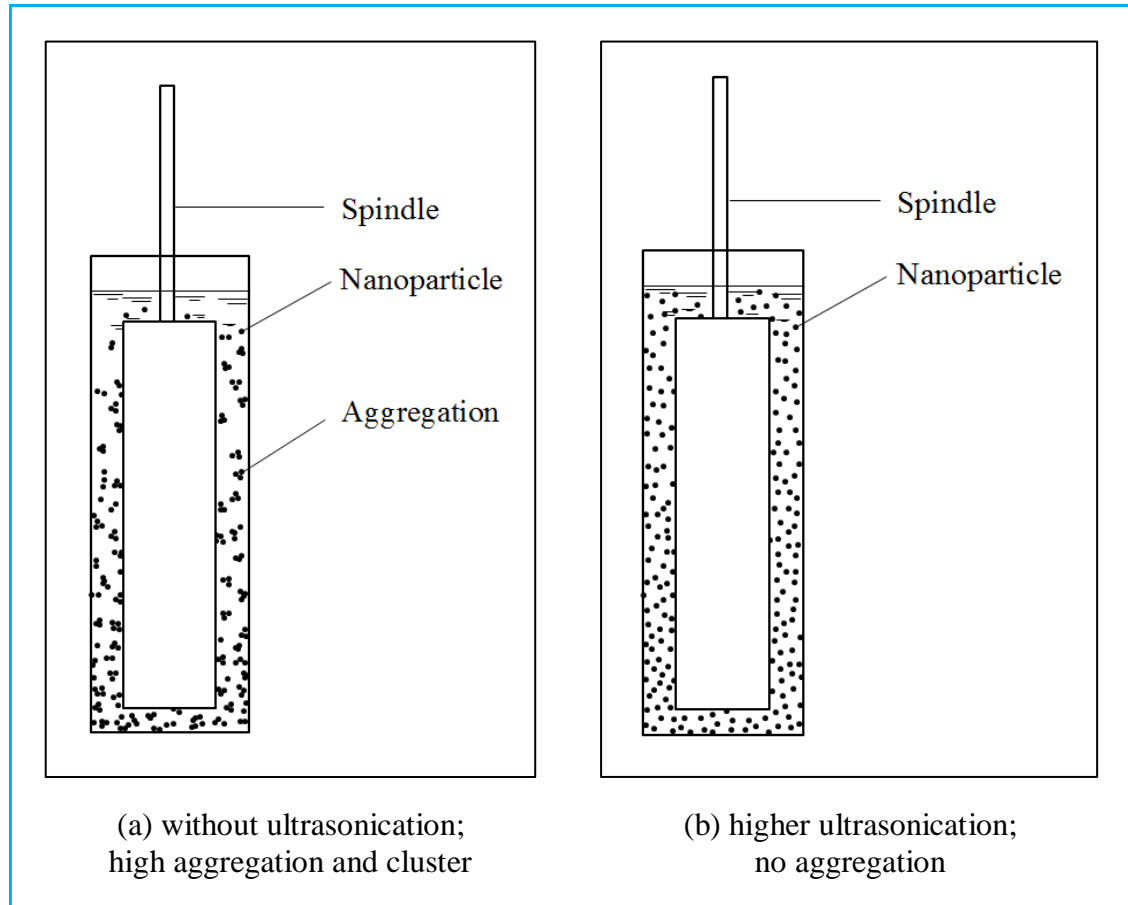


Figure 4.31: Mechanism of influence of ultrasonication duration on viscosity.

The effects of temperatures on the viscosity enhancement percentage of 0.5 vol.% of Al_2O_3 -water nanofluid are shown in Figure 4.32 for the nanofluids prepared at different ultrasonication durations. It can be seen that the viscosity of the ultrasonicated nanofluid significantly decreased as the temperature was increased from 10 to 50 °C. The decrease in the viscosity with increasing temperature is due to the weakening of inter particle adhesion forces. When temperature increases, the heat energy provided extra energy to separate the molecules, resulting in the reduction of attractive forces between molecules. A higher nanofluid temperature intensifies the Brownian motion of the nanoparticles and reduces the viscosity of the nanofluid (Murshed et al., 2008c). At 10 °C, the viscosity of the Al_2O_3 -water nanofluid without ultrasonication (0 h) was the highest compared to those of the other ultrasonicated nanofluids. This can be explained

by the fact that, without ultrasonication, the nanoparticles were able to spread homogeneously in the base fluid and, therefore, a strong agglomeration occurred. Furthermore, this study started with the measurement of viscosity of 10 °C, and the particles could not get enough time to sediment, so the strong clusters of nanoparticles made resistance to the spindle, and viscosity increased. Therefore, from 10 to 20 °C, the viscosity of the nanofluids dropped sharply mainly because of two effects: One is the rotation of the spindle of the rheometer, which was 60 rpm. It took about 20 min to change the temperature of the bath from 10 to 20 °C, and the spindle was rotating during this period. Therefore, some clusters broken down and reduced the resistance to flow. The second reason is the temperature intensification, which is related to Brownian motion, and particles started to move from the cluster. The experimental results of this study were compared with the studies of Nguyen et al. (2007) and Namburu et al. (2007a). They also found the similar trend as decrease of viscosity ratio with the intensification of temperature. Namburu et al. (2007a) observed a higher viscosity enhancement percentage because they used 1 vol.% concentration, also their base fluid was 60/40 mixture of ethylene glycol and water, which has a higher viscosity than water.

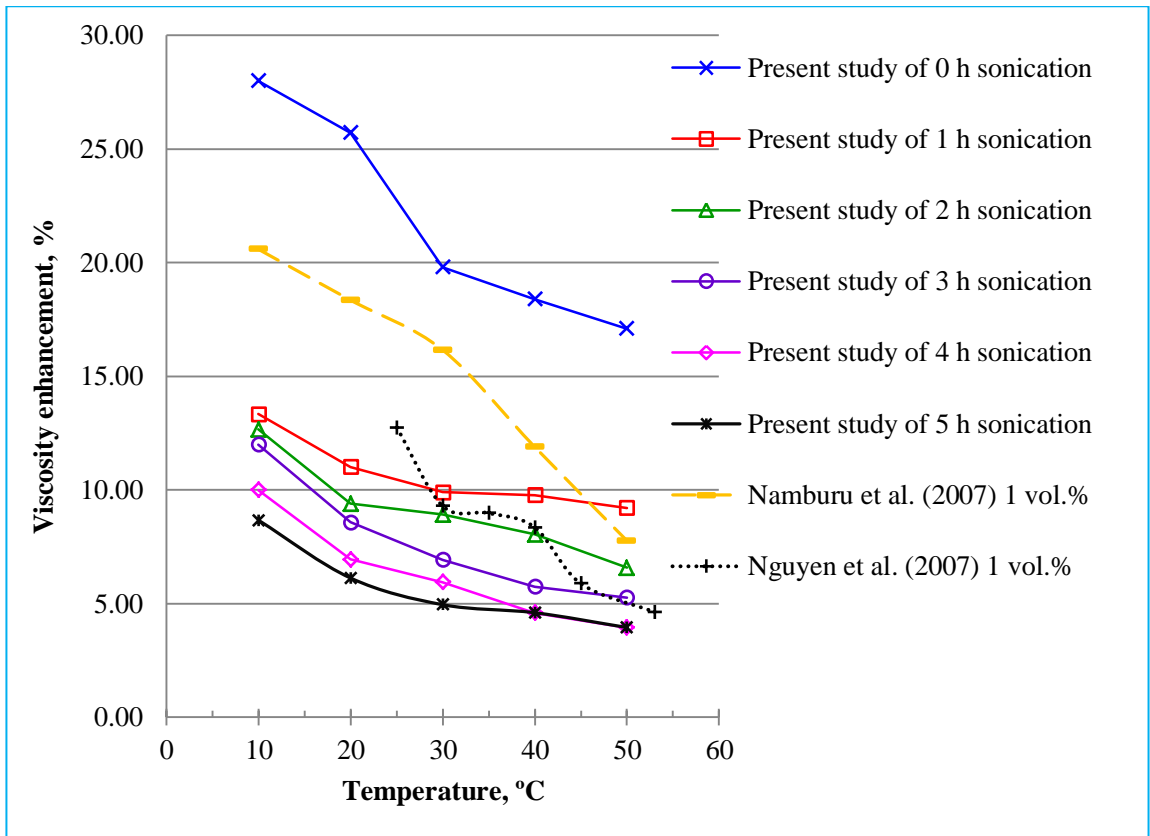


Figure 4.32: Variations of viscosity enhancement with temperatures.

Furthermore, viscosity values were measured at 25 °C temperature after 0, 10, 20, and 30 days of the preparation of the samples and reported in Figure 4.33. It can be seen in Figure 4.33 that the viscosity ratio was decreased with the periods sample kept until 30 days. The reason is the sedimentation of particles over time. As the sedimented particles do not have participation in the flow therefore, the resistance to flow is decreased and as a result viscosity values are decreased. It is found that after 30 days of sample preparation, viscosity enhancement was decreased about 6.09% for the nanofluid prepared by 5 h of ultrasonication duration. However, this decrement was found to be 25.80% for the nanofluid prepared by 0 h of ultrasonication. Therefore, the effect of ultrasonication duration was effective over the viscosity enhancement percentage until 30 days of preparation. The lowest viscosity enhancement was observed for the nanofluid prepared by 0 h of sonication and after 30 days of preparation that was about 0.64%. The reason behind this is the sedimentation of most of the particles and they

took place at bottom and the supernatant level was found to be water like. The measured values of effective viscosities at 25 °C temperature after 0, 10, 20, and 30 days of sample preparation have reported in Figure C4 (Appendix C).

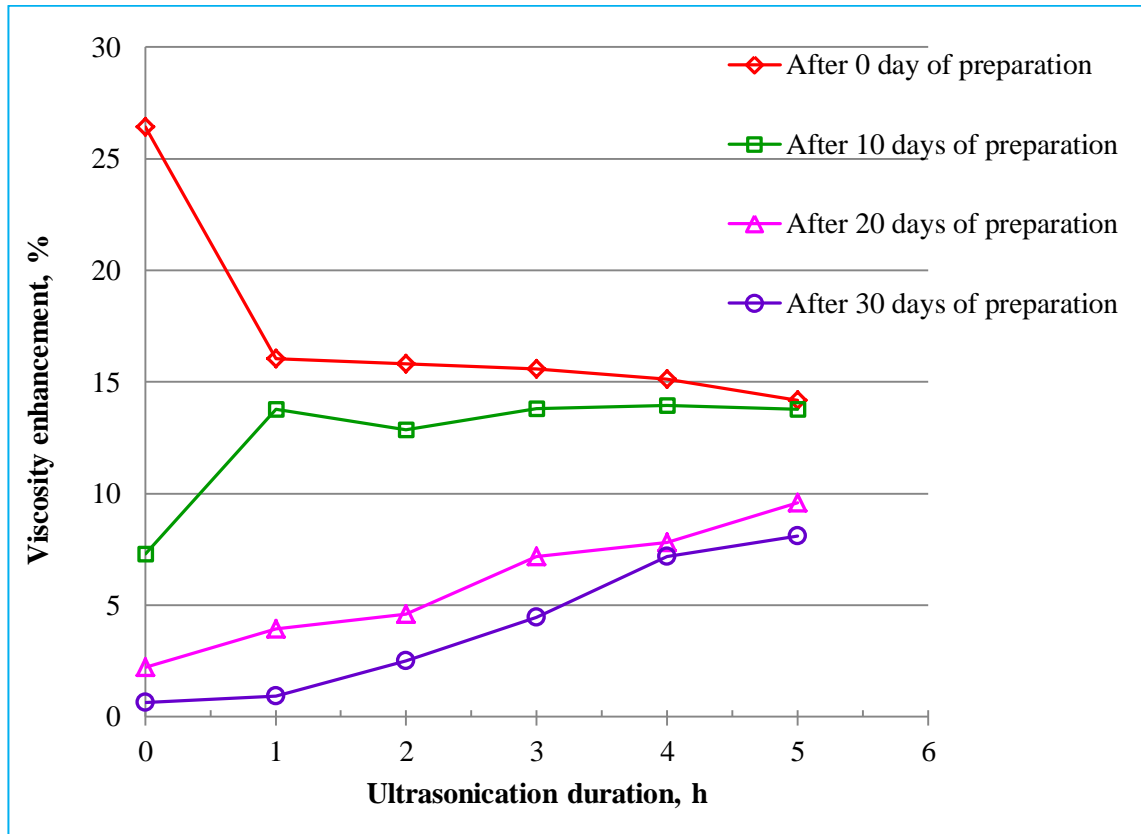


Figure 4.33: Enhancement percentage of viscosity at 25 °C temperature after different durations of sample preparation.

4.4.3 Density

The effect of ultrasonication duration on density enhancement percentage of Al_2O_3 -water nanofluid is shown in Figure 4.34. It can be seen in Figure 4.34 that the density enhancement ratio of nanofluid increased with increasing ultrasonication duration. The reason behind this could be discussed with the aid of Figure 4.35. At lower ultrasonication period, nanoparticles are not well dispersed as reported in Figure 4.35 (a), which was also seen in TEM micrograph of Figure 4.3 and 4.4. Therefore, density of base fluid was found to be dominating and lower density was observed in comparison

to prolonged ultrasonicated nanofluid. The density meter is designed to measure the liquid samples only. Therefore, the effect of not properly dispersed nanoparticles is not sensed by the device. Due to the gravitational effect, aggregated particles are rapidly sediment. Also the sedimented nanoparticles are not suctioned by the nozzle of the device. Therefore, nanoparticles are properly dispersed with base fluid with higher sonication time, as seen in Figure 4.35 (b). Therefore, density enhancement percentage of nanofluid was found to be increased as the high density nanoparticles mixed with fluid and increased the density of the suspension. An almost linear increasing trend of density enhancement was observed with sonication time. Moreover, the enhancement percentage of density of nanofluid was found to be very low (below 0.5%). Therefore, the effect of ultrasonication duration of nanofluid was not significant on density enhancement ratio. The measured effective density values at different temperatures for the nanofluid prepared by different durations of ultrasonication have reported in Figure C5 (Appendix C).

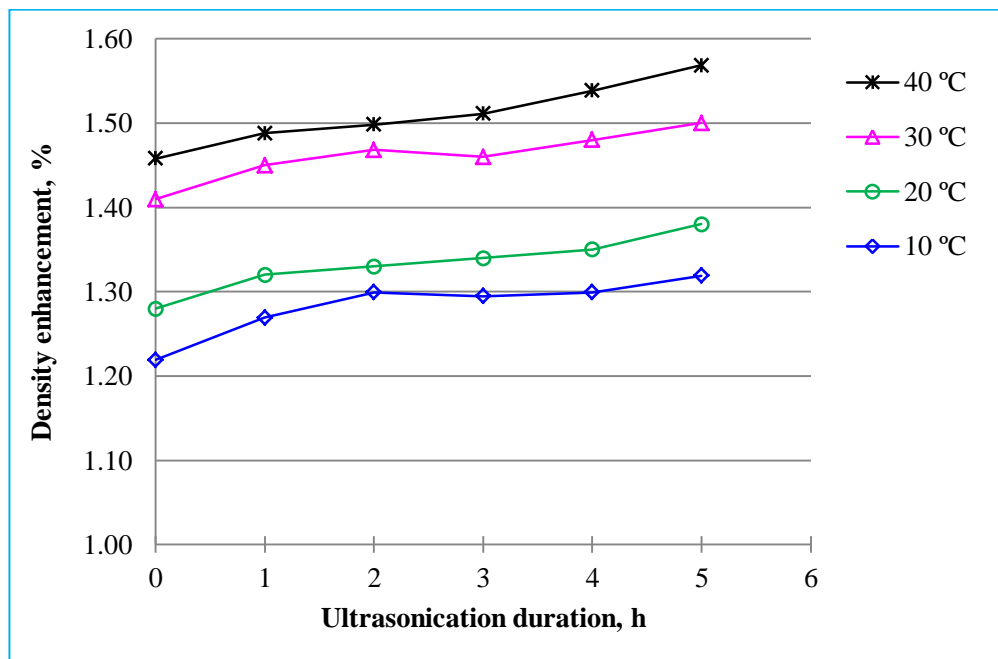


Figure 4.34: Enhancement percentage of density of 0.5 vol.% of Al_2O_3 -water nanofluids after different duration of ultrasonication.

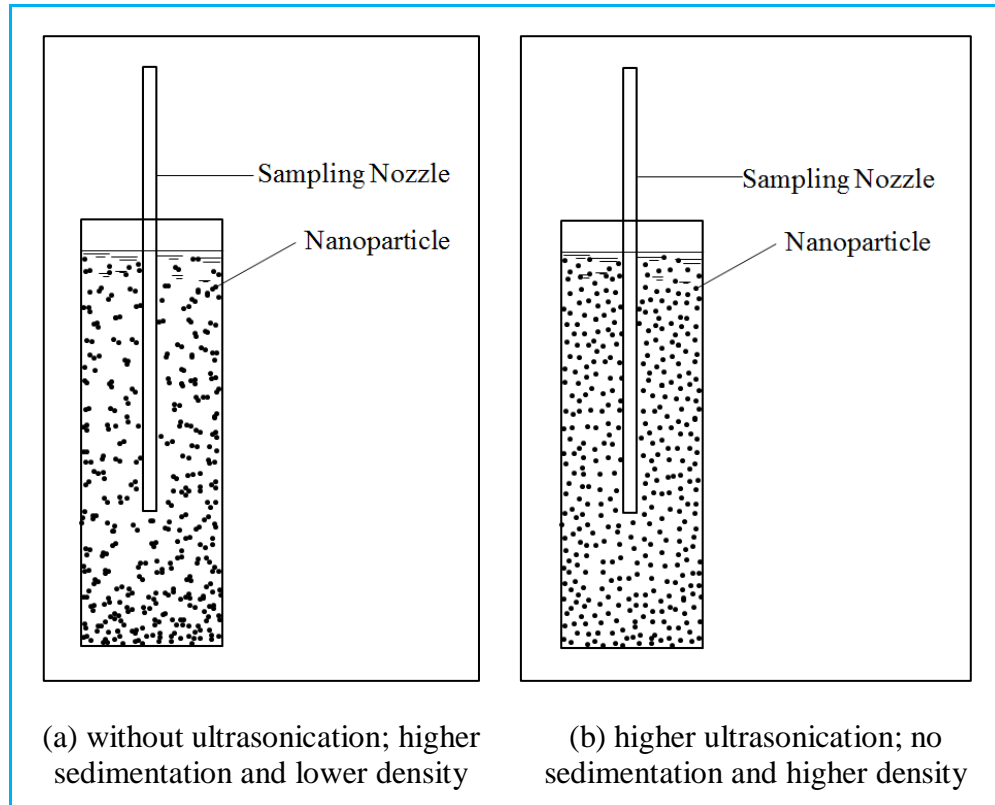


Figure 4.35: Mechanism of influence of ultrasonication duration on density.

The effect of temperature on density enhancement percentage of nanofluid is shown in Figure 4.36. It can be seen in Figure 4.36 that the density enhancement percentage of nanofluids was increased with the increase of temperature. The rate of enhancement percentage was very low with increasing temperature. The result of this study was compared with the study of Vajjha and Das (2012) and Elias et al. (2014). Vajjha and Das (2012) found overall higher density enhancement percentage because they used 1 vol.% of particles. However, they observed a slight decreasing trend of density enhancement with increasing temperature. Elias et al. (2014) found a slight increase of density enhancement with increasing temperature. However, the overall density enhancement percentage was very low. This may be because they used commercial radiator coolant as base fluid, which already has some ingredients for antirust and others. Therefore, the

dispersion of nanoparticle did not have significant effect on density enhancement. The experimental result of this study was also compared with the prediction of Pak and Cho (1998) density model. The prediction of this correlation was also show an increase of density enhancement with temperature. However, the increment ratio was very low.

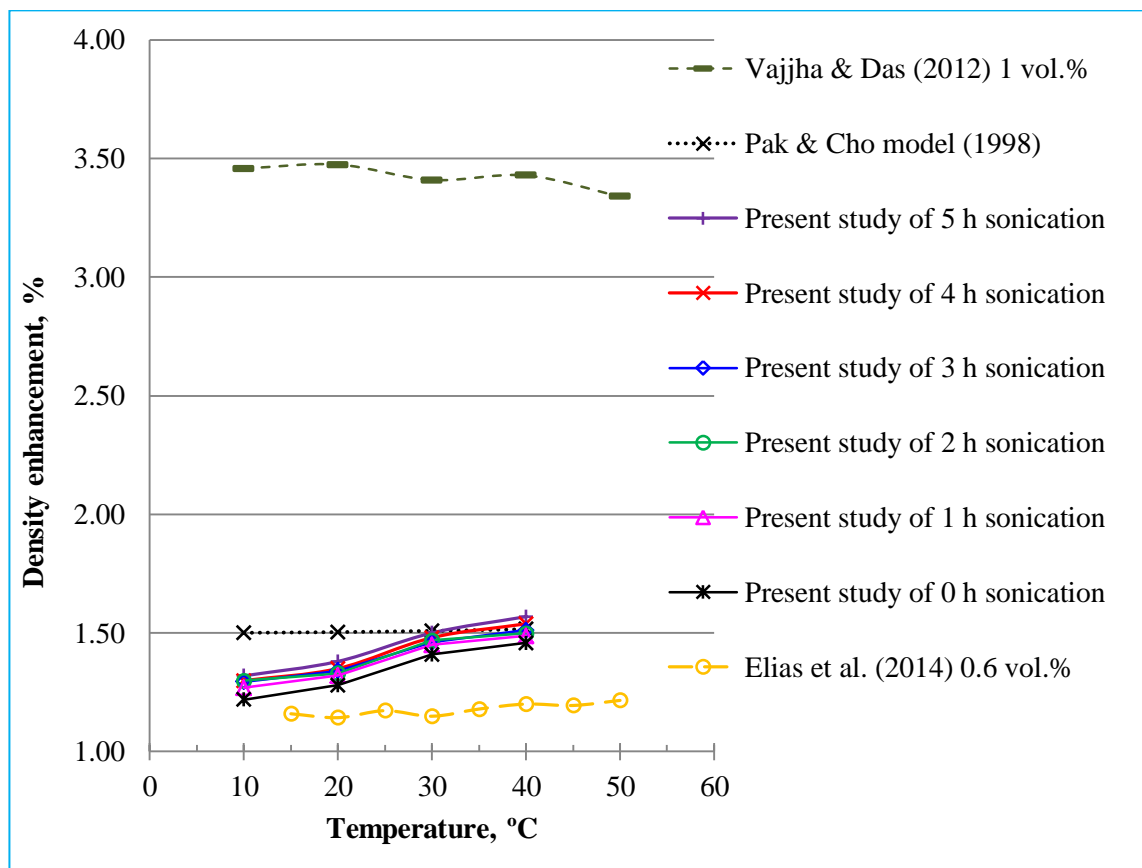


Figure 4.36: Variations of density enhancement with temperatures.

Again, density values were measured at 25 °C temperature after 0, 10, 20, and 30 days of the preparation of the samples and reported in Figure 4.37. It can be seen in Figure 4.37 that the density ratio was decreased with the periods sample kept until 30 days. The reason is the sedimentation of particles over time. As the sedimented particles are took place at bottom as a result density values are decreased. It is found that after 30 days of sample preparation, density enhancement was decreased about 0.47% for the nanofluid prepared by 5 h of ultrasonication duration. However, this decrement was found to be

1.00% for the nanofluid prepared by 0 h of ultrasonication. Therefore, the effect of ultrasonication duration was not so effective over the density enhancement percentage until 30 days of preparation. The measured values of effective densities at 25 °C temperature after 0, 10, 20, and 30 days of sample preparation have reported in Figure C6 (Appendix C).

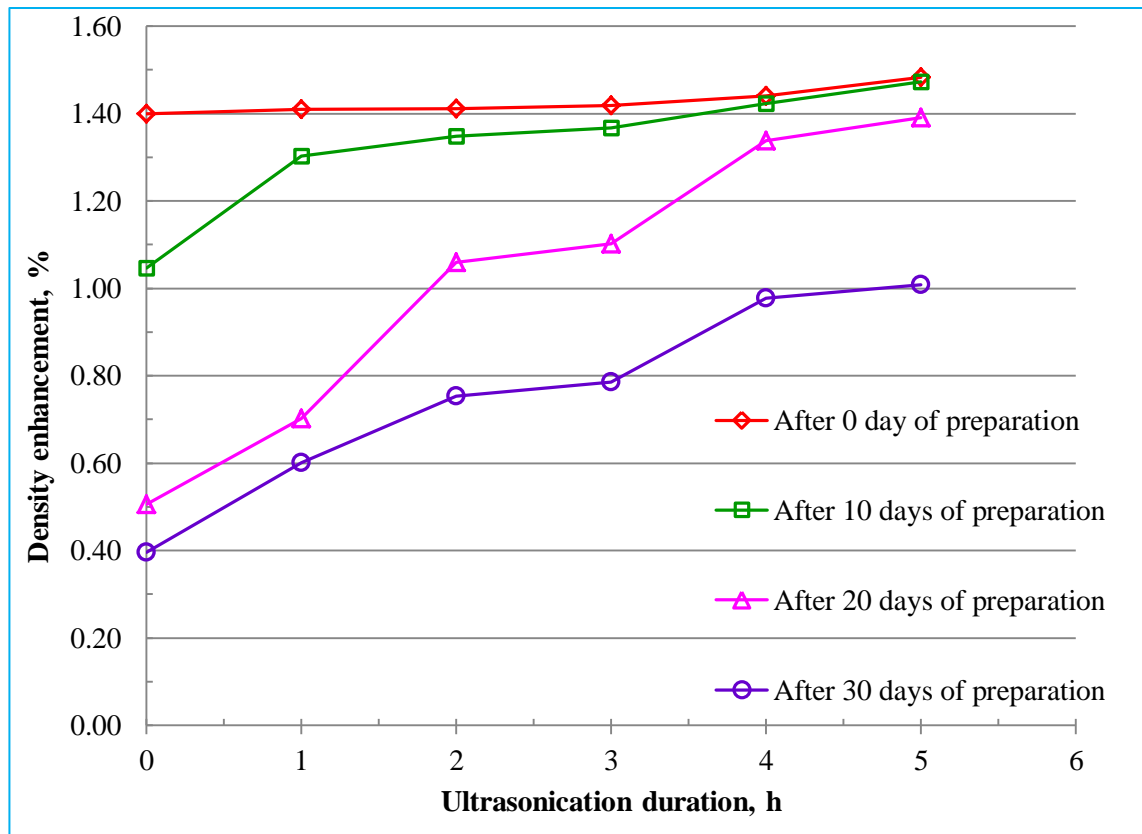


Figure 4.37: Enhancement percentage of density at 25 °C temperature after different durations of sample preparation.

4.5 Rheology

Figure 4.38 shows the trend of shear stresses at different shear rates from 12.23 to 305.75 s⁻¹. To make a clear understanding of the Figure 4.38, only the data for 10, 30, and 50 °C temperatures have been plotted. Flow behavior for the specific temperatures is indicated by circles. It is observed from Figure 4.38 that initially the nanofluid showed Newtonian behavior at 10 °C temperature and the trend continued almost up to

150 s⁻¹ shear rates, even the Newtonian trend continued up to 150 s⁻¹ shear rates for the nanofluid prepared by without ultrasonication (0 h). After that, at higher shear rate, the nanofluid found to be non-Newtonian (dilatant and shear thickening fluid). It is also observed from Figure 4.38 that at 30 °C temperatures, initially the nanofluid showed Newtonian behavior and existed up to 100 s⁻¹ shear rates. Then it became non-Newtonian as dilatant and shear thickening fluid. Almost similar trend of rheological behavior was observed at 50 °C temperature. However, in the case of 50 °C temperature, Newtonian behavior continued up to 73.38 s⁻¹ shear rates only.

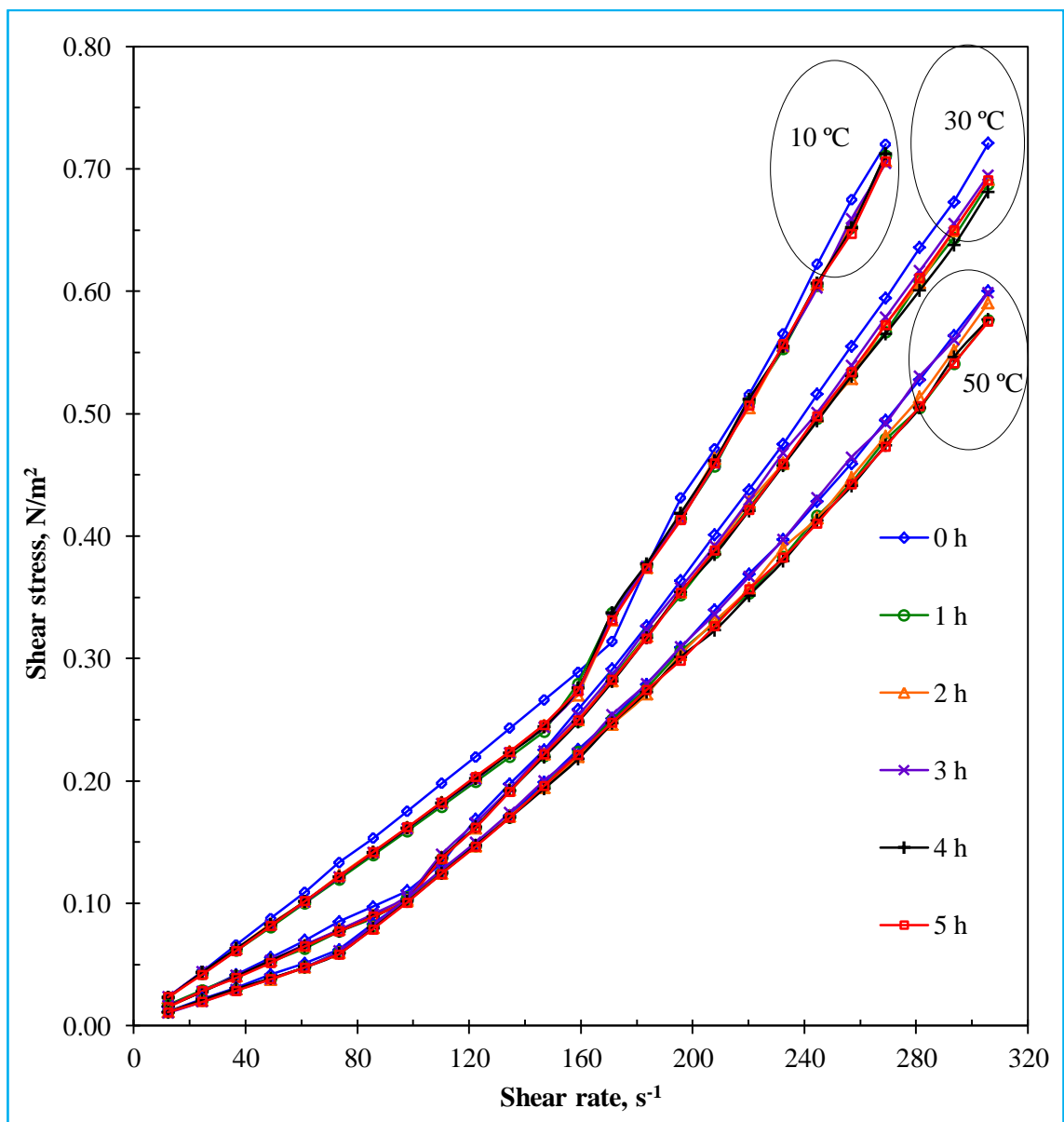


Figure 4.38: Relation of shear stress of Al₂O₃-water nanofluid with shear rates.

Figure 4.39 represents the flow behavior of the nanofluids prepared by different ultrasonication periods, which could give better understanding of the effect of sonication time. The nanofluids prepared by 0 (without ultrasonication), 1, 2, 3, 4, and 5 h of ultrasonication have been portrayed in Figure 4.39 (a), (b), (c), (d), (e), and (f), respectively. It is clear from the Figure 4.39 that, almost similar flow behavior was found for the nanofluid prepared by different durations of ultrasonication. It is observed that, at the start of ultrasonication, shear stresses of nanofluid were found to be decreased by the increase of ultrasonication periods. The shear stresses values (Y-axis) of Figure 4.39 (b) which are the values for 1 h of ultrasonication were found to be lower than the values of Figure 4.39 (a) (for 0 h of ultrasonication). However, further ultrasonication, the shear stresses values (Y-axis) were found to be almost similar (very small changes were observed) as seen in Figure 4.39 (b)–(f). Initially, without ultrasonication the nanoparticles were in highly clustered form and aggregated that has been observed in Figure 4.3 as TEM image. These clusters are not taken part into the flow rather making resistance to flow; as a result, shear stress was increased. Again, flow behavior was changed by the increase of temperatures and shear rates. From the Figure 4.39, it is clear that, the shear stresses of nanofluid significantly decreased by the increase of temperature from 10 °C to 50 °C, which were found to be more significant at higher shear rates.

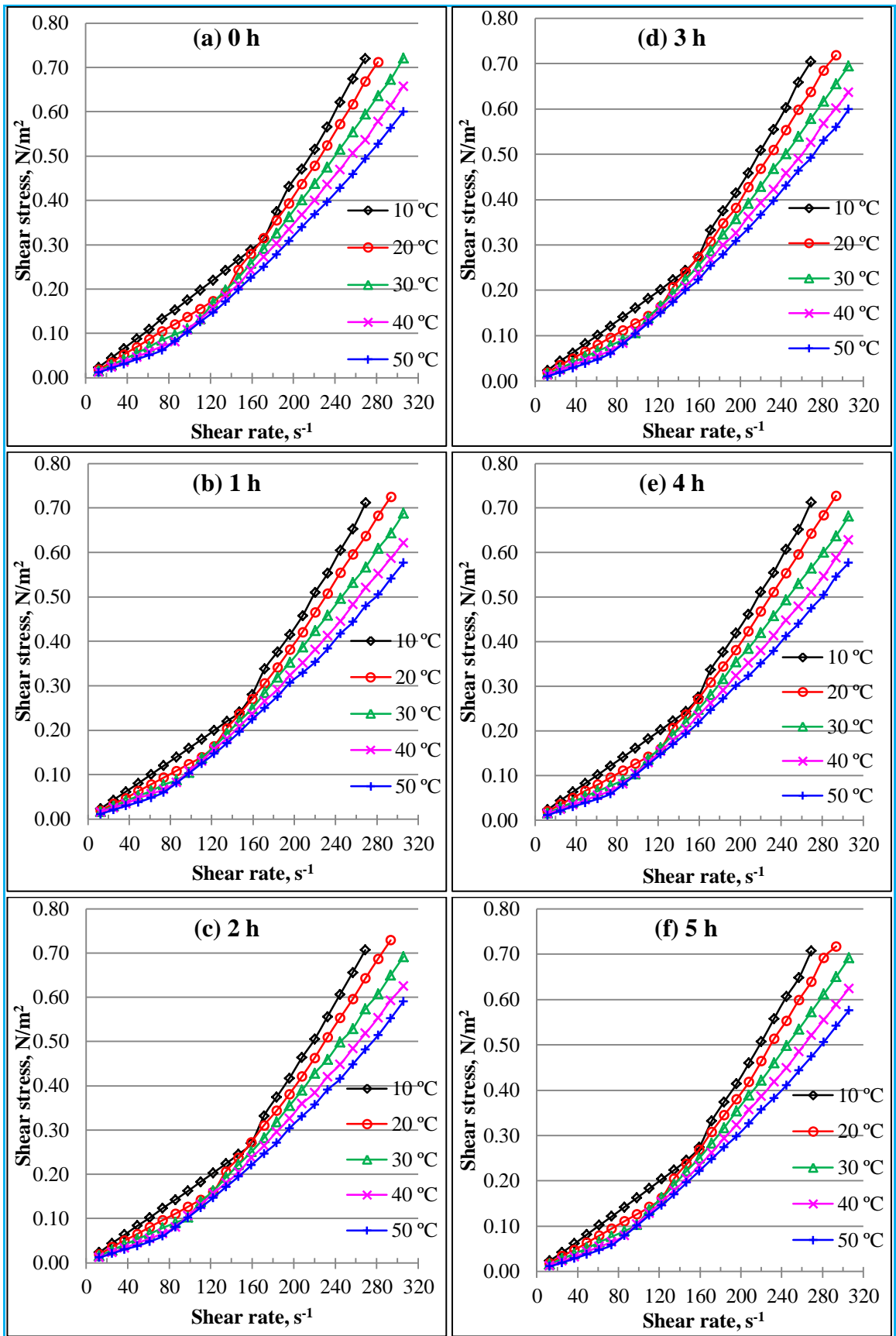


Figure 4.39: Shear stresses at different shear rates for the Al₂O₃-water nanofluid prepared by (a) 0, (b) 1, (c) 2, (d) 3, (e) 4, and (f) 5 h of ultrasonication.

The effect of ultrasonication duration on the rheological properties of 0.5 vol.% Al₂O₃-water nanofluid have been observed at 10, 20, 30, 40 and 50 °C temperatures. Figure 4.40 shows the trend of viscosity at different shear rates (from 36.69 to 305.75 s⁻¹). To make a clear understanding of the Figure 4.40, only the data for 10, 30, and 50 °C temperatures have been plotted. Flow behavior for the specific temperatures is indicated by circles. It is observed from Figure 4.40 that initially the nanofluid showed Newtonian behavior at 10 °C temperature and the trend continued almost up to 150 s⁻¹ shear rates. After that, at higher shear rate, the nanofluid found to be non-Newtonian as dilatant and shear thickening fluid. For all the nanofluids prepared by different ultrasonication durations were found to be similar characteristics as discussed above at 10 °C temperatures. However, nanofluid prepared without ultrasonication (0 h) showed higher viscosity compared with others and exhibited Newtonian behavior for the longer range of shear rates. It is also observed from Figure 4.40 that at 30 °C temperature, initially the nanofluid showed Newtonian behavior and existed up to 100 s⁻¹ shear rates. Then it became non-Newtonian as dilatant and shear thickening fluid. Almost similar trend of rheological behavior was observed at 50 °C temperature. However, in the case of 50 °C temperature, Newtonian behavior continued up to 70 s⁻¹ shear rates only.

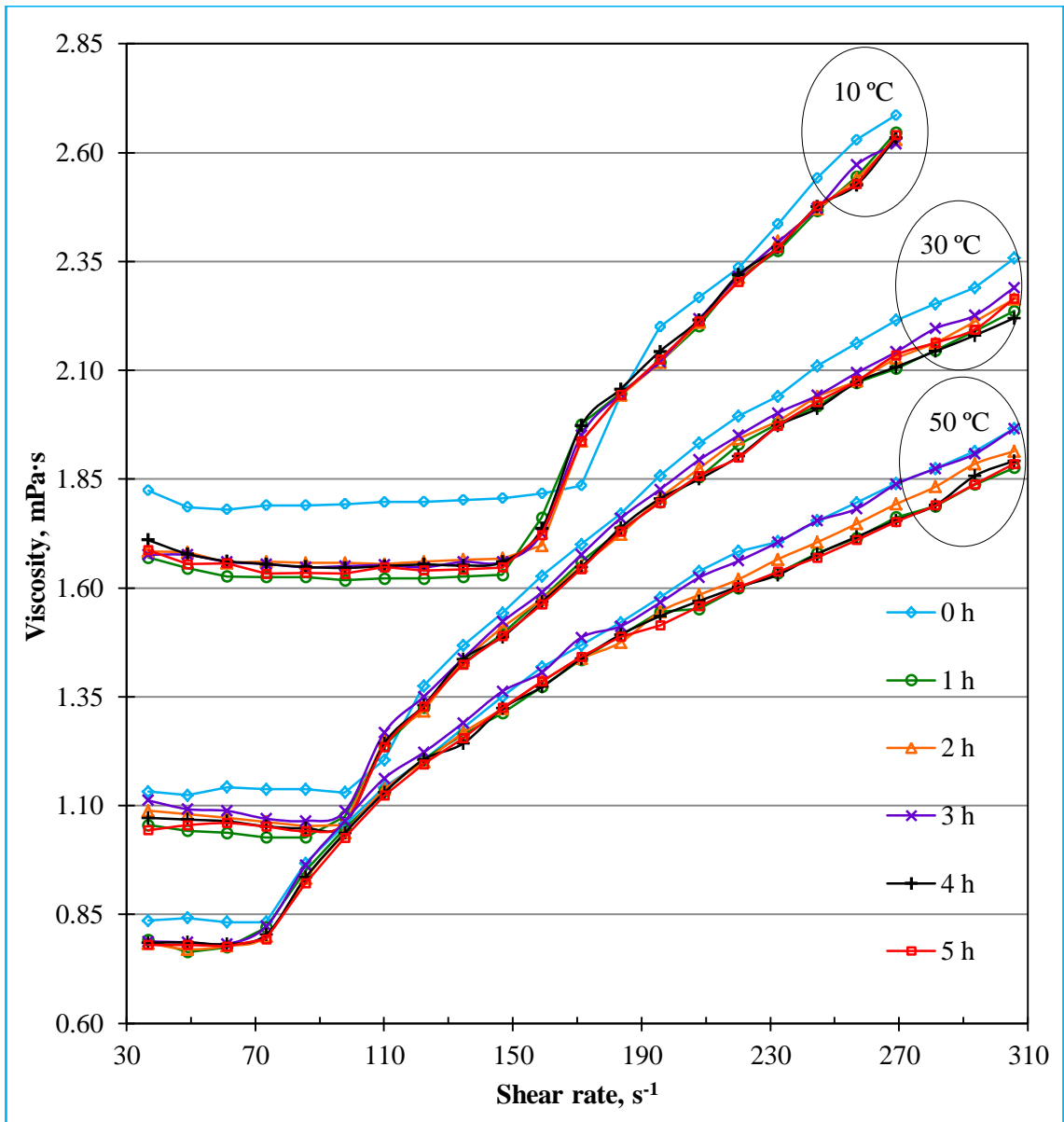


Figure 4.40: Viscosity of Al₂O₃–water nanofluid at different shear rates.

For better understanding of flow behavior of the nanofluids prepared by different ultrasonication durations have been again presented in Figure 4.41. The nanofluids prepared by 0 (without ultrasonication), 1, 2, 3, 4, and 5 h of ultrasonication have been portrayed in Figure 4.41 (a), (b), (c), (d), (e), and (f), respectively. It is clear from the Figure 4.41 that, almost similar flow behavior was found for the nanofluid prepared by different durations of ultrasonication. However, at the start of ultrasonication, viscosity of nanofluid was found to be decreased by the increase of ultrasonication durations. The viscosity values (Y-axis) of Figure 4.41 (b) which are the values for 1 h of

ultrasonication were found to be lower than the values of Figure 4.41 (a) (for 0 h of ultrasonication). However, further ultrasonication, the viscosity values (Y-axis) were found to be almost similar (very small changes were observed) as seen in Figure 4.41 (b)–(f). Nevertheless, flow behavior was changed by the increase of temperatures and shear rates. It is also found from the Figure 4.41 that there are interactions between temperature and sonication period with the viscosity of nanofluid. This phenomenon is due to the effect of Brownian motion and van der Waals force. At the lower temperatures, the decrease of viscosity with the increase of ultrasonication duration was found to be higher compare to higher temperature. From the Figure 4.41, it is clear that, the viscosity of nanofluid significantly decreased by the increase of temperature from 10 to 50 °C. This is because of the weakening of inter particle adhesion forces that decrease in the increase of temperatures (Murshed et al., 2008c). It is found that viscosity of nanofluid decreased by the increase of ultrasonication duration. The similar trend has also been observed by Yang et al. (2006). Initially, the nanoparticles are in highly clustered form and aggregated that have been seen in Figure 4.3 as TEM micrograph. These clusters are not taken part into the flow rather making resistance to flow; as a result, viscosity was increased. The TEM microstructure of Figure 4.4 also supports the above statement. As in the micrograph, it has been seen that with 1 h of ultrasonication and so on, nanoparticles started to disperse that create less resistance to flow and viscosity decreased.

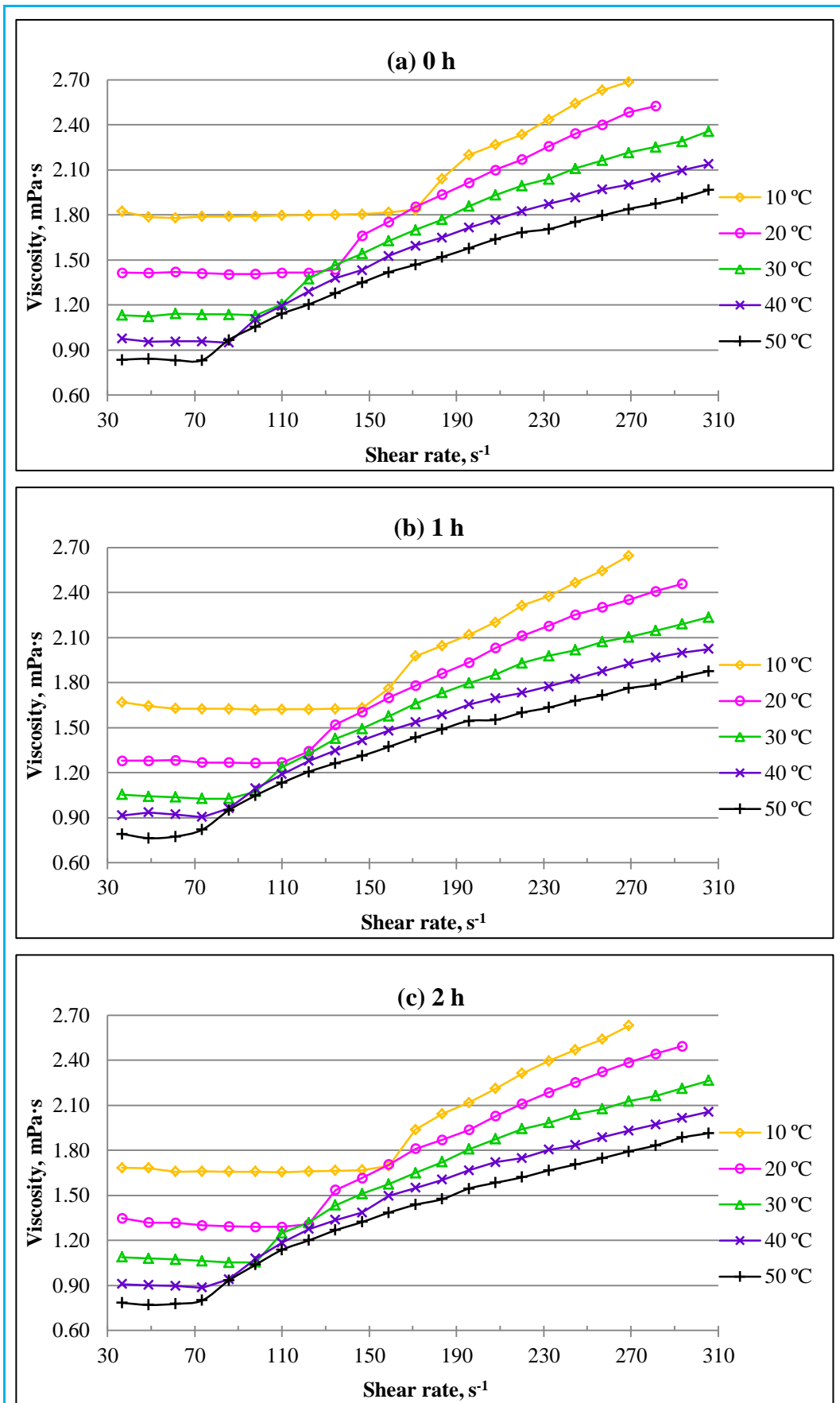


Figure 4.41, continued

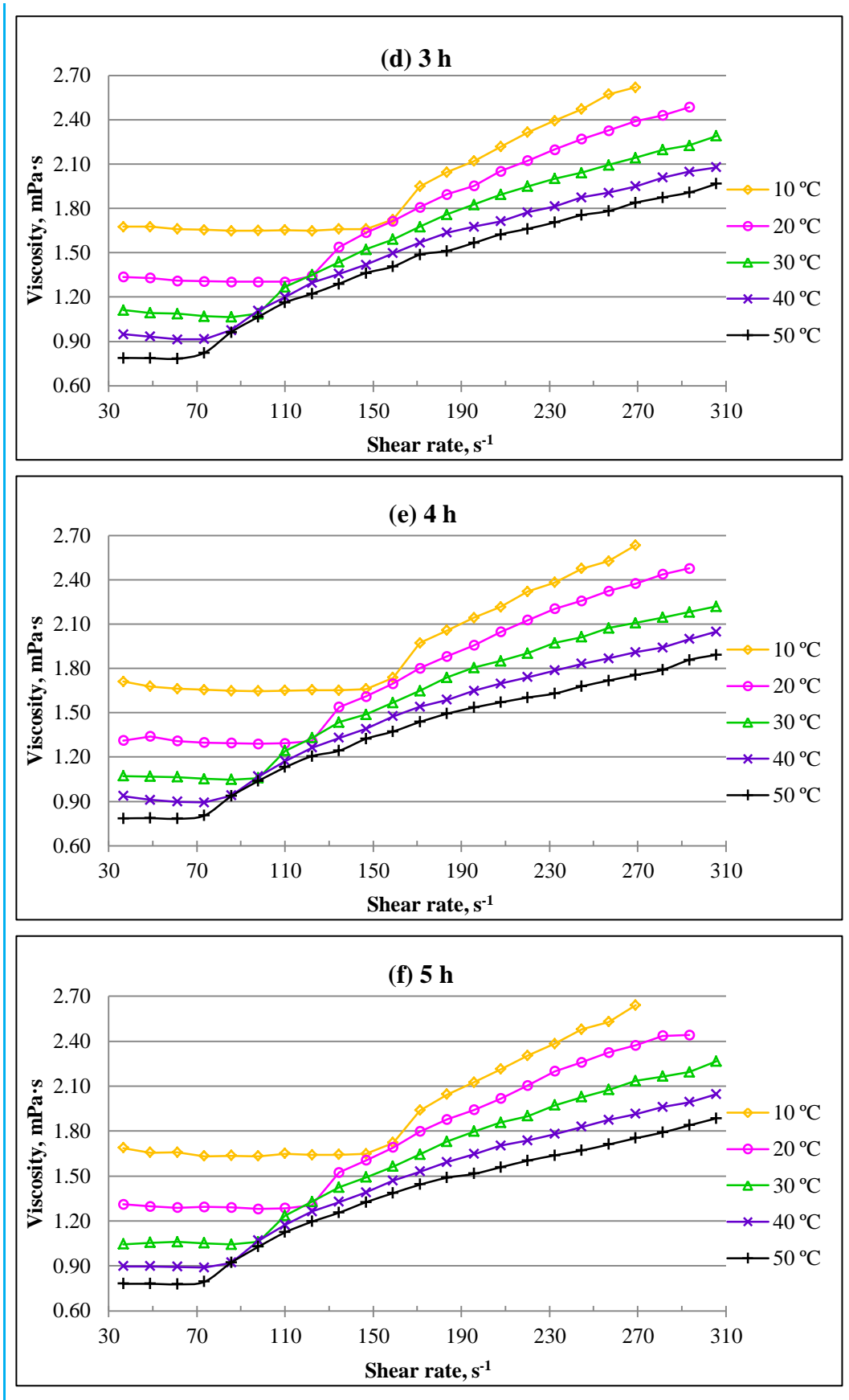


Figure 4.41: Viscosity at different shear rates for the Al_2O_3 -water nanofluid prepared by (a) 0, (b) 1, (c) 2, (d) 3, (e) 4, and (f) 5 h of ultrasonication.

The relations of microstructures of colloids with rheological behavior could be discussed from the study of Mueller et al. (2010), which have been portrayed in Figure 4.42. They stated that, in the case of very low volume concentrations of nanoparticles, where the particles are sufficiently well separated, and then the interactions among the nanoparticles are negligible. By applying and increasing shear rates' viscosity do not changes and a Newtonian flow characteristic is observed in such as cases and yield stress is supposed to be zero. Nevertheless, the addition of particles will increase the viscosity of suspension. For adding very low concentration of particles, viscosity increases linearly, however, for slightly higher particle concentration, viscosity increases nonlinearly (Mueller et al., 2010). Figure 4.42 (a) shows the pictorial example of the addition of low concentration of particles in a fluid. For intermediate or higher particle concentration, non-Newtonian fluid is observed. However, the flow behavior can be shear thinning or shear thickening. With the increase of applied shear rates, particles can be organized in the fluid and viscosity will be decreased (Wagner & Brady, 2009). In some cases, particles become separated although it is very small but the applied force (shear rate) squeezed the fluid to pass through the gaps and viscosity decreases. Such an approach is called shear thinning behavior, which has shown in Figure 4.42 (b). Even the increase of shear rate can form chain and network among neighboring particles. In such cases, particle face difficulties to flow and viscosity are abruptly increases and yield stress also developed. The above condition is called shear thickening, which has shown in Figure 4.42 (c). The blue color particles of Figure 4.42 (c) are showing the example of network. In this study, most of the micrograph of the Figure 4.3 to 4.8 show that there were some typical networks of particles, which were termed as cluster or aggregation of particles. The PSD results of Figure 4.17 and 4.19 also proof that there were small networks among nanoparticles. Average cluster size of this study was over 100 nm however; the average diameter of a single particle is about

13 nm. Therefore, there were some small nano-clusters were existed in the nanoparticles and in this study, shear thickening behavior was observed for this reason.

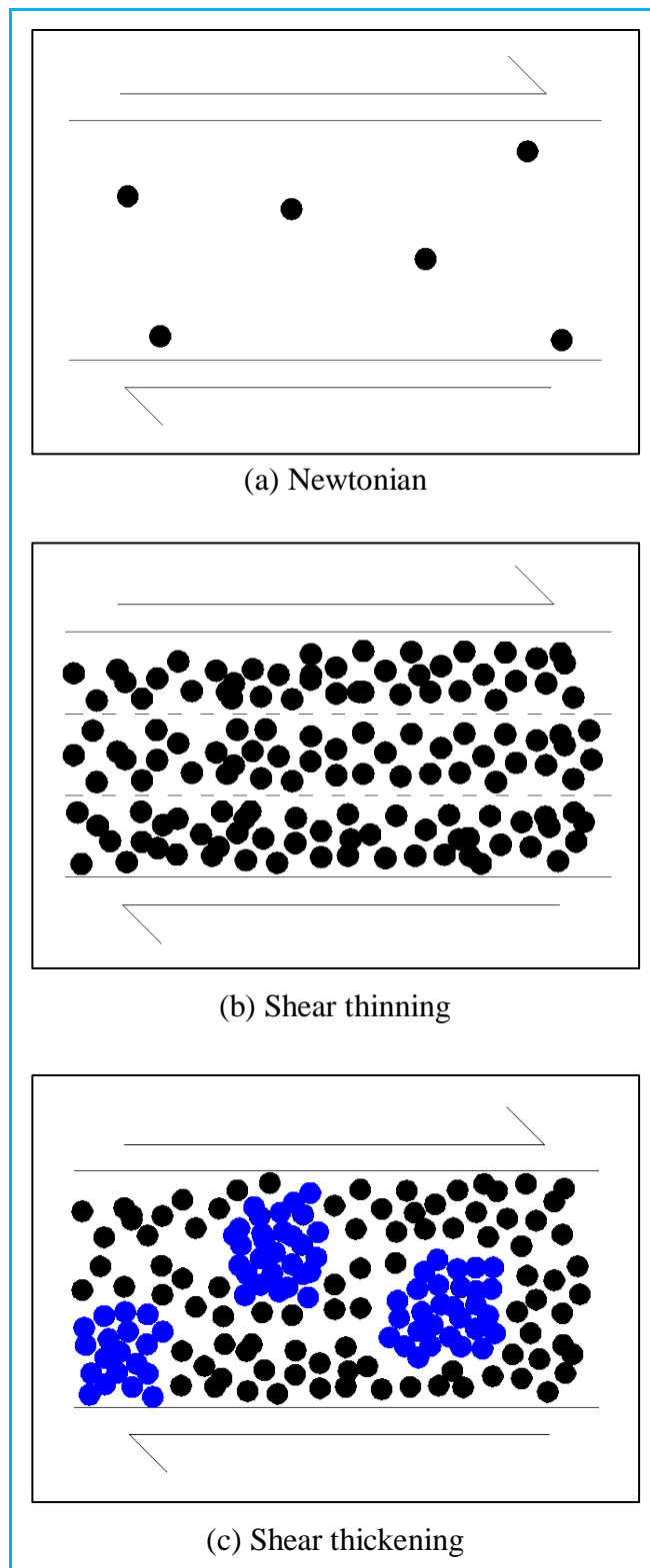


Figure 4.42: Relations of microstructure of colloids with rheology.

The yield stress for the nanofluids prepared by different ultrasonication durations was analyzed with Herschel-Bulkey rheological model (Herschel & Bulkley, 1926). A very good agreement with the model has been observed as the average confidence of fit was found to be 99.87% (R^2 in %), which were within the confidence probability between 99.55% to 99.96%. The details of the fitting parameters have reported in Table D1 (Appendix D). Figure 4.43 shows the effect of the ultrasonication periods (used to prepare nanofluid) on yield stress point. It is found that yield stress rapidly decreased with the start of ultrasonication (as the variation of yield stress point significantly decreased from 0 to 1 h). Again, with further ultrasonication, yield stress slowly decreased.

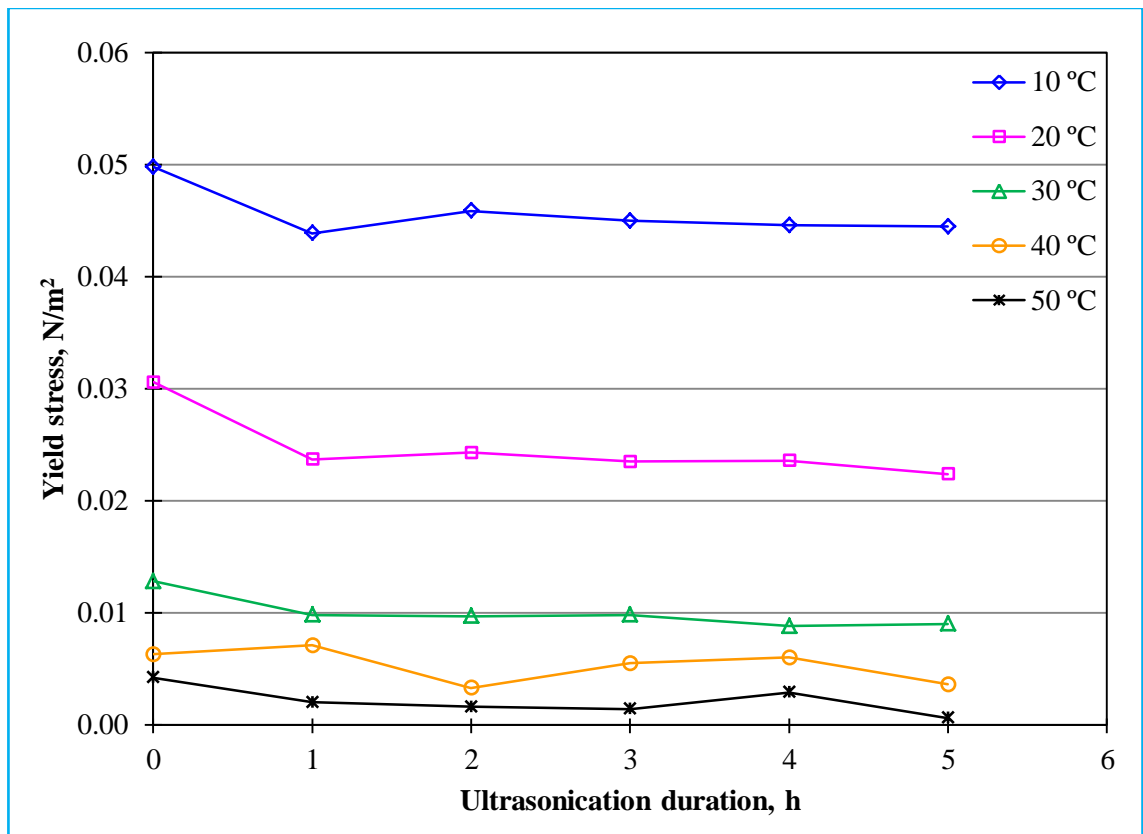


Figure 4.43: Effect of ultrasonication duration on yield stress point of Al_2O_3 -water nanofluid.

The result of Figure 4.43 could be discussed with the aid of Figure 4.31. The clusters of Figure 4.31 (a) are not taken part into the flow rather making resistance to flow and higher yield stress was observed. As there is less aggregation of particles observed in Figure 4.31 (b), therefore, the nanoparticles take part in the flow and create less resistance to the spindle and lower yield stress was observed. Moreover, yield stress decreased with the increase of temperatures. As with the increase of temperature, the inter particle adhesion forces become weak and yield stress point was decreased.

The flow characteristics of the nanofluids prepared by 0, 1, 2, 3, 4, and 5 h of ultrasonication duration were analyzed with Power-Law rheological model. A very good agreement with the model was observed as the average confidence of fit was 98.77% (R^2 in %), which was found to be 97.77% as the lowest. The details of the fitting parameters have been reported in Table D1 (Appendix D). The flow index values were plotted in Figure 4.40. The parameters were calculated for the experimental values at 10, 20, 30, 40, and 50 °C. It is noted that, the types of fluid depend on the value of this power-law index n ; as $n < 1$ means pseudo plastic or shear thinning, $n = 1$ means Newtonian fluid, and $n > 1$ means dilatant or shear thickening behavior. It is found from Figure 4.40 that the flow index value increased by the increase of temperatures, which indicate that the nanofluids were strong non-Newtonian with shear thickening behavior with increasing temperature. It is also found that at lower temperature (10 °C), the values of n were lower for the nanofluid prepared by without ultrasonication (0 h). That is why in Figure 4.38 to 4.41, the longer Newtonian trend has been observed for the nanofluids at 10 °C, especially for the nanofluid prepared by 0 h. It is observed from Figure 4.44 that the flow behavior index varies for 0 and 1 h of ultrasonication. However, in the case of 2, 3, 4, and 5 h of ultrasonication, the values of n were almost similar.

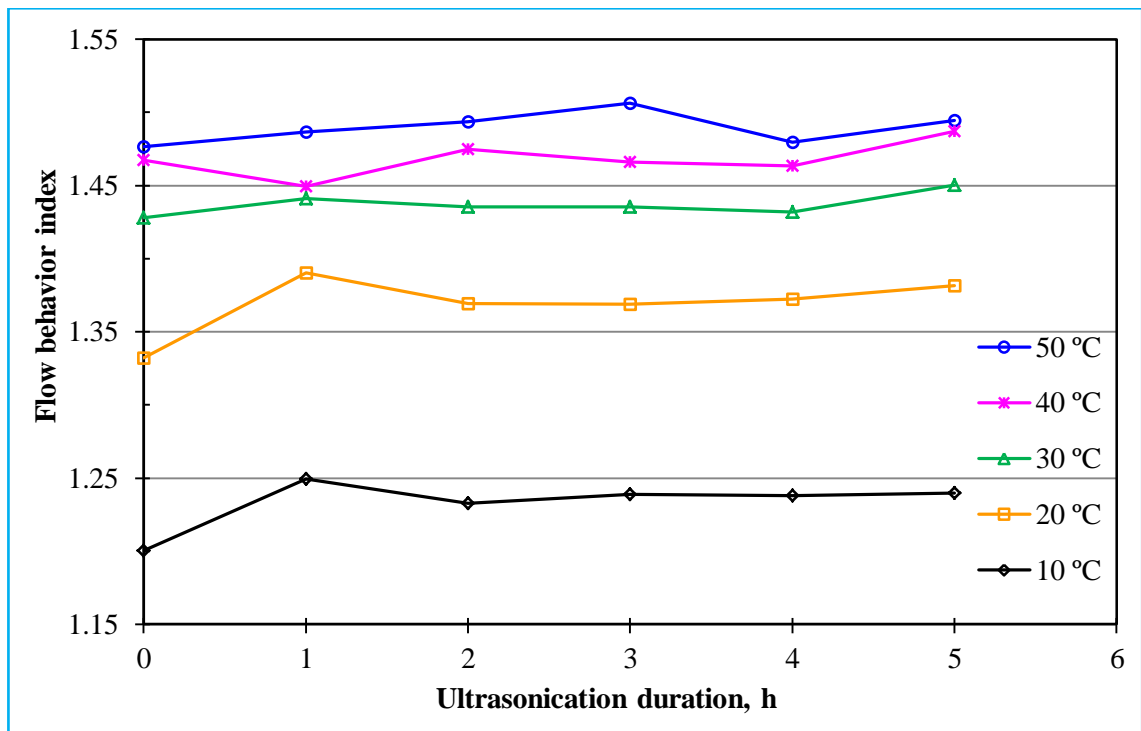


Figure 4.44: Effect of ultrasonication duration on flow behavior index for the Al_2O_3 -water nanofluid.

The effect of ultrasonication duration of nanofluid on the consistency index (k) was determined by using Power law model and portrayed in From Figure 4.45. It can be seen from Figure 4.45 that the consistency index was decreased with increasing temperature. This is because, flow consistency index k is proportional to viscosity and viscosity decreased by the increase of temperature as seen in Figure 4.32. It is also observed that, the consistency index decreased by the increase of ultrasonication durations. The values of k were found to be higher for the nanofluid prepared by without ultrasonication and it rapidly decreased by the increase of the ultrasonication period. Similar to the viscosity, a very slow decrement rate of k was observed after 1 h of ultrasonication.

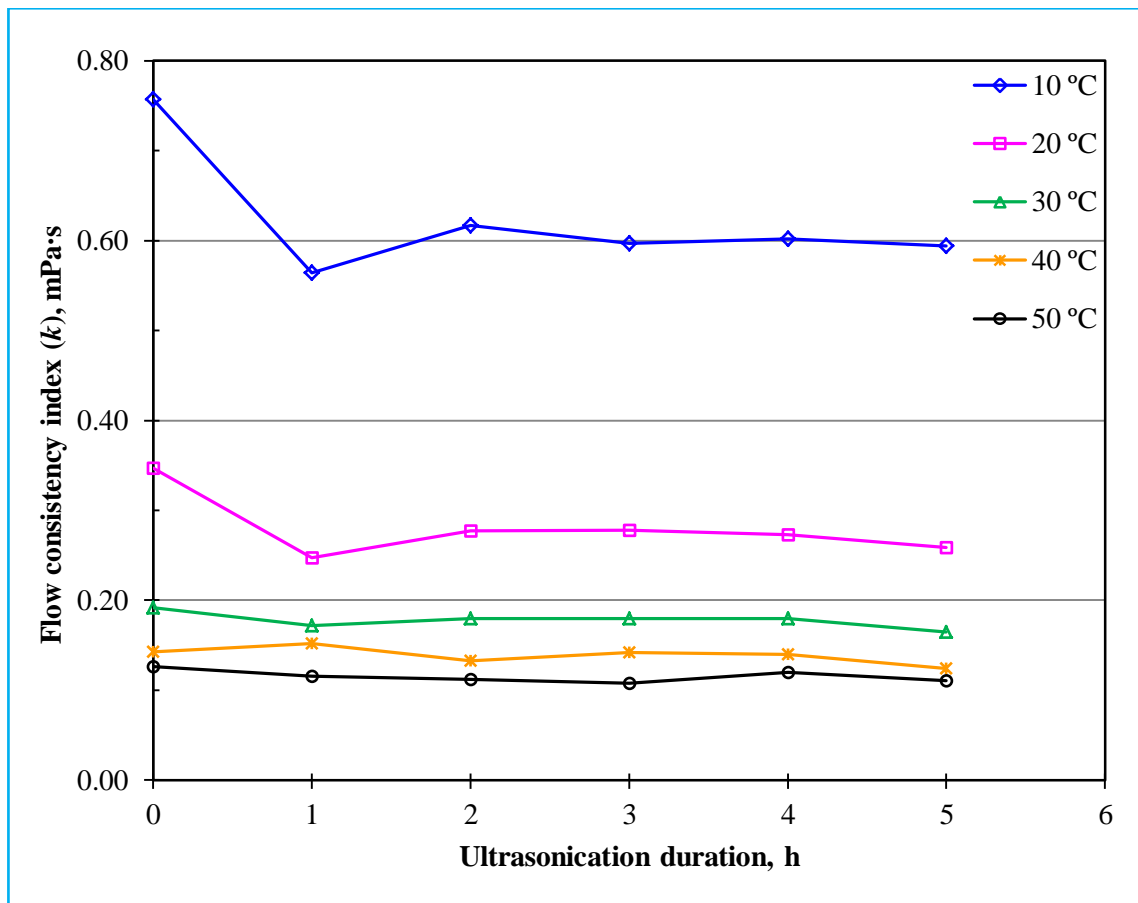


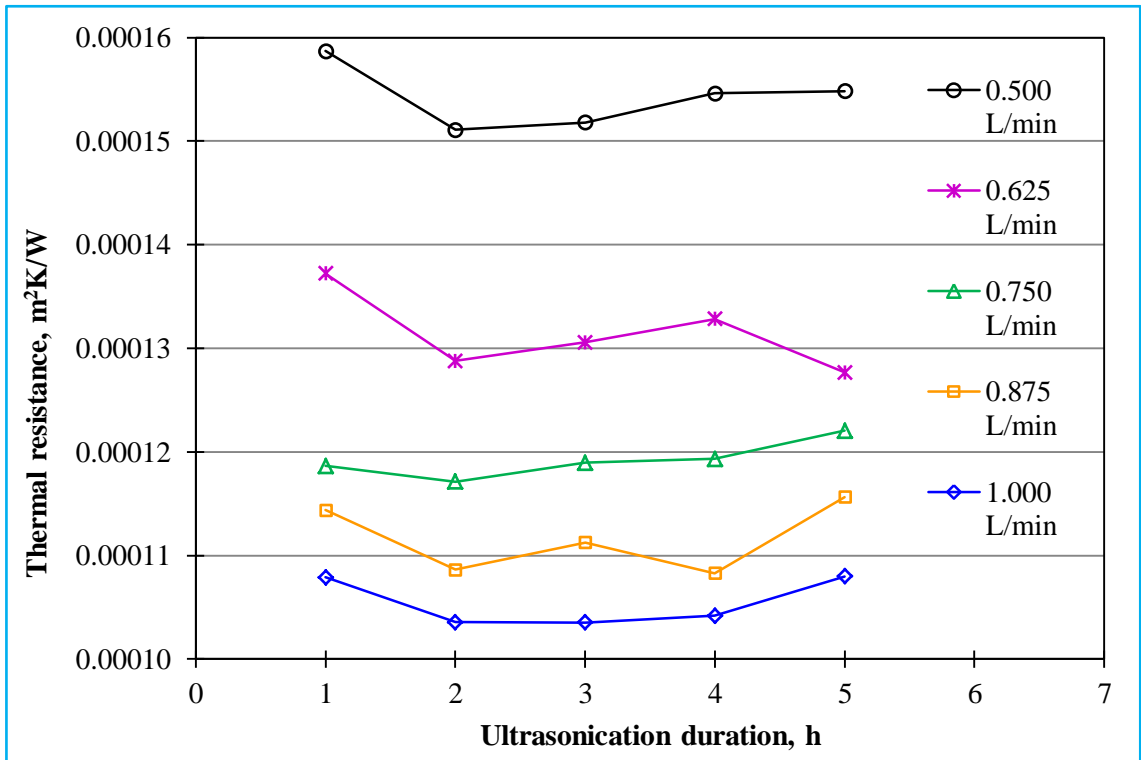
Figure 4.45: Effect of ultrasonication duration on flow consistency index for the Al_2O_3 -water nanofluid.

4.6 Thermal performance characteristics

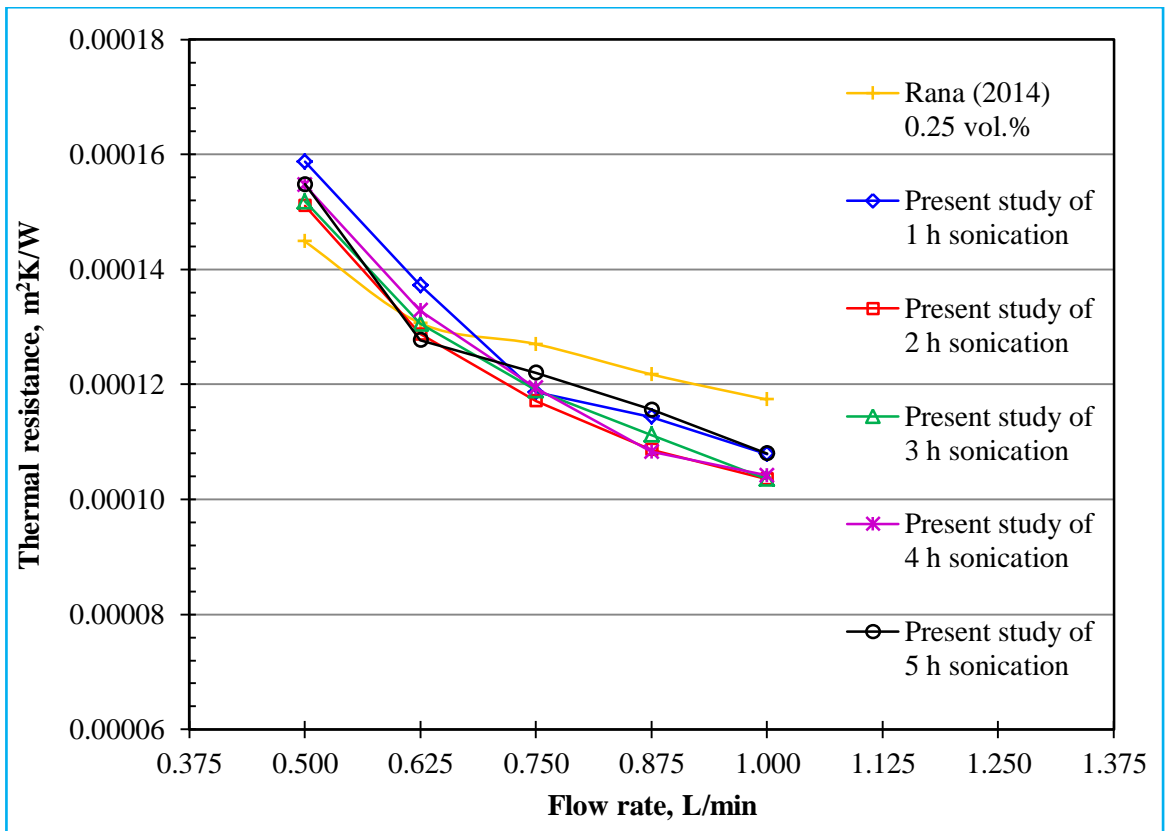
The effect of ultrasonication duration of nanofluid preparation on the thermal performance parameters of a mini channel heat sink was investigated. Thermal resistance, log mean temperature difference, heat transfer coefficient, pumping power, and FOM were investigated for the ultrasonication duration of 1, 2, 3, 4, and 5 h.

The effect of ultrasonication duration of nanofluid on the thermal resistance of the heat sink is shown in Figure 4.46. It can be seen in Figure 4.46 (a) that the highest thermal resistance was observed for the nanofluid prepared by 1 h of ultrasonication duration. The highest thermal resistance observed for 1 h of sonication could be due to the huge agglomeration of particles for that period as seen in Figure 4.4 and Figure 4.19.

Moreover, this may be because of the lower thermal conductivity values that were observed for 1 h of sonication in Figure 4.24. Then thermal resistance was found to be decreased for 2 h of sonication. Further ultrasonication after 2 h showed the different trend of thermal resistance at different flow rates. This irregular trend may be due to the temperature variation, which could be influenced by the outside temperature (room temperature). Thermal resistance is calculated based on the following three parameters: surface area, temperature difference, and generated heat. Among them, area is constant for all samples. Heat generated by the cartridge heater supposed to be constant as there was no electrical power disruption or fluctuation was observed during the experiments. Nevertheless, the heater had an accuracy of $\pm 3.5\%$. The other controlling parameters of thermal resistance are: bond line thickness, surface roughness, and thermal conductivity of the material (Hirschi, 2008) were constant. Therefore, only the variable parameter is the temperature, which is mainly influenced by heater, coolant (nanofluid) performance, and room temperature. Again, the nanofluid performance depends on flow rate and the extra radiator cooler in the mini channel heat sink that was used to cold down the nanofluid exerted from the heat sink to return it in room temperature. The highest difference of the thermal resistance decrement for the nanofluids with different ultrasonication durations were within 5.74% only, which is related to the deviation of thermal conductivity enhancement of the nanofluids that was within 1.90% for different durations of ultrasonication and the accuracy of the heater ($\pm 3.5\%$). Therefore, the use of higher ultrasonication duration is not significant in thermal resistance decrement of the system.



(a) Thermal resistance for different ultrasonication periods

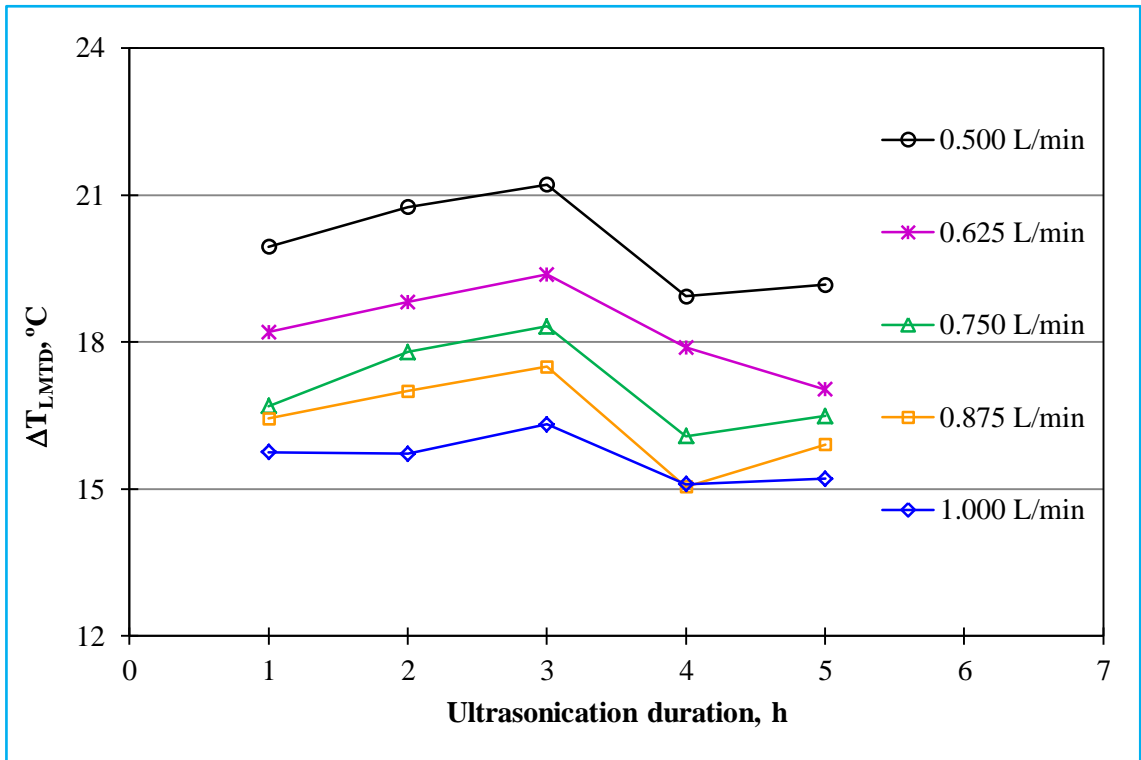


(b) Thermal resistance at different flow rates

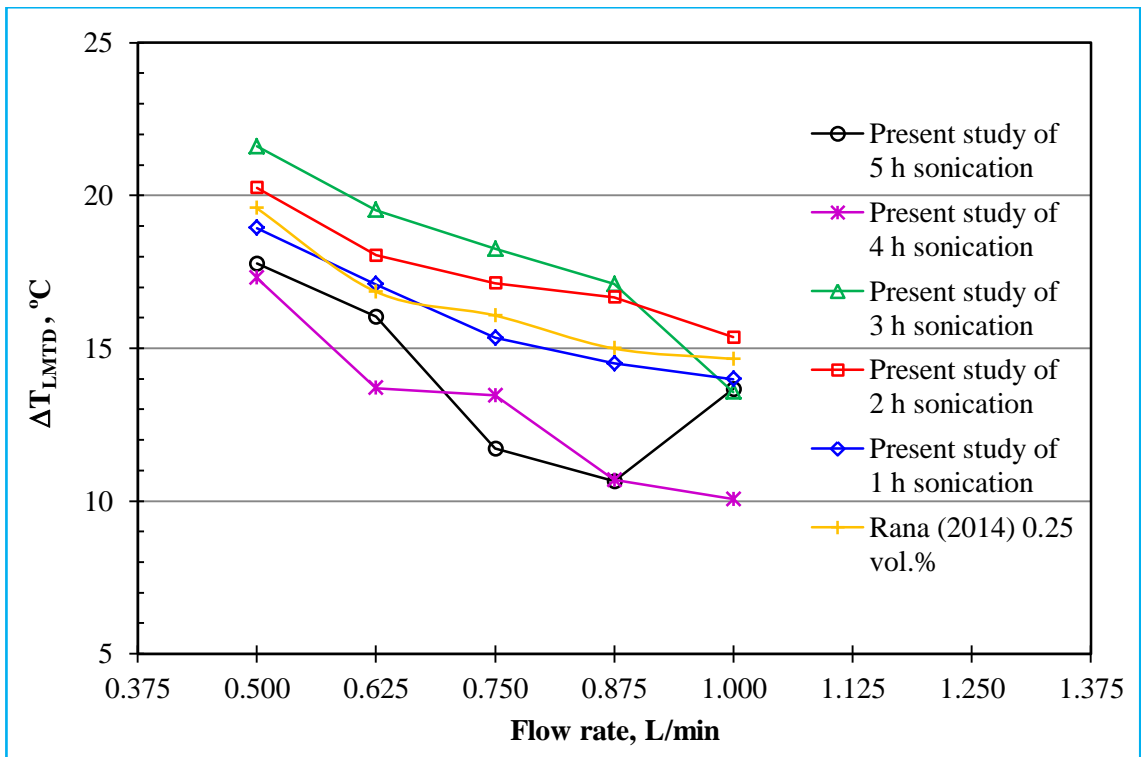
Figure 4.46: Effect of ultrasonication duration on thermal resistance of the mini channel heat sink.

Again, the experimental results of this study was compared with the study of Rana (2014) and plotted in Figure 4.46 (b). He (Rana, 2014) studied with the same setup and same nanofluid but with 0.25 vol.% and with a lower ultrasonication duration of about 30 min. It can be seen from Figure 4.46 (b) that at lower flow rates (0.500–0.625 L/min), thermal resistance of this study was higher than the studies of Rana (2014), which could be an error of any of the study. At higher flow rates (0.750–1.000 L/min), the result of this study was found to be lower than the study of Rana (2014). The higher thermal resistance of his study is mainly for the use of low concentration of particles. It is also seen from Figure 4.46 (b) that higher thermal resistance was observed at lower flow rates. Thermal resistance was found to be decreased with the increase of nanofluid flow rates. At higher flow rates, nanofluid prepared by 5 h of ultrasonication also showed higher thermal resistance, which could be due to the reason of tip erosion as seen in Figure 4.8.

The logarithmic mean temperature difference (LMTD) was determined for the effect of ultrasonication duration and shown in Figure 4.47. Initially, LMTD was found to be increased with the ultrasonication period until 3 h as seen in Figure 4.47 (a). Further ultrasonication after 3 h, LMTD was found to be decreased for 4 h of sonication time. The above trend was found to be similar for all the used flow rates as seen in Figure 4.47 (a) and (b). In the case of nanofluid prepared by 5 h of sonication time, different trends were observed, which could be due to the erosion of ultrasound probe as seen in Figure 4.8.



(a) Log mean temperature difference for different ultrasonication periods



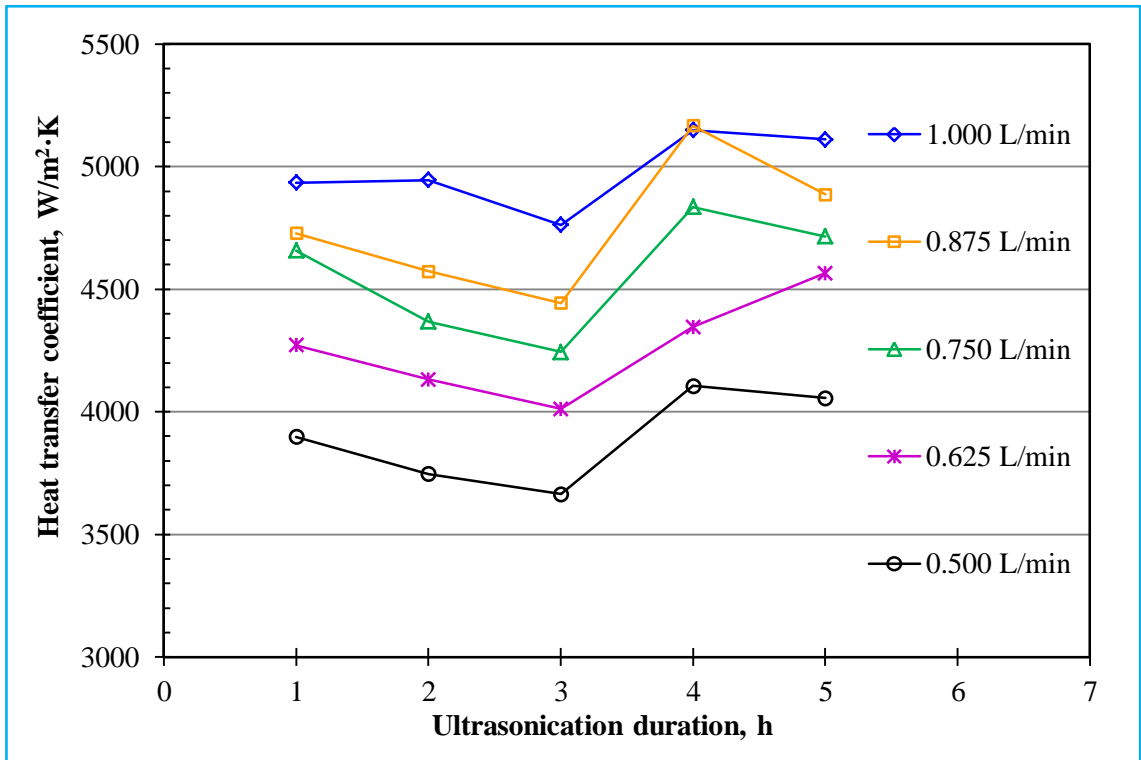
(b) Log mean temperature difference at different flow rates

Figure 4.47: Effect of ultrasonication duration on log mean temperature difference of the mini channel heat sink.

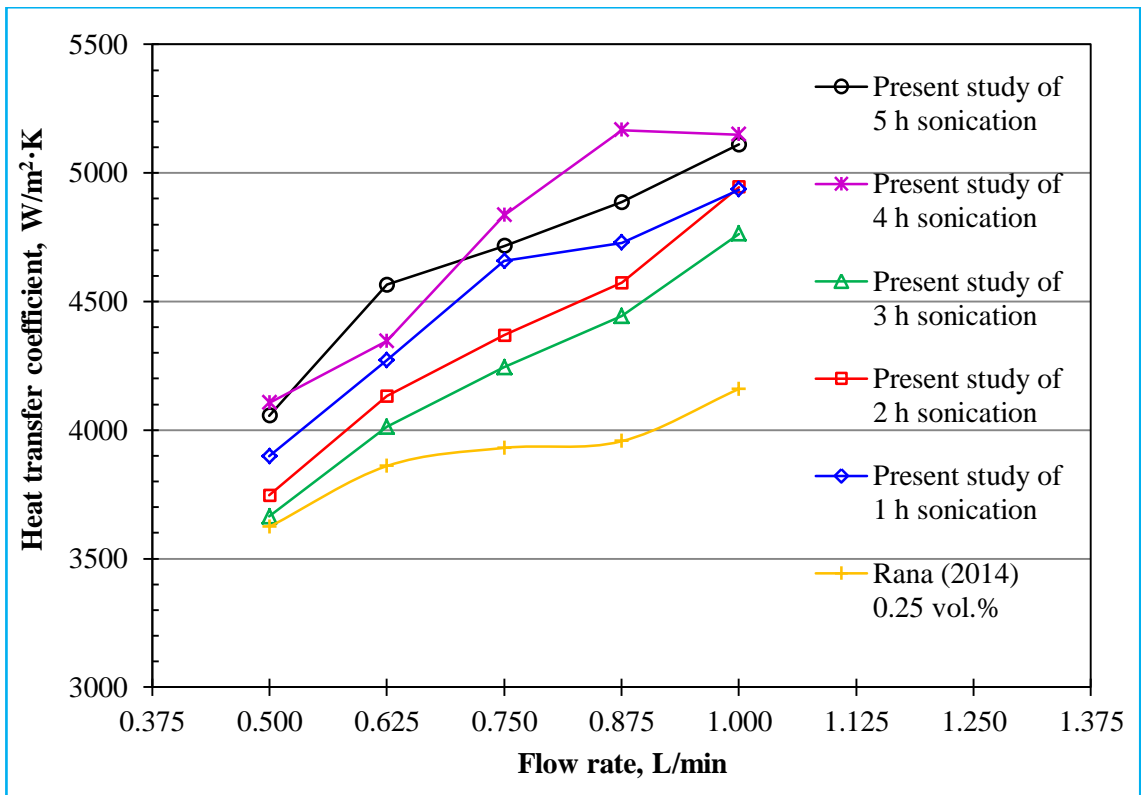
The experimental results of this study was compared with the study of Rana (2014) and plotted in Figure 4.47 (b). The similar trend of decreasing LMTD with increasing flow rates was observed. It can be seen in Figure 4.47 (b) that the lower LMTD was observed at higher flow rates but it was higher at lower flow rates. However, the results of this study for 2 h and 3 h of ultrasonication were found to be higher than the study of Rana (2014), which could be an error of any of the study. Because, he studied for 0.25 vol.% of alumina nanoparticle. It could be noted that LMTD is inversely proportional to the HTC of a system. Therefore, the higher decrement percentage of the LMTD is better for thermal performance.

HTC of the mini channel heat sink operated with Al_2O_3 -water nanofluids was analyzed at different flow rates. Figure 4.48 shows the effect of 1, 2, 3, 4 and 5 h of ultrasonication duration on HTC of the heat sink. From Figure 4.48 (a), it can be seen that initially, a decreasing trend of HTC with increasing the ultrasonication duration until 3 h was observed. The highest HTC was observed for 4 h of ultrasonication. Almost a similar trend was observed at different applied flow rates until 4 h of sonication time. After 4 h of ultrasonication, different trends of HTC were seen in Figure 4.48 (a). At 5 h of ultrasonication and at 0.875 L/min flow rates, HTC was decreased. However, at 0.625 L/min flow rates, it was increased. The higher HTC values are in agreement with the thermal conductivity values observed in Figure 4.24 where, higher thermal conductivity values were observed for 4 and 5 h of ultrasonication durations. The highest increment of HTC was found to be 13.60% at 0.875 L/min flow rate for 4 h of ultrasonication. It can be seen that HTC was increased with increasing the ultrasonication duration until 4 h. Further enhancement was not observed for the nanofluids prepared by 5 h periods. Maximum variation of HTC enhancement was observed about 13% for the samples prepared at different durations of

ultrasonication. Therefore, the effect of ultrasonication of nanofluid is significant in HTC enhancement. It is established that HTC is proportional to thermal conductivity. An increase in HTC enhancement values were observed with the increase of flow rates as seen in Figure 4.48 (b). The experimental results of this study was compared with the analysis of Rana (2014) who found a similar trend as seen in Figure 4.48 (b). However, as he used 0.25 vol.% of nanoparticles therefore, his HTC enhancement was found to be lower than this study. Another study reported by Garg et al. (2009) found highest increment about 32% for the 1 wt.% MWCNT in DIW with GA in a straight tube. In most cases, HTC is proportional to thermal conductivity of the used fluid. Therefore, the highest increment of Garg et al. (2009) was higher because of using the high thermal conductivity MWCNT.



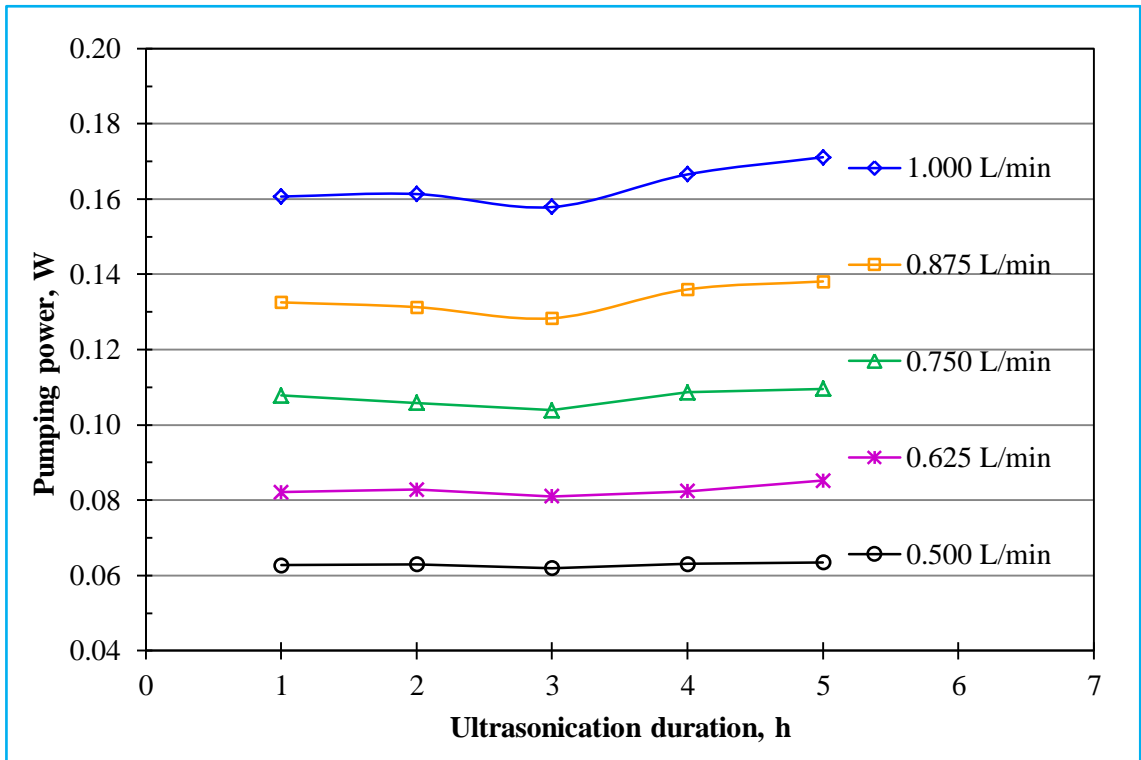
(a) Heat transfer coefficient difference for the variation ultrasonication periods



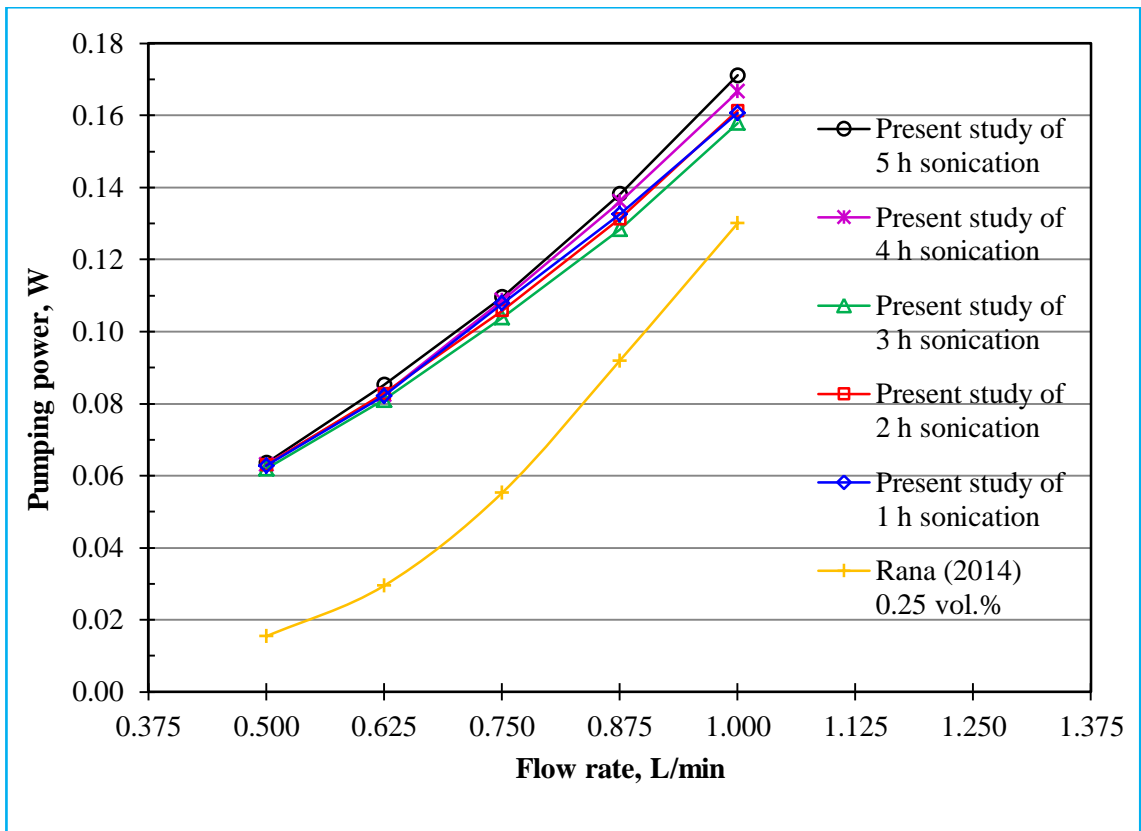
(b) Heat transfer coefficient difference at different flow rates

Figure 4.48: Effect of ultrasonication duration on the heat transfer coefficient of the mini channel heat sink.

Pumping power of the mini channel heat sink was calculated based on the measured pressure drop at different flow rates. The effect 1, 2, 3, 4, and 5 h of ultrasonication of Al_2O_3 -water nanofluids on pumping power of the system is shown in Figure 4.49. It can be seen in Figure 4.49 (a) that pumping power enhancement was decreased with increasing sonication durations up to 3 h. After that, pumping power was again increased with sonication time. The highest pumping power enhancement was observed at 5 h of ultrasonication. The microstructure of Al_2O_3 nanoparticles reported in Figure 4.6 showed that there were very few clusters of particles were available after 3 h of sonication. Also, viscosity of the nanofluids was found to be decreasing with the increase of sonication time as seen in Figure 4.30. The increase of pumping power from 4 h of ultrasonication could be because of the erosion of the ultrasound probe. It is quite impossible to stop the erosion of sonicator tip and the amount of erosion is exponentially increased with the sonication period. The TEM images of Figure 4.7 and 4.8 showed that there were some aggregations of particles as well as erosion of the ultrasound tip. The highest difference of pumping power enhancement was found about 10% for the nanofluid prepared at different ultrasonication durations. Nevertheless, the highest viscosity difference was found to be 5.5%. Therefore, the effect of ultrasonication duration on pumping power enhancement of the system was found to be significant.



(a) Pumping power difference for the variation ultrasonication periods



(b) Pumping power difference at different flow rates

Figure 4.49: Effect of ultrasonication duration of Al_2O_3 -water nanofluids on pumping power of the mini channel heat sink.

The analysis of this study was compared with the study of Rana (2014) and found almost similar trend as reported in Figure 4.49 (b). However, he found a lower pumping power enhancement as he used lower particle concentration that was 0.25 vol.%. It can be seen in Figure 4.49 (b) that the pumping power was found to be higher with high-flow rates. This is because when the flow rate increases, it creates extra force and resistance to the flow; and pressure difference is increased. It can be seen in Figure 4.49 (b) that at lower flow rates (0.500 L/min), the difference of pumping power enhancement was lower for the nanofluids prepared by 1–5 h of ultrasonication. The difference of pumping power enhancement was found to be higher at high-flow rates.

It could be noted that HTC is the key performance parameter of a heat exchanger system, which was found to be higher at 4 and 5 h of ultrasonication in this study. Nevertheless, highest pumping power was also observed at 5 h of ultrasonication and it is a negative impact. Therefore, to get the maximum benefit from nanofluid for the mini channel heat sink, FOM were determined by considering both HTC and pumping power. The effect of ultrasonication duration of Al₂O₃–water nanofluids on FOM of the mini channel heat sink is shown in Figure 4.50, which are the ratio of HTC and pumping power of nanofluid divided by those values of base fluid. From Figure 4.50, it can be seen that mostly, highest FOM values were found to be for the nanofluid prepared by 4 h of ultrasonication at all flow rates except 0.625 L/min. However, at 0.625 L/min the peak of FOM was observed for 5 h of ultrasonication duration. The peak of the FOM (among all) was found at 0.875 L/min flow rate for 4 h of ultrasonication.

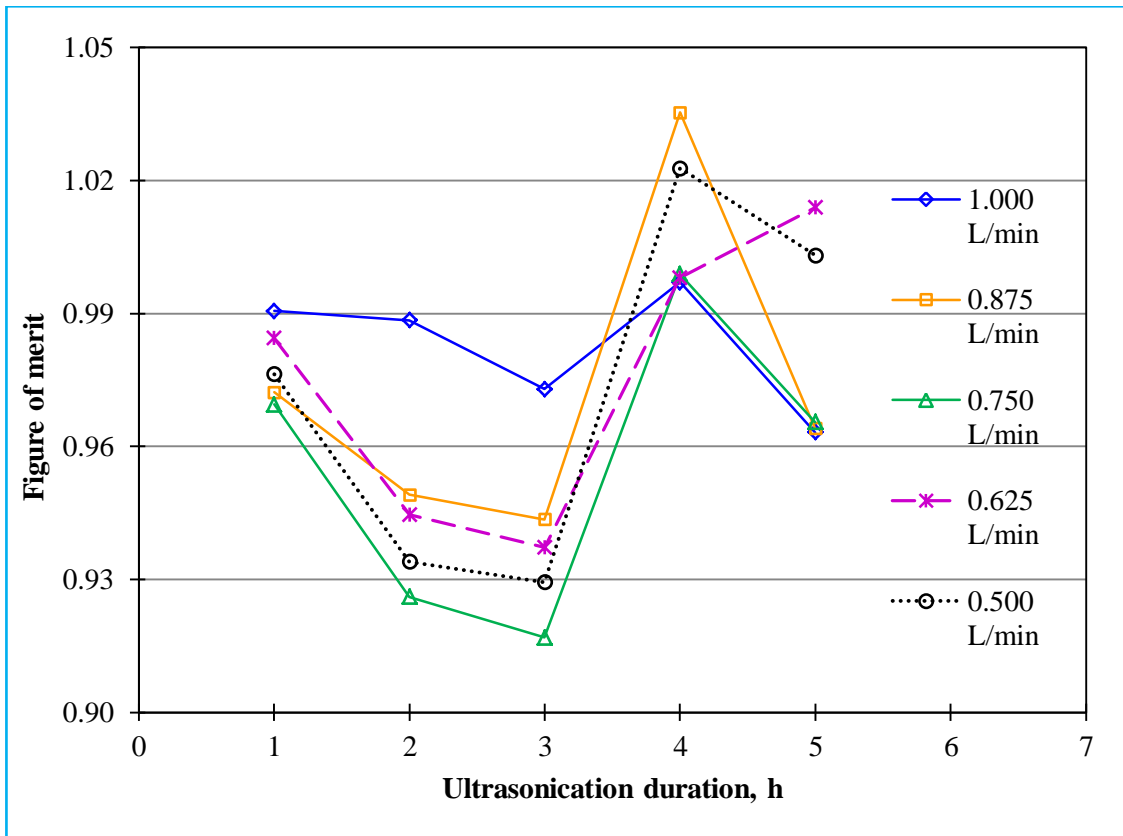


Figure 4.50: Figures of merit of the mini channel heat sink after different durations of ultrasonication.

CHAPTER 5: CONCLUSIONS AND RECOMMENDATIONS

5.1 Introduction

This chapter is divided into three sections. The first section starts with some concluding remarks, second section discussing the limitation of the study, and the third section is about some recommendations for future work and precautions during ultrasonication.

5.2 Conclusions

The effects of ultrasonication treatment on colloidal dispersion characteristics, thermophysical and rheological properties, and thermal performance analysis (in a mini channel heat sink) of 0.5 vol.% Al₂O₃-water nanofluid were investigated. From the experimental analysis, the followings conclusions can be drawn.

- ❖ Based on FESEM microstructure, nanoparticles were in loosely aggregated form before being suspended in water. TEM analyses showed that nanoparticles start dispersing with ultrasonication. Ultrasonication with higher amplitude takes shorter duration for proper dispersion of particles. A 1 h of ultrasonication is not sufficient for proper dispersion of nanoparticles and better dispersion was observed for nanofluid prepared by ~3 h of ultrasonication with 50% amplitude of sonicator power. However, further ultrasonication after 3 h showed more spreading of nanoparticles but there were few nano-clusters were existed. The higher dispersion of particles was observed after 5 h of ultrasonication in the case of 25% amplitude. However, there were some aggregations; therefore, further ultrasonication may disperse the particles more. Erosion of the sonicator tip was observed at 5 h of ultrasonication, especially for the operation with 50% amplitude of power. The mean particle size decreased with increasing ultrasonication duration until 3 h and further sonication could not change the average particle diameter. PSD analysis showed that

cluster size decreased with increasing ultrasonication duration and initially, it decreased rapidly. In addition, the higher the amplitude, the lower the aggregate size was observed. Polydispersity index was decreased with the start of ultrasonication until 2 h and after 2 h it was increased with sonication periods. The highest zeta potential value 58.4 mV was observed for 3 h of ultrasonication with 50% amplitude of power and further sonication until 5 h could not increase the value. In the case of 25% amplitude, the zeta potential value was slowly increased until 5 h of sonication and the highest value was 57.5 mV at this ultrasonication period (5 h). Therefore, it could be predicted that with 50% amplitude, the nanoparticles received highest ultrasound energy at 3 h of duration. However, in the case of 25% amplitude, the ultrasound energy was effective until 5 h period; even further ultrasonication could increase the charge. After 30 days of preparation, the zeta potential values were almost same for the nanofluid prepared by 4 h and above durations of ultrasonication with 50% amplitude. The pH of the samples subjected to ultrasonication for 1–5 h was almost same and was far from the isoelectric point. In brief, better particle dispersion, lower aggregate size, and higher zeta potential were obtained with the 50% amplitude of sonicator power and the optimum duration was found to be 3~4 h.

❖ Thermal conductivity was found to be increased by the rise of temperature and ultrasonication durations. However, thermal conductivity enhancement percentage was not enough in respect to the used ultrasonication duration. Maximum thermal conductivity enhancement was observed 1.90% only for the use of ultrasonication duration until 5 h. An average increase of 1.33% of thermal conductivity enhancement was observed for the temperatures variations from 10 to 50 °C. If thermal conductivity value of a nanoparticle is too high then the effect of ultrasonication duration and temperature will be significant. Again the effect of

ultrasonication period on thermal conductivity enhancement was found to be negligible after 30 days of sample preparation. The deviation was about 1.57% on an average. The viscosity of Al₂O₃–water nanofluid decreased with increasing temperature. Moreover, the viscosity of the nanofluid decreased with increasing sonication time toward the viscosity of the base fluid. During the 1st h of ultrasonication, it decreased rapidly and further ultrasonication decreased slowly. The viscosity enhancement was decreased about 8–15% from 0 to 1 h of ultrasonication. However, from 1–5 h of ultrasonication, it was decreased only 5–6% at different temperature. Therefore, first hour of ultrasonication is more effective for minimization of viscosity enhancement. It is also observed that, the nanofluid with higher temperature needs less energy to become well dispersed to get a lower viscosity. The effect of ultrasonication duration was effective over sedimentation time for the viscosity. It is found that after 30 days of sample preparation, viscosity enhancement was decreased about 6.09% for the nanofluid prepared by 5 h of ultrasonication duration. However, this decrement was found to be 25.80% for the nanofluid prepared by 0 h of ultrasonication. As like thermal conductivity, density ratio of nanofluid was increased with increasing ultrasonication time and temperature. However, the change of density enhancement was very low and negligible (below 0.5%). The effect of ultrasonication duration was not so effective over the density enhancement percentage considering sedimentation time. It is found that after 30 days of sample preparation, density enhancement was decreased about 0.47% for the nanofluid prepared by 5 h of ultrasonication duration. However, this decrement was found to be 1.00% for the nanofluid prepared by 0 h of ultrasonication. Therefore, prolonged ultrasonication does not have a significant effect over thermophysical properties after a certain level.

❖ Shear stress values were found to be decreased with increasing temperatures and the decrements were more significant at higher shear rates. At lower temperatures and lower shear rates, nanofluids were found to be Newtonian. However, at higher temperature, nanofluids were found to be almost non-Newtonian with shear thickening behavior. Shear stresses were slowly decreased with the start of ultrasonication. Nevertheless, further prolonged ultrasonication, could not significantly change the shear stresses. The rapid decrease of yield stresses was observed with the increase of temperatures for all the nanofluids prepared by different durations of ultrasonication. Yield stress was decreased rapidly with the start of ultrasonication. However, it decreased slowly with further ultrasonication. The flow index values were indicative of strong non-Newtonian and shear thickening behavior. In a nutshell, the effect of ultrasonication duration was not significant over rheological properties of the nanofluid.

❖ Irregular trend of thermal resistance was observed with ultrasonication duration at different flow rates. Log mean temperature difference was found to be increasing with increasing ultrasonication duration until 3 h. Further ultrasonication after 3 h, LMTD was found to be decreased for 4 and 5 h of sonication time. Heat transfer coefficient was initially decreased with increasing ultrasonication duration until 3 h and it was found to be higher at 4 h of sonication period. Maximum variation of HTC enhancement was observed about 13% for the samples prepared at different durations of ultrasonication. Pumping power was initially decreased until 3 h of ultrasonication. Further ultrasonication, they were increased to the maximum at 5 h of sonication time. Figure of merit analysis showed that 4 h of ultrasonication duration was the optimum by considering enhancement of HTC and penalty of pumping power.

- ❖ Therefore, throughout this study, it was found that initially, the ultrasonication process changes the colloidal dispersion states and prolonged ultrasonication did not have significant effect, rather small nano-cluster and erosion of ultrasound tip was observed. Also, no major effects of ultrasonication on the thermal conductivity, density and rheological properties were observed. It can be concluded that, the use of high ultrasound energy during nanofluid preparation could not increase significant thermal efficiency.

5.3 Limitations of the study

- ❖ There are very limited experimental facilities existing.
- ❖ The availabilities of some equipment are not adequate specially: electron microscopes.

5.4 Recommendations

- ❖ Specific heat capacity and surface tension are two important fundamental properties. These are directly related to the heat transfer performance analysis. These two parameters need to be determined experimentally for the effect of ultrasound sonication.
- ❖ There need to make some standards of nanofluid preparation process (duration, amplitudes, and pulses). More types of nanoparticles at various concentrations with different base fluids are needed to be analyzed.
- ❖ The agitation of ultrasonic horn increases the temperature. Therefore, a temperature bath is necessary to control the bulk heating during ultrasonication to avoid

vaporization. It is better to place an ultrasound homogenizer inside a sound enclosure box. Otherwise, sound protection ear plugs need to be used.

- ❖ Maintenance of an ultrasound tip is necessary whether it is a replaceable or continuous type. Over life time, tips are eroded and reduce the performance of an ultrasonic homogenizer. Nevertheless, the erosion of a tip is an unescapable side effect of ultrasonication (Taurozzi et al., 2012). The example of the end surface of a ½ inch new tip and worn tip are shown in Figure 5.1 (a) and (b), respectively. The bottom surface of the tip of an ultrasonic homogenizer need to inspect before of using every time. Based on the manufacturer guidelines, a worn tip should be reconstructed.

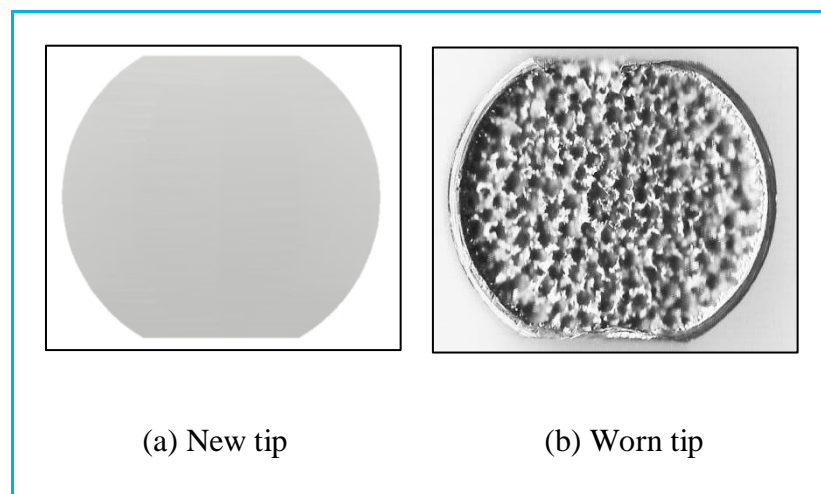


Figure 5.1: Example of ultrasound tip erosion.

REFERENCES

- American Chemical Society. (2014, July 2). Toward a new way to keep electronics from overheating. *ScienceDaily*. Retrieved from <http://www.sciencedaily.com/releases/2014/07/140702111011.htm>.
- Amrollahi, A., Hamidi, A., & Rashidi, A. (2008). The effects of temperature, volume fraction and vibration time on the thermo-physical properties of a carbon nanotube suspension (carbon nanofluid). *Nanotechnology*, *19*(31), 315701.
- Anoop, K. B., Kabelac, S., Sundararajan, T., & Das, S. K. (2009). Rheological and flow characteristics of nanofluids: Influence of electroviscous effects and particle agglomeration. *Journal of Applied Physics*, *106*(3), 034909.
- Baheta, A. T., & Woldeyohannes, A. D. (2013). Effect of Particle Size on Effective Thermal Conductivity of Nanofluids. *Asian Journal of Scientific Research* *6*, 339-345.
- Banerjee, D. (2013). Guest Editorial for the Special Issue on Micro/Nanoscale Transport Phenomena. *Journal of Nanotechnology in Engineering and Medicine*, *3*, 030301.
- Bi, S., Guo, K., Liu, Z., & Wu, J. (2011). Performance of a domestic refrigerator using TiO₂-R600a nano-refrigerant as working fluid. *Energy Conversion and Management*, *52*(1), 733-737.
- Bi, S., Shi, L., & Zhang, L. (2008). Application of nanoparticles in domestic refrigerators. *Applied Thermal Engineering*, *28*(14-15), 1834-1843.
- Chakraborty, S., Mukherjee, J., Manna, M., Ghosh, P., Das, S., & Denys, M. B. (2012). Effect of Ag nanoparticle addition and ultrasonic treatment on a stable TiO₂ nanofluid. *Ultrasonics Sonochemistry*, *19*(5), 1044-1050.
- Chandrasekar, M., Suresh, S., & Chandra Bose, A. (2010). Experimental investigations and theoretical determination of thermal conductivity and viscosity of Al₂O₃/water nanofluid. *Experimental Thermal and Fluid Science*, *34*(2), 210-216.
- Chandrasekar, M., Suresh, S., & Senthilkumar, T. (2012). Mechanisms proposed through experimental investigations on thermophysical properties and forced convective heat transfer characteristics of various nanofluids – A review. *Renewable and Sustainable Energy Reviews*, *16*(6), 3917-3938.

- Chen, H., Ding, Y., He, Y., & Tan, C. (2007a). Rheological behaviour of ethylene glycol based titania nanofluids. *Chemical Physics Letters*, 444(4-6), 333-337.
- Chen, H., Ding, Y., Lapkin, A., & Fan, X. (2009a). Rheological behaviour of ethylene glycol-titanate nanotube nanofluids. *Journal of Nanoparticle Research*, 11(6), 1513-1520.
- Chen, H., Ding, Y., & Tan, C. (2007b). Rheological behaviour of nanofluids. *New Journal of Physics*, 9(10), 367.
- Chen, H., Witharana, S., Jin, Y., Kim, C., & Ding, Y. (2009b). Predicting thermal conductivity of liquid suspensions of nanoparticles (nanofluids) based on rheology. *Particuology*, 7(2), 151-157.
- Chevalier, J., Tillement, O., & Ayela, F. (2007). Rheological properties of nanofluids flowing through microchannels. *Applied Physics Letters*, 91(23), 233103.
- Choi, S. U. S., & Eastman, J. A. (1995, November 12-17). *Enhancing thermal conductivity of fluids with nanoparticles*. Paper presented at the ASME International Mechanical Engineering Congress & Exposition, San Francisco, CA.
- Chung, S. J., Leonard, J. P., Nettleship, I., Lee, J. K., Soong, Y., Martello, D. V., & Chyu, M. K. (2009). Characterization of ZnO nanoparticle suspension in water: Effectiveness of ultrasonic dispersion. *Powder Technology*, 194(1-2), 75-80.
- Ding, Y., Alias, H., Wen, D., & Williams, R. A. (2006). Heat transfer of aqueous suspensions of carbon nanotubes (CNT nanofluids). *International Journal of Heat and Mass Transfer*, 49(1-2), 240-250.
- Eastman, J., Choi, S., Li, S., Yu, W., & Thompson, L. (2001). Anomalously increased effective thermal conductivities of ethylene glycol-based nanofluids containing copper nanoparticles. *Applied Physics Letters*, 78(6), 718-720.
- Elcioglu, E. B., & Okutucu-Ozyurt, T. (2014, June 12-15). *An experimental study on the dispersion stability of alumina-water nanofluids via particle size distribution and zeta potential measurements*. Paper presented at the International Conference on Thermophysical and Mechanical Properties of Advanced Materials, Cesme - Izmir, Turkey.
- Elias, M. M., Mahbulul, I. M., Saidur, R., Sohel, M. R., Shahrul, I. M., Khaleduzzaman, S. S., & Sadeghipour, S. (2014). Experimental investigation on the thermo-physical properties of Al₂O₃ nanoparticles suspended in car radiator coolant. *International Communications in Heat and Mass Transfer*, 54, 48-53.

- Everett, D. H. (1988). *Basic principles of colloid science*. London: Royal Society of Chemistry.
- Garg, P., Alvarado, J. L., Marsh, C., Carlson, T. A., Kessler, D. A., & Annamalai, K. (2009). An experimental study on the effect of ultrasonication on viscosity and heat transfer performance of multi-wall carbon nanotube-based aqueous nanofluids. *International Journal of Heat and Mass Transfer*, 52(21-22), 5090-5101.
- Ghadimi, A., & Metselaar, I. H. (2013). The influence of surfactant and ultrasonic processing on improvement of stability, thermal conductivity and viscosity of titania nanofluid. *Experimental Thermal and Fluid Science*, 51, 1-9.
- Ghadimi, A., Saidur, R., & Metselaar, H. S. C. (2011). A review of nanofluid stability properties and characterization in stationary conditions. *International Journal of Heat and Mass Transfer*, 54(17-18), 4051-4068.
- Goharshadi, E., Ding, Y., Jorabchi, M., & Nancarrow, P. (2009). Ultrasound-assisted green synthesis of nanocrystalline ZnO in the ionic liquid [hmim][NTf₂]. *Ultrasonics Sonochemistry*, 16(1), 120-123.
- Hays, A., Marsh, C. P., Alvarado, J., & Franks, R. (2006, July 17-20). *The effect of nanoparticle agglomeration on enhanced nanofluidic thermal conductivity*. Paper presented at the International Refrigeration and Air Conditioning Conference, Purdue University.
- He, Y., Jin, Y., Chen, H., Ding, Y., Cang, D., & Lu, H. (2007). Heat transfer and flow behaviour of aqueous suspensions of TiO₂ nanoparticles (nanofluids) flowing upward through a vertical pipe. *International Journal of Heat and Mass Transfer*, 50(11-12), 2272-2281.
- Herschel, W. H., & Bulkley, R. (1926). Konsistenzmessungen von gummi-benzollösungen. *Kolloid-Zeitschrift*, 39(4), 291-300.
- Hiemenz, P. C., & Rajagopalan, R. (1997). *Principles of Colloid and Surface Chemistry, Third edition, revised and expanded*. New York, NY: Marcel Dekker, Inc.
- Hirschi, D. (2008). Understanding Thermal Performance Data: Improve your ability to recommend the right thermal interface material, *Dow Corning Case Study*. Midland, MI: Dow Corning Corporation.
- Ho, C. J., & Chen, W. C. (2013). An experimental study on thermal performance of Al₂O₃/water nanofluid in a minichannel heat sink. *Applied Thermal Engineering*, 50(1), 516-522.

- Hong, K. S., Hong, T.-K., & Yang, H.-S. (2006). Thermal conductivity of Fe nanofluids depending on the cluster size of nanoparticles. *Applied Physics Letters*, 88(3), 031901.
- Hong, T.-K., Yang, H.-S., & Choi, C. J. (2005). Study of the enhanced thermal conductivity of Fe nanofluids. *Journal of Applied Physics*, 97(6), 064311.
- Hunter, R. J. (1981). *Zeta potential in colloid science: principles and applications*. London: Academic Press Ltd.
- Ijam, A., Saidur, R., & Ganesan, P. (2012). Cooling of minichannel heat sink using nanofluids. *International Communications in Heat and Mass Transfer*, 39(8), 1188-1194.
- Ijam, A., Saidur, R., Ganesan, P., & Moradi Golsheikh, A. (2015). Stability, thermo-physical properties, and electrical conductivity of graphene oxide-deionized water/ethylene glycol based nanofluid. *International Journal of Heat and Mass Transfer*, 87(0), 92-103.
- Islam, M. M. (2012). *Investigation of fundamental properties of nanorefrigerants*. (Unpublished master's thesis). University of Malaya, Kuala Lumpur.
- Jiang, W., Ding, G., & Peng, H. (2009a). Measurement and model on thermal conductivities of carbon nanotube nanorefrigerants. *International Journal of Thermal Sciences*, 48(6), 1108-1115.
- Jiang, W., Ding, G., Peng, H., Gao, Y., & Wang, K. (2009b). Experimental and Model Research on Nanorefrigerant Thermal Conductivity. *HVAC&R Research*, 15(3), 651-669.
- Kabir, M. E., Saha, M. C., & Jeelani, S. (2007). Effect of ultrasound sonication in carbon nanofibers/polyurethane foam composite. *Materials Science and Engineering: A*, 459(1-2), 111-116.
- Khaleduzzaman, S. S., Saidur, R., Mahbubul, I. M., Ward, T. A., Sohel, M. R., Shahrul, I. M., . . . Rahman, M. M. (2014). Energy, Exergy, and Friction Factor Analysis of Nanofluid as a Coolant for Electronics. *Industrial & Engineering Chemistry Research*, 53(25), 10512-10518.
- Kole, M., & Dey, T. K. (2010). Viscosity of alumina nanoparticles dispersed in car engine coolant. *Experimental Thermal and Fluid Science*, 34(6), 677-683.

- Kole, M., & Dey, T. K. (2012). Effect of prolonged ultrasonication on the thermal conductivity of ZnO–ethylene glycol nanofluids. *Thermochimica Acta*, 535, 58-65.
- Kulkarni, D. P., Das, D. K., & Vajjha, R. S. (2009). Application of nanofluids in heating buildings and reducing pollution. *Applied Energy*, 86(12), 2566-2573.
- Kwak, K., & Kim, C. (2005). Viscosity and thermal conductivity of copper oxide nanofluid dispersed in ethylene glycol. *Korea-Australia Rheology Journal*, 17(2), 35-40.
- Lam, C.-k., Lau, K.-t., Cheung, H.-y., & Ling, H.-y. (2005). Effect of ultrasound sonication in nanoclay clusters of nanoclay/epoxy composites. *Materials Letters*, 59(11), 1369-1372.
- Lee, J., Hwang, K., Jang, S., Lee, B., Kim, J., Choi, S., & Choi, C. (2008). Effective viscosities and thermal conductivities of aqueous nanofluids containing low volume concentrations of Al₂O₃ nanoparticles. *International Journal of Heat and Mass Transfer*, 51(11-12), 2651-2656.
- Leong, Y. K., Scales, P. J., Healy, T. W., Boger, D. V., & Buscall, R. (1993). Rheological evidence of adsorbate-mediated short-range steric forces in concentrated dispersions. *Journal of the Chemical Society, Faraday Transactions*, 89(14), 2473-2478.
- Li, Y., Zhou, J. e., Tung, S., Schneider, E., & Xi, S. (2009). A review on development of nanofluid preparation and characterization. *Powder Technology*, 196(2), 89-101.
- LotfizadehDehkordi, B., Ghadimi, A., & Metselaar, H. S. (2013). Box–Behnken experimental design for investigation of stability and thermal conductivity of TiO₂ nanofluids. *Journal of Nanoparticle Research*, 15, 1369.
- Mahbubul, I. M., Saidur, R., & Amalina, M. A. (2012). Latest developments on the viscosity of nanofluids. *International Journal of Heat and Mass Transfer*, 55(4), 877-888.
- Mahbubul, I. M., Saidur, R., & Amalina, M. A. (2013). Influence of particle concentration and temperature on thermal conductivity and viscosity of Al₂O₃/R141b nanorefrigerant. *International Communications in Heat and Mass Transfer*, 43, 100-104.
- Mandzy, N., Grulke, E., & Druffel, T. (2005). Breakage of TiO₂ agglomerates in electrostatically stabilized aqueous dispersions. *Powder Technology*, 160(2), 121-126.

- Mariano, A., Pastoriza-Gallego, M. J., Lugo, L., Camacho, A., Canzonieri, S., & Piñeiro, M. M. (2013). Thermal conductivity, rheological behaviour and density of non-Newtonian ethylene glycol-based SnO₂ nanofluids. *Fluid Phase Equilibria*, 337, 119-124.
- Mewis, J., & Wagner, N. J. (2012). *Colloidal Suspension Rheology*. Cambridge: Cambridge University Press.
- Mueller, S., Llewellyn, E. W., & Mader, H. M. (2010). The rheology of suspensions of solid particles. [Journal Article]. *Proceedings of the Royal Society A: Mathematical, Physical and Engineering Science*, 466(2116), 1-28.
- Müller, R. H. (1996). *Zetapotential und Partikelladung in der Laborpraxis* (First ed.). Stuttgart, Germany: Wissenschaftliche Verlagsgesellschaft.
- Murshed, S., Leong, K., & Yang, C. (2008a). Investigations of thermal conductivity and viscosity of nanofluids. *International Journal of Thermal Sciences*, 47(5), 560-568.
- Murshed, S., Leong, K., & Yang, C. (2008b). Thermophysical and electrokinetic properties of nanofluids – A critical review. *Applied Thermal Engineering*, 28(17-18), 2109-2125.
- Murshed, S. S., Tan, S.-H., & Nguyen, N.-T. (2008c). Temperature dependence of interfacial properties and viscosity of nanofluids for droplet-based microfluidics. *Journal of Physics D: Applied Physics*, 41(8), 085502.
- Namburu, P., Kulkarni, D., Misra, D., & Das, D. (2007a). Viscosity of copper oxide nanoparticles dispersed in ethylene glycol and water mixture. *Experimental Thermal and Fluid Science*, 32(2), 397-402.
- Namburu, P. K., Kulkarni, D. P., Dandekar, A., & Das, D. K. (2007b). Experimental investigation of viscosity and specific heat of silicon dioxide nanofluids. *Micro & Nano Letters*, 2(3), 67-71.
- Naphon, P., & Nakharintr, L. (2013). Heat transfer of nanofluids in the mini-rectangular fin heat sinks. *International Communications in Heat and Mass Transfer*, 40, 25-31.
- Nguyen, C., Desgranges, F., Roy, G., Galanis, N., Mare, T., Boucher, S., & Anguemintsa, H. (2007). Temperature and particle-size dependent viscosity data for water-based nanofluids – Hysteresis phenomenon. *International Journal of Heat and Fluid Flow*, 28(6), 1492-1506.

- Nguyen, V. S., Rouxel, D., Hadji, R., Vincent, B., & Fort, Y. (2011). Effect of ultrasonication and dispersion stability on the cluster size of alumina nanoscale particles in aqueous solutions. *Ultrasonics Sonochemistry*, 18(1), 382-388.
- Özcan-Taşkin, N. G., Padron, G., & Voelkel, A. (2009). Effect of particle type on the mechanisms of break up of nanoscale particle clusters. *Chemical Engineering Research and Design*, 87(4), 468-473.
- Özeringç, S., Kakaç, S., & Yazıcıoğlu, A. G. (2010). Enhanced thermal conductivity of nanofluids: a state-of-the-art review. *Microfluidics and Nanofluidics*, 8(2), 145-170.
- Pak, B. C., & Cho, Y. I. (1998). Hydrodynamic and heat transfer study of dispersed fluids with submicron metallic oxide particles. *Experimental heat transfer*, 11(2), 151-170.
- Patel, H. E., Sundararajan, T., & Das, S. K. (2010). An experimental investigation into the thermal conductivity enhancement in oxide and metallic nanofluids. *Journal of Nanoparticle Research*, 12(3), 1015-1031.
- Paul, G., Chopkar, M., Manna, I., & Das, P. K. (2010). Techniques for measuring the thermal conductivity of nanofluids: A review. *Renewable and sustainable energy reviews*, 14(7), 1913-1924.
- Paul, G., Philip, J., Raj, B., Das, P. K., & Manna, I. (2011). Synthesis, characterization, and thermal property measurement of nano-Al₁₉₅Zn₀₅ dispersed nanofluid prepared by a two-step process. *International Journal of Heat and Mass Transfer*, 54(15-16), 3783-3788.
- Phuoc, T. X., Massoudi, M., & Chen, R.-H. (2011). Viscosity and thermal conductivity of nanofluids containing multi-walled carbon nanotubes stabilized by chitosan. *International Journal of Thermal Sciences*, 50(1), 12-18.
- Rana, M. S. (2014). *Enhancing the cooling performance of electronic devices using nanofluids*. (Unpublished master's thesis). University of Malaya, Kuala Lumpur.
- Rashmi, W., Ismail, A., Sopyan, I., Jameel, A., Yusof, F., Khalid, M., & Mubarak, N. (2011). Stability and thermal conductivity enhancement of carbon nanotube nanofluid using gum arabic. *Journal of Experimental Nanoscience*, 6(6), 567-579.
- Ruan, B., & Jacobi, A. M. (2012). Ultrasonication effects on thermal and rheological properties of carbon nanotube suspensions. *Nanoscale Research Letters*, 7(1), 127.

- Sadeghi, R., Etemad, S. G., Keshavarzi, E., & Haghshenasfard, M. (2014). Investigation of alumina nanofluid stability by UV–vis spectrum. *Microfluidics and Nanofluidics*, DOI: 10.1007/s10404-10014-11491-y.
- Saidur, R., Leong, K. Y., & Mohammad, H. A. (2011). A review on applications and challenges of nanofluids. *Renewable and Sustainable Energy Reviews*, *15*(3), 1646-1668.
- Sanchez, C., Renard, D., Robert, P., Schmitt, C., & Lefebvre, J. (2002). Structure and rheological properties of acacia gum dispersions. *Food Hydrocolloids*, *16*(3), 257-267.
- Shah, S. K. (2015). *Energy, exergy and entropy generation analyses of Al₂O₃ nanofluid as a coolant for electronics*. (Unpublished master's thesis). University of Malaya, Kuala Lumpur.
- Shahrul, I. M., Mahbubul, I. M., Khaleduzzaman, S. S., Saidur, R., & Sabri, M. F. M. (2014). A comparative review on the specific heat of nanofluids for energy perspective. *Renewable and sustainable energy reviews*, *38*, 88-98.
- Sitprasert, C., Dechaumphai, P., & Juntasaro, V. (2009). A thermal conductivity model for nanofluids including effect of the temperature-dependent interfacial layer. *Journal of Nanoparticle Research*, *11*(6), 1465-1476.
- Smalley, R. E. (2005). Future global energy prosperity: the terawatt challenge. *MRS Bulletin*, *30*(6), 412-417.
- Smith, G. J., Wilding, W. V., Oscarson, J. L., & Rowley, R. L. (2003, June 22-27). *Correlation of Liquid Viscosity at the Normal Boiling Point* Paper presented at the Fifteenth Symposium on Thermophysical Properties, Boulder, CO.
- Sohel, M. R., Khaleduzzaman, S. S., Saidur, R., Hepbasli, A., Sabri, M. F. M., & Mahbubul, I. M. (2014). An experimental investigation of heat transfer enhancement of a minichannel heat sink using Al₂O₃–H₂O nanofluid. *International Journal of Heat and Mass Transfer*, *74*, 164-172.
- Taurozzi, J., Hackley, V., & Wiesner, M. (2012). Preparation of nanoparticle dispersions from powdered material using ultrasonic disruption, *NanoEHS Protocols* (Version 1.1 ed.). Gaithersburg, MD: National Institute of Standards and Technology.
- Timofeeva, E. V., Routbort, J. L., & Singh, D. (2009). Particle shape effects on thermophysical properties of alumina nanofluids. *Journal of Applied Physics*, *106*(1), 014304.

- Timofeeva, E. V., Smith, D. S., Yu, W., France, D. M., Singh, D., & Routbort, J. L. (2010). Particle size and interfacial effects on thermo-physical and heat transfer characteristics of water-based α -SiC nanofluids. *Nanotechnology*, *21*, 215703.
- Timofeeva, E. V., Yu, W., France, D. M., Singh, D., & Routbort, J. L. (2011). Nanofluids for heat transfer: an engineering approach. *Nanoscale Research Letters*, *6*(1), 182.
- Tseng, W. J., & Chen, C. N. (2003). Effect of polymeric dispersant on rheological behavior of nickel-terpineol suspensions. *Materials Science and Engineering A*, *347*(1-2), 145-153.
- Tseng, W. J., & Lin, K. C. (2003). Rheology and colloidal structure of aqueous TiO₂ nanoparticle suspensions. *Materials Science and Engineering A*, *355*(1-2), 186-192.
- Tseng, W. J., & Wu, C. H. (2002). Aggregation, rheology and electrophoretic packing structure of aqueous Al₂O₃ nanoparticle suspensions. *Acta Materialia*, *50*(15), 3757-3766.
- Tullius, J. F., Vajtai, R., & Bayazitoglu, Y. (2011). A Review of Cooling in Microchannels. *Heat Transfer Engineering*, *32*(7-8), 527-541.
- Turgut, A., Tavman, I., Chirtoc, M., Schuchmann, H. P., Sauter, C., & Tavman, S. (2009). Thermal Conductivity and Viscosity Measurements of Water-Based TiO₂ Nanofluids. *International Journal of Thermophysics*, *30*(4), 1213-1226.
- Vajjha, R. S., & Das, D. K. (2012). A review and analysis on influence of temperature and concentration of nanofluids on thermophysical properties, heat transfer and pumping power. *International Journal of Heat and Mass Transfer*, *55*(15-16), 4063-4078.
- Wagner, N. J., & Brady, J. F. (2009). Shear thickening in colloidal dispersions. *Physics Today*, *62*(10), 27-32.
- Wang, X., & Guo, L. (2006). Effect of preparation methods on rheological properties of Al₂O₃/ZrO₂ suspensions. *Colloids and Surfaces A: Physicochemical and Engineering Aspects*, *281*(1-3), 171-176.
- Wang, X., Xu, X., & Choi, S. U. S. (1999). Thermal conductivity of nanoparticle-fluid mixture. *Journal of Thermophysics and Heat Transfer*, *13*(4), 474-480.

- Wen, D., & Ding, Y. (2005). Formulation of nanofluids for natural convective heat transfer applications. *International Journal of Heat and Fluid Flow*, 26(6), 855-864.
- Xie, H., Chen, L., & Wu, Q. (2008). Measurements of the viscosity of suspensions (nanofluids) containing nanosized Al₂O₃ particles. *High Temperatures High pressures*, 37(2), 127-135.
- Xie, X. L., Liu, Z. J., He, Y. L., & Tao, W. Q. (2009). Numerical study of laminar heat transfer and pressure drop characteristics in a water-cooled minichannel heat sink. *Applied Thermal Engineering*, 29(1), 64-74.
- Yang, Y., Grulke, E. A., Zhang, Z. G., & Wu, G. (2006). Thermal and rheological properties of carbon nanotube-in-oil dispersions. *Journal of Applied Physics*, 99, 114307.
- Yu, H., Hermann, S., Schulz, S. E., Gessner, T., Dong, Z., & Li, W. J. (2012a). Optimizing sonication parameters for dispersion of single-walled carbon nanotubes. *Chemical Physics*, 408, 11-16.
- Yu, J., Grossiord, N., Koning, C. E., & Loos, J. (2007). Controlling the dispersion of multi-wall carbon nanotubes in aqueous surfactant solution. *Carbon*, 45(3), 618-623.
- Yu, W., France, D. M., Timofeeva, E. V., Singh, D., & Routbort, J. L. (2010). Thermophysical property-related comparison criteria for nanofluid heat transfer enhancement in turbulent flow. *Applied Physics Letters*, 96, 213109.
- Yu, W., France, D. M., Timofeeva, E. V., Singh, D., & Routbort, J. L. (2012b). Comparative review of turbulent heat transfer of nanofluids. *International Journal of Heat and Mass Transfer*, 55(21-22), 5380-5396.
- Yu, W., Xie, H., Li, Y., & Chen, L. (2011). Experimental investigation on thermal conductivity and viscosity of aluminum nitride nanofluid. *Particuology*, 9(2), 187-191.
- Zhang, P., Ouyang, G., & Bai, L. (2010, August 24-26). *Simulation on thermal performance parameters of gas-fired in cylinder based on Boost software*. Paper presented at the International Conference on Computer, Mechatronics, Control and Electronic Engineering, Changchun.
- Zhu, H.-t., Lin, Y.-s., & Yin, Y.-s. (2004). A novel one-step chemical method for preparation of copper nanofluids. *Journal of Colloid and Interface Science*, 277(1), 100-103.

- Zhu, H., Li, C., Wu, D., Zhang, C., & Yin, Y. (2010). Preparation, characterization, viscosity and thermal conductivity of CaCO₃ aqueous nanofluids. *Science China Technological Sciences*, 53(2), 360-368.
- Zhu, H., Liu, S., Xu, L., & Zhang, C. (2007). Preparation, characterization and thermal properties of nanofluids. In D. M. Sabatini (Ed.), *Leading Edge Nanotechnology Research Developments* (pp. 5-38). New York, NY: Nova Science Publishers, Inc.
- Zhu, H., Zhang, C., Liu, S., Tang, Y., & Yin, Y. (2006). Effects of nanoparticle clustering and alignment on thermal conductivities of Fe₃O₄ aqueous nanofluids. *Applied Physics Letters*, 89(2), 023123.

LIST OF PUBLICATIONS AND PAPERS PRESENTED

Journal:

1. **Mahbubul, I. M.**, Chong, T. H., Khaleduzzaman, S. S., Shahrul, I. M., Saidur, R., Long, B. D. and Amalina, M. A. 2014. Effect of Ultrasonication Duration on Colloidal Structure and Viscosity of Alumina–water Nanofluid, *Industrial and Engineering Chemistry Research*, 53, 6677-6684. (ISI Cited Publication)
2. **Mahbubul, I. M.**, Saidur, R., Amalina, M. A., Elcioglu, E. B. and Okutucu-Ozyurt, T. Effective Ultrasonication Process for Better Colloidal Dispersion of Nanofluid, *Ultrasonics Sonochemistry* (Accepted), DOI: 10.1016/j.ultsonch.2015.01.005.
3. **Mahbubul, I. M.**, Shahrul, I. M., Khaleduzzaman, Saidur, R., Amalina, M. A. and Turgut, A. Experimental Investigation on Effect of Ultrasonication duration on Colloidal Dispersion and Thermophysical Properties of Alumina–water Nanofluid, *International Journal of Heat and Mass Transfer* (Accepted), DOI: 10.1016/j.ijheatmasstransfer.2015.04.048.
4. **Mahbubul, I. M.**, Saidur, R., Amalina, M. A. and Hepbasli, A. Experimental Investigation of the Relation between Yield Stress and Ultrasonication Period of Nanofluid (Under preparation).
5. **Mahbubul, I. M.**, R. Saidur and Amalina, M. A. Influence of Sonication Time on Rheological Properties of Nanofluid (Under preparation).
6. **Mahbubul, I. M.**, Khaleduzzaman, S. S., Saidur, R., Amalina, M. A. and Sohel, M. R. Effect of Ultrasonication Treatment of Nanofluid on Thermal Performance of a Mini Channel Heat Sink (Under preparation).

Conference:

1. **Mahbubul, I.M.**, Saidur, R. and Amalina, M.A. 2014. Effective Ultrasonic duration for Better Dispersion of Nanofluid. International Conference on Thermophysical and Mechanical Properties of Advanced Materials. 12-15 June 2014, Boyalik Beach Hotel, Cesme-Izmir, Turkey [Paper no. 74].
2. **Mahbubul, I.M.**, Shahrul, I.M., Khaleduzzaman, S.S., Saidur, R. and Amalina, M.A. Effect of Ultrasonic Duration on Thermal Conductivity and Viscosity of Alumina–Water Nanofluid. International Conference on Thermophysical and Mechanical Properties of Advanced Materials. 12-15 June 2014, Boyalik Beach Hotel, Cesme-Izmir, Turkey [Paper no. 60].

APPENDIX A: ELEMENTAL COMPOSITION OF NANOPARTICLES BY FESEM-EDAX ANALYSIS

Table A1: Elemental composition of Al₂O₃ nanoparticles by EDAX analysis at point 1.

| Element | Wt. % | At% |
|---------|------------|-------|
| OK | 44.73 | 57.71 |
| AlK | 55.27 | 42.29 |
| Matrix | Correction | ZAF |

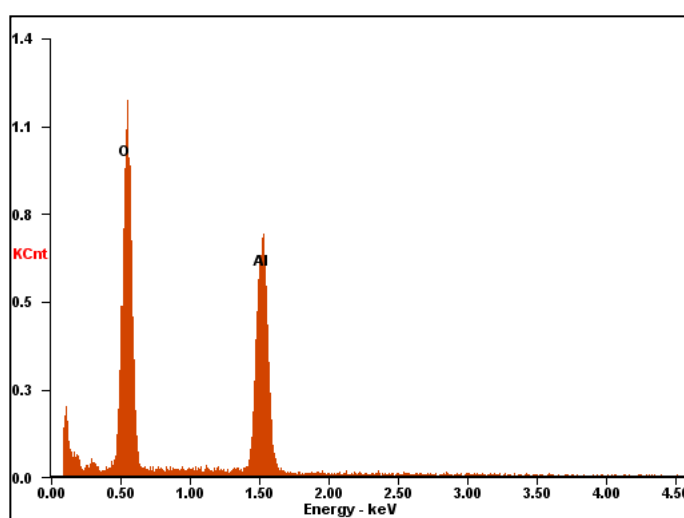


Figure A1: EDAX analysis of Al₂O₃ nanoparticles at point 1.

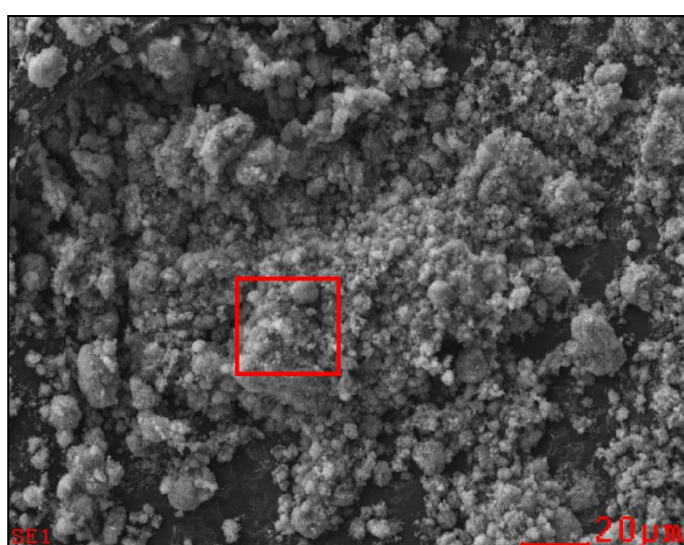


Figure A2: FESEM image of Al₂O₃ nanoparticles during EDAX analysis with the marking of point 1.

Table A2: Elemental composition of Al₂O₃ nanoparticles by EDAX analysis at point 2.

| Element | Wt.% | At% |
|---------|------------|-------|
| OK | 44.72 | 57.71 |
| AlK | 55.28 | 42.29 |
| Matrix | Correction | ZAF |

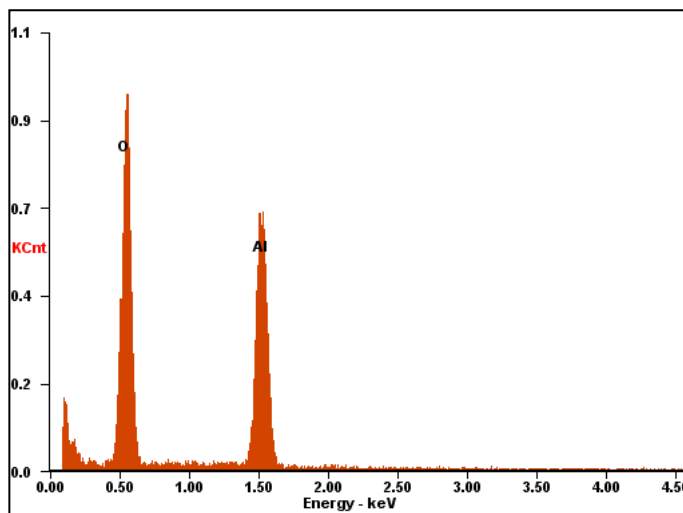


Figure A3: EDAX analysis of Al₂O₃ nanoparticles at point 2.

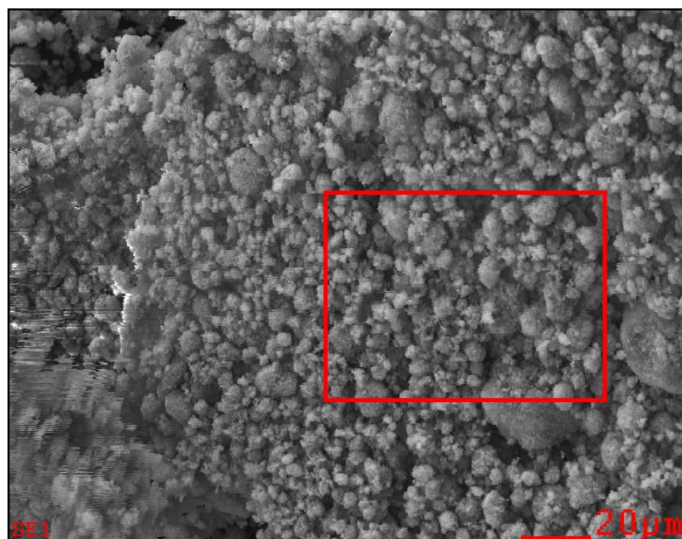


Figure A4: FESEM image of Al₂O₃ nanoparticles during EDAX analysis with the marking of point 2.

APPENDIX B: PARTICLES SIZE MEASUREMENT AFTER ULTRASONICATION

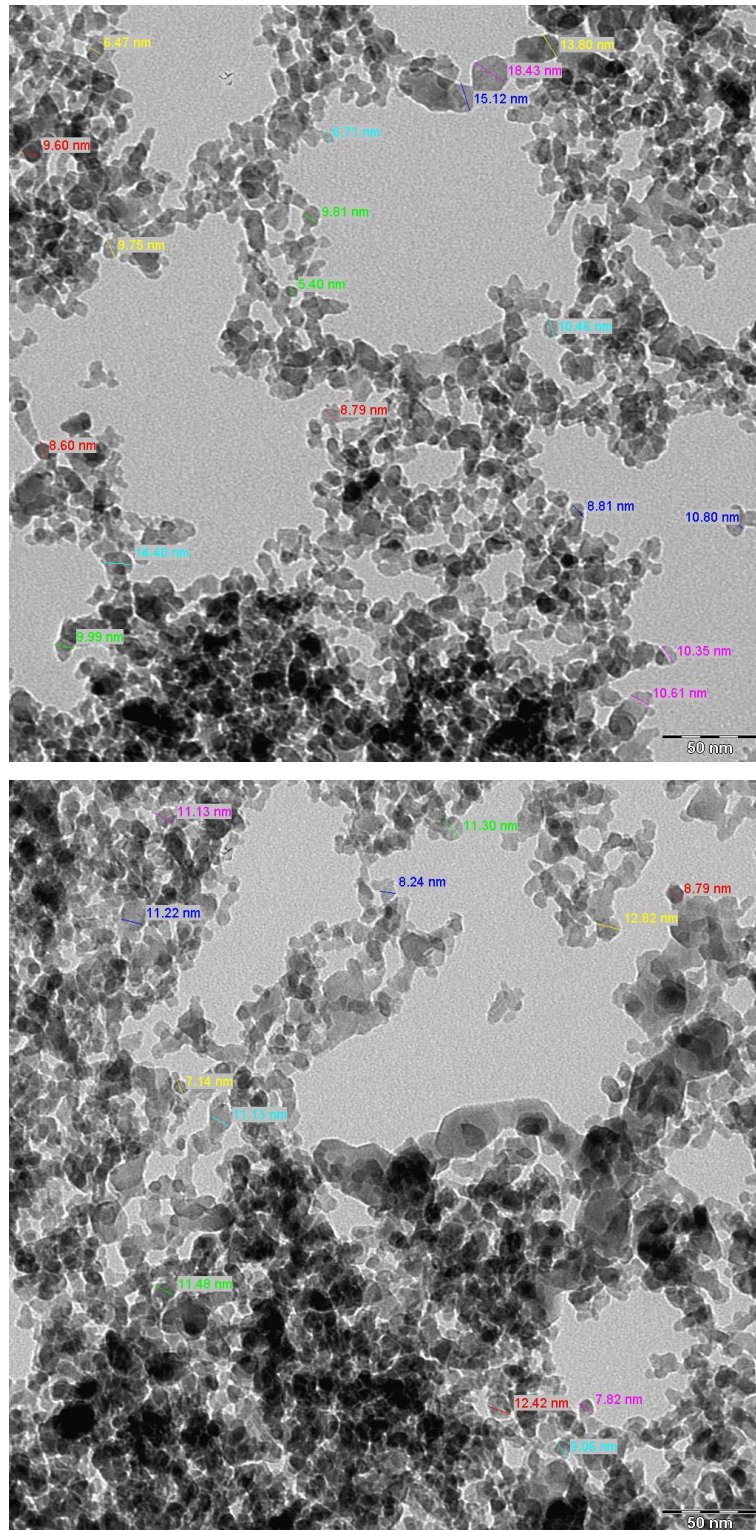


Figure B1: TEM microstructure of Al_2O_3 -water nanofluid prepared by without ultrasonication (0 h) on a 50 nm scale ($31500\times$ magnifications) with particle size measurements.

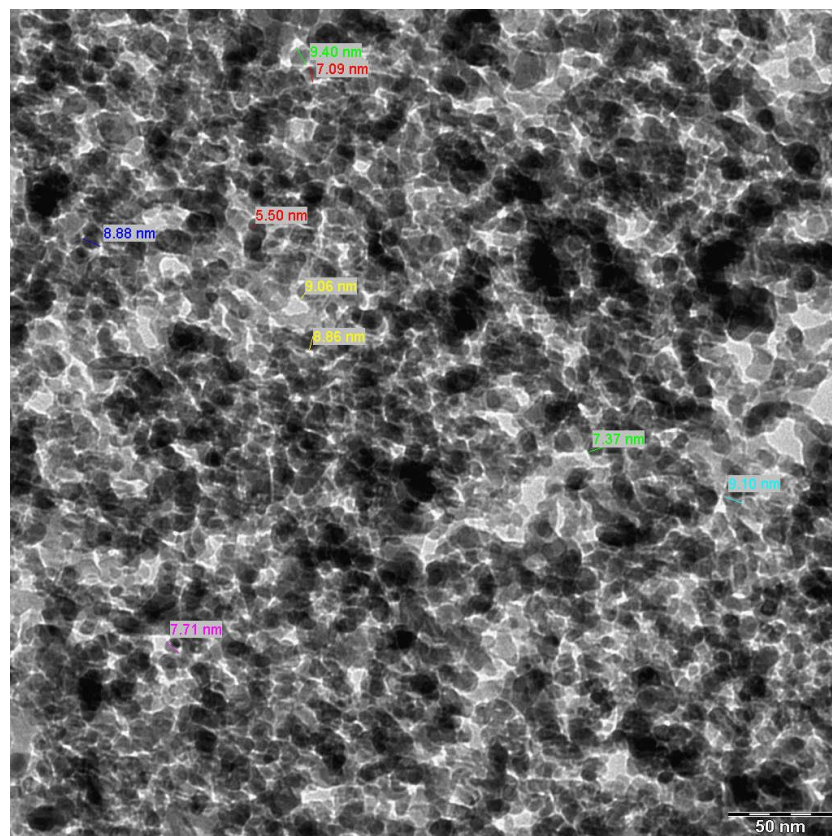
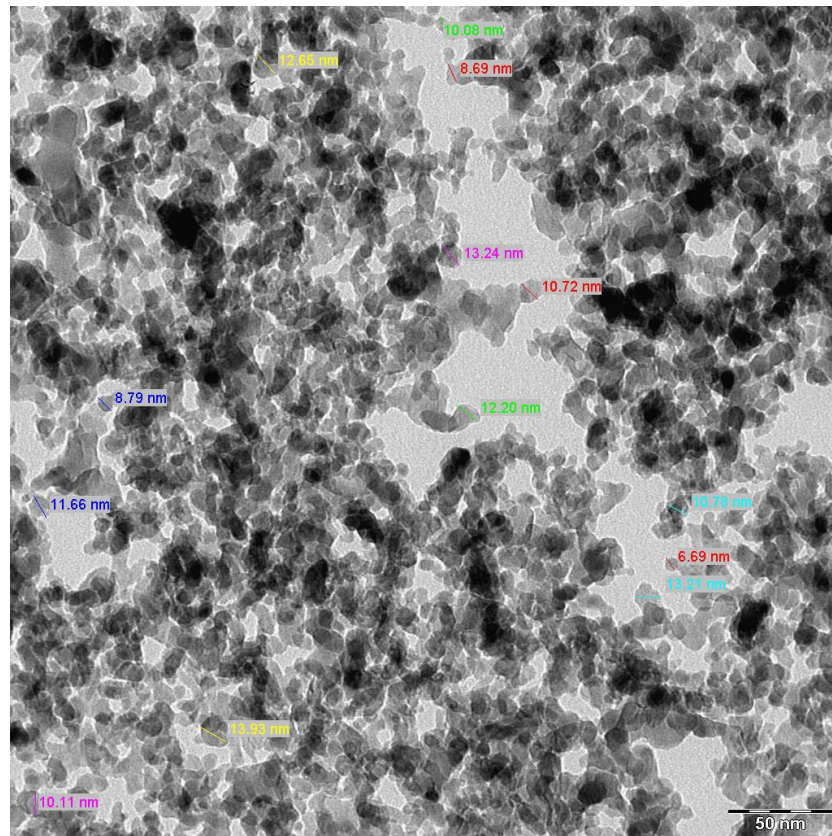


Figure B2: TEM microstructure of Al_2O_3 -water nanofluid prepared by 1 h of ultrasonication on a 50 nm scale ($31500\times$ magnifications) with particle size measurements.

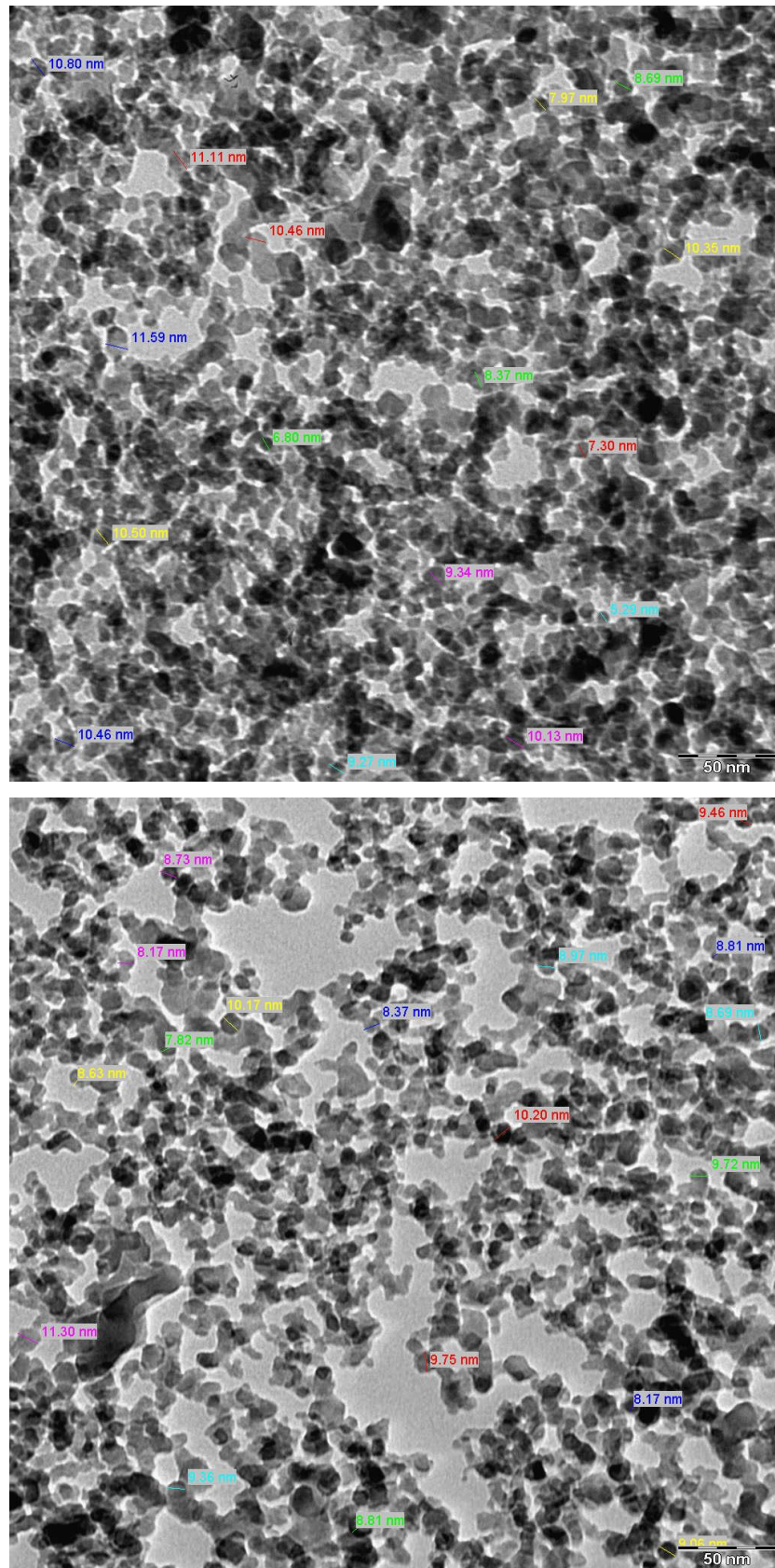


Figure B3: TEM microstructure of Al₂O₃-water nanofluid prepared by 2 h of ultrasonication on a 50 nm scale (31500× magnifications) with particle size measurements.

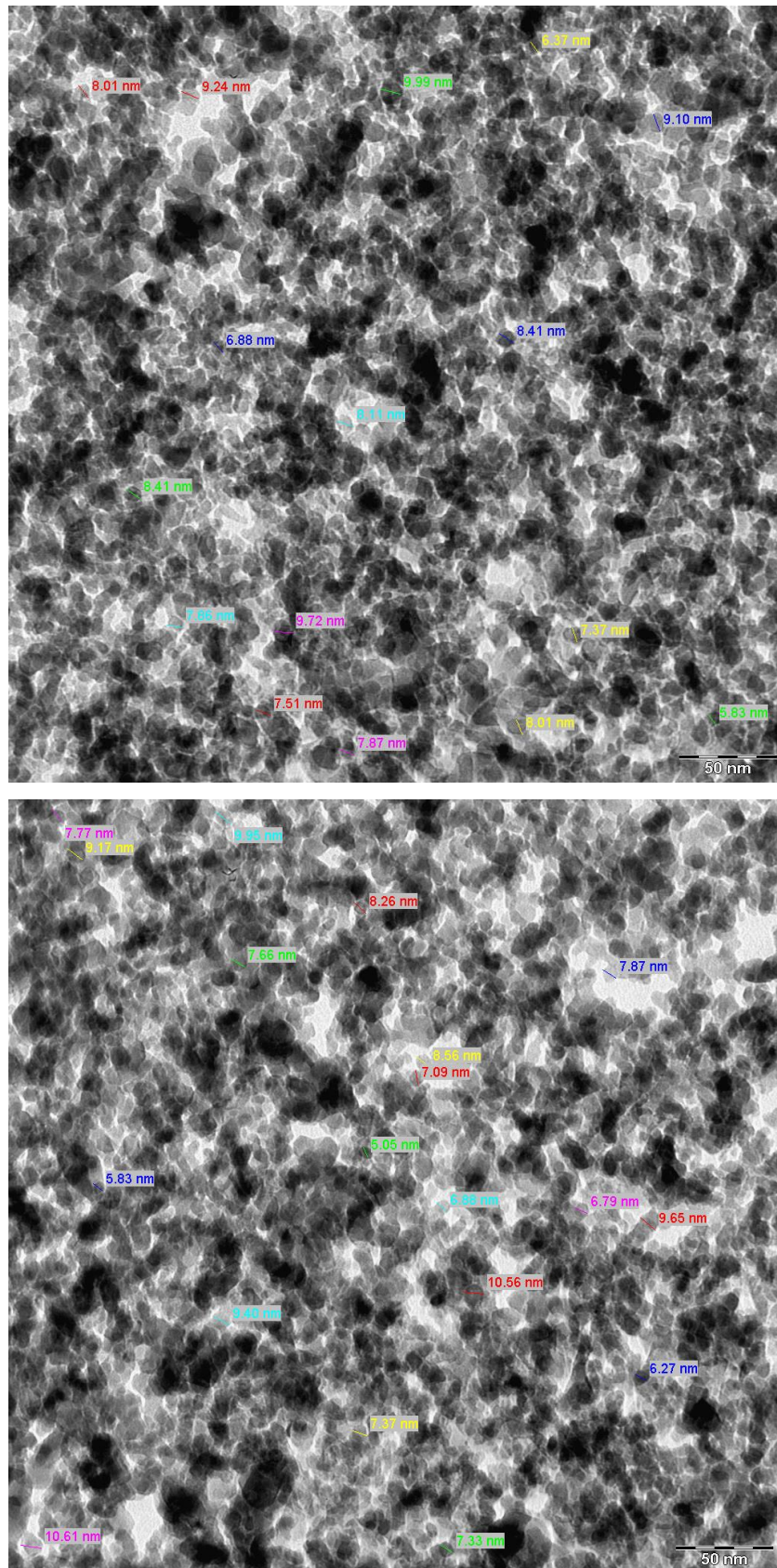


Figure B4: TEM microstructure of Al₂O₃-water nanofluid prepared by 3 h of ultrasonication on a 50 nm scale (31500× magnifications) with particle size measurements.

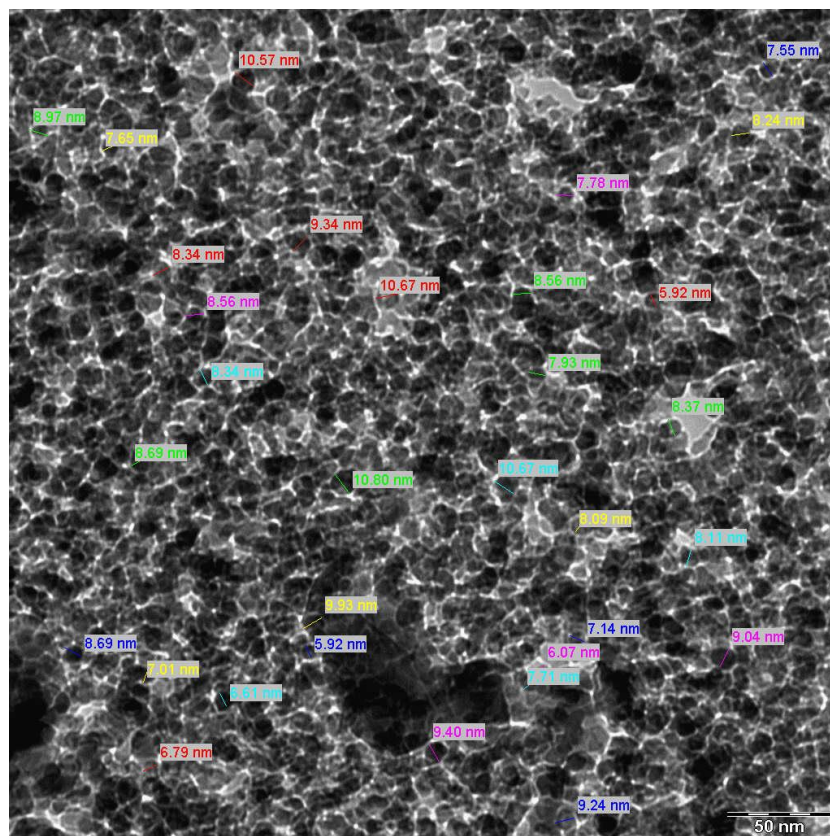
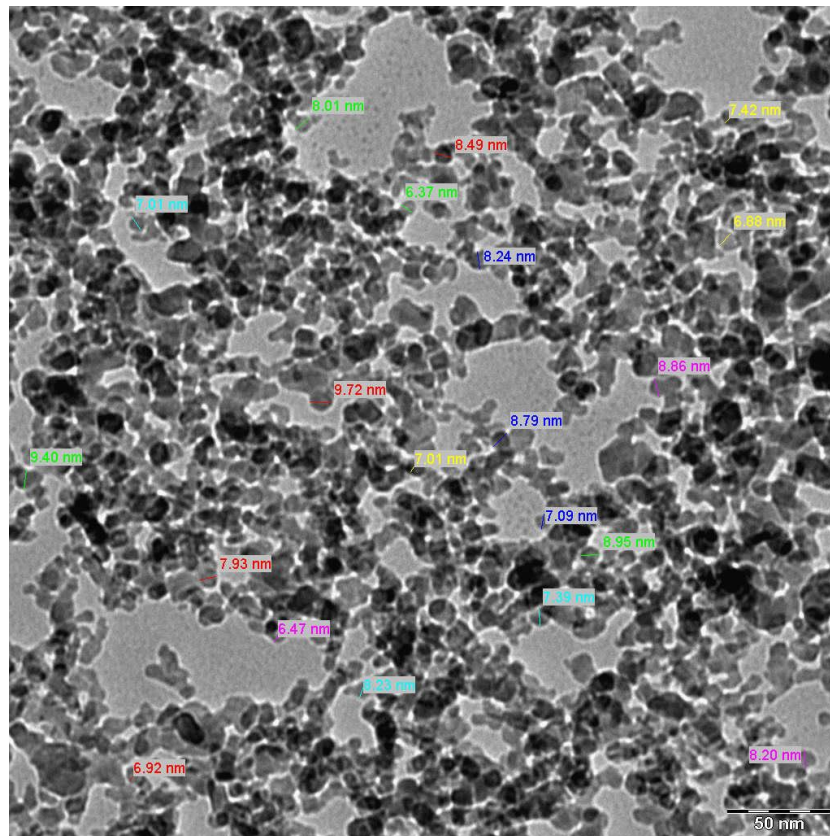


Figure B5: TEM microstructure of Al₂O₃-water nanofluid prepared by 4 h of ultrasonication on a 50 nm scale (31500× magnifications) with particle size measurements.

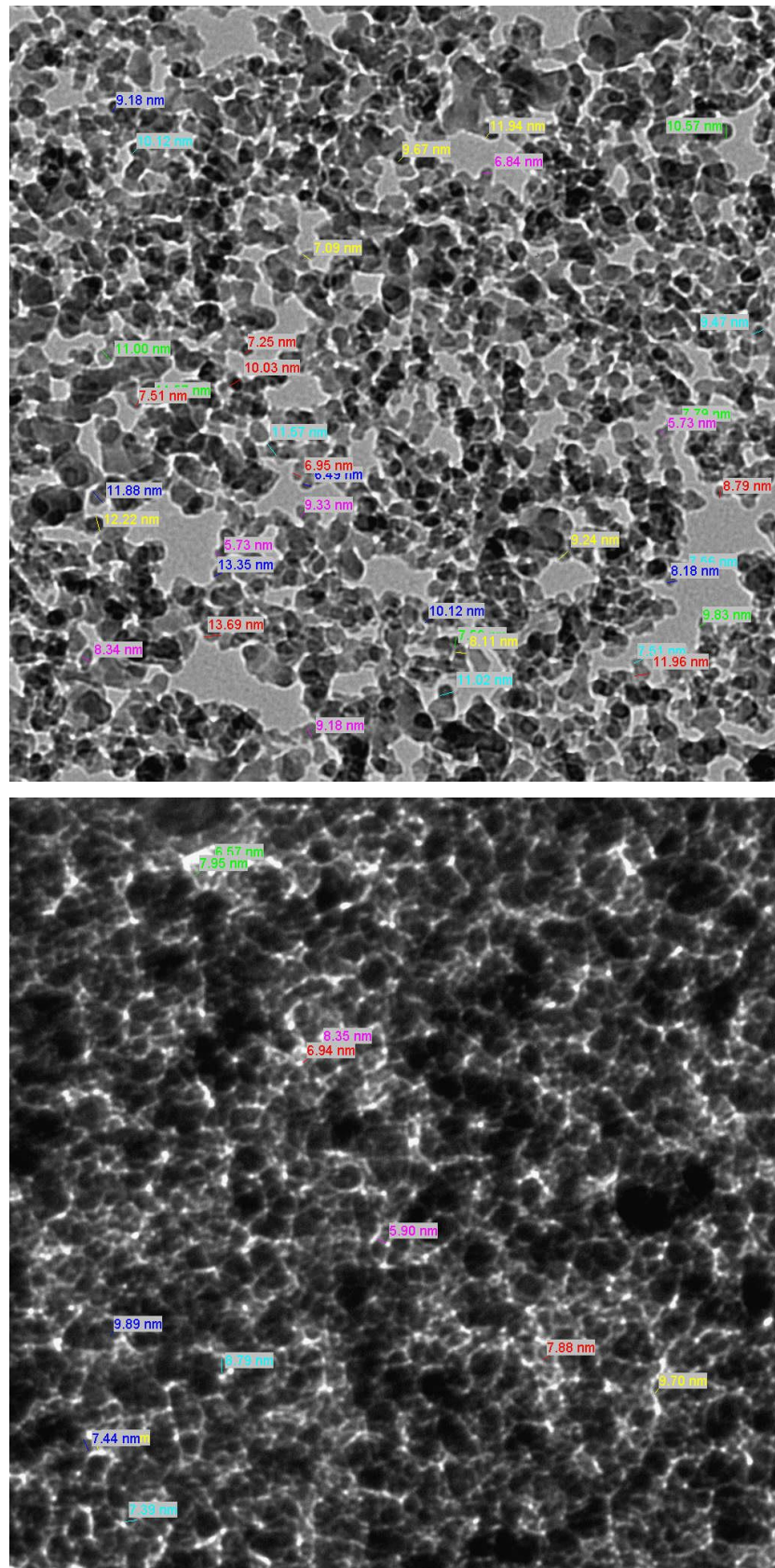


Figure B6: TEM microstructure of Al₂O₃-water nanofluid prepared by 5 h of ultrasonication on a 50 nm scale (31500× magnifications) with particle size measurements.

**APPENDIX C: MEASURED VALUES OF EFFECTIVE THERMOPHYSICAL
PROPERTIES**

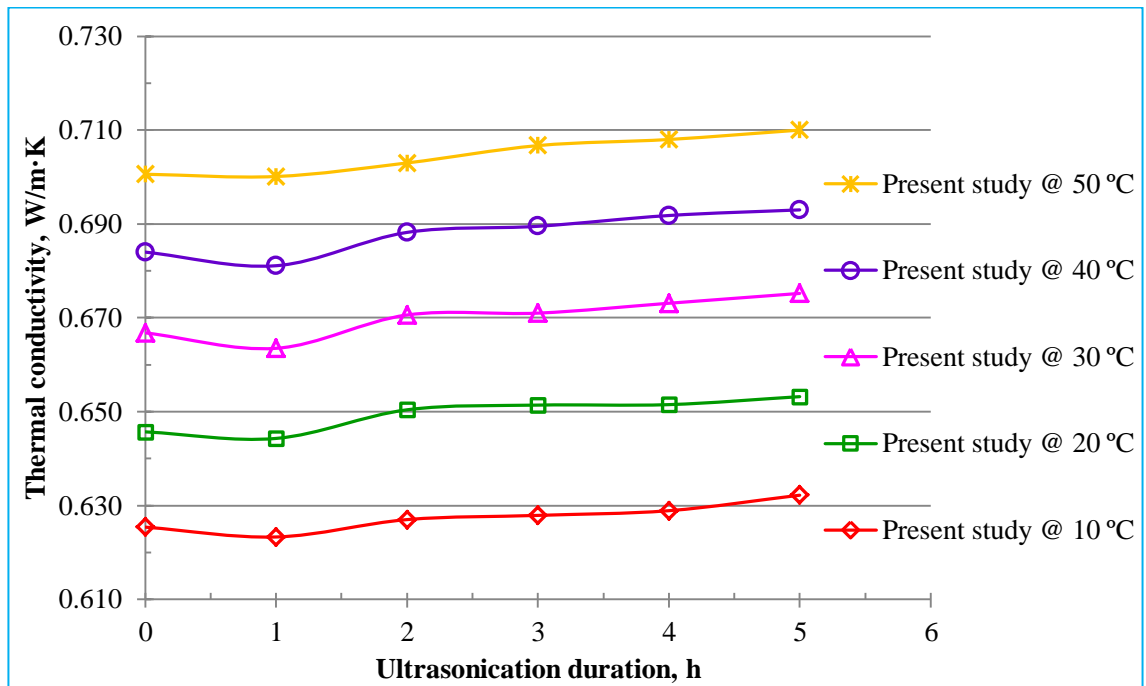


Figure C1: Thermal conductivity of 0.5 vol.% of Al₂O₃-water nanofluids after different duration of ultrasonication.

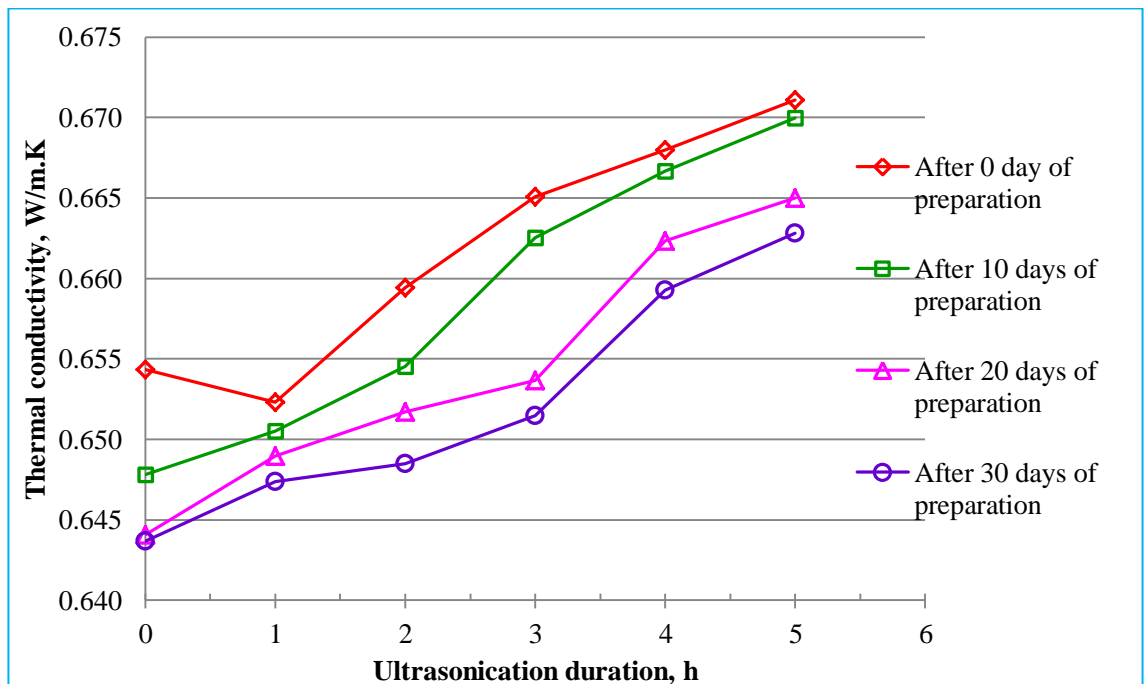


Figure C2: Effective thermal conductivity of 0.5 vol.% of Al₂O₃-water nanofluids at 25 °C after different periods from sample preparation.

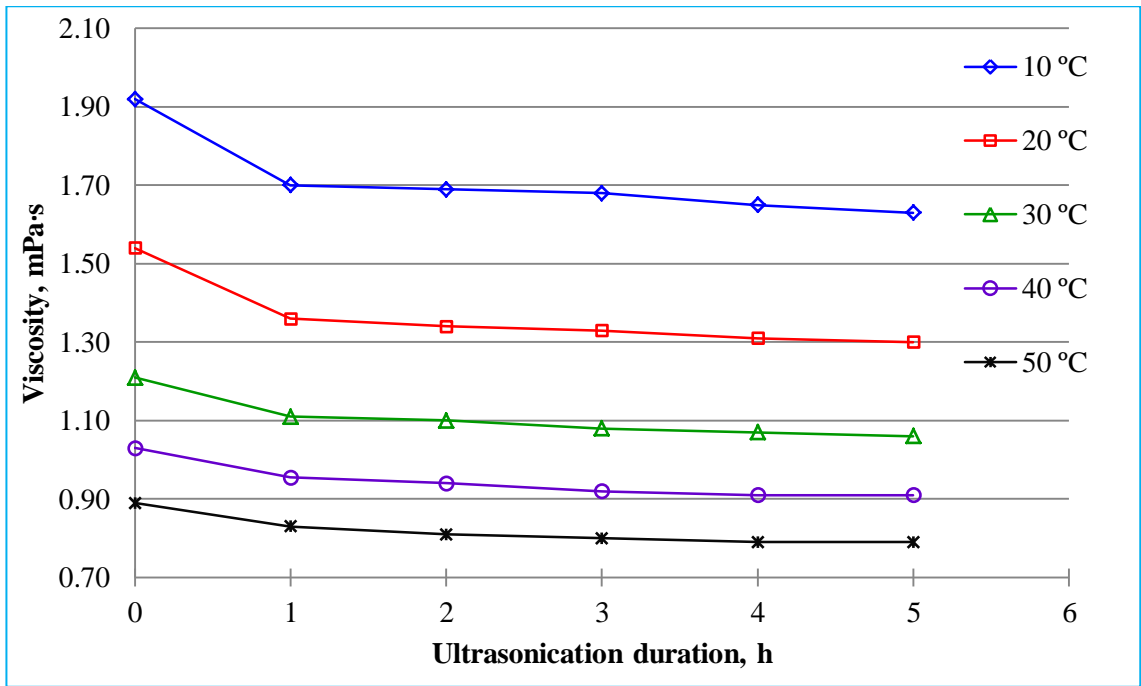


Figure C3: Effective viscosity of 0.5 vol.% of Al₂O₃–water nanofluids after different duration of ultrasonication.

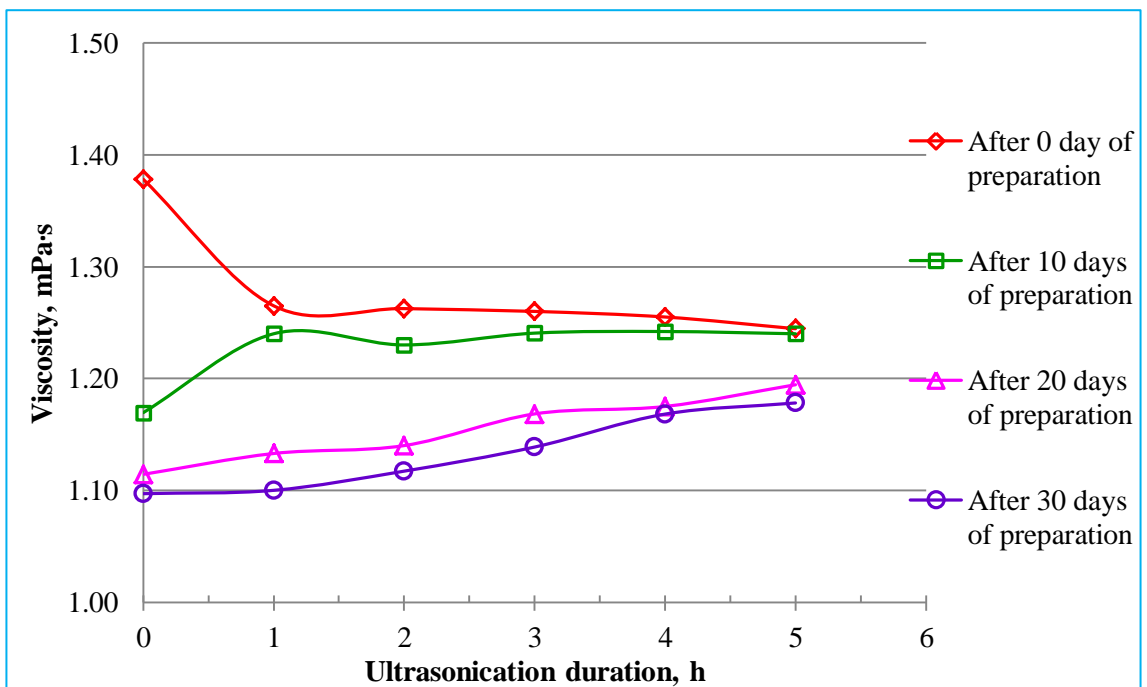


Figure C4: Effective viscosity of 0.5 vol.% of Al₂O₃–water nanofluids at 25 °C after different periods from sample preparation.

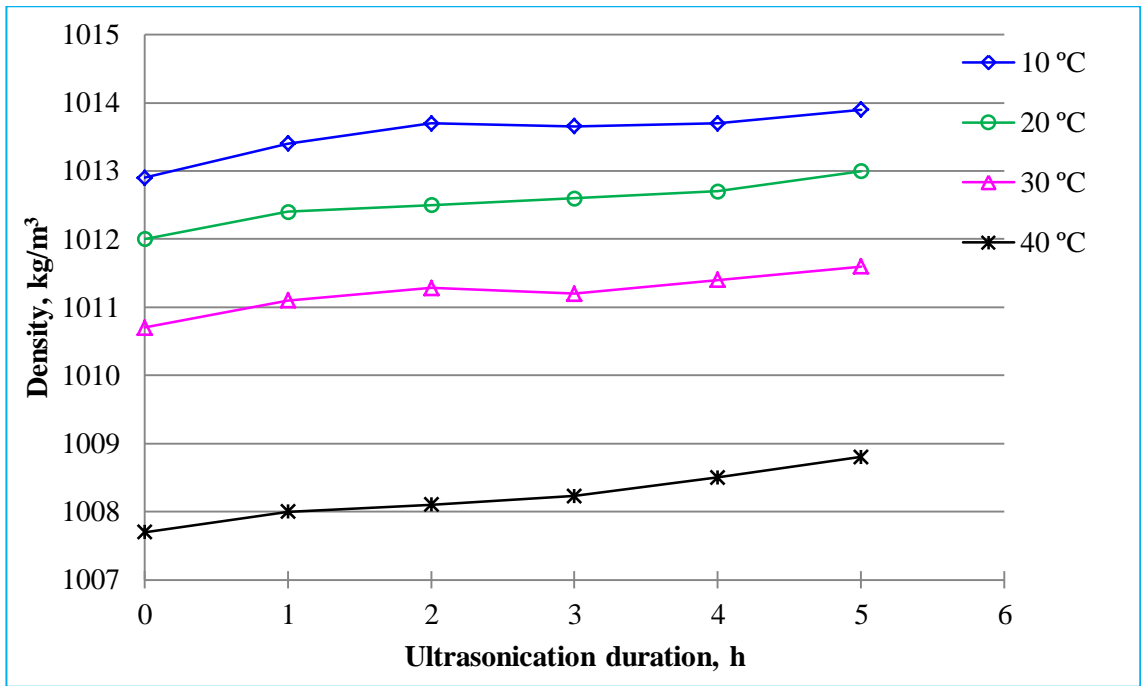


Figure C5: Effective density of 0.5 vol.% of Al₂O₃-water nanofluids after different duration of ultrasonication.

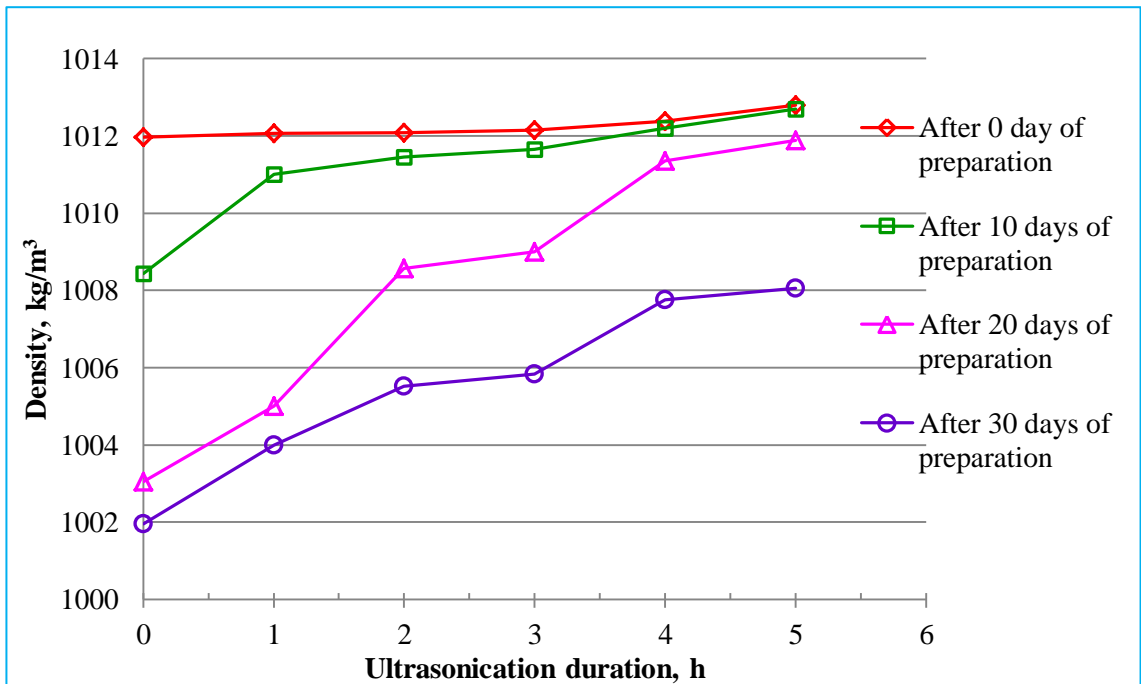


Figure C6: Effective density of 0.5 vol.% of Al₂O₃-water nanofluids at 25 °C after different periods from sample preparation.

APPENDIX D: FITTING PARAMETERS FOR RHEOLOGICAL MODELS

Table D1: Fitting parameters for rheological models.

| Temp., °C | Dura- tion, h | Herschel-Bulkey | | | | Power law | | |
|--------------|---------------------|-----------------|-----------|--------|-----------|-----------|--------|-----------|
| | | τ_0 | k | n | CoF, % | k | n | CoF, % |
| 10 | 0 | 0.0498 | 0.0283680 | 1.7997 | 99.55 | 0.7570 | 1.2002 | 98.08 |
| | 1 | 0.0439 | 0.0229870 | 1.8360 | 99.75 | 0.5640 | 1.2492 | 97.79 |
| | 2 | 0.0459 | 0.0227740 | 1.8370 | 99.68 | 0.6170 | 1.2327 | 97.73 |
| | 3 | 0.0450 | 0.0232390 | 1.8335 | 99.72 | 0.5970 | 1.2389 | 97.79 |
| | 4 | 0.0446 | 0.0244410 | 1.8251 | 99.72 | 0.6020 | 1.2379 | 97.74 |
| | 5 | 0.0445 | 0.0250220 | 1.8197 | 99.71 | 0.5940 | 1.2398 | 97.96 |
| 20 | 0 | 0.0306 | 0.0294500 | 1.7840 | 99.86 | 0.3470 | 1.3319 | 98.00 |
| | 1 | 0.0237 | 0.0385030 | 1.7314 | 99.90 | 0.2470 | 1.3904 | 98.35 |
| | 2 | 0.0243 | 0.0387350 | 1.7293 | 99.89 | 0.2770 | 1.3694 | 98.09 |
| | 3 | 0.0235 | 0.0421970 | 1.7141 | 99.87 | 0.2780 | 1.3690 | 98.27 |
| | 4 | 0.0236 | 0.0401090 | 1.7231 | 99.88 | 0.2730 | 1.3723 | 98.13 |
| | 5 | 0.0224 | 0.0421390 | 1.7136 | 99.86 | 0.2590 | 1.3817 | 98.35 |
| 30 | 0 | 0.0128 | 0.0638140 | 1.6292 | 99.92 | 0.1920 | 1.4280 | 98.87 |
| | 1 | 0.0098 | 0.0739200 | 1.5962 | 99.91 | 0.1720 | 1.4409 | 98.87 |
| | 2 | 0.0097 | 0.0736590 | 1.5976 | 99.90 | 0.1800 | 1.4354 | 98.82 |
| | 3 | 0.0098 | 0.0775530 | 1.5903 | 99.91 | 0.1800 | 1.4353 | 98.89 |
| | 4 | 0.0088 | 0.0810920 | 1.5787 | 99.89 | 0.1800 | 1.4317 | 98.84 |
| | 5 | 0.0090 | 0.0724320 | 1.6012 | 99.92 | 0.1650 | 1.4501 | 98.95 |

Table D1, continued

| Temp., °C | Dura- tion, h | Herschel-Bulkey | | | | Power law | | |
|--------------|---------------------|-----------------|-----------|--------|-----------|-----------|--------|-----------|
| | | τ_0 | k | n | CoF, % | k | n | CoF, % |
| 40 | 0 | 0.0063 | 0.0808560 | 1.5725 | 99.94 | 0.1430 | 1.4673 | 99.25 |
| | 1 | 0.0071 | 0.0895780 | 1.5451 | 99.94 | 0.1520 | 1.4494 | 99.35 |
| | 2 | 0.0033 | 0.0984730 | 1.5305 | 99.94 | 0.1330 | 1.4746 | 99.40 |
| | 3 | 0.0055 | 0.0895760 | 1.5500 | 99.95 | 0.1420 | 1.4659 | 99.36 |
| | 4 | 0.0060 | 0.0850350 | 1.5547 | 99.94 | 0.1400 | 1.4635 | 99.32 |
| | 5 | 0.0036 | 0.0918220 | 1.5429 | 99.94 | 0.1240 | 1.4869 | 99.45 |
| 50 | 0 | 0.0042 | 0.0902560 | 1.5374 | 99.96 | 0.1260 | 1.4764 | 99.55 |
| | 1 | 0.0020 | 0.1103800 | 1.4956 | 99.93 | 0.1160 | 1.4867 | 99.61 |
| | 2 | 0.0016 | 0.1093300 | 1.4980 | 99.96 | 0.1120 | 1.4937 | 99.55 |
| | 3 | 0.0014 | 0.1005600 | 1.5190 | 99.96 | 0.1080 | 1.5061 | 99.65 |
| | 4 | 0.0029 | 0.0998320 | 1.5128 | 99.95 | 0.1200 | 1.4798 | 99.52 |
| | 5 | 0.0006 | 0.1135400 | 1.4905 | 99.94 | 0.1110 | 1.4947 | 99.59 |

APPENDIX E: UNCERTAINTIES IN MEASUREMENTS

Table E1: Uncertainties in aggregate size measurement for 50% power amplitude.

| Ultrasonication (min) | Uncertainty, % |
|----------------------------------|-----------------------|
| 0 | 1.08 |
| 30 | 22.32 |
| 60 | 0.48 |
| 90 | 0.58 |
| 120 | 1.40 |
| 150 | 0.09 |
| 180 | 2.99 |
| 210 | - |
| 240 | 0.98 |
| 270 | - |
| 300 | 0.24 |

Table E2: Uncertainties in polydispersity index measurement for 50% power amplitude.

| Ultrasonication (h) | Uncertainty, % |
|----------------------------|-----------------------|
| 0 | 2.94 |
| 1 | 26.09 |
| 2 | 2.33 |
| 3 | 33.10 |
| 4 | 9.80 |
| 5 | - |

Table E3: Uncertainties in zeta potential measurement for 50% power amplitude.

| Ultrasonication (min) | Uncertainty, % |
|-----------------------|----------------|
| 0 | - |
| 30 | - |
| 60 | - |
| 90 | - |
| 120 | - |
| 150 | - |
| 180 | 3.77 |
| 210 | - |
| 240 | 3.65 |
| 270 | - |
| 300 | 0.09 |

Table E4: Uncertainties in thermal conductivity measurement.

| Temp. (°C) | Uncertainty, % | | | | | |
|------------|----------------|------|------|------|------|------|
| | 0 h | 1 h | 2 h | 3 h | 4 h | 5 h |
| 10 | 2.97 | 2.02 | 1.49 | 1.25 | 4.13 | 2.27 |
| 20 | 3.06 | 3.85 | 1.79 | 4.54 | 4.58 | 2.37 |
| 30 | 5.04 | 6.10 | 3.60 | 4.02 | 4.62 | 5.56 |
| 40 | 6.43 | 4.45 | 6.09 | 6.96 | 5.25 | 5.98 |
| 50 | 6.81 | 4.71 | 6.44 | 5.62 | 6.31 | 6.45 |

Table E5: Uncertainties in thermal conductivity measurement after certain periods at 25 °C.

| Day(s) | Uncertainty, % | | | | | |
|--------|----------------|------|------|------|------|------|
| | 0 h | 1 h | 2 h | 3 h | 4 h | 5 h |
| 0 | 6.88 | 5.67 | 3.38 | 4.13 | 2.45 | 1.37 |
| 10 | 3.77 | 4.86 | 3.40 | 5.04 | 3.07 | 5.04 |
| 20 | 3.34 | 3.73 | 4.88 | 3.95 | 3.31 | 3.53 |
| 30 | 2.67 | 3.67 | 2.86 | 2.67 | 4.12 | 3.88 |

Table E6: Uncertainties in viscosity measurement.

| Temp. (°C) | Uncertainty, % | | | | | |
|---------------|----------------|------|------|------|------|------|
| | 0 h | 1 h | 2 h | 3 h | 4 h | 5 h |
| 10 | 0.43 | 0.49 | 0.29 | 0.00 | 0.49 | 0.31 |
| 20 | 0.00 | 0.74 | 0.51 | 0.37 | 0.38 | 0.39 |
| 30 | 1.68 | 0.44 | 0.00 | 0.46 | 0.47 | 0.47 |
| 40 | 0.96 | 1.85 | 0.92 | 0.53 | 0.00 | 0.89 |
| 50 | 0.56 | 0.77 | 0.85 | 0.64 | 0.59 | 0.59 |

Table E7: Uncertainties in viscosity measurement after certain periods at 25 °C.

| Day(s) | Uncertainty, % | | | | | |
|--------|----------------|------|------|------|------|------|
| | 0 h | 1 h | 2 h | 3 h | 4 h | 5 h |
| 0 | 0.52 | 0.40 | 0.52 | 0.51 | 0.40 | 0.63 |
| 10 | 0.83 | 1.02 | 0.49 | 0.65 | 1.05 | 0.76 |
| 20 | 0.44 | 1.35 | 0.53 | 0.91 | 0.76 | 0.70 |
| 30 | 0.58 | 0.86 | 1.36 | 1.52 | 1.67 | 0.81 |

Table E8: Uncertainties in density measurement.

| Temp. (°C) | Uncertainty, % | | | | | |
|---------------|----------------|------|------|------|------|------|
| | 0 h | 1 h | 2 h | 3 h | 4 h | 5 h |
| 10 | 0.06 | 0.07 | 0.01 | 0.03 | 0.00 | 0.01 |
| 20 | 0.01 | 0.00 | 0.01 | 0.00 | 0.00 | 0.01 |
| 30 | 0.01 | 0.01 | 0.02 | 0.00 | 0.01 | 0.00 |
| 40 | 0.00 | 0.01 | 0.04 | 0.00 | 0.01 | 0.00 |

Table E9: Uncertainties in density measurement after certain periods at 25 °C.

| Day(s) | Uncertainty, % | | | | | |
|--------|----------------|------|------|------|------|------|
| | 0 h | 1 h | 2 h | 3 h | 4 h | 5 h |
| 0 | 0.01 | 0.02 | 0.01 | 0.01 | 0.01 | 0.01 |
| 10 | 0.18 | 0.00 | 0.00 | 0.01 | 0.01 | 0.00 |
| 20 | 0.07 | 0.01 | 0.00 | 0.02 | 0.12 | 0.12 |
| 30 | 0.01 | 0.01 | 0.10 | 0.12 | 0.07 | 0.08 |

Table E10: Uncertainties in rheology measurement at 10 °C.

| rpm | Shear rate, s ⁻¹ | Uncertainties (%) in shear stress measurement | | | | | | Uncertainties (%) in viscosity measurement | | | | | |
|-----|-----------------------------|---|------|------|------|------|------|--|------|------|------|------|------|
| | | 0 h | 1 h | 2 h | 3 h | 4 h | 5 h | 0 h | 1 h | 2 h | 3 h | 4 h | 5 h |
| 10 | 12.23 | 2.13 | 2.97 | 2.22 | 2.13 | 0.00 | 4.76 | 2.80 | 5.21 | 2.72 | 2.63 | 1.54 | 6.54 |
| 20 | 24.46 | 1.80 | 2.59 | 1.15 | 1.86 | 2.86 | 3.11 | 1.92 | 2.85 | 1.43 | 0.84 | 2.10 | 0.74 |
| 30 | 36.69 | 1.92 | 2.78 | 2.34 | 4.09 | 2.42 | 2.20 | 0.82 | 3.58 | 2.42 | 3.57 | 1.62 | 1.31 |
| 40 | 48.92 | 2.35 | 1.19 | 1.70 | 1.42 | 2.78 | 2.32 | 2.14 | 1.25 | 1.48 | 1.39 | 2.72 | 1.93 |
| 50 | 61.15 | 1.54 | 0.69 | 0.49 | 2.52 | 1.18 | 1.92 | 1.38 | 1.49 | 0.66 | 2.25 | 1.22 | 2.33 |
| 60 | 73.38 | 3.20 | 0.36 | 0.80 | 1.88 | 1.12 | 2.06 | 1.53 | 1.05 | 0.43 | 2.11 | 1.03 | 0.51 |
| 70 | 85.61 | 1.79 | 0.31 | 0.00 | 1.96 | 1.37 | 2.13 | 1.53 | 1.05 | 0.26 | 1.98 | 1.18 | 0.68 |
| 80 | 97.84 | 1.78 | 0.44 | 0.27 | 1.86 | 0.91 | 2.21 | 1.74 | 0.99 | 0.26 | 1.82 | 1.13 | 0.51 |
| 90 | 110.07 | 1.69 | 0.61 | 0.27 | 1.93 | 1.23 | 2.21 | 1.64 | 1.03 | 0.30 | 1.98 | 1.27 | 1.69 |
| 100 | 122.30 | 1.74 | 0.65 | 0.41 | 1.87 | 0.91 | 2.02 | 1.63 | 1.03 | 0.43 | 1.98 | 0.90 | 0.43 |
| 110 | 134.53 | 1.36 | 0.75 | 0.37 | 1.79 | 0.83 | 2.00 | 1.33 | 1.07 | 0.30 | 1.81 | 0.89 | 0.50 |
| 120 | 146.76 | 1.38 | 0.62 | 0.53 | 1.95 | 1.00 | 1.89 | 1.43 | 0.87 | 0.50 | 1.81 | 1.01 | 0.50 |
| 130 | 158.99 | 1.35 | 2.11 | 0.26 | 1.01 | 1.13 | 1.15 | 1.31 | 2.04 | 0.26 | 0.87 | 1.00 | 1.13 |
| 140 | 171.22 | 0.94 | 0.82 | 0.50 | 1.50 | 0.85 | 1.88 | 0.90 | 0.94 | 0.43 | 1.54 | 0.98 | 2.04 |
| 150 | 183.45 | 0.95 | 1.23 | 0.22 | 0.22 | 0.97 | 0.53 | 0.87 | 1.31 | 0.41 | 0.24 | 0.83 | 0.83 |
| 160 | 195.68 | 0.73 | 0.42 | 0.60 | 0.69 | 1.34 | 1.21 | 0.76 | 0.50 | 0.84 | 0.67 | 1.34 | 1.04 |
| 170 | 207.91 | 0.78 | 0.66 | 1.51 | 0.99 | 1.05 | 1.07 | 0.79 | 0.61 | 0.70 | 1.00 | 0.36 | 0.49 |
| 180 | 220.14 | 1.19 | 0.20 | 0.94 | 1.15 | 0.33 | 1.38 | 1.10 | 0.35 | 0.19 | 1.12 | 0.55 | 1.37 |
| 190 | 232.37 | 0.44 | 0.43 | 0.39 | 0.30 | 0.76 | 1.02 | 0.42 | 0.43 | 0.43 | 0.68 | 0.82 | 0.49 |
| 200 | 244.60 | 0.77 | 0.27 | 0.21 | 0.68 | 0.97 | 0.61 | 0.63 | 0.69 | 0.00 | 0.65 | 0.41 | 0.47 |
| 210 | 356.83 | 1.03 | 0.60 | 0.23 | 1.43 | 0.57 | 0.75 | 0.99 | 0.74 | 0.39 | 1.44 | 0.85 | 0.58 |
| 220 | 269.06 | 0.21 | 0.82 | 1.00 | 0.58 | 0.41 | 0.90 | 0.30 | 0.47 | 0.81 | 0.54 | 0.30 | 0.34 |

Table E11: Uncertainties in rheology measurement at 20 °C.

| rpm | Shear rate, s ⁻¹ | Uncertainties (%) in shear stress measurement | | | | | | Uncertainties (%) in viscosity measurement | | | | | |
|-----|-----------------------------|---|------|------|------|------|------|--|------|------|------|------|------|
| | | 0 h | 1 h | 2 h | 3 h | 4 h | 5 h | 0 h | 1 h | 2 h | 3 h | 4 h | 5 h |
| 10 | 12.23 | 4.68 | 4.30 | 2.70 | 2.56 | 2.56 | 2.70 | 5.06 | 1.96 | 5.13 | 1.89 | 3.02 | 2.83 |
| 20 | 24.46 | 1.25 | 2.40 | 2.33 | 2.86 | 2.33 | 5.21 | 2.49 | 1.77 | 2.69 | 1.74 | 2.62 | 3.39 |
| 30 | 36.69 | 3.93 | 6.97 | 1.26 | 6.06 | 4.54 | 4.31 | 3.51 | 7.59 | 1.19 | 4.38 | 2.07 | 3.15 |
| 40 | 48.92 | 1.15 | 4.35 | 2.01 | 3.55 | 1.14 | 3.10 | 1.39 | 3.54 | 1.62 | 3.19 | 1.25 | 2.91 |
| 50 | 61.15 | 1.63 | 3.27 | 0.62 | 3.19 | 1.41 | 2.97 | 1.80 | 3.50 | 0.63 | 3.15 | 1.32 | 2.17 |
| 60 | 73.38 | 3.65 | 2.83 | 1.47 | 2.21 | 1.36 | 2.58 | 1.26 | 2.97 | 1.22 | 2.19 | 1.38 | 2.70 |
| 70 | 85.61 | 0.93 | 3.29 | 1.36 | 2.05 | 1.17 | 2.63 | 0.80 | 3.36 | 1.38 | 2.26 | 0.86 | 2.53 |
| 80 | 97.84 | 1.30 | 3.23 | 1.41 | 2.51 | 1.19 | 2.61 | 1.27 | 3.19 | 1.55 | 2.26 | 1.23 | 2.75 |
| 90 | 110.07 | 1.33 | 3.27 | 1.60 | 2.06 | 0.91 | 2.61 | 1.46 | 3.36 | 1.55 | 2.26 | 1.01 | 2.39 |
| 100 | 122.30 | 1.16 | 1.99 | 0.94 | 1.14 | 0.52 | 1.18 | 1.06 | 2.07 | 0.63 | 1.22 | 0.33 | 0.38 |
| 110 | 134.53 | 0.26 | 0.78 | 0.49 | 1.51 | 0.48 | 1.09 | 0.58 | 0.66 | 0.33 | 1.62 | 0.54 | 1.18 |
| 120 | 146.76 | 0.50 | 0.85 | 0.63 | 0.49 | 0.70 | 0.86 | 0.50 | 0.93 | 0.93 | 0.31 | 0.76 | 0.78 |
| 130 | 158.99 | 0.59 | 1.49 | 1.79 | 1.19 | 1.12 | 0.61 | 0.49 | 1.53 | 1.52 | 1.20 | 0.80 | 0.97 |
| 140 | 171.22 | 0.57 | 1.69 | 1.17 | 0.53 | 0.75 | 0.64 | 0.27 | 1.28 | 1.30 | 0.95 | 0.65 | 0.52 |
| 150 | 183.45 | 0.73 | 1.47 | 0.76 | 0.35 | 0.76 | 1.06 | 0.78 | 1.46 | 0.53 | 0.46 | 0.62 | 1.00 |
| 160 | 195.68 | 1.29 | 1.53 | 0.11 | 0.94 | 1.58 | 0.94 | 1.39 | 3.28 | 0.58 | 0.91 | 1.54 | 1.00 |
| 170 | 207.91 | 0.20 | 1.66 | 0.39 | 0.58 | 0.49 | 0.91 | 0.34 | 1.90 | 0.64 | 0.53 | 0.85 | 1.24 |
| 180 | 220.14 | 0.44 | 1.36 | 0.47 | 0.24 | 0.28 | 0.75 | 0.41 | 1.84 | 0.58 | 0.38 | 0.39 | 0.71 |
| 190 | 232.37 | 0.47 | 1.14 | 0.57 | 1.00 | 0.32 | 1.11 | 0.37 | 1.04 | 0.40 | 0.88 | 0.46 | 1.00 |
| 200 | 244.60 | 0.87 | 1.02 | 0.38 | 0.23 | 0.21 | 1.02 | 0.76 | 1.25 | 0.19 | 0.79 | 0.52 | 0.94 |
| 210 | 356.83 | 0.56 | 1.56 | 0.22 | 0.79 | 0.80 | 0.78 | 0.49 | 1.61 | 0.17 | 0.74 | 0.80 | 0.70 |
| 220 | 269.06 | 0.12 | 1.55 | 0.59 | 0.98 | 0.45 | 0.75 | 0.20 | 1.60 | 0.63 | 0.95 | 0.87 | 1.01 |
| 230 | 281.29 | 0.62 | 1.59 | 0.88 | 1.09 | 0.38 | 1.17 | 0.85 | 1.34 | 1.02 | 0.86 | 0.33 | 0.74 |
| 240 | 293.52 | - | 0.93 | 0.52 | 1.87 | 0.46 | 0.42 | - | 0.91 | 0.19 | 0.45 | 0.92 | 0.41 |

Table E12: Uncertainties in rheology measurement at 30 °C.

| rpm | Shear rate, s ⁻¹ | Uncertainties (%) in shear stress measurement | | | | | | Uncertainties (%) in viscosity measurement | | | | | |
|-----|-----------------------------|---|------|------|------|------|------|--|------|------|------|------|------|
| | | 0 h | 1 h | 2 h | 3 h | 4 h | 5 h | 0 h | 1 h | 2 h | 3 h | 4 h | 5 h |
| 10 | 12.23 | 3.23 | 4.80 | 5.44 | 6.78 | 5.10 | 2.84 | 4.26 | 3.55 | 4.08 | 3.71 | 3.71 | 2.09 |
| 20 | 24.46 | 2.82 | 2.82 | 2.92 | 2.92 | 4.51 | 1.53 | 3.24 | 2.09 | 3.40 | 2.15 | 3.31 | 2.14 |
| 30 | 36.69 | 4.46 | 3.63 | 1.97 | 3.09 | 5.77 | 6.50 | 5.07 | 6.88 | 1.87 | 2.44 | 3.46 | 5.36 |
| 40 | 48.92 | 2.70 | 2.83 | 1.56 | 2.80 | 2.49 | 2.90 | 2.67 | 4.56 | 1.13 | 2.20 | 2.00 | 3.18 |
| 50 | 61.15 | 2.93 | 3.60 | 0.66 | 1.96 | 1.79 | 2.87 | 2.50 | 3.63 | 0.40 | 1.96 | 1.94 | 2.98 |
| 60 | 73.38 | 4.34 | 4.86 | 1.73 | 1.89 | 2.05 | 2.81 | 2.00 | 3.67 | 0.78 | 1.75 | 2.27 | 2.87 |
| 70 | 85.61 | 1.34 | 3.48 | 0.48 | 0.91 | 2.00 | 3.13 | 1.57 | 3.67 | 0.41 | 1.05 | 1.85 | 2.56 |
| 80 | 97.84 | 1.18 | 1.70 | 0.69 | 1.56 | 0.48 | 0.48 | 1.08 | 1.40 | 0.82 | 1.36 | 0.41 | 0.00 |
| 90 | 110.07 | 1.56 | 1.10 | 0.81 | 1.63 | 0.73 | 1.12 | 1.71 | 1.55 | 0.57 | 1.80 | 0.67 | 1.12 |
| 100 | 122.30 | 0.98 | 0.62 | 0.50 | 0.74 | 0.51 | 1.49 | 1.21 | 0.38 | 0.33 | 0.94 | 0.53 | 1.65 |
| 110 | 134.53 | 0.44 | 1.10 | 1.07 | 0.58 | 1.28 | 0.58 | 0.57 | 1.20 | 1.29 | 0.68 | 1.36 | 0.78 |
| 120 | 146.76 | 0.54 | 1.61 | 0.22 | 0.32 | 0.84 | 1.47 | 0.54 | 1.44 | 0.42 | 0.49 | 0.56 | 0.55 |
| 130 | 158.99 | 0.17 | 1.44 | 0.82 | 0.81 | 1.57 | 1.05 | 0.27 | 1.68 | 0.95 | 0.89 | 1.83 | 1.05 |
| 140 | 171.22 | 1.17 | 1.19 | 0.73 | 0.72 | 1.31 | 0.97 | 1.25 | 1.65 | 0.74 | 0.89 | 1.51 | 0.49 |
| 150 | 183.45 | 1.44 | 1.55 | 0.88 | 0.32 | 1.45 | 0.67 | 1.47 | 1.34 | 0.48 | 0.36 | 1.64 | 0.73 |
| 160 | 195.68 | 0.81 | 1.80 | 0.50 | 0.63 | 0.73 | 1.31 | 0.96 | 2.13 | 0.46 | 0.89 | 0.28 | 1.03 |
| 170 | 207.91 | 0.81 | 1.12 | 1.20 | 0.45 | 0.72 | 1.06 | 0.67 | 0.88 | 1.33 | 0.72 | 0.76 | 1.03 |
| 180 | 220.14 | 0.75 | 1.07 | 1.11 | 0.69 | 0.81 | 1.23 | 0.75 | 1.31 | 0.43 | 0.73 | 0.44 | 1.12 |
| 190 | 232.37 | 0.94 | 1.18 | 0.54 | 0.52 | 0.28 | 1.20 | 1.20 | 1.48 | 0.66 | 0.86 | 0.67 | 1.13 |
| 200 | 244.60 | 1.12 | 1.50 | 0.69 | 0.69 | 0.40 | 0.69 | 1.21 | 1.15 | 0.69 | 0.37 | 0.22 | 0.54 |
| 210 | 356.83 | 1.04 | 1.70 | 0.49 | 0.56 | 0.73 | 0.93 | 1.15 | 1.68 | 0.72 | 0.49 | 0.53 | 1.10 |
| 220 | 269.06 | 1.13 | 1.58 | 0.61 | 0.99 | 1.44 | 0.49 | 0.75 | 1.55 | 0.55 | 0.91 | 1.76 | 0.70 |
| 230 | 281.29 | 0.93 | 1.85 | 0.55 | 0.48 | 0.22 | 0.88 | 1.27 | 1.27 | 0.83 | 0.46 | 0.48 | 0.95 |
| 240 | 293.52 | 0.45 | 1.49 | 0.23 | 0.18 | 0.39 | 1.38 | 0.31 | 1.61 | 0.18 | 0.46 | 0.92 | 0.98 |
| 250 | 305.75 | 0.84 | 1.57 | 0.19 | 0.63 | 0.48 | 0.74 | 0.76 | 1.28 | 0.60 | 1.00 | 0.32 | 0.91 |

Table E13: Uncertainties in rheology measurement at 40 °C.

| rpm | Shear rate, s ⁻¹ | Uncertainties (%) in shear stress measurement | | | | | | Uncertainties (%) in viscosity measurement | | | | | |
|-----|-----------------------------|---|-------|------|------|------|------|--|-------|------|------|------|------|
| | | 0 h | 1 h | 2 h | 3 h | 4 h | 5 h | 0 h | 1 h | 2 h | 3 h | 4 h | 5 h |
| 10 | 12.23 | 5.85 | 3.23 | 4.35 | 5.83 | 5.83 | 5.44 | 4.20 | 2.44 | 5.10 | 2.53 | 4.30 | 5.79 |
| 20 | 24.46 | 4.56 | 0.00 | 2.22 | 3.40 | 5.13 | 4.69 | 5.22 | 1.33 | 2.63 | 1.49 | 2.55 | 3.56 |
| 30 | 36.69 | 4.59 | 13.26 | 1.30 | 2.15 | 3.22 | 7.57 | 3.53 | 11.83 | 2.25 | 2.53 | 3.14 | 3.95 |
| 40 | 48.92 | 5.83 | 6.59 | 1.69 | 2.25 | 3.14 | 3.41 | 4.53 | 8.93 | 1.98 | 2.08 | 2.69 | 3.95 |
| 50 | 61.15 | 3.92 | 8.47 | 0.79 | 1.95 | 1.36 | 2.45 | 3.49 | 8.41 | 0.48 | 2.37 | 1.21 | 2.72 |
| 60 | 73.38 | 4.18 | 6.12 | 2.73 | 2.20 | 1.98 | 3.48 | 3.41 | 6.65 | 0.56 | 2.50 | 2.00 | 3.52 |
| 70 | 85.61 | 2.62 | 1.49 | 1.08 | 2.31 | 0.54 | 1.46 | 2.23 | 1.70 | 0.75 | 2.11 | 0.67 | 0.89 |
| 80 | 97.84 | 0.77 | 1.04 | 1.23 | 1.50 | 1.25 | 1.19 | 0.98 | 1.02 | 1.21 | 1.55 | 0.78 | 0.64 |
| 90 | 110.07 | 0.99 | 1.38 | 0.66 | 0.82 | 0.34 | 0.59 | 0.72 | 1.19 | 0.73 | 1.02 | 0.37 | 0.40 |
| 100 | 122.30 | 0.83 | 1.38 | 0.53 | 1.30 | 0.54 | 0.92 | 1.10 | 1.28 | 0.39 | 1.43 | 0.66 | 1.33 |
| 110 | 134.53 | 0.89 | 1.03 | 0.99 | 1.18 | 0.46 | 1.15 | 0.89 | 1.09 | 1.02 | 1.18 | 0.92 | 1.35 |
| 120 | 146.76 | 1.55 | 1.13 | 1.14 | 1.04 | 1.25 | 0.95 | 1.59 | 1.06 | 1.05 | 1.04 | 1.14 | 1.02 |
| 130 | 158.99 | 1.56 | 1.70 | 2.89 | 0.80 | 0.55 | 1.20 | 1.34 | 1.13 | 2.85 | 0.68 | 0.59 | 1.33 |
| 140 | 171.22 | 1.02 | 1.13 | 0.94 | 0.76 | 1.55 | 1.45 | 0.94 | 0.66 | 1.00 | 0.85 | 1.48 | 1.10 |
| 150 | 183.45 | 0.71 | 0.65 | 0.90 | 0.68 | 1.19 | 1.02 | 0.74 | 0.73 | 0.85 | 0.68 | 1.03 | 0.93 |
| 160 | 195.68 | 1.02 | 0.55 | 1.42 | 1.11 | 1.35 | 1.69 | 0.97 | 0.62 | 1.88 | 0.67 | 1.04 | 1.47 |
| 170 | 207.91 | 0.68 | 1.12 | 1.13 | 1.14 | 0.83 | 0.99 | 0.73 | 1.09 | 0.82 | 2.35 | 0.47 | 0.49 |
| 180 | 220.14 | 0.37 | 0.85 | 0.55 | 0.80 | 0.46 | 1.51 | 0.47 | 0.85 | 0.67 | 1.16 | 1.22 | 1.44 |
| 190 | 232.37 | 0.20 | 0.98 | 0.31 | 0.75 | 0.92 | 1.19 | 0.23 | 0.92 | 0.44 | 1.02 | 1.15 | 0.79 |
| 200 | 244.60 | 1.09 | 1.11 | 0.44 | 1.78 | 0.67 | 0.90 | 1.00 | 1.13 | 0.89 | 1.71 | 0.85 | 0.98 |
| 210 | 356.83 | 0.60 | 0.82 | 0.43 | 0.85 | 0.26 | 0.96 | 0.62 | 0.99 | 0.42 | 1.08 | 0.23 | 0.67 |
| 220 | 269.06 | 1.09 | 0.77 | 0.81 | 1.09 | 0.50 | 1.26 | 0.65 | 1.19 | 0.73 | 1.45 | 0.88 | 0.89 |
| 230 | 281.29 | 1.01 | 0.71 | 1.10 | 1.45 | 1.28 | 1.16 | 1.14 | 0.52 | 0.67 | 1.71 | 0.96 | 1.08 |
| 240 | 293.52 | 1.40 | 1.23 | 0.35 | 2.02 | 0.49 | 1.02 | 1.41 | 1.28 | 0.40 | 1.73 | 0.20 | 0.74 |
| 250 | 305.75 | 0.95 | 0.44 | 0.42 | 1.88 | 0.62 | 0.87 | 1.44 | 1.23 | 0.73 | 2.31 | 0.78 | 1.16 |

Table E14: Uncertainties in rheology measurement at 50 °C.

| rpm | Shear rate, s ⁻¹ | Uncertainties (%) in shear stress measurement | | | | | | Uncertainties (%) in viscosity measurement | | | | | |
|-----|-----------------------------|---|------|------|------|------|------|--|------|------|------|------|------|
| | | 0 h | 1 h | 2 h | 3 h | 4 h | 5 h | 0 h | 1 h | 2 h | 3 h | 4 h | 5 h |
| 10 | 12.23 | 7.53 | 9.72 | 4.35 | 4.76 | 7.42 | 6.43 | 9.59 | 0.00 | 5.44 | 5.44 | 5.44 | 4.88 |
| 20 | 24.46 | 4.55 | 4.67 | 2.44 | 2.56 | 3.89 | 5.73 | 6.31 | 3.02 | 3.02 | 2.55 | 2.92 | 2.94 |
| 30 | 36.69 | 4.56 | 3.47 | 2.11 | 2.56 | 3.86 | 6.88 | 5.54 | 4.68 | 4.08 | 2.59 | 2.11 | 7.25 |
| 40 | 48.92 | 6.64 | 1.80 | 1.15 | 2.66 | 2.81 | 1.80 | 7.26 | 1.78 | 1.64 | 2.49 | 2.07 | 1.28 |
| 50 | 61.15 | 5.88 | 0.91 | 0.91 | 1.47 | 2.28 | 2.65 | 5.72 | 1.12 | 0.56 | 1.39 | 1.70 | 2.31 |
| 60 | 73.38 | 4.24 | 3.79 | 2.01 | 4.18 | 1.07 | 0.81 | 4.52 | 4.95 | 0.79 | 5.19 | 1.27 | 0.59 |
| 70 | 85.61 | 2.56 | 2.41 | 1.53 | 3.11 | 1.04 | 1.70 | 2.87 | 3.24 | 0.89 | 2.88 | 0.93 | 1.46 |
| 80 | 97.84 | 0.00 | 1.04 | 0.81 | 2.67 | 0.85 | 0.94 | 0.46 | 2.28 | 0.80 | 2.86 | 1.25 | 0.92 |
| 90 | 110.07 | 1.00 | 0.80 | 1.05 | 1.62 | 0.67 | 1.23 | 1.40 | 1.15 | 0.73 | 1.65 | 0.63 | 1.22 |
| 100 | 122.30 | 1.57 | 0.61 | 1.61 | 1.79 | 0.92 | 0.47 | 1.45 | 0.66 | 1.77 | 1.59 | 1.12 | 0.94 |
| 110 | 134.53 | 1.36 | 0.73 | 1.24 | 0.70 | 1.25 | 1.20 | 1.25 | 0.66 | 1.41 | 0.69 | 0.35 | 0.40 |
| 120 | 146.76 | 1.21 | 2.18 | 0.85 | 1.17 | 1.85 | 0.86 | 1.24 | 0.63 | 0.98 | 1.41 | 1.28 | 0.38 |
| 130 | 158.99 | 1.39 | 3.64 | 1.40 | 0.94 | 1.34 | 0.93 | 1.37 | 0.95 | 1.20 | 0.96 | 0.60 | 0.36 |
| 140 | 171.22 | 0.89 | 2.76 | 0.58 | 0.62 | 0.86 | 1.31 | 0.79 | 0.35 | 0.76 | 0.69 | 0.76 | 1.11 |
| 150 | 183.45 | 0.66 | 2.89 | 1.39 | 2.24 | 0.55 | 1.52 | 0.72 | 0.00 | 1.69 | 2.72 | 0.56 | 1.37 |
| 160 | 195.68 | 0.88 | 3.00 | 1.10 | 2.74 | 0.33 | 1.99 | 0.74 | 0.97 | 1.33 | 2.87 | 0.33 | 1.60 |
| 170 | 207.91 | 1.50 | 3.47 | 2.24 | 3.12 | 0.68 | 1.84 | 1.18 | 0.48 | 2.02 | 2.74 | 0.45 | 0.58 |
| 180 | 220.14 | 1.31 | 4.88 | 1.37 | 3.68 | 0.74 | 2.07 | 1.04 | 0.44 | 1.51 | 3.93 | 1.20 | 1.07 |
| 190 | 232.37 | 1.32 | 4.27 | 1.70 | 3.91 | 1.31 | 0.92 | 1.37 | 0.62 | 1.99 | 4.16 | 0.43 | 0.67 |
| 200 | 244.60 | 1.10 | 5.80 | 2.13 | 4.77 | 0.36 | 1.70 | 1.06 | 0.53 | 1.52 | 4.28 | 0.69 | 1.51 |
| 210 | 356.83 | 1.73 | 6.45 | 1.21 | 4.59 | 0.67 | 1.17 | 1.30 | 0.29 | 1.17 | 4.97 | 0.63 | 0.95 |
| 220 | 269.06 | 1.13 | 3.78 | 2.06 | 4.92 | 0.40 | 1.39 | 0.97 | 0.62 | 1.91 | 4.60 | 0.49 | 1.11 |
| 230 | 281.29 | 1.02 | 1.49 | 2.12 | 4.53 | 0.35 | 1.08 | 1.10 | 0.74 | 1.87 | 5.12 | 0.40 | 1.21 |
| 240 | 293.52 | 0.68 | 1.57 | 2.15 | 4.48 | 0.46 | 1.23 | 1.08 | 0.63 | 1.89 | 4.39 | 0.45 | 1.19 |
| 250 | 305.75 | 0.65 | 1.49 | 1.40 | 4.45 | 0.63 | 1.24 | 0.41 | 1.37 | 2.03 | 4.20 | 0.62 | 1.46 |

Table E15: Uncertainties in the measured parameters of the heat sink.

| Parameter (unit) | Flow rate, L/min | Uncertainty, % | | | | | |
|-------------------------|------------------|----------------|------|------|------|------|------|
| | | Water | 1 h | 2 h | 3 h | 4 h | 5 h |
| Inlet temperature (°C) | 1.000 | 0.29 | 2.80 | 0.54 | 0.98 | 5.73 | 2.87 |
| | 0.875 | 0.33 | 0.32 | 0.28 | 0.13 | 2.48 | 0.60 |
| | 0.750 | 0.94 | 0.61 | 0.60 | 0.37 | 1.15 | 0.44 |
| | 0.625 | 1.10 | 1.84 | 0.29 | 0.25 | 0.50 | 1.16 |
| | 0.500 | 0.85 | 1.96 | 0.36 | 0.40 | 0.17 | 0.66 |
| Outlet temperature (°C) | 1.000 | 0.43 | 1.55 | 3.48 | 1.38 | 3.00 | 2.64 |
| | 0.875 | 0.49 | 0.27 | 0.33 | 0.34 | 2.40 | 0.61 |
| | 0.750 | 1.00 | 0.56 | 0.80 | 0.34 | 0.82 | 0.81 |
| | 0.625 | 1.00 | 2.15 | 0.39 | 0.45 | 0.73 | 1.09 |
| | 0.500 | 3.78 | 1.04 | 0.49 | 0.94 | 0.54 | 0.45 |
| Base temperature (°C) | 1.000 | 0.52 | 0.99 | 0.24 | 0.72 | 2.11 | 1.94 |
| | 0.875 | 0.42 | 0.44 | 0.24 | 0.17 | 1.86 | 0.48 |
| | 0.750 | 0.62 | 0.33 | 0.41 | 0.24 | 0.52 | 0.61 |
| | 0.625 | 0.70 | 1.41 | 0.31 | 0.30 | 0.44 | 1.04 |
| | 0.500 | 2.83 | 0.70 | 0.35 | 0.49 | 0.43 | 0.14 |
| Pressure drop (Pa) | 1.000 | 0.20 | 0.41 | 0.34 | 0.32 | 0.84 | 0.47 |
| | 0.875 | 0.14 | 0.12 | 0.16 | 0.20 | 0.35 | 0.23 |
| | 0.750 | 0.14 | 0.15 | 0.12 | 0.12 | 0.39 | 0.64 |
| | 0.625 | 0.09 | 0.30 | 0.14 | 0.11 | 0.18 | 0.17 |
| | 0.500 | 7.05 | 0.20 | 0.12 | 0.11 | 0.11 | 0.10 |